

**THE NOTCH1-C-MYC PATHWAY MEDIATES LEUKEMIA-  
INITIATING CELL ACTIVITY IN MOUSE T-ALL MODELS**

**A Dissertation Presented**

**By**

**JESSICA MARIE TESELL**

Submitted to the Faculty of the  
University of Massachusetts Graduate School of Biomedical Sciences, Worcester  
in partial fulfillment of the requirements for the degree of

**DOCTOR OF PHILOSOPHY**

**MAY 10, 2013**

**CANCER BIOLOGY**

**THE NOTCH1-C-MYC PATHWAY MEDIATES LEUKEMIA-INITIATING CELL  
ACTIVITY IN MOUSE T-ALL MODELS**

**A Dissertation Presented  
By  
JESSICA MARIE TESELL**

**The signatures of the Dissertation Defense Committee signify completion  
and approval as to style and content of the Dissertation**

---

**Michelle Kelliher Ph.D., Thesis Advisor**

---

**Lucio Castilla, Ph.D., Member of Committee**

---

**Rachel Gerstein, Ph.D., Member of Committee**

---

**Brian Lewis, Ph.D., Member of Committee**

---

**Patricia Ernst, Ph.D., Member of Committee**

**The signature of the Chair of the Committee signifies that the written  
dissertation meets the requirements of the Dissertation Committee**

---

**Stephen Jones, Ph.D., Chair of Committee**

**The signature of the Dean of the Graduate School of Biomedical Sciences  
signifies that the student has met all graduation requirements for the  
school**

---

**Anthony Carruthers, Ph.D.  
Dean of the Graduate School of Biomedical Sciences  
Cancer Biology  
May 10, 2013**

## Acknowledgments

First, I would like to thank my mentor, Michelle Kelliher, for her support and guidance over the last five years. I also need to thank the members of the Kelliher Lab, both past and present for their help and friendship. Specifically, I would like to thank Kate Cullion, Nicole Hermance, Justine Roderick, and A Hyun Choi for their help with experiments directly related to my thesis. The Cancer Biology Department has been a great place to learn and grow and I need to thank them for supporting me, especially with the T32 training grant. I also appreciate the advice and criticisms from my committee, Stephen Jones, Brian Lewis, Rachel Gerstein, Lucio Castilla, and Patricia Ernst.

I thank Sudhir Rao at Merck for the GSI compound MRK-003 and corresponding pharmacokinetics and technical support. I thank James Bradner and Jun Qi at DFCI for the JQ1 compound. I learned challenging surgical techniques from Kimie Hattori at Harvard Medical School (Benoist/Mathis lab). Todd Ashworth, in the lab of Jon Aster, helped perform 5' Notch1 deletion analysis in Chapter III.

Last but far from least, I need to thank my family and friends for their constant love and support. My parents who have always taught me that hard work pays off and to my sister Rachel who has taught me what it means to follow your dreams and be truly happy. Finally, to my little nuclear family, my husband Mark and our fur-child Diego: you keep me sane. Going home to them each night helps give me perspective and helps me to remember what I have done all this work for.

## Abstract

Although cure rates have significantly improved for children with T-cell acute lymphoblastic leukemia (T-ALL), 20-30% undergo induction failure or relapse with most succumbing to disease. Leukemia-initiating cells (L-ICs) are hypothesized to be resistant to conventional chemotherapy and radiation and are thereby responsible for disease recurrence. Using an *in vivo* limiting dilution assay, we previously showed that the murine T-ALL L-IC is quite rare, with only 0.003-0.05% of cells capable of initiating disease, and demonstrated that the L-IC is a subset of the leukemic DN3 thymic progenitor population. Work described in this thesis validates the L-IC assay using two transplantation methods to rule out effects of homing and/or microenvironment on T-ALL L-IC survival and maintenance. Using this assay, we demonstrate that sustained Notch1 signaling is required for T-ALL initiation *in vivo* and show that treatment with a Notch1 inhibitor reduces or in some cases eliminates the L-IC population. We further analyze the effects of inhibiting c-Myc, a Notch1-regulated gene, on L-IC frequency and uncover an essential role for c-Myc in L-IC survival and expansion. Suppressing c-Myc by using specific shRNAs or a c-Myc inhibitor reduces the L-IC population and interferes with leukemia initiation. Together, these findings reveal a critical role of the Notch1-c-Myc pathway in T-ALL initiation and suggest that therapeutics targeted at this pathway could be used to treat and/or prevent disease relapse in patients.

## TABLE OF CONTENTS

Signature Page	ii
Acknowledgments	iii
Abstract	iv
Table of Contents	v
List of Tables	viii
List of Figures	ix
List of Abbreviations	xi
Chapter I: Introduction	1
Chapter II: Thymic microenvironment does not influence frequency or activity of murine T-ALL leukemia-initiating cells	44
Introduction	46
Results	49
Discussion	52

Methods	55
Figures	57

### Chapter III: Notch1 inhibition targets the leukemia-initiating cells in a *Tal1/Lmo2*

mouse model of T-ALL	65
Introduction	67
Results	70
Discussion	75
Methods	79
Figures	82

### Chapter IV: c-Myc silencing or inhibition prevents disease initiation in mice and

impairs the growth of relapsed pediatric T-ALL cells	95
Introduction	97
Results	99
Discussion	108
Methods	112

Figures	116
Chapter V: Discussion	132
Appendix I: Clonal selection for Pten loss occurs upon T-ALL transplant	152
Appendix II: Attempts to further characterize the L-IC population	168
Appendix III: c-Myb plays a role in T-ALL L-IC survival and/or activity	182
Appendix IV: Microarray following JQ1 treatment <i>in vivo</i>	198
List of Primers	205
List of Antibodies	206
References	207

## List of Tables

Table 1.	<i>Lck-Tal1/Lmo2</i> T-ALLs are functionally heterogeneous
Table 2.	L-IC frequency is not influenced by mode of transplant.
Table 3.	TCR-V $\beta$ clonal selection is not influenced by mode of transplant.
Table 4.	Multiple <i>Notch1</i> mutations are detected in preleukemic <i>Lck-Tal1/Lmo2</i> thymic progenitors.
Table 5.	Notch1 inhibition reduces L-IC frequency and/or activity.
Table 6.	Notch1 inhibition reduces L-IC frequency and/or activity.
Table 7.	Summary of GSI responses <i>in vivo</i> .
Table 8.	Silencing of c-Myc reduces L-IC frequency.
Table 9.	Silencing of c-Myc reduces L-IC frequency.
Table 10.	Most shMyc leukemic mice contained GFP+ and proviral+ cells.
Table 11.	JQ1 treatment reduces L-IC frequency.
Table 12.	JQ1 treatment reduces L-IC frequency.
Table 13.	Loss of Pten expression correlates with decreased GSI sensitivity and increased p-Akt.
Table 14.	c-Kit expression on <i>Lck-Tal1/Lmo2</i> preleukemic and leukemic thymic subsets
Table 15.	CD27 expression on <i>Lck-Tal1/Lmo2</i> preleukemic and leukemic thymic subsets
Table 16.	Silencing of c-Myb reduces L-IC frequency.
Table 17.	Silencing of c-Myb reduces L-IC frequency.
Table 18.	Top 50 repressed and induced genes following JQ1 treatment <i>in vivo</i>



## List of Figures

- Figure 1. Thymocyte development
- Figure 2. Notch1 signaling pathway
- Figure 3. Models for tumor-initiating cell heterogeneity
- Figure 4. Functional heterogeneity among mouse *Lck-Tal1/Lmo2* T-ALLs
- Figure 5. Intrathymic injection of T-ALL cells does not alter disease progression.
- Figure 6. Leukemia-Initiating Cell (L-IC) frequency does not differ with mode of transplant.
- Figure 7. L-ICs are maintained with both IT and IP injection.
- Figure 8. Method of T-ALL injection alters disease presentation.
- Figure 9. Notch1-active *Lck-Tal1/Lmo2* thymic progenitors are oligoclonal.
- Figure 10. Notch1 protein expression is similar in leukemic DN3 and DP cells.
- Figure 11. GSI treatment reduces Notch1 protein expression in primary T-ALLs after 48 hours *in vitro*.
- Figure 12. GSI administration to leukemic mice results in decreased Notch1 target gene expression.
- Figure 13. Notch inhibition targets the L-IC in *Lck-Tal1/Lmo2* mouse T-ALLs.
- Figure 14. Transplanted mice treated with GSI continued to gain weight throughout the treatment period.
- Figure 15. Mouse T-ALLs examined in the GSI treatment study express high levels of intracellular Notch1, harbor insertions/deletions that result in PEST truncation and express aberrant 3' transcripts.
- Figure 16. GSI targets the L-IC population in *Lck-Tal1/Lmo2* T-ALLs
- Figure 17. Sort purity of shRNA-infected leukemic cells prior to transplant.

- Figure 18. Silencing of c-Myc prolongs survival in mice transplanted with murine T-ALL cells.
- Figure 19. Reduced c-Myc protein levels and impaired growth in vitro in c-Myc-silenced leukemic cells.
- Figure 20. Myc-silenced mice that develop disease contain GFP+ cells but do not exhibit Myc knockdown.
- Figure 21. No GFP-positive cells remained in transplanted animals 120 days post-transplant.
- Figure 22. JQ1 treatment induces rapid cell cycle arrest and apoptosis of murine T-ALL cells.
- Figure 23. JQ1 treatment reduces c-Myc mRNA and expression of its target genes.
- Figure 24. JQ1 treatment of leukemic mice significantly prolongs survival and reduces c-Myc expression.
- Figure 25. JQ1 treatment extends survival of recipient mice when cells are transplanted in limiting dilution.
- Figure 26. Similar growth inhibition is observed among T-ALLs following JQ1 treatment.
- Figure 27. A model for T-ALL development
- Figure 28. Pten protein decreases upon transplant and results in increased Akt signaling
- Figure 29. miR-19b and Pten mRNA expression in T-ALLs after transplant
- Figure 30. BrdU uptake assays do not reveal a quiescent DN3 population
- Figure 31. Silencing of c-Myb prolongs survival in mice transplanted with murine T-ALL cells.
- Figure 32. Impaired cell growth and reduced c-Myb expression in c-Myb-silenced leukemic cells.
- Figure 33. c-Myb-silenced mice that develop disease contain GFP+ cells and exhibit Myb knockdown.
- Figure 34. No GFP-positive cells remained in transplanted animals 120 days post-transplant.

### List of Abbreviations

ADAM	A disintegrin and metalloprotease
AML	Acute myelogenous leukemia
ANK	Ankyrin repeats
B-ALL	B-cell acute lymphoblastic leukemia
bHLH	Basic-helix-loop-helix
BRD4	bromodomain-4
CADASIL	cerebral autosomal dominant arteriopathy with subcortical infarcts and leukoencephalopathy
CD	cluster of differentiation
CDK	cyclin-dependent kinase
CLP	Common lymphoid progenitor
CML	Chronic myelogenous leukemia
CMP	Common myeloid progenitor
CNA	copy number abnormality
CNS	central nervous system
CSL	CBF1 ,RBP-J, Su(H), Lag1
DLL	Delta-like
DN	Double negative
DP	Double positive
EGF	Epidermal growth factor
ETP	Early thymic progenitor
GSI	gamma secretase inhibitor
GVH	Graft versus host
HD	heterodimerization domain

HSC	Hematopoietic stem cell
ICN1	Intracellular Notch1
IF	Induction failure
ISP	Immature single positive
Jag1/2	Jagged-1 or Jagged-2
L-IC	Leukemia-initiating cell
Lin	Lineage
LMO1/2	LIM-only protein 1 or 2
LT-HSC	Long term hematopoietic stem cell
MAML	Mastermind-1 like 1
MAPK	mitogen-activated protein kinase
MCS	Myc core signature
MDR	Multidrug resistance
MDSR	Myc-dependent serum response
MoMLV	Moloney murine leukemia virus
MPP	Multipotent progenitor
mTOR	Mammalian target of rapamycin
NEC	Notch1 extracellular domain
NICD	Notch1 intracellular domain
NK	Natural killer
NLS	nuclear localization sequence
NOD/SCID	non-obese diabetic/severe combined immunodeficient
NRR	Negative regulatory region
NSC	neuronal stem cell
NTM	Notch1 transmembrane domain

p70S6K	ribosomal protein kinase 6
PEST	Pro-Glu-Ser-Thr
PI3K	Phosphatidylinositol 3-kinase
Pre-TCR	Pre-T-cell receptor
Pre-T $\alpha$	Pre-T-cell antigen receptor alpha
Pten	Phosphatase and tensin homolog
Rag 1/2	Recombinase activating genes 1 and 2
RMA	Robust Multi-Array Analysis
SCID	Severe combined immunodeficiency
SCF	Stem cell factor
SCL	Stem cell leukemia
SIL	Scl interrupting locus
SP	single positive
ST-HSC	Short term hematopoietic stem cell
T-ALL	T-cell acute lymphoblastic leukemia
T-IC	Tumor-initiating cell
TACE	TNF- $\alpha$ converting enzyme
TAD	Transactivation domain
TAL1	T-cell acute lymphoblastic leukemia -1
TCR	T-cell receptor

# **CHAPTER I**

## **Introduction**

## T-ALL

T-cell acute lymphoblastic leukemia (T-ALL) is a disease of immature T-lymphocytes and accounts for 15% of pediatric and 25% of adult cases of ALL, for a total of approximately 500 children and 250 adults diagnosed each year in the United States<sup>1,2</sup>. Patients often present with fever, bone pain, bleeding, lymphadenopathy, mediastinal mass, and extremely high white blood cell counts with evidence of atypical blasts in the periphery<sup>3-5</sup>. Classification of ALL is based on morphology of the cells found in blood smears and on flow cytometry of defined cell surface markers<sup>6</sup>.

T-ALL is a high-risk group within ALL as a whole. This is partly due to the fact that T-ALL cells will often infiltrate the CNS, causing neurological symptoms and increased mortality. T-cells express the CCR7 receptor on the cell surface, which permits the cells to cross into the CNS<sup>7</sup>. Overall survival for pediatric patients with T-ALL is estimated at 70%, compared to an 85% survival rate overall for ALL<sup>8-10</sup>. This prognosis is worse for adults (50%)<sup>11</sup> and patients with an early precursor T-cell subtype (~57%)<sup>12-14</sup>. Once disease has relapsed the outlook for patients, both children and adults, is very poor with median survival being only one year and only 25% of relapsed patients surviving to 3 years<sup>11,15</sup>.

Current chemotherapies are rigorous and harsh, especially on young children. First line therapy for T-ALL is a multidrug regimen consisting of three separate phases: induction, consolidation, and maintenance<sup>8</sup>. Induction therapy

consists of weekly treatment with vincristine, cortical steroids, asparaginase, and doxorubicin<sup>9,16</sup>; approximately 90% of patients will achieve a remission (as judged by bone marrow biopsy) after this phase<sup>16</sup>. Consolidation therapy is begun after remission is attained from induction therapy and consists of cytarabine, methotrexate, doxorubicin, cyclophosphamide, and etoposide<sup>17</sup>. These drugs are given in different combinations for up to six months and are adjusted according to each patients risk group and response rate<sup>18</sup>. Patients are lastly put on a less intensive maintenance therapy that can last 2-3 years. This usually consists of oral 6-mercaptopurine and periodic intrathecal methotrexate, with some patients also receiving low doses of vincristine and steroids<sup>19–21</sup>.

Relapse will occur in approximately 20-25% of children<sup>8,10,22</sup> and 50% of adults<sup>11</sup> diagnosed with T-ALL. An estimated 3% of patients will die from toxicities associated with treatment, including cardiac events and infections<sup>23</sup>. Notably, to prevent central nervous system (CNS) involvement, patients are often treated with cranial irradiation and intrathecal high-dose chemotherapy<sup>8</sup>. This has led to the development of learning disorders in children and secondary malignancies later in life<sup>24,25</sup>. It is critical that targeted therapies be developed to help abate some of these side effects, while improving successful remission rates.



## **Self-renewal plays a role in thymocyte development**

T-ALL results from proliferation of immature thymocytes, so it is important to understand the normal steps in thymocyte maturation in order to better understand the progression of the disease. Murine thymocyte development is being increasingly well defined as flow cytometry and genomics techniques become more sophisticated. The steps and regulation of human thymocyte development are not as well defined, but is presumed to occur in an analogous fashion. Flow cytometry and monoclonal antibodies have allowed for the fractionation of hematopoietic stem cells (HSCs) and their progeny from murine bone marrow, using a combination of cluster of differentiation (CD) molecules and SLAM markers. These populations can then be sorted, reconstituted in mice, and their gene expression profile determined. T-cells go through a regimented developmental program of commitment and differentiation steps before becoming functional lymphocytes (outlined in Figure 1). These steps are often defined by the presence or absence of T-lineage markers CD4 and CD8 on the cell surface (reviewed in<sup>26</sup> and <sup>27</sup>).

All blood lineages can be derived from the HSCs, which reside in the bone marrow and can be divided into two groups: long-term (LT-HSC) and short-term (ST-HSC)<sup>28,29</sup>. LT-HSCs have a surface expression profile of CD34<sup>-</sup>, Flt3<sup>-</sup>, lineage (Lin)<sup>-</sup>, c-Kit<sup>+</sup>, Thy<sup>lo</sup>, Sca<sup>+</sup>, CD150/Slamf1<sup>+</sup>, CD48/Slamf2<sup>-30-36</sup>. These cells have unlimited self-renewal capacity and the potential to give rise to any blood

lineage. ST-HSCs have a similar cell surface expression pattern with CD34 being expressed in addition to those on LT-HSC population. ST-HSCs have limited self-renewal capacity compared to LT-HSCs, but still have the capacity to give rise to all progenitors necessary for blood development (reviewed in<sup>37</sup>). The HSC differentiates into the short-lived multipotent progenitor population (MPP)<sup>38</sup> with the expression of Flt3 and then is able to give rise to the lymphoid-primed multipotent progenitor<sup>39</sup> and common myeloid progenitors (LMPPs and CMPs, respectively).

The LMPP resides in the bone marrow and has the ability to spawn both the B and T lineages. LMPP cells that express CCR9, c-Kit, Sca, and Flt3 will egress and migrate to the thymus where they have the option to become a T-cell (reviewed in<sup>40</sup>). The first stage of T-cell development is termed the double-negative 1 (DN1) population and has a surface marker profile of Lin<sup>-</sup>, CD44<sup>+</sup>, CD25<sup>-</sup>, c-Kit<sup>+</sup><sup>41</sup>. These cells are not fully committed to the T-cell lineage and may reverse at any time to differentiate into B-cells, natural killer (NK) cells, dendritic cells, mast cells, or monocytes<sup>42-44</sup>. The early thymic precursor (ETP) population is a subset of the DN1 population, can be found in and outside of the thymus, and has the cell surface expression pattern Lin<sup>-</sup>/CD4<sup>lo</sup>, Sca<sup>+</sup>, c-Kit<sup>high</sup>, IL7R $\alpha$ <sup>-</sup>, and CCR9<sup>+</sup>, and includes Flt3L<sup>+</sup> and Flt3L<sup>-</sup> subsets<sup>41,45,46</sup>. There is also evidence that once an ETP cell no longer expresses Flt3L, it no longer has B-cell potential and has the ability to differentiate into a mature T-lymphocyte<sup>42,47</sup>. Notch1

signaling is required early on in these stages to commit these progenitor cells to the T-cell lineage<sup>48–50</sup>.

T-cells physically move through the thymus as they change their differentiation status to express new markers and critical T-cell genes. The DN2 population begins to express CD25 and decreases surface expression of c-Kit (reviewed in<sup>51</sup> and<sup>40</sup>). This population is divided into DN2a and DN2b subsets and is characterized by a massive burst of proliferation. DN2a cells are plastic, like the DN1 population, and are not fully committed to the T-cell lineage. DN2b cells can begin to express CD3<sup>52</sup> and can differentiate along the  $\gamma\delta$  or  $\alpha\beta$  T-cell lineages. Rag1/2 proteins begin to rearrange the T-cell receptor (TCR)  $\delta$ ,  $\gamma$ , and  $\beta$  loci to determine to which lineage the cell will differentiate<sup>53</sup>. Cells that do not successfully rearrange one of these loci will undergo apoptosis. Cells that rearrange the TCR $\beta$  locus will continue to develop in the thymus while less is known about the development of the  $\gamma\delta$  T-cells<sup>54</sup>.

Once the cells reach the DN3 stage in thymocyte development, they begin to express the TCR $\beta$  chain on the cell surface and decrease CD44 and Kit expression. At this point they are fully committed to the T-cell differentiation program and cannot reverse direction. This population can be divided into DN3a and DN3b cells based on CD27 expression and CD25 staining intensity<sup>53</sup>. DN3a cells undergo proliferation arrest and express a high amount of Pre-T $\alpha$  on the surface to form the Pre-TCR complex with the TCR $\beta$  chain and promote positive

selection of the thymocytes<sup>55,56</sup>. Pre-TCR signaling is critical for cells to move past the DN3 stage in development as it starts a MAPK signaling cascade and activates phospholipase-C, which activate critical T-cell transcription factors such as Ets-1, Id3, Runx-1, NFAT, NFκB, Myb, Gata3, Gfi1, and Lef1<sup>56-62</sup>. Cells at the DN3b stage increase CD27 expression and resume proliferation. Here they start to reduce the expression of Notch1 target genes and increase expression of more mature TCR complex members such as Zap70. Cells then move into the DN4 stage of development as they lose expression of CD25<sup>26,40</sup>.

Cells continue to proliferate as they rearrange the TCRα chain at the double-positive (DP) stage of thymocyte development. Here, cells will express both CD4 and CD8, preceded by a transient immature single-positive (ISP) stage. At this stage, thymocytes undergo both positive and negative selection before they can mature to either CD4 or CD8 single positive cells and enter the periphery<sup>63,64</sup>. Only approximately 5% of cells will make it all the way through development; most will die in the thymus<sup>65</sup>.

Recent evidence has shown that thymocytes do have an intrinsic ability to self-renew and that this traditional path from bone marrow to T-cell may not always be taken (reviewed in<sup>66</sup>). In times of stress or reduced thymic import, T-cells are able to repopulate the thymus to prevent a shortage of mature T-cells in the periphery. The target cell for this self-renewal phenotype in normal thymocytes is controversial, but evidence shows that it probably does not reside

in the immature ETP population<sup>67,68</sup>. A more differentiated cell has an intrinsic ability to self renew, but will only do so if necessary, as using this method of thymic repopulation reduces heterogeneity in the T-cell receptor  $\alpha$  and  $\beta$  chains<sup>67</sup>.

### **Activation of oncogenes and loss of tumor suppressors drive T-ALL**

Identifying the underlying genetic mutations driving T-ALL is one step towards finding targeted therapeutics. Oncogenic events in T-ALL enhance proliferation, inhibit differentiation, and possibly promote self-renewal of thymocytes. T-ALL is a multi-step process and none of these events are ever implicated in isolation. In order for leukemia to develop, mutations must occur in two separate pathways: one involving cell proliferation and one that disrupts normal hematopoietic development<sup>69</sup>. Unlike other leukemias such as acute myelogenous leukemia (AML), chronic myelogenous leukemia (CML), and B-cell ALL (B-ALL), translocation events are rare in T-ALL, but usually involve the TCR when they do occur.

Genetic profiling of hundreds of patient samples has revealed that T-ALL is often associated with mutations or overexpression of *TAL1*, *LMO1*, *LMO2*, *HOX11*, *NOTCH1*, *c-MYC*, *TLX3*, *c-MYB*, or *LYL1*<sup>70–80</sup>. In addition to oncogene activation, there are a number of tumor suppressors that are inactivated in T-ALL patients and often result in activation of oncogenic pathways or loss of growth control. Mutations, deletions, and loss of heterozygosity have been found in

*FBW7*, *PTEN*, *p16INK4a*, *p14ARF*, *p53*, and *IKAROS* in T-ALL patient samples (reviewed in<sup>71</sup>). Loss of *FBW7* and *IKAROS* can result in increased *NOTCH1* signaling while loss of *PTEN* increases cell growth and metabolism through the activation of the PI3K pathway. Inactivation of *p53*, *p16INK4a*, and/or *p14ARF* results in loss of apoptosis or cell cycle control, which can then allow for oncogenic growth to go unchecked.

### **Tal1 as an oncogenic driver of T-ALL**

Tal1, also called SCL or TCL5, encodes a basic-helix-loop-helix (bHLH) transcription factor critical for hematopoiesis. Expression of Tal1 initiates in the mouse embryo at day 7.5 and is seen in the brain, endothelial cells, and the erythroid, mast, megakaryocyte, and myeloid lineages at that time<sup>81–83</sup>. Tal1 is absolutely essential for development of all blood lineages<sup>84,85</sup>. Tal1-null mice die at embryonic day 8.5–10 due to complete lack of blood and defects in yolk sac hematopoiesis<sup>86</sup>. Without Tal1, the embryo has defective angiogenesis and the organism is unable to form megakaryocytes or HSCs<sup>85–88</sup>. Tal1 is expressed in HSCs and MPPs, but expression in thymocytes is downregulated very early in T-cell development. There is little to no detection of Tal1 expression after the DN1/DN2 stage in thymocyte development and the protein has no role in T-cell maturation<sup>89,90</sup>.

bHLH transcription factors are divided into two groups: Class I and II. Class I bHLH proteins can bind DNA as homodimers or heterodimers while Class

II proteins can only bind DNA as heterodimers with Class I bHLH proteins. Tal1 is a Class II bHLH transcription factor and binds DNA with E-proteins such as E2-2, E47, E12, and Heb<sup>91–93</sup>. This heterodimer then becomes part of a transcriptional complex in hematopoietic cells along with Lmo2, Ldb1, Gata1/2 and Sp1<sup>94–96</sup>. Once bound to E-box/Gata sequences, the complex recruits transcriptional coactivators such as p300<sup>97</sup> and p/CAF<sup>98</sup>, or transcriptional repressors such as mSin3A<sup>99</sup> to modulate transcription.

T-ALL patient samples often misexpress TAL1 resulting from a variety of genetic events, not all of which are well understood. Rare translocation events have been reported, one of which brings TAL1 into the TCR $\delta$  locus (t(1;14)(q33;11))<sup>100</sup> and one which brings it into the TCR $\beta$  locus (t(1;7)(p32;q35))<sup>101</sup>. In approximately 20% of T-ALL patients, a 90kb genomic deletion event occurs which deletes the TAL1 proximal promoter and places TAL1 within range of the SIL promoter, which is strongly expressed in a variety of tissues, including the thymus<sup>102–104</sup>. These cryptic deletions only occur in  $\alpha\beta$  T-cells, suggesting that the same machinery is used to create the SIL deletion as T-cell gene rearrangement<sup>105</sup>. It is estimated that 60% of pediatric and 45% of adult T-ALL patients express TAL1, so there is clearly a large portion of patients where Tal1 is misexpressed by an unknown mechanism<sup>104</sup>.

### Tal1 mouse models of T-ALL

Because of the high frequency of TAL1 expression in patients, mouse models of T-ALL have attempted to use Tal1 as a driver of the disease, however few have been successful. The *CD2* promoter<sup>106</sup> expressed in early T-cell development and the *SIL* (*Scl Interrupting Locus* promoter)<sup>107,108</sup> have been used to transgenically drive the expression of Tal1 in the thymus, but none of the mice developed T-ALL. When the *Lck* promoter (expressed at the DN2/DN3 stage of thymocyte development) was used to drive Tal1 expression in mice, 27% of the mice developed a lymphoblastic disease similar to T-ALL with T-cell blasts found in the thymus, kidney, liver, spleen, bone marrow, and central nervous system of the animals. The average latency of disease for these mice was 9-10 months, indicating that there must be additional oncogenic events that cooperate with Tal1 before disease is initiated<sup>109</sup>.

In T-ALL patients, TAL1 is found coordinately expressed with LMO1, LMO2, NOTCH1, and c-MYC as well as loss of the p14/ARF and p16/INK4A tumor suppressors (reviewed in<sup>71</sup>). In the *Lck-Tal1* model of T-ALL, retroviral mutagenesis was performed with Moloney murine leukemia virus (MoMLV), which identified Notch1, c-Myc, and a dominant negative form of Ikaros as cooperating events in Tal1-driven T-ALL<sup>110</sup>. In the same mouse model, heterozygous loss of the *INK4a/Arf* locus accelerated leukemia development and increased disease penetrance to 100%<sup>111</sup>. The same was found when *Lck-Tal1*



mice were mated to mice that expressed Lmo1 or Lmo2 in the developing thymus<sup>112,113</sup>. In T-ALL, Tal1 is oncogenic, but must cooperate with other events in order to successfully initiate disease. These events include, but are not limited to, the loss or epigenetic silencing of the *Ink4a/Arf* locus, activation of the Notch1 pathway, and misexpression of Lmo1/2.

When Tal1 is misexpressed in the developing thymus, T-cell differentiation is blocked at the DN3 stage of thymocyte development<sup>114</sup>. At this stage, critical events take place that commit thymocytes to maturation: TCR $\beta$  is rearranged and the pre-TCR $\alpha$  complex is assembled. These events take place with the help of the Rag1/2 proteins, which rearrange the DNA at the TCR loci to produce successful signaling proteins (reviewed in<sup>40</sup>). There is evidence that Tal1 expression at this stage disrupts the transcriptional activity of E-proteins such as E47 and HEB<sup>91,114</sup>. These E-proteins can drive the transcription of Rag 1/2<sup>114,115</sup> as well as other T-cell development genes such as PreT $\alpha$ <sup>116</sup> and CD4<sup>117</sup>. The DNA-binding activity is not required for the development of T-ALL<sup>112,118</sup>, so it is probable that Tal1 binds the E-proteins and sequesters them away from the promoter, resulting in decreased transcription of genes like Rag1/2, PreT $\alpha$ , and CD4. This idea was further confirmed when *Lck-Tal1* mice were mated to Heb<sup>+/-</sup> and E47<sup>+/-</sup> mice and the developmental block was enhanced and T-ALL was accelerated<sup>114</sup>.

### **Tal1 promotes gene expression as a member of a transcriptional complex**

Recent ChIP-seq and microarray expression data in T-ALL patient samples and human cell lines point to an even more complex regulatory circuit. In erythroid cells, TAL1 and E-proteins bind E-boxes often adjacent to GATA1 sites to initiate transcription. However, in T-ALL, ChIP-seq experiments have shown that TAL1 binds E-boxes not only adjacent to GATA3 sites, but also RUNX and ETS sites. The TAL1 complex in T-ALL cells also contains RUNX1 and Ets as members<sup>119,120</sup>. RUNX1 (and RUNX3) and ETS are critical genes in T-cell differentiation<sup>58,121,122</sup>, but their roles in T-ALL initiation and maintenance is unclear. In T-ALL, the TAL1 complex has been shown to inhibit differentiation, apoptosis, and tumor suppressor genes<sup>119,120</sup>, all of which contribute to the pathogenesis of the disease. These new data indicate that TAL1 not only acts as an inhibitor of normal E-protein function, but also can drive *de novo* transcription of a distinct set of target genes.

### **Lmo2 collaborates with Tal1 to initiate leukemia**

The LIM-only domain proteins LMO1/2 are misexpressed in 80% of T-ALL patients positive for (or expressing) TAL1, and LMO2 misexpression alone is found in 9% of T-ALL patients<sup>70,71,123</sup>. The protein was discovered after mapping the t(11;14)(p13;q11) translocation in T-ALL, in which RAG proteins rearrange the LMO2 locus into the TCR locus<sup>70,124–126</sup>. LMO2 was also implicated as the oncogenic driver in leukemias resulting from gene therapy of SCID-X1 patients.

In four patients, retroviral insertion at the LMO2 locus induced T-ALL after a long latency<sup>127–130</sup>.

LMO2 is critical for normal hematopoiesis and forms a complex with TAL1/SCL, GATA-1, and LDB1 at erythroid gene promoters in order to drive hematopoietic gene expression<sup>95,131,132</sup>. Lmo2-null mice fail to survive past embryonic day 10.5 due to major defects in yolk sac erythropoiesis, a result that parallels Tal1-null mice<sup>133</sup>. While it does not bind DNA directly, LMO2 is considered a transcription factor that activates and represses target genes by binding with different protein complexes(reviewed in<sup>134,135</sup>).

Lmo proteins have been shown to cooperate with Tal1/Scl to accelerate leukemia in mice<sup>112,113</sup> and this cooperation is not dependent on the DNA-binding activity of Tal1<sup>112</sup>. The differentiation block seen in the bi-transgenic mice is more pronounced than with either oncogene alone, suggesting that Lmo1/2 help Tal1 sequester proteins from the promoter of genes critical in T-cell differentiation. Transgenic expression of Lmo2 alone in mice is also sufficient to initiate T-ALL at low penetrance and after long latency<sup>112,136</sup>. McCormack and colleagues also showed that forced Lmo2 expression early in the developing thymus results in aberrant self-renewal of thymocytes<sup>137</sup>, which could potentially explain the long latency found in the SCID-X1 patients and mouse models. The expression of LMO2 in these patients could allow the target cells time to accumulate secondary mutations in proliferation pathways, thus leading to leukemic transformation.

## Notch1 structure and signaling

Notch1 is a prominent oncogene in T-ALL, with activating mutations found in every subtype of patients analyzed<sup>138</sup>. Notch1 is a single pass transmembrane receptor first described in *Drosophila melanogaster* in 1917 when a heterozygous mutation resulted in a notched wing phenotype (Morgan 1917). Since then, countless experiments have been conducted in flies (*Drosophila melanogaster*), worms (*Caenorhabditis elegans*), and mammals to elucidate Notch1 structure and function. There are four Notch homologues in mammals, designated Notch1-4, and all have diverse functions in lineage commitment, developmental pathways, and human malignancies<sup>139–143</sup>.

Notch1 and Notch2 are broadly expressed throughout the body while Notch3 and Notch4 are more restricted. Notch1 is expressed in the brain, liver, bone marrow, heart, lung, thymus, kidney, stomach, intestine, eye, skeletal muscle, and spinal cord. Notch2 is expressed in the brain, kidney, liver and stomach. Notch3 expression is restricted to smooth muscle, central nervous system and hematopoietic cells while Notch4 is solely expressed in vascular endothelial cells. This varied expression pattern can control the temporal and spatial patterning of Notch1 signaling *in vivo* (reviewed in<sup>144</sup>).

Notch1-4 bind five different ligands that are most often expressed on adjacent cells: Jagged1 (Jag1), Jagged 2 (Jag2), and Delta-like 1,3,4 (Dll1,3,4)<sup>145–147</sup>. The ligands have a very similar structure to one another, with

Jag1 and Jag2 expressing an increased number of EGF repeats compared to the Dll ligands and also containing a cysteine-rich region that aids in protein interactions and signal transduction<sup>145</sup>.

The Notch receptors have two main functional domains: the extracellular (NEC) and transmembrane domains (NTM)<sup>148</sup>. The NEC domain contains EGF repeats and a negative regulatory region (NRR) for ligand recognition<sup>149</sup>. The NRR contains the heterodimerization domain (HD) and a series of Notch repeats. The NTM domain contains RAM and ankyrin repeat (ANK) domains for protein interactions<sup>150,151</sup>. Notch1 and Notch2 contain sizeable transactivation (TAD) domains, but these are much smaller and less important in Notch3 and Notch4<sup>152</sup>. All the Notch receptors also contain a PEST domain at the C-terminus of the NTM, which controls receptor turnover<sup>153</sup>.

Three cleavage events take place in order to release the Notch1 intracellular domain (ICD) that is capable of activating target genes (Figure 2). The first event takes place in the Golgi as the final step in the protein maturation process. A Furin protease cleaves the NEC from the NTM; these two domains will remain covalently linked as they make their way into the plasma membrane at the cell surface<sup>148</sup>. Upon ligand binding<sup>154–156</sup>, TACE, a member of the ADAM family of proteases, cleaves the NEC from the NTM at the HD region<sup>157</sup>. This then signals the gamma-secretase complex, which cleaves the NTM at Valine

1744, thus releasing the ICD from the membrane. The nuclear localization sequence (NLS) then allows translocation the ICD to the nucleus<sup>158</sup>.

The Notch1 ICD, also called ICN1, binds CSL (named for CBF1/RBPJ in mammals, Suppressor of Hairless in *D. melanogaster*, Lag1 in *C. elegans*) in the nucleus along with coactivators Mastermind-like 1 (MAML) and CBP/p300<sup>159–161</sup>. CSL is a transcriptional repressor that binds DNA at the consensus site TGGGAA almost constitutively<sup>162,163</sup>. When ICN1 is not present, CSL is bound with repressors such as KyoT2, CIR, N-Cor/SMRT, SKIP, Sin3A, SAP18, SAP30, RBAp46/48, or HDACs<sup>164–169</sup>. ICN1 displaces these repressors on its specific target genes such as Deltex1, Notch3, Nrarp, Prtcra, Cyclin D3, p21, c-Myc, CDK4/6 and CD25 and activates their transcription<sup>110,170–172</sup>. Recent structural evidence has shown that Notch1 must dimerize at the promoter of some of its target genes critical for T-cell development and leukemogenesis, such as Pre-Tα and c-Myc, but not others, such as Hey1 and CD25<sup>173</sup>. This indicates that Notch1 transcriptional activation is more complex than previously thought, and could reveal another layer of transcriptional regulation.

### **Regulation of Notch1 signaling**

Because of their role in so many critical developmental processes, tight regulation of the Notch receptors is required for the control of apoptosis, proliferation, differentiation, and self-renewal. This is accomplished by a few different mechanisms and can be cell-type specific. The Fringe family of

enzymes (Lunatic, Manic, and Radical) modifies the EGF repeats on the Notch receptors, which result in changes in ligand binding specificity<sup>174,175</sup>. In general these modifications result in increased interactions with Dll ligands and decreased affinity for Jag ligands<sup>176</sup>. Depending on the cell type and availability of ligands, these modifications could increase or decrease Notch signaling.

The regulation of Notch protein stability is an additional way cells control the amount of Notch signaling at any given time. This is accomplished by three main proteins: Itch, Numb, and Fbxw7. Itch is an E3 ligase of the HECT family that targets Notch proteins for degradation by the lysosome<sup>177–179</sup> and Numb is a protein that negatively regulates Notch by recruiting ubiquitination machinery such as Itch to the Notch1 receptor<sup>180</sup>.

Fbw7 (also called Fbxw7, Sel-10, or hCdc4) controls Notch1 protein stability by degrading Notch through the ubiquitination-proteasome pathway<sup>181–184</sup>. Fbw7 is a member of the Skip-Cullin-Fbox (SCF) degradation complex, an E3 ubiquitin ligase complex that targets the protein for degradation in the proteasome<sup>185</sup>. The CyclinC/CDK8 complex is recruited by MAML and phosphorylates Notch1 in the TAD and PEST domains. Fbw7 then binds the phosphorylated residues in the PEST domain, targeting it for degradation<sup>186</sup>. Fbw7 and the SCF complex also target other proteins such as Cyclin E, c-Myc, c-Jun, and mTOR for degradation<sup>187–190</sup>. Fbw7 often undergoes inactivating

mutations in T-ALL that results in increased stability of these oncogenes, underscoring the importance of Fbw7 in controlling cell growth.

### **Notch1 signaling in development**

Notch receptor signaling is critical for many developmental pathways, as demonstrated by the embryonic lethality of Notch1 and Notch2 knockout mice, which die by embryonic day 11.5<sup>191,192</sup>. Ligands Dll1, Dll4, and Jag1 are also critical for development, as knockout mice die from embryonic day 9.5-12.5 from various defects<sup>193,194</sup>. Notch3 and Notch4 are less crucial for developmental processes as whole body knockout mice are viable, however they do often present with vascular defects<sup>195</sup>. In humans, Alagille Syndrome is characterized by a JAG1 deletion. Patients with this syndrome present with liver, heart, eye, bone, and kidney defects, pointing to the broad role of NOTCH signaling in human development<sup>196,197</sup>. There is also a stroke disorder called CADASIL (cerebral autosomal dominant arteriopathy with subcortical infarcts and leukoencephalopathy) that is characterized by mutations in the Notch3 gene<sup>198</sup>.

Notch1 signaling is required for the successful commitment of several different lineages in mammals. In skin, Notch1 is involved in follicle development by maintaining the epithelial stem cells and is thought to maintain pigment cells. There has also been a role reported for activated Notch1 in the pathogenesis of melanoma (reviewed in<sup>199</sup>). In contrast, loss of CSL or Notch1 results in hyperkeratinization of the epidermis and squamous cell carcinoma. Because



Notch1 can act as both an oncogene and a tumor suppressor in the skin (reviewed in<sup>200</sup>), this points to an important role for Notch signaling in maintaining the balance of specialized cells in the skin<sup>201–203</sup>. In the vasculature, Notch1 signaling pushes vascular endothelial cells towards an arterial fate instead of a venous one. In animals where Notch1 signaling has been perturbed, there is often an imbalance in arteries and veins resulting in severe vascular defects<sup>195,204,205</sup>. Finally, in the intestine, Notch1 signaling controls the balance of absorptive enterocytes and secretory goblet cells. Notch1 signaling promotes the formation of enterocytes at the expense of goblet cells and Notch1 inhibition through use of gamma-secretase inhibitors switches this fate to an increase in goblet cells. This results in gastrointestinal toxicity due to excessive mucus secretion and lack of nutrient absorption<sup>206–208</sup>.

In lymphopoiesis, Notch1 is required for the specification of the T-cell lineage over the B-cell lineage. Conditional Notch1 knockout mice have a decrease in overall T-cells and a huge increase in B-cells while Notch1 overexpression models show the opposite phenotype<sup>49,209,210</sup>. Ligands Jag1, Jag2, Dll1, Dll3, and Dll4 are expressed on thymic epithelial cells as well as the bone marrow stroma, facilitating the Notch1 signaling cascade<sup>27,140,144,211–213</sup>. Notch1 is especially critical at specifying T-cell lineage commitment at the DN1 stage of development. At this stage, DN1 cells can still become B-cells if Notch1 signaling does not promote T-cell differentiation<sup>41,43,171,214</sup>. Notch1 signaling is required through T-cell development up through the DN3 stage at which point it is

downregulated. Conditional knockout mice showed a developmental block at the DN3 stage and defects in TCR signaling, pointing to a critical role of Notch1 at this particular stage in development<sup>210,215</sup>.

Self-renewal of stem cells is critical for maintaining adult tissues and emerging evidence suggest a role for self-renewal in malignancy. Stem cells are defined as cells that have the ability to generate an unlimited amount of daughter stem cells (self-renewal) and still are able to expand and differentiate into a desired tissue(reviewed in<sup>216,217</sup>). Notch1 signaling is required for the maintenance of several types of adult tissue stem cells from neuronal to endothelial to mammary and intestinal lineages<sup>206,218–222</sup>. In the neuronal stem cell (NSC), Notch signaling is required for the maintaining stem cell numbers, as evidenced by knockout mice that displayed a decreased number of NSCs<sup>221,222</sup>. Similarly, in the intestine, loss of CSL confers a decrease in intestinal stem cell number while forced expression of Notch1 results in stem cell hyperplasia<sup>206</sup>.

The role of Notch1 signaling in HSCs is a current topic of debate. It is clear that Notch1 is required for generation of HSCs in the embryo, but it is less clear whether Notch1 is required for the maintenance of HSC self-renewal in the adult<sup>223</sup>. Increasing Notch1 signaling results in a block in differentiation consistent with an increase in HSCs and increased HSC self renewal *ex vivo*<sup>224–226</sup>. However, loss of Notch1 signaling either by dominant negative (DN)-MAML or genetic deletion of Jag1 or Notch1 itself has no effect on HSC self-

renewal<sup>227,228</sup>. A recent report of *Itch*<sup>-/-</sup> mice implicates *Itch* in the negative regulation of HSCs. *Itch*<sup>-/-</sup> mice harbored HSCs with increased proliferative capacity coordinate with increased Notch1 signaling, but retained self-renewal capabilities<sup>229</sup>. This suggests that Notch1 plays a role in maintaining the number of HSCs in the bone marrow, but does not alter the self-renewal capacity of the cells. Another report suggests that Notch2 is in control of HSC homeostasis, but neither Notch2 nor Notch1 have any role in HSC self-renewal once homeostasis is reached<sup>230</sup>. Overall, there is still controversy surrounding the exact role of Notch1 in hematopoiesis, but these data along with the requirement for Notch1 signaling in the development of T-cells, marginal zone B-cells, and megakaryocytes (reviewed in<sup>171</sup>) could indicate that Notch1 signaling only plays a role in promoting the differentiation and proliferation of the HSCs.

### **Notch1 is a prominent oncogene in T-ALL**

The NOTCH1 pathway is upregulated in approximately 70% of T-ALL patients either by activating mutations in the NOTCH1 receptor itself (50%) or by inactivating mutations in the negative regulator FBW7 (20%)<sup>71,74,231–233</sup>. *NOTCH1* was discovered as an oncogene in T-ALL when the t(7;9)(q34;q34.3) translocation was mapped. This translocation is very rare in T-ALL and the subtype only accounts for 1% of T-ALL cases. The translocation puts *NOTCH1* into the *TCR* locus resulting in a truncated NOTCH1 protein with the strong TCR enhancer<sup>234</sup>. This allele, sometimes called the *TAN1* allele, has been shown to

transform cells *in vitro* and also results in a T-ALL disease *in vivo* when transduced into adult bone marrow<sup>235–237</sup>. It has been shown that the ANK, TAD, and NLS are all required for this transformation event<sup>163,238</sup>.

Most of the NOTCH1 mutations found in T-ALL patient samples have been mapped to either the HD or PEST regions of the receptor. HD mutations result in ligand-independent cleavage of the receptor while PEST mutations result in increased ICN1 protein stability<sup>138,182,239</sup>. These mutations can occur together in the same patient either on the same or separate alleles. When these two mutations occur on the same allele, a 10-fold increase in NOTCH1 reporter activity has been observed<sup>138</sup>. A 5' deletion event that mimics an HD mutation was reported in one patient sample (1/69), but it is unclear how common these events are in the human disease<sup>240</sup>. In a small subset of patients with mutant NOTCH1 (3%), a tandem duplication of the JME region occurs resulting in ligand independent activation<sup>241</sup>. These NOTCH1 alleles found in patients have not been shown to be transforming on their own in mouse models and are not as strong as the ICD resulting from the TAN allele. However, these alleles have been shown to cooperate and accelerate disease in a model of K-Ras induced T-ALL<sup>242</sup>. This implies that while NOTCH1 mutations are prevalent in T-ALL patients, these mutations are rarely initiating events; additional mutations must occur before a cell is fully transformed.

NOTCH2 mutations have not been found in patient samples, but alleles have been found that are able to transform immortalized rat kidney cells<sup>235</sup>. NOTCH2 has the potential to be oncogenic, but appears to be irrelevant in terms of human T-ALL. NOTCH3, however, has been shown to be mutated in a subset of relapsed T-ALL patients<sup>243</sup>. This oncogenicity has been confirmed in a mouse model as well where Notch3 was overexpressed in murine bone marrow and resulted in a T-ALL like disease<sup>244</sup>.

Activating Notch1 mutations have also been found in several mouse models of T-ALL<sup>113,245–248</sup>. In the *Lck-Ta11* model, Notch1 mutations were found in 74% of the leukemias examined. Most of these mutations (91.5%) were found in the PEST domain while HD mutations were quite rare (8.5%)<sup>248</sup>. In this same model, however, many T-ALLs have upstream intragenic deletions in the *Notch1* locus that essentially mimicked the HD mutations found in patient samples<sup>(249</sup> and Chapter III). So while murine leukemias do not often harbor HD mutations for ligand-independent Notch1 cleavage, they have adapted a unique mutation event to end at the same result<sup>250</sup>. In the *Lck-Ta11/Lmo2* and the *pSil-TSCL/Lck-LMO1* mouse models of T-ALL, Notch1 mutations were also found in preleukemic thymi, confirming that Notch1 mutations are a critical transforming feature of murine T-ALL<sup>113,251</sup>. The *Lck-Ta11* T-ALLs were sequenced for mutations in the other 3 Notch receptors, but no mutations were found, solidifying a unique role for Notch1 in the pathogenesis of T-ALL<sup>248</sup>.

### GSI as an anti-leukemic agent

The gamma-secretase ( $\gamma$ -secretase) complex initiates the final cleavage event that releases the NICD from the cell membrane so that it is able to translocate to the nucleus and activate target genes (Figure 2). The complex is composed of four essential proteins: nicastrin, presenilin, APH-1, and PEN-2<sup>158,252–254</sup>. Notch1 is not the only substrate of the  $\gamma$ -secretase complex; it also cleaves Notch1 ligands, ErbB4, CD44, growth hormone receptor, N-cadherin, E-cadherin, and amyloid precursor protein<sup>255–258</sup>. In T-ALL, administration of  $\gamma$ -secretase inhibitors (GSIs) to murine cell lines results in a G1 cell cycle arrest and apoptosis<sup>110,246</sup>. Human cell lines are not as sensitive, but most do achieve the G1 cell cycle arrest after extended treatment<sup>172,259,260</sup>. Treatment of moribund mice with GSIs significantly extended survival<sup>261</sup> and GSIs have been shown to decrease disease initiation *in vivo* when cells were pretreated with GSI *in vitro*<sup>251,262</sup>.

GSI treatment of T-ALL cell lines and primary mouse tumors results in decreased Notch1 expression and decreased expression of known Notch1 target genes<sup>110,251,261</sup>. This effect is very similar to that of overexpression of DN-MAML<sup>263</sup>. In T-ALL, forced Notch1 expression is sufficient to rescue the cell cycle arrest observed with GSI treatment, suggesting that the other substrates of the  $\gamma$ -secretase complex are not significantly affected by GSI in this cell type<sup>110</sup>. c-Myc will also rescue the phenotype<sup>110,172,259</sup>, but other Notch1 target genes such as

Hes1 and Hes5 have no effect<sup>263</sup>. Partial rescue of the GSI phenotype was seen with forced expression of Cyclin D3 and CDK4/6, which was probably not complete due to upregulation of CDK inhibitors such as p27 upon GSI treatment<sup>170</sup>.

Other methods to inhibit Notch1 and/or NICD are being investigated, but none have been entirely effective (reviewed in<sup>264</sup>). Monoclonal antibodies against human NOTCH1 have made it to clinical trials, but other ideas such as DN-MAML mimics<sup>265,266</sup> and ADAM protease inhibitors<sup>267</sup> have not. Unfortunately, GSIs have not been very successful in the clinic due to on-target gastrointestinal toxicity. Because of the critical expression of Notch1 in the intestinal enterocytes, GSIs force a lineage switch to goblet cells and this causes massive diarrhea in patients accompanied by temporary hair loss and hair pigment loss<sup>208,268</sup>. These trials used a continuous administration of GSI. It has recently been shown that an intermittent dosing regimen may decrease gastrointestinal toxicity while not compromising efficacy<sup>261</sup>. Clinical trials with this dosing regimen have been completed in breast cancer and melanoma, but results have not yet been released<sup>269,270</sup>. It is also possible that administration of glucocorticoids along with the GSI will help abate these side effects with an added bonus of the steroids having intrinsic anti-leukemic activity<sup>208</sup>. Bristol-Myers-Squibb have begun a clinical trial with a GSI-dexamethasone combination for the treatment of T-ALL<sup>271</sup>.

### **c-Myc expression is oncogenic in T-ALL**

c-Myc is a direct transcriptional target of Notch1, as shown through GSI rescue experiments, chromatin immunoprecipitation (ChIP), and gene expression arrays<sup>110,172,259</sup>. Forced expression of c-Myc rescues the G1 arrest and apoptosis phenotype caused by GSI treatment in both human and mouse T-ALL cell lines. Both human and mouse T-ALL cell lines often have deletions or epigenetic modifications in the p53 and/or Ink4Arf loci, thus counteracting the overexpression of c-Myc<sup>71,111,272</sup>. Rescue does not occur in 100% of lines (8/10 mouse lines, 3/5 human lines)<sup>110</sup>, however, indicating that while c-Myc is important to Notch1-induced T-ALL, it is not the only critical target gene for the pathogenesis of the disease.

c-Myc is an immediate early response gene for many ligands and cellular processes including Notch1, Wnt, and many receptor tyrosine kinases<sup>110,172,259,273–276</sup>. The gene was first discovered by a translocation event in Burkitt's lymphoma, t(8;14), which juxtaposes the c-MYC locus and the IgH enhancer, driving its overexpression in B-cells<sup>277–279</sup>. c-Myc is also the cellular homologue of the v-myc oncogene in the avian myelocytoma virus MC29, which causes leukemia and sarcoma in chickens<sup>280,281</sup>.

Overexpression or deregulation of c-Myc is found in approximately 70% of human cancers. In addition to Burkitt's lymphoma, c-Myc is implicated in the pathogenesis of multiple myeloma, colon, breast, and mast cell tumors (reviewed



in<sup>282</sup>). In multiple myeloma, c-Myc activation is accomplished by translocations into the IgH, IgL, and Igk loci or by amplification events<sup>283</sup>. In other cancers, c-Myc expression is upregulated by driving oncogenic activation of the Wnt-APC pathway in colon cancer<sup>276</sup> or the Notch1 pathway in T-ALL<sup>110,172,259</sup>. Ectopic expression of c-Myc can transform mouse embryonic fibroblasts in conjunction with additional oncogenes<sup>284</sup> and forced c-Myc expression in transgenic mice results in a variety of malignancies<sup>285–287</sup>. In most mouse models, however, secondary events are required for malignancy, as mice present with disease after a long latency<sup>288–290</sup>.

### **c-Myc structure and regulation**

c-Myc is a basic-helix-loop-helix leucine zipper (bHLH-Zip) transcription factor which binds E-box sequences as a dimer with the bHLH-Zip transcription factor Max<sup>291–295</sup>. In normal cells, c-Myc promotes cell cycle progression and contributes to growth-related pathways such as ribosome biogenesis, nucleotide metabolism, DNA replication, and RNA processing (reviewed in<sup>282</sup>). c-Myc mostly activates target genes at the transcriptional level, however it can also modulate protein expression by activating oncogenic miRNAs such as miR-17-92 cluster, and inhibiting tumor suppressor miRNAs, such as let-7<sup>296–298</sup>. It is also thought that c-Myc has a non-transcriptional role in cap-dependent translation, although this is not entirely understood<sup>299,300</sup>. Finally, c-Myc can act as a transcriptional repressor. Although the precise mechanism and conditions under which this

occurs is not clear, it is thought that c-Myc binds to Miz-1 to inhibit a subset of target genes<sup>275,301</sup>.

Because of its critical role in many growth pathways, c-Myc is normally under tight regulation to prevent overgrowth of cells and development of cancer. When c-Myc is overexpressed, cells undergo apoptosis through the p53-ARF pathway<sup>302,303</sup> and through p53-independent mechanisms<sup>304,305</sup>. c-Myc expression is activated at the transcriptional level, and in some cases is regulated at the transcriptional level<sup>306</sup>. Secondary DNA structures can slow down the transcription of c-Myc mRNA and the binding of bromodomain proteins, such as Brd4, to activated histones can increase transcriptional elongation by recruiting Pol II, Mediator, and additional factors. In the absence of Brd4, transcription at the c-Myc promoter is drastically decreased<sup>307,308</sup>. c-Myc expression is controlled at the protein level by having a very short half-life of 15-20 minutes<sup>309,310</sup>. c-Myc is phosphorylated at Ser62 and Thr58, often by GSK3 $\beta$ , which recruits the E3 ligase Fbw7 and targets the protein for degradation in the proteasome<sup>311,312</sup>. In malignancy, many tumors have adapted ways to decrease either or both of these steps to ensure that c-Myc protein levels remain high in tumor cells and maintain a rapid growth program.

### **c-Myc controls proliferation of hematopoietic stem cells**

In adult hematopoietic stem cells, c-Myc is required for commitment to terminal differentiation but not self-renewal of the stem cells. Loss or reduction of

c-Myc results in an accumulation of the HSC pool while overexpressing c-Myc results in a decrease in HSCs<sup>313</sup>. Consistent with this, when c-Myc expression is reduced, there is a decrease in differentiated cells from the lymphoid and myeloid lineages and an accumulation of p21, a cell cycle inhibitor. Therefore, c-Myc is required for pushing HSCs into the cell cycle in order to promote the formation of differentiated blood lineages<sup>314</sup>. This balance is controlled by the Fbw7-targeted degradation of c-Myc; Fbw7-null HSCs mimic the phenotype of c-Myc overexpression<sup>315,316</sup>.

c-Myc also mediates the release of HSCs from the hematopoietic niche in the bone marrow, which helps them to mobilize and differentiate. When c-Myc protein levels were decreased in the bone marrow of mice, increased expression of N-cadherin, a cell surface adhesion molecule, correlated with the HSC accumulation<sup>314</sup>. Recently, it was shown that c-Myc plays a similar role in the CML L-IC. Increased c-Myc resulted in the switch from quiescence to proliferation in the L-IC population and sensitized cells to Imatinib treatment<sup>317,318</sup>. Likewise, in T-cell development, c-Myc is required for the proliferative burst in DN3/DN4 cells before the DP stage in development, but not for the self-renewal of these cells<sup>319</sup>.

### **The c-Myc transcriptional signature**

Many high-throughput technologies have been used to try and define a specific c-Myc signature, but none have truly succeeded. One group defined a

Myc-dependent serum response (MDSR)<sup>320</sup> list that contained genes involved in growth pathways while other groups have shown a Myc core signature (MCS)<sup>321</sup> of 50 genes induced by c-Myc, with the most prominent pathway involved being ribosome biogenesis. Interestingly, the MCS is cell-type specific. Whole genome analysis revealed that the c-Myc preferred E-box 5'-CACGTG-3' is the most frequent DNA-binding motif in the entire human genome<sup>322</sup>. It is estimated that at any given time, 15% of the genome is occupied by the c-Myc transcription factor<sup>323</sup>.

Because there seems to be no definitive c-Myc signature and so much of the genome is transcribed by c-Myc, researchers hypothesized that c-Myc could be a universal transcriptional amplifier and not necessarily a specific transcription factor. c-Myc has also been shown to recruit p-TEFb, a transcriptional elongation factor, to active promoters and initiate Pol II pause release, which contributes to this theory<sup>324</sup>. Recently, using ChIP-seq to c-Myc and Pol II, mRNA quantification, and analysis of active histone marks, two independent groups found that c-Myc is indeed a transcriptional amplifier in many cell types, including T-cells<sup>325,326</sup>. c-Myc overexpression leads to overall increased levels of mRNA in cells and amplifies the existing transcriptional programs of each given cell type. It still seems as though c-Myc regulates proliferation and overall biomass accumulation in a cell-dependent manner, i.e. when expressed in T-cells, c-Myc will amplify T-cell genes to promote proliferation<sup>321</sup>.

### **c-Myc as a target for therapeutics**

While many tumors use c-Myc expression to promote proliferation and cell growth, not all of these tumors are addicted to c-Myc. In a normal, non-Myc addicted cell, c-Myc inhibition causes the cell to retreat to the G1 phase of the cell cycle<sup>327</sup>. In general, these cells will not die due to withdrawal of c-Myc. In a cell where c-Myc is overexpressed by translocations, amplifications, or additional oncogenes, cells often undergo apoptosis upon c-Myc withdrawal<sup>328,329</sup>. Tumors will often regress after c-Myc withdrawal, some to the point of cure even after brief withdrawal periods<sup>330</sup>. When this happens, tumors are said to be addicted to c-Myc. This addiction allows for a therapeutic window where normal cells should not be affected by c-Myc inhibition.

The fact that c-Myc is aberrantly expressed in approximately 70% of human cancers coupled with this recent data demonstrating that c-Myc is a universal amplifier makes c-Myc a very desirable target as a cancer therapeutic. In theory, if one could fully inhibit c-Myc in a tumor, it is possible that this would also inhibit other active oncogenic pathways by reducing the total mRNA of targets within those other pathways. Inhibition of BET bromodomain proteins, which activate c-Myc expression<sup>307,308</sup>, has been successful at inhibiting c-Myc transcription in murine models of multiple myeloma<sup>307</sup> and AML<sup>331</sup> as well as cell lines derived from human hematopoietic malignancies. There have also been attempts at developing small molecules to inhibit Myc-Max interactions, but these

have not as been successfully tested in *in vivo* models of disease<sup>332,333</sup>. Researchers are also screening drugs that target known Myc target genes as well as synthetic lethal genes<sup>334,335</sup>. Inhibiting c-Myc in human cancers may result in decreased tumor burden, but it remains to be seen if these therapeutics could eradicate disease by inhibiting the initiating cells.

### **Leukemia-initiating cells often follow a cancer stem cell, hierarchical model**

Leukemia-Initiating cells (L-ICs) are thought to facilitate relapse in multiple malignancies, including T-cell acute lymphoblastic leukemia (T-ALL)<sup>113,251,336,337</sup>. L-ICs are a rare population of leukemic cells that possess the ability to initiate disease in recipient mice, differentiate, and self-renew. These cells are thought to be resistant to conventional therapies and therefore able to repopulate disease once treatment is ceased, mediating relapse. In hematopoietic malignancies, the L-IC is often found to be a phenotypically immature cell such as a stem cell or a transformed progenitor cell(reviewed in<sup>217</sup>). There is still controversy in the field as to whether an L-IC could arise from a more mature cell, and there are cases of initiating activity found throughout the developmental hierarchy, such as in melanoma and B-ALL. A summary of the controversy in the field is highlighted in different models for tumor/leukemia heterogeneity (Figure 3).

Pathways that drive L-IC proliferation, survival, and maintenance are likely similar to those that drive the differentiated leukemia, as many models suggest that leukemia arises from a small pool of L-ICs. Evidence also suggests that

pathways critical for stem cell maintenance may be involved in L-IC survival and self-renewal(reviewed in<sup>338</sup>). Levels of Pten expression have been shown to maintain the balance between normal stem cells and leukemia-stem cells (LSC), thus implicating PI3K/Akt/mTOR signaling in LSC survival and proliferation<sup>339,340</sup>. Aberrant expression of HSC genes such as Lmo2 in T-ALL<sup>137</sup> and upregulation of Wnt signaling in CML have also been implicated in L-IC generation and self-renewal<sup>341</sup>. In general, an L-IC must have genetic mutations in at least one set of genes that deregulate/block differentiation and in another pathway that promotes rapid proliferation of the cells.

L-ICs were first described in AML as a population of patient cells able to initiate disease in non-obese diabetic/severe combined immunodeficient (NOD/SCID or NS) mice. This L-IC population expresses CD34 on the surface of cells, but not CD38, a phenotype very similar to normal HSCs<sup>342–344</sup>. Most subtypes of AML are organized in a hierarchical manner, like normal hematopoiesis, with the initiating mutation(s) occurring in the HSC. The inherent capacity of self-renewal found in the HSC is very important because it results in the long-term persistence of the stem cell, allowing the accumulation of multiple mutations in oncogenes and tumor suppressors that can eventually lead to malignancy(reviewed in<sup>345</sup>).

Recently, there has been increasing evidence that L-ICs can also arise from committed progenitor populations. Mouse models of AML have shown that

expression of fusion proteins such as MLL-ENL<sup>346</sup>, MLL-GAS7<sup>347</sup>, MLL-AF9<sup>348,349</sup>, MOZ-TIF2<sup>350</sup>, and Cbf $\beta$ -SMMHC<sup>351</sup> are able to transform progenitor cells with little or no inherent self-renewal capabilities. Similar to these AML subtypes, CML L-ICs also originate in a progenitor population<sup>352,353</sup>. In both mouse models and patient samples, granulocyte-macrophage progenitors (GMPs) gain the ability to self renew by activation of the  $\beta$ -catenin pathway through mutation of its negative regulator Gsk3 $\beta$ <sup>341</sup>. Progenitor populations have vast proliferative capabilities, as well as the ability to differentiate, but must somehow acquire the ability to self renew through transforming mutations if they are to become successful L-ICs. Identifying these mutations that confer self-renewal properties may be one way to target the L-ICs in human malignancy.

Murine T-ALL L-ICs arise from a committed thymic progenitor, in a subset of the DN3/4 stage of thymocyte development<sup>113,251</sup>. In xenotransplantation assays, functional activity of T-ALL patient samples has also been analyzed. An immature progenitor population defined by surface markers was found to be capable of initiating disease in immunodeficient, NOD/SCID/IL2 $\gamma^{-/-}$  (NSG) mice. Researchers sorted CD34<sup>+</sup> (found on HSCs) and CD7<sup>+</sup> (a human marker for immature T-cells) cells and found that these cells were enriched in disease initiating activity compared to their CD7<sup>-</sup> or CD34<sup>-</sup>negative counterparts<sup>354</sup>. The NOTCH1 pathway, active in T-cell progenitors, was also shown to be involved in human T-ALL initiation in NSG mice<sup>262,355</sup>. It is possible for T-ALL to initiate in the bone marrow in cases of murine retroviral infection models<sup>238,242,356</sup>, but it is not



entirely clear if bone marrow derived progenitors or stem cells are capable of being transformed into T-ALL L-ICs in the human disease.

Aside from self-renewal, an L-IC must adapt additional qualities of normal stem cells in order to remain active long-term and evade current anti-leukemia treatments. While not shown for all hematopoietic malignancies, it is thought that L-ICs are able to enter a state of quiescence in order to escape chemotherapies that target rapidly dividing cells, a common behavior of normal stem cells<sup>357–359</sup>. A quiescent L-IC population has been described in AML using mouse models<sup>360,361</sup> and clonal tracking techniques<sup>342</sup>. A correlation between slow-cycling cells and tumor-initiating cells (T-ICs) was also found in solid tumors such as colon<sup>362</sup> and breast cancers<sup>363</sup>. Normal stem cells are able to exit quiescence<sup>357,359,361,364,365</sup>, and so it is thought that this exit may be a major mediator of relapse, especially because relapse can often occur years or even decades after initial treatment ceases<sup>366,367</sup>. Pushing quiescent L-ICs into cycle may be a viable treatment method to induce L-IC exhaustion and make cells more responsive to traditional chemotherapy, thus preventing disease relapse<sup>361,364</sup>.

Initiating cells in both leukemia and solid tumors have been shown to have intrinsic resistance to chemotherapy and radiation. In CML patients where disease was driven by BCR-ABL, L-ICs were found to be resistant to tyrosine kinase inhibitors such as imatinib while the bulk leukemia cells remained

sensitive to the drug<sup>368–373</sup>. In breast cancer, T-ICs were enriched in patients after cytotoxic chemotherapy<sup>374</sup>. The mechanism for this resistance could be linked to quiescence (as explained above), or could be due to increased expression of multi-drug resistance (MDR) transporters or other intracellular factors<sup>375</sup>. In AML, L-ICs and surrounding stromal cells were found to overexpress anti-apoptotic genes such as Bcl-XL and Bcl-2 to counteract cell death triggered by chemotherapy and radiation<sup>376,377</sup>. In solid tumors, CD133-positive gliomas express proteins to counteract DNA damaging agents<sup>378</sup> and breast cancers express free radical scavengers<sup>379</sup>. Preleukemic thymocytes overexpressing Lmo2 showed increased resistance to radiation<sup>137</sup>, but the mechanism is currently unknown. The fact that these mechanisms exist highlights the need for specific anti-L-IC therapies not based on targeting rapidly dividing cells.

### **Alternative models of cancer heterogeneity**

Contrary to the idea of a hierarchical organization of leukemia/cancer, B-cell acute lymphoblastic leukemia (B-ALL) is thought to undergo clonal evolution (reviewed in<sup>338</sup>). This model of malignancy takes place in situations where a tumor/leukemia has a high amount of genetic heterogeneity (Figure 3A). B-ALL has been profiled using copy number abnormality (CNA) analysis<sup>380,381</sup> and in situ hybridization<sup>382</sup> to find that there are many subclones in any given patient and each of these subclones has a different functional capability to transplant the leukemia in xenograft models.

One major difference between the hierarchical model (Figure 3B) and the clonal evolution model (Figure 3A) is the presence of epigenetic versus genetic heterogeneity. In the cancer stem model, heterogeneity in the tumor/leukemia is most often attained by differentiation of the tumor/leukemia to a cell type where disease-initiating capabilities are not possible. This is often achieved by epigenetic changes in the individual cells causing irreversible changes in gene expression profiles<sup>383</sup>. In contrast, in the clonal evolution model of tumorigenesis, the functional heterogeneity of each clone is achieved by individual oncogenic events (reviewed in<sup>384</sup>). There is likely epigenetic heterogeneity in addition to genetic mutations in the clonal evolution model. Because epigenetic changes can be transient and reversible, tumors with this type of heterogeneity may be difficult to target therapeutically.

One last model of cancer heterogeneity has been described. In this model, tumor microenvironment and available ligands dictate the ability of any given cell to initiate a tumor. This model is most often found in solid tumors, which differ from leukemias that tend to be systemic and therefore not entirely dependent on any given niche. In this model, any cell can be a disease-initiating cell if it is in the proper location. This functionality is very plastic and reversible; as a cell moves from one ligand source, its prominent gene expression profile changes to reflect the new microenvironment<sup>385,386</sup>.

Clonal evolution may take place in T-ALL even though there is evidence of a functional L-IC hierarchy in the disease(reviewed in<sup>338</sup>). It is entirely possible for a single leukemia to inherit heterogeneity from multiple sources: developmental hierarchy, epigenetic changes, genetic mutations, and effects of a particular niche. Recent evidence suggests that there are multiple clones within T-ALL patient samples that have varying functional capabilities. The most aggressive of these clones manifest in relapsed patient samples and can be mapped back to the diagnostic sample<sup>336</sup>. In cases like this, a different approach towards therapy and relapse must be used, as targeting one leukemia-initiating clone may leave others untouched and therefore in a prime position to mediate relapse. Clonal evolution also takes place in pancreatic cancer and is thought to be one of the reasons why the disease has such a low survival rate even after treatment<sup>387</sup>.

### **Methods for assaying cancer stem cells**

Recently, lineage tracing has been used to define and characterize T-ICs in solid tumors<sup>388–390</sup> but prior to this, the main assay for determining L-IC frequency was through transplantation. With this method, tumor or leukemia cells are taken from the original source, made into a single cell suspension, and transplanted into histocompatible hosts in limiting dilution. This artificial system has been used to determine T-IC/L-IC frequency and functional populations in these malignancies for decades(reviewed in<sup>217</sup>). Gene expression profiling has identified SLAM family genes enriched in HSCs, and then these receptors were

functionally confirmed with *in vivo* transplantation assays<sup>35</sup>. In other cases, specific developmental surface markers have enriched for a T-IC/L-IC population. Recently, less biased methods such as lineage tracing and clonal tracking have been used to determine the identity and function of normal and malignant stem cells without having to use transplantation methods<sup>388–390</sup>.

Therapeutic strategies to target the L-IC have been an interest to the field since their discovery. In AML, the adhesion molecule CD44 was targeted with monoclonal antibodies, which resulted in oxidative stress followed by terminal differentiation of the AML<sup>391</sup>. This terminal differentiation resulted in ablation of the LSC population from patient samples<sup>392</sup>. Similarly, in acute promyelocytic leukemia (APL), an AML subtype, terminal differentiation by use of all trans retinoic acid (ATRA) has been successful in patients<sup>393</sup>. Because T-ALL does not have the features of a normal HSC and is often composed of cells at various stages of differentiation, specific oncogenic pathways will need to be targeted in lieu of inducing differentiation in the cells.

In this thesis, I will focus on defining and targeting the L-ICs in the *Lck-Tal1/Lmo2* mouse model of T-ALL. I will discuss transplant comparisons in a mouse model of T-ALL to validate our current L-IC assay. Using this assay, I will present data where we have successfully targeted the L-IC in this mouse model using shRNA and therapeutic approaches to inhibit Notch1 and c-Myc.

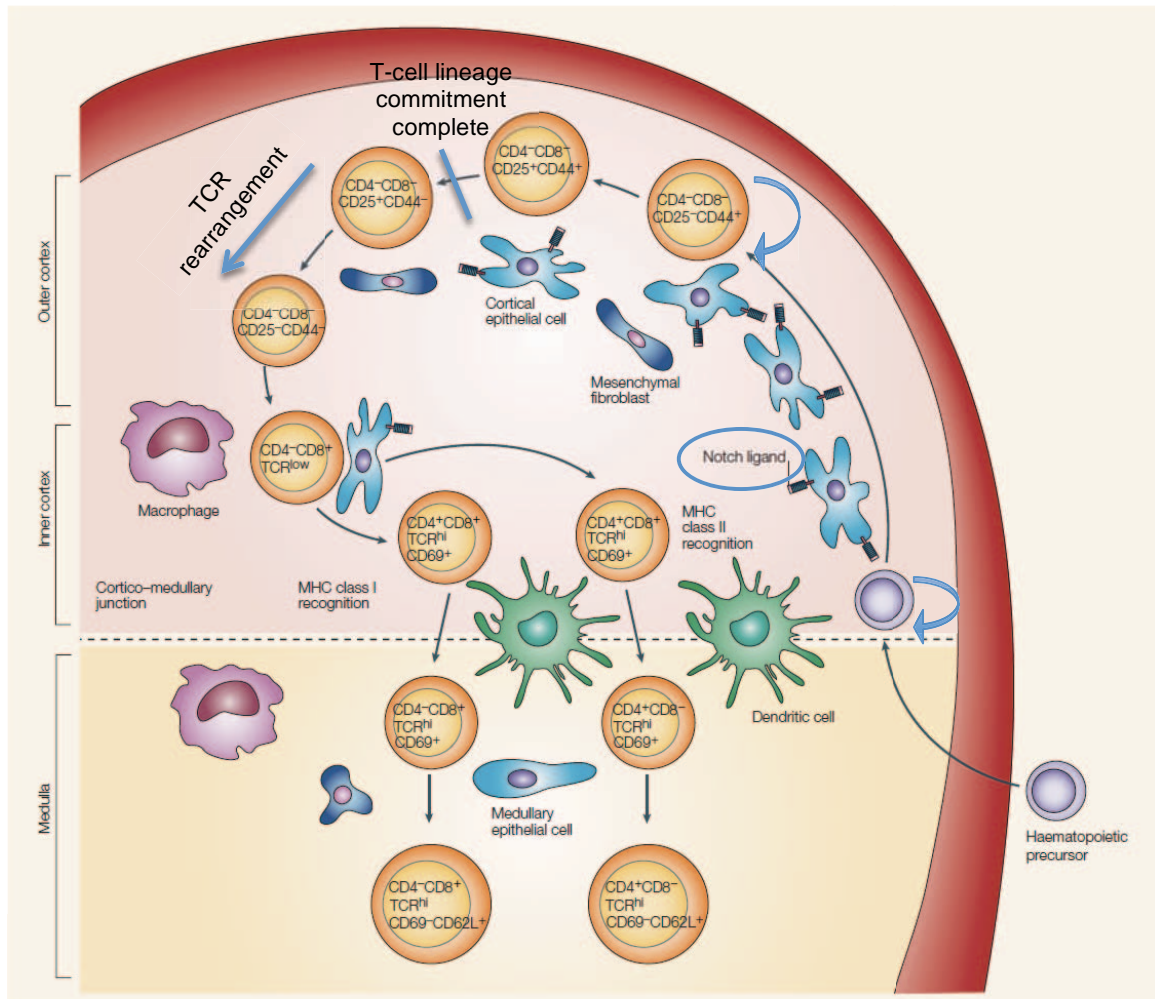


**Figure 1. Thymocyte development.** Thymocyte precursors are imported from the bone marrow. Upon entering the thymus and encountering Notch1 ligands, cells enter a series of discrete differentiation steps. Cells travel through the thymus and interact with the microenvironment as they differentiate and change their surface expression profile. They start by going through the four DN stages, then to the DP stage and finally reaching the CD4 or CD8 single-positive stages. At the end of the differentiation process, cells egress into the circulation and execute adaptive immune responses. (Adapted from: Zuniga Pflucker, JC. 2004. *Nature Reviews Immunology* 4, 67-72)

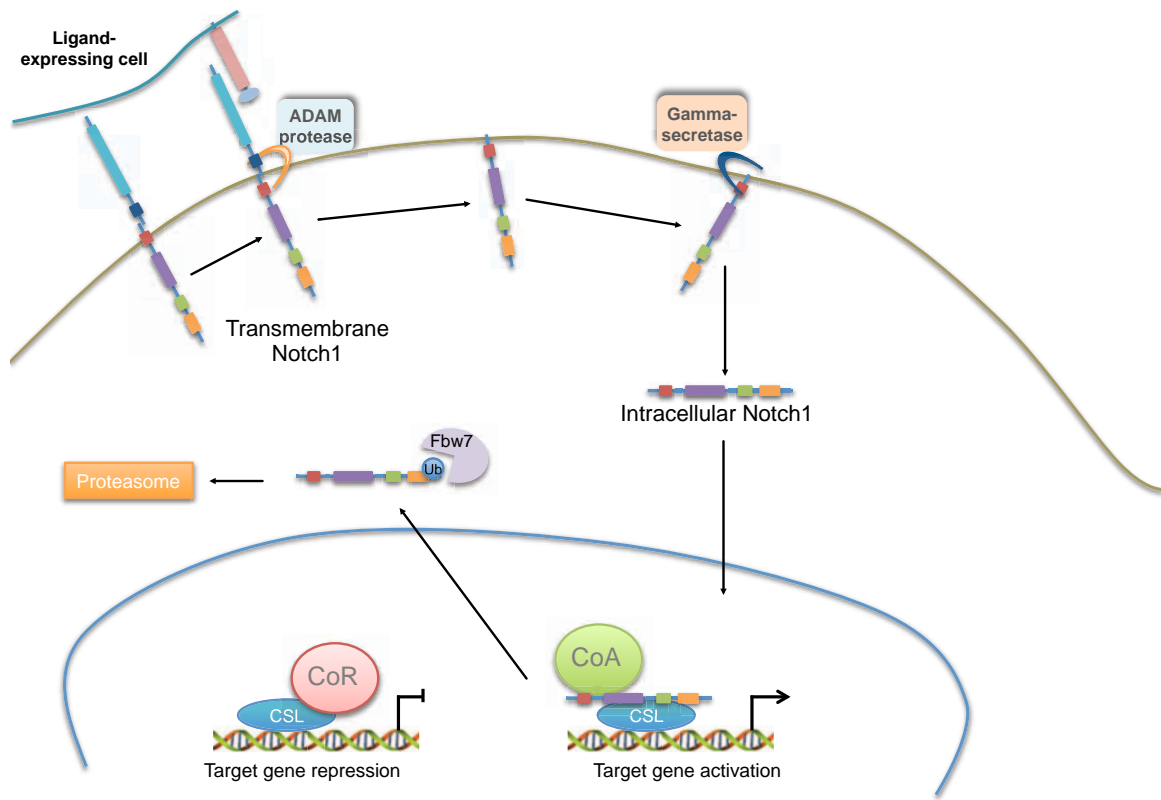


**Figure 2. Notch1 signaling pathway.** Upon ligand (Jag1, Jag2, Dll1, Dll3, Dll4) engagement, an ADAM protease cleaves the protein at the HD region. The receptor is endocytosed and the gamma-secretase complex releases the Notch1 intracellular domain from the membrane where it then translocates to the nucleus and binds CSL. Upon CSL binding, corepressors are released and transcriptional coactivators are recruited to activate Notch1 target genes. Fbw7 then targets the Notch1 protein for degradation in the proteasome.

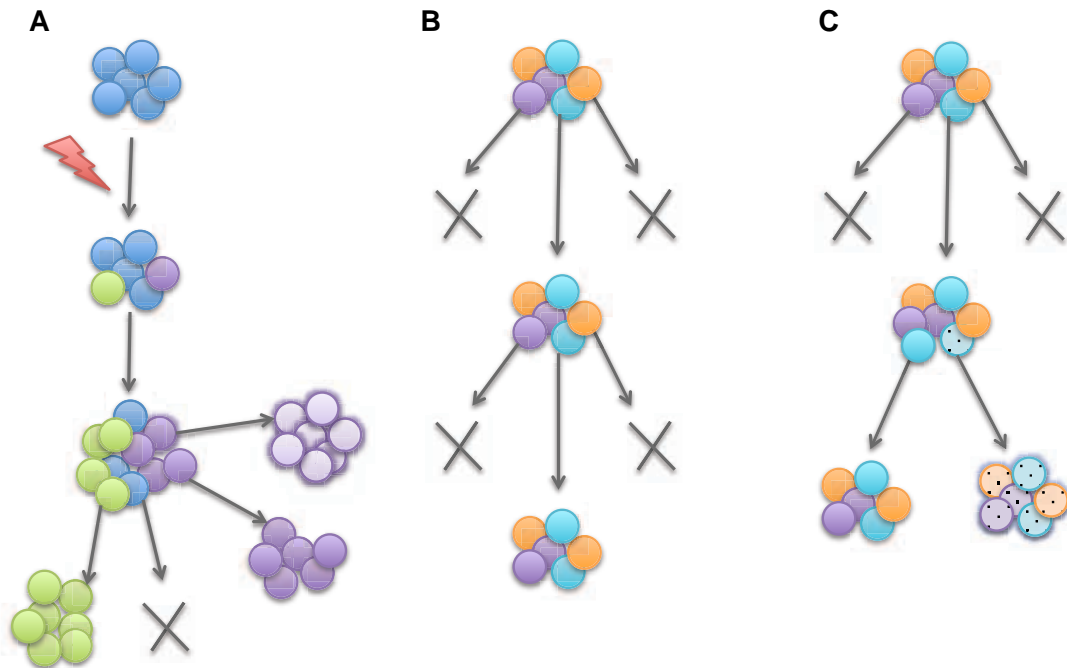


**Figure 3. Models for tumor initiating cell heterogeneity.** Current evidence supports a variety of models for how cancers gain the ability to initiate disease in secondary recipients, or how cancers can initiate relapse in a patient. **A.** The clonal evolution model suggests that there are a number of cells within a tumor that have gained mutations making them capable of initiating disease. **B.** The cancer stem cell (hierarchical) model proposes that a normal stem or progenitor cell with intrinsic self-renewal capabilities gains oncogenic mutations and is able to serially transplant disease while differentiated progeny cannot. **C.** These models can occur in isolation or combination within a single individual or malignancy.



## **CHAPTER II**

**Thymic microenvironment does not  
influence frequency or activity of murine T-  
ALL leukemia-initiating cells**

Data from the following Chapter were submitted as a manuscript not yet in print:

**Tatarek, J. \***, Hermance, N., Kelliher, M. (2013) T-cell acute lymphoblastic leukemia-initiating cell frequency is not influenced by method of transplant or microenvironment. *J. Exp. Med*, *submitted*

Transplant surgeries were performed by Jessica Tesell and Nicole Hermance. Additional experiments and all data analysis were performed by Jessica Tesell.

## Introduction

Leukemia-Initiating cells (L-ICs) are thought to mediate relapse in hematopoietic malignancies such as AML, CML, and T-ALL<sup>337,343,352</sup>. L-ICs are a rare population of leukemic cells that possess the ability to initiate disease in recipient mice, differentiate, and self-renew. It is also thought that these cells are able to evade conventional chemotherapy and radiation by remaining quiescent, expressing drug pumps on their surface, or counteracting damage by expressing survival proteins and free radical scavengers<sup>370,377–379,394</sup>. In murine *Lck-Tal1/Lmo2* T-ALL, the L-IC is quite rare, with only 0.003-0.05% of cells enriched in the ability to initiate disease in recipient mice<sup>251</sup>. This frequency is much lower than other hematopoietic malignancies where frequencies have been reported on the range of 0.05%-1% of cells being able to initiate disease<sup>113,344,395</sup>. This discrepancy could reflect intrinsic characteristics of the T-ALL L-IC or it could reflect limitations in the assay used to determine the frequency.

Current assays for determining murine L-IC frequency involve transplanting a primary leukemia into syngeneic, histocompatible recipient mice (reviewed in<sup>338</sup>). Recently, concerns have been raised about whether this L-IC assay accurately measures L-IC activity and whether it is influenced by factors such as engraftment, homing (to the thymus), survival in the circulation, and/or adaption to a foreign microenvironment. The conventional transplantation method for L-IC assays is either through the tail vein (IV) or peritoneum (IP). These

routes of transplant place cells into microenvironments that may not be ideal for the T-ALL L-ICs to initiate disease. Cells injected into the blood stream or peritoneum must endure shear stress on the order of  $20\text{dyn/cm}^2$ , a force that even normal lymphocytes must struggle to overcome<sup>396,397</sup>. Leukemic blasts derived from the mouse thymus may not express the necessary adhesion molecules to survive such forces and may die upon transplant, thus resulting in an apparently low L-IC frequency. It is imperative that we understand and accurately quantitate the L-ICs in this disease so that we can successfully develop and test anti-LIC therapies in animal models.

Murine T-ALLs are immunophenotypically and functionally heterogeneous (Figure 4 and Table 1). We and others have demonstrated that the L-IC in T-ALL is a committed thymic DN3/4 progenitor, not a traditional stem cell<sup>113,251</sup>. These cells are present in *Lck-Tal1/Lmo2* T-ALLs and are maintained upon transplant. This thymic progenitor has been shown to have the intrinsic ability to self renew when *Lmo2* is overexpressed in developing thymocytes<sup>137</sup> and we have shown that leukemic DN3 cells can transplant disease and give rise to more differentiated leukemic DP blasts<sup>251</sup>. Thymic progenitors require specific signals from the epithelium/microenvironment in order to successfully differentiate and exit the thymus to function as mature lymphocyte<sup>40,398</sup>. Notch1 signaling is critical for early thymocyte specification and development, especially through the DN3 stage of thymocyte development<sup>41,43,214</sup>. Thus, access to Notch1 ligands such as

Dll4 and Jag2 in the thymic epithelium could be critical for L-IC survival and maintenance of L-IC activity.

Here, we aimed to validate the L-IC assay by estimating L-IC frequency using two methods of transplant. We compared the effects of injecting cells into the peritoneum (IP) versus directly into the thymus (IT) on L-IC frequency, disease kinetics, and disease presentation in recipient animals. We found that L-IC frequency is not influenced by site of injection and that the same leukemic clones expanded *in vivo* irrespective of method of transplant. This study confirms that the current assay for measuring L-IC frequency accurately estimates an intrinsic activity within these cells and suggests that this assay will accurately and sensitively assess effects of anti-LIC therapies.

## Results

### ***Mode of transplant does not alter disease kinetics or leukemia-initiating cell frequency***

The thymic microenvironment is critical in promoting successful differentiation of DN3 cells, by supplementing the developing thymocytes with Notch1 ligands, cytokines such as IL7, and morphogenetic proteins such as BMP2 and Wnt<sup>399-401</sup>. We hypothesized that these cytokines and growth factors could influence the survival of leukemic DN3 (L-IC) population. In order to determine whether L-IC frequency is influenced by the ability of cells to home to the thymus, we serially diluted four independent *Lck-Tal1/Lmo2* T-ALLs and transplanted each into syngeneic recipient mice by IP or IT injection under limiting dilution conditions. Mice transplanted with leukemic cells by IT injection were sublethally irradiated before leukemic cells were surgically implanted into the recipient thymus<sup>402,403</sup>. Transplanted mice were monitored for signs of leukemia and sacrificed when moribund.

In all four T-ALLs examined, mode of transplant did not significantly affect disease latency, with p-values ranging from 0.15-0.88 (Figure 5 A-D). Leukemia-initiating cell frequency was calculated for each T-ALL injected IP versus IT (Figure 6 A-D) and a mean L-IC frequency was also calculated (Table 2). L-IC frequencies were found to be within the range of what we had previously published (0.009-0.042%, Table 2) and mode of transplant did not significantly

alter the frequency of L-ICs in any of the T-ALLs examined. This finding suggests that the leukemia-initiating cell frequency is a cell autonomous feature of the leukemia and is not influenced by differences in microenvironment or ability to survive in the circulation or peritoneum.

***Clonal selection is not influenced by method of injection***

Due to the diverse methods of transplant examined, we hypothesized that different leukemic clones may expand in the IT or IP microenvironments. In order to determine if mode of transplant preferentially selected for certain leukemic clones, we analyzed leukemic tissues from recipient mice. Immunophenotyping conducted using flow cytometry for T-cell surface markers revealed that the leukemic DN3, L-IC, population was detected in all recipient animals, regardless of mode of transplant (Figure 7). Small increases in CD44-positive cells in the IP injected animals most likely reflect endogenous CD44 expression found in the mesenteric lymph node<sup>404</sup> (site of leukemic burden and immunophenotype analysis), and likely do not contribute to disease pathogenesis. This slight increase in CD44 expression is seen in all IP injected animals from this study and others in our lab (data not shown).

We also assessed TCR-V $\beta$  clonality by PCR, as previously described<sup>251</sup>, to determine if the IT or IP method of injection or corresponding microenvironment selected for certain leukemic clones. Wild-type thymi are polyclonal in terms of TCR-V $\beta$  expression while *Lck-Tal1/Lmo2* mouse T-ALLs

are oligoclonal. In each T-ALL examined, clonal selection did occur upon transplant; overall the number of TCR-V $\beta$  families expressed was reduced in recipient mice compared to the primary T-ALL. However, in each T-ALL, the same leukemic TCR-V $\beta$  clones were selected irrespective of whether cells were transplanted IT or IP (Table 3). This demonstrates that site of T-ALL cell injection does not select for particular leukemic clones. This finding also reaffirms the functional heterogeneity of murine T-ALLs; only certain leukemic clones are able to initiate disease in recipient mice.

***Disease presentation differs significantly with mode of transplant***

Although L-IC frequency and clonal selection did not significantly change in IT versus IP transplant, differences in site of leukemic burden were observed. Mice transplanted with cells via IP injection presented with greatest disease burden in the spleen, whereas mice transplanted with cells via IT injection presented with leukemic cells mainly in the thymus (Figure 8). While disseminated leukemia did develop in all animals, the greatest burden was found at the injection site, suggesting that cells expand at the injection site prior to entering the bloodstream and infiltrating other organs.



## Discussion

Here, we validated the assay to estimate the L-IC frequency in murine T-ALL by demonstrating that L-IC activity is not influenced by extrinsic factors such as transplant microenvironment or survival of cells in the bloodstream. T-ALL cells were transplanted by two independent methods, both of which resulted in similar disease latencies and no significant differences in estimates of L-IC frequency. Leukemic DN3 cells were detected with both methods of transplant and identical clones expanded in IP or IT injected mice. This study validates our L-IC estimates and provides evidence that this assay can be used to evaluate anti-LIC therapies.

Recent reports have demonstrated that normal thymocytes have the ability to self-renew when there is a lack of bone marrow progenitor import into the thymus<sup>67,68</sup>. *Lmo2*, a collaborating oncogene in our mouse model, increases the self-renewal capacities of thymocytes, specifically at the DN3 stage in development<sup>137</sup>. *Lmo2* upregulates a transcriptional program consistent with HSCs by inducing the expression of *Hhex*, *Lyl1* and *Gfi1*<sup>137,405</sup>. Thus, in the *Lck-Tal1/Lmo2* mouse model, the DN3 population may gain properties of stem cells via the expression of *Lmo2* that enable the cell to self-renew and gain further mutations needed for leukemic transformation.

Mature SP T-cells leave the thymus and intravasate into the blood stream and have the ability to then extravasate into tissues, processes that require

adhesion molecules and a tolerance for shear stress of the circulation<sup>396,397,406–408</sup>. In T-ALL, specific T-cell adhesion molecules may be present on the cell surface to aid in migration of these cells. The immunoglobulin adhesion molecule EVA1 is expressed on thymic epithelial cells and developing thymocytes. It is required for progression of ETP/DN1 progenitors to DN3 thymocytes. Mice with EVA1 deletions exhibit impaired thymocyte engraftment 10-fold, so this protein could play a critical role in the transplantation of T-ALL cells<sup>409,410</sup>. Integrins in general are important in adhesion and migration of normal and cancer cells and could be important in engraftment of the T-ALL L-IC after transplant. In particular  $\alpha\beta 1$  is important for B- and T-lymphocyte entry in and out of the CNS<sup>411</sup>, and MadCAM1 is critical for T-cell entry to lymph nodes<sup>412,413</sup>.

Our data suggest that once a preleukemic cell is transformed to an L-IC, it is able to adapt and proliferate in varied microenvironments and is no longer dependent on the thymus for its survival. This study confirms that the T-ALL L-IC has unique, intrinsic properties that allow the cell to adapt and initiate disease in recipient mice in a thymus-independent manner. Further study is necessary to determine what these exact properties are, but first the T-ALL L-IC must be purified based on cell surface markers or biological characteristics. We are confident that the L-IC assay accurately measures an activity within these cells, therefore future studies will analyze leukemic the DN3/4 population for the expression of adhesion molecules, T-cell co-stimulatory molecules, surface

transporters, and stem cell markers. We can then continue to use this assay to test the effects of therapeutics on targeting the L-IC in T-ALL.

## Methods

### Mice

A cohort of *Lck-Ta11/Lmo2* transgenic mice were maintained and monitored daily for development of leukemia<sup>112</sup>. *Lck-Ta11/Lmo2* leukemic cells were transplanted into syngeneic recipient FVB/N mice (4-6 weeks old, The Jackson Laboratory) via intraperitoneal<sup>251</sup> or intrathymic (see below) injection. The University of Massachusetts Medical School Institutional Animal Care and Use Committee approved all animal procedures.

### Intrathymic injections

Protocol performed as described previously<sup>402,403</sup>. Mice were sublethally irradiated with 400rads using a cesium irradiator prior to the procedure. Mice were anesthetized using Avertin (2, 2, 2-Tribromoethanol) and immobilized ventral side up. An incision was made from the sternum to the base of the chin, approximately 2-3cm. Two curved forceps were used to gently open the rib cage and remove salivary gland tissue above the trachea and thymus. Once thymus was visible at top of rib cage, 10ul of cell solution was injected into each lobe of the thymus using a 25ul fine-needle syringe (Hamilton #7654-01). Approximately 3-4 staples (Protech International #205016) were used to close incision.

### L-IC statistics

Mice were transplanted with *Lck-Ta11/Lmo2* leukemic cells via IP or IT injection. Leukemia-initiating cell (L-IC) frequency was calculated using Poisson distribution analysis and the ELDA software<sup>388</sup>. Kaplan-Meier survival curves and

statistical analyses were performed using GraphPad Prism software, Version 5.0. The hazard ratio and its 95% confidence interval was also measured, comparing the designated groups and adjusting for the dilutions of leukemic cells, using the Cox proportional hazards model analysis. A 2-sided  $P < .05$  was considered statistically significant.

### **FACS analysis**

Single-cell suspensions of *Lck-Tal1/Lmo2* leukemic cells were stained with cell surface antibodies as described previously. Flow cytometric analysis was performed on the LSRII or FACSCalibur machines (BD Biosciences). Data were analyzed using FlowJo Version 9.1 software (TreeStar).

### **TCR-V $\beta$ Clonality analysis**

To determine clonality of each T-ALL, RNA was isolated from thymic tissue and cDNA synthesized. Rearrangements of the TCR $\beta$ -chain were assayed by standard qualitative PCR analysis as described previously<sup>251</sup>.

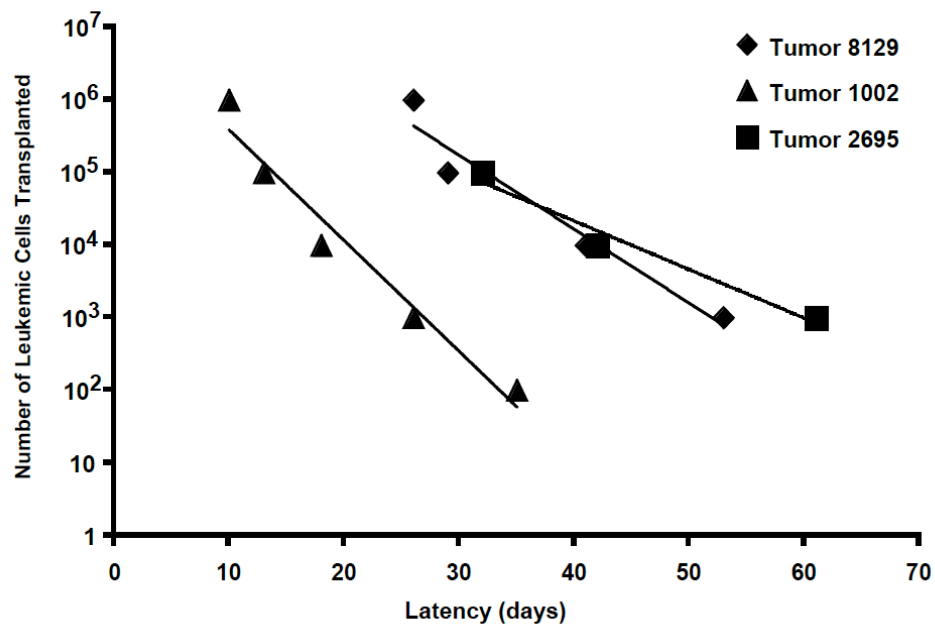


**Figure 4. Functional heterogeneity among mouse *Lck-Tal1/Lmo2* T-ALLs.** Leukemic cells from seven *Lck-Tal1/Lmo2* mice were transplanted through limiting dilution into syngeneic mice. Three representative *Lck-Tal1/Lmo2* mouse T-ALLs are shown. Time to leukemia following transplantation of the indicated numbers of cells is shown. L-IC frequency for each mouse T-ALL was calculated by applying Poisson statistics using the Limiting Dilution software (StemCell Technologies). (4 of the 7 T-ALLs were transplanted and analyzed by Kathleen Cullion)

Table 1. *Lck-Tal1/Lmo2* T-ALLs are functionally heterogeneous

Dilution	Disease Penetrance					
	8129	2695	1002	2697	2692	1450
$10^6$	4/4	N.D.	8/8	N.D.	N.D.	N.D.
$10^5$	3/3	4/4	8/8	2/2	4/4	3/3
$10^4$	3/4	3/4	8/8	1/3	2/4	N.D.
$10^3$	1/4	2/4	7/8	0/3	0/4	2/3
$10^2$	N.D.	N.D.	2/8	N.D.	N.D.	0/3
Est. L-IC frequency	1:30,735	1:4,579	1:2,209	1:10,725	1:16,085	1:4,962
% DN3	1.04	11.08	29.29	4.12	67.61	5.47

N.D. not determined

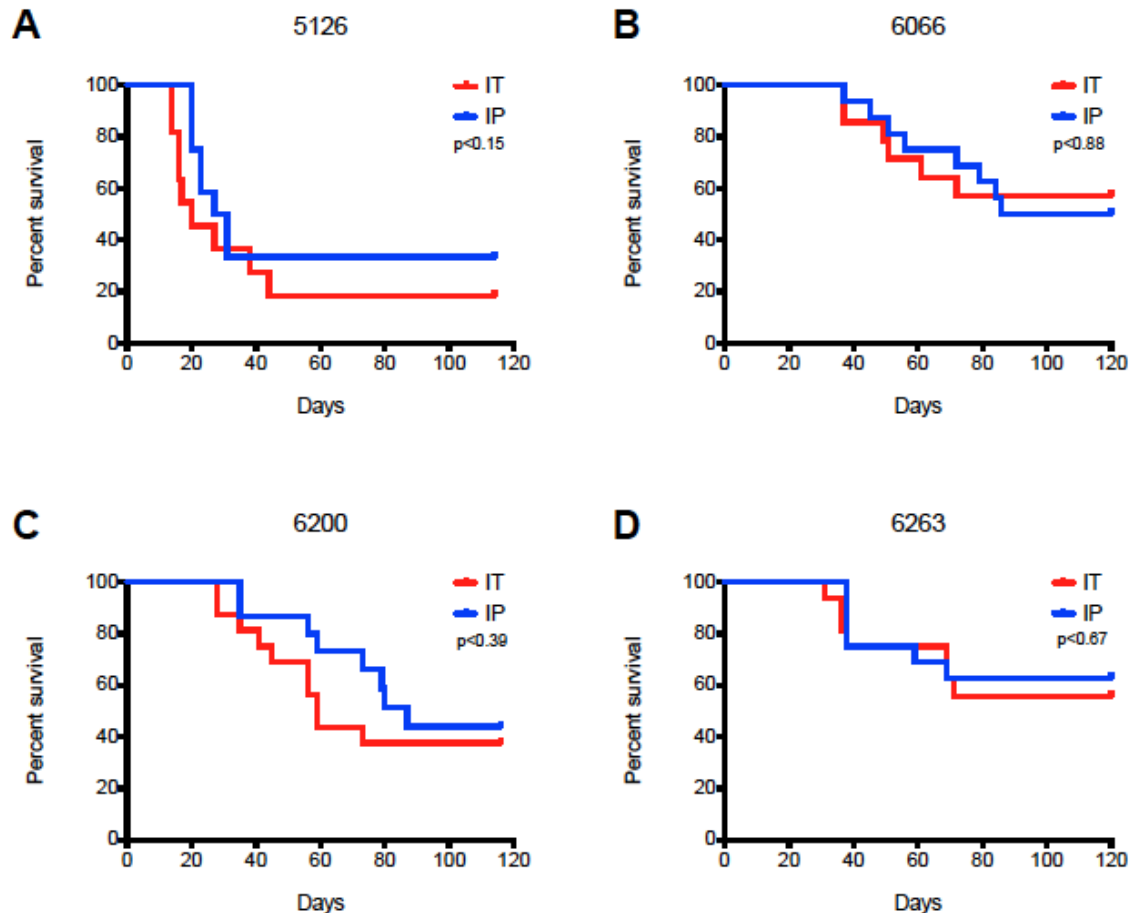


**Figure 5. Intrathymic injection of T-ALL cells does not alter disease progression.** *Lck-Tal1/Lmo2* tumor cells were injected into syngeneic wild type recipients via intraperitoneal (IP) or intrathymic (IT) injection and monitored for disease. The survival curve for each group of mice was estimated by the Kaplan-Meier method and the difference in overall survival between the two groups assessed by the log-rank test. We further estimated the hazard ratio and its 95% confidence interval, comparing the IP with the IT group and adjusting for the three levels of cell dilution, using the Cox proportional hazards model analysis. A two-sided P value of  $<0.05$  was considered to indicate statistical significance. Four independent tumors were analyzed. **A.** 5126  $p < 0.15$ , **B.** 6066  $p < 0.88$ , **C.** 6200  $p < 0.39$ , **D.** 6263  $p < 0.67$ .



**Table 2. L-IC frequency is not influenced by mode of transplant.**

<b>Injection Method</b>	<b><u>Number of Cells Injected</u></b>				<b>#diseased/ total</b>	<b>L-IC freq</b>	<b>CI</b>
	<b>100,000</b>	<b>10,000</b>	<b>1,000</b>	<b>100</b>			
<b>IT</b>	14/14	12/15	7/14	0/13	33/56	0.024%	0.009-0.027%
<b>IP</b>	15/15	10/15	5/13	0/13	30/56	0.015%	0.013-0.042%

CI: Confidence Interval

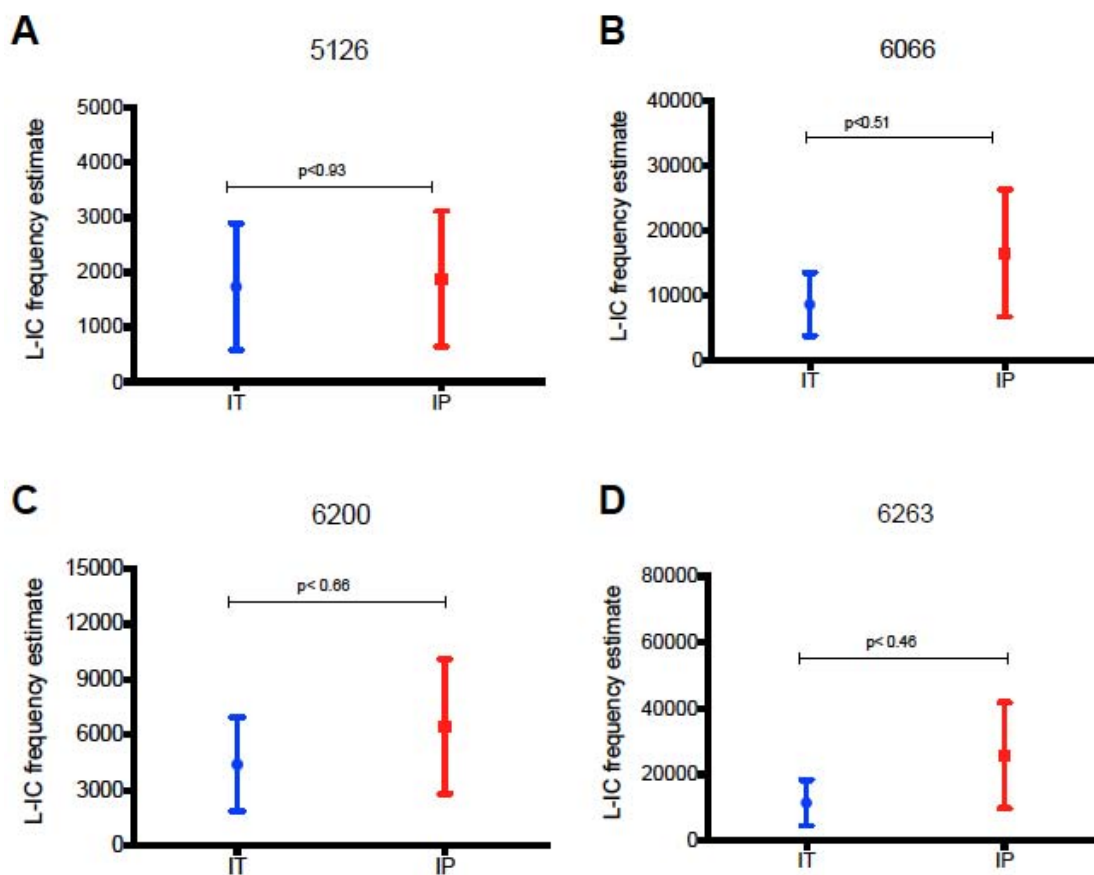


**Figure 6. Leukemia-Initiating Cell (L-IC) frequency does not differ with mode of transplant.** Murine T-ALL cells were injected into syngeneic wild type recipients (with carrier cells) in limiting dilution via intraperitoneal (IP) or intrathymic (IT) injection. Estimated L-IC frequencies are shown. L-IC frequency was calculated using *Poisson* statistics and ELDA software<sup>414</sup>. Four independent tumors were analyzed. **A.** 5126  $p < 0.93$ , **B.** 6066  $p < 0.51$ , **C.** 6200  $p < 0.66$ , **D.** 6263  $p < 0.46$ .

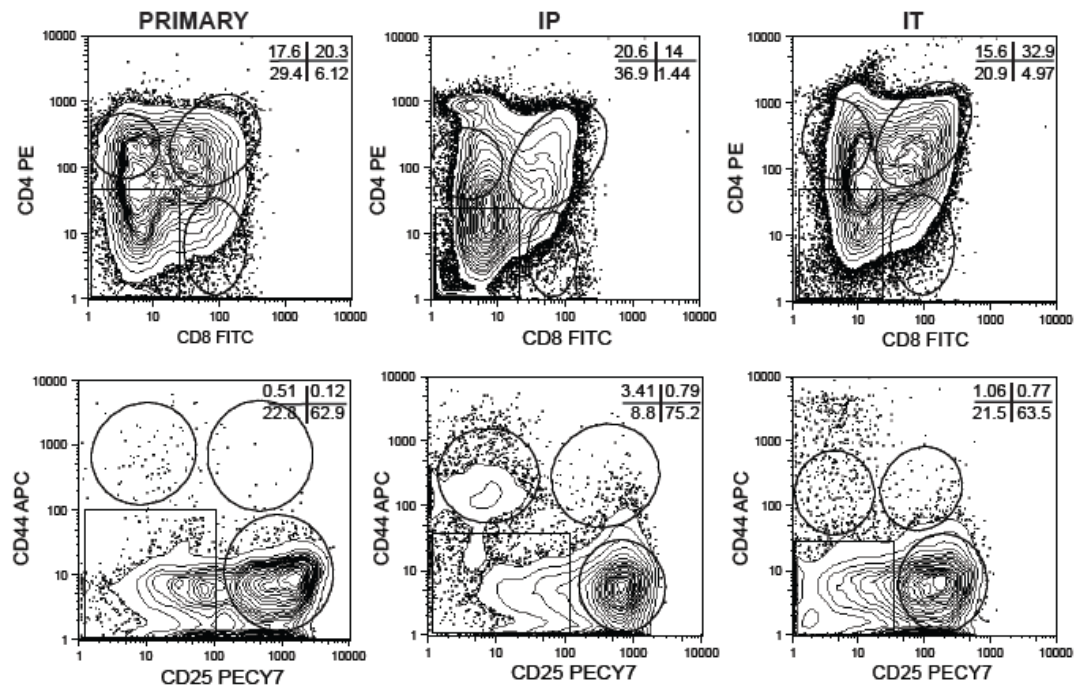


**Figure 7. The leukemic DN3 population is maintained with both IT and IP injection.** *Lck-Tal1/Lmo2* tumor cells were injected via IP or IT injection into syngeneic recipient mice. At sacrifice, the immunophenotype of the transplanted tumor was reanalyzed by flow cytometry and compared to the primary tumor. Four tumors were analyzed; one representative T-ALL (6200) is shown.

**Table 3. TCR-V $\beta$  clonal selection is not influenced by mode of transplant.**

	1	2	3	4	5.1	5.2	5.3	6	7	8.1	8.2	8.3	9	10	11	12	13	14	15	16	17	18
<b>WT</b>	X	X	X	X	X	X		X	X	X			X	X	X				X	X	X	X
<b>6066 Primary</b>	X	X		X	X													X				
<b>6066 IT recipient</b>	X			X														X				
<b>6066 IP recipient</b>	X			X														X				
<b>6200 Primary</b>		X						X														X
<b>6200 IT recipient</b>								X														X
<b>6200 IP recipient</b>								X														X
<b>6263 Primary</b>	X			X				X														
<b>6263 IT recipient</b>				X				X														
<b>6263 IP recipient</b>				X				X														

**Table 3.** To determine clonality of each T-ALL, RNA was isolated from thymic tissue and cDNA synthesized. Rearrangements of the TCR-V $\beta$  chain were assayed by standard qualitative PCR analysis as described previously<sup>251</sup>. Expression of each TCR-V $\beta$  clone are displayed as analyzed on a 2% agarose gel. Each X represents an average of three independent experiments.

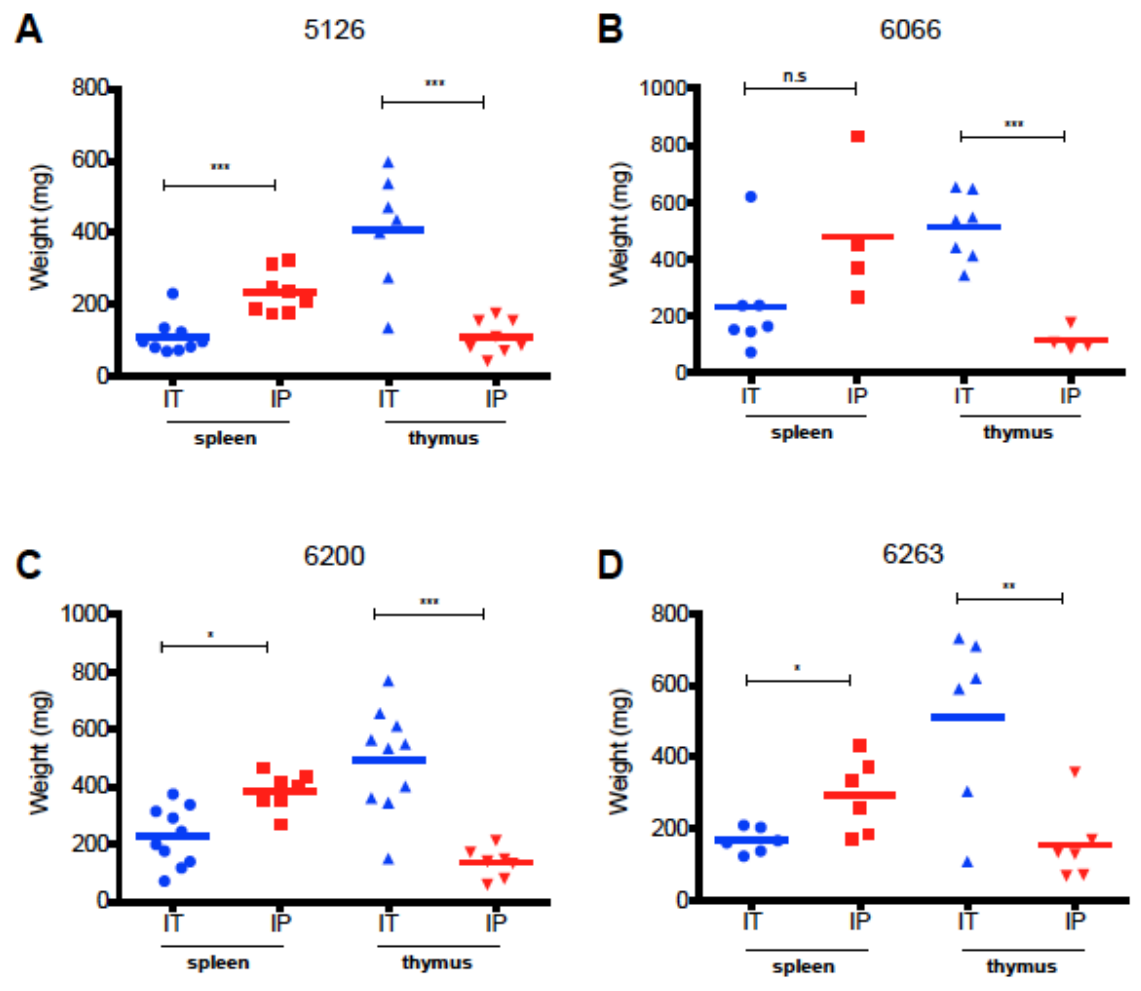


**Figure 8. Method of T-ALL injection alters primary site of leukemic infiltration.** T-ALL cells were injected into syngeneic wild-type recipients via intraperitoneal (IP) or intrathymic (IT) injection and monitored for disease. Upon sacrifice, spleen and thymus were harvested and measured; weights are shown in milligrams. An unpaired t-test was performed with a  $p < 0.05$  being considered significant. NS, not significant; \*  $p < 0.05$ , \*\*\* $p < 0.0005$ . **A.** 5126, **B.** 6066, **C.** 6200, **D.** 6263.

## **CHAPTER III**

**Notch1 inhibition targets the leukemia-initiating cells in a *Tal1/Lmo2* mouse model of T-ALL**

Data from the following Chapter were published as:

**Tatarek, J. \***, Cullion, K. \*, Ashworth, T., Gerstein, R., Aster, J., Kelliher, M. (2011) Notch1 inhibition targets the leukemia-initiating cells in a *Tal1/Lmo2* mouse model of T-ALL. *Blood*, Aug 11;118(6):1579-90 \*equal contribution

The manuscript has been edited for this thesis so that the results only include experiments performed by Jessica (Tatarek) Tesell; data generated by others are noted.

## Introduction

Experiments performed in Chapter II validate the method we are using to measure L-IC frequency and allow us to use this assay to identify pathways that contribute to L-IC frequency. The NOTCH1 pathway has been implicated in T-ALL initiation in a xenotransplant model using patient samples<sup>262</sup> and Notch1 inhibition has been shown to have anti-leukemia effects in our mouse model<sup>261</sup>. These studies led us to start testing the effects of Notch1 inhibition on the murine T-ALL L-IC.

Spontaneous gain of function *Notch1* mutations are frequently observed in murine T-ALL models and occur mainly in the PEST domain<sup>245,246,248,415</sup>. Recently 5' activating deletions in *Notch1* have been found in multiple mouse T-ALL models including the model used in this study<sup>249,250</sup>. Two types of deletions have been described in these mouse models, designated Type 1 and 2. Type 1 deletions are Rag1/2 mediated and remove the 5' proximal promoter of Notch1. Transcription initiates at a cryptic promoter in exon 25, where changes in histone marks occur that allow this internal transcription initiation. The mechanism that creates the Type 2 deletions is not as well understood, but could result from random DNA breaks. These mutations leave the 5' proximal promoter intact, but remove from exon 2 to either exon 26 or 28. Both types of mutations result in translation initiation from an internal methionine, M1727. The truncated protein lacks the extracellular domain of the Notch1, but still inserts into the cell membrane and is sensitive to cleavage by the  $\gamma$ -secretase complex<sup>249</sup>.



These 5' deletion events are common in mouse T-ALLs (6 out of 7 *Lck-Tal1/Lmo2* T-ALLs) but occur rarely, in human T-ALL. Only one patient sample with a 5' deletion has been reported to date<sup>240</sup>. Instead, human T-ALLs often present with mutations in the HD domain of Notch1 resulting in ligand-independent activation. The deletions described in mouse T-ALLs also result in ligand independent activation of the Notch1 signaling cascade, thus in mouse T-ALL the *Notch1* locus undergoes two mutation events. The deletion events or HD mutations allow for ligand-independent cleavage by ADAM proteases in situations where ligand may be limiting and then the PEST (or FBW7 in patients) mutations increase ICN1 protein stability. Together, these mutations result in constitutively active Notch1 signaling.

To monitor Notch activity during leukemogenesis, we mated our *Lck-Tal1/Lmo2* mice with the Transgenic Notch Reporter (TNR) mouse line. The TNR mouse contains a transgene with four CSL-binding sites, a minimal SV40 promoter, followed by an enhanced green fluorescent protein (GFP) sequence<sup>416,417</sup>. The TNR mouse has been shown to accurately report Notch activity during early thymocyte and neuronal development, angiogenesis, and hair follicle formation<sup>201,416–418</sup>. Using these mice, we detected Notch-active cells in the expanded DN population of preleukemic *TNR/Tal1/Lmo2* animals. The proportion of GFP-positive, Notch-active, DN thymocytes in preleukemic *TNR/Tal1/Lmo2* animals was significantly greater than that observed in control littermates with no significant increase in Notch-active cells observed in the DP, CD4SP, or CD8SP

populations(Kate Cullion<sup>251</sup>). Although Notch1 activity is normally down-regulated at the DN4 stage<sup>419</sup>, we detected an expansion of GFP+, Notch-active DN3 and DN4 progenitors in the mice predisposed to leukemia.

To examine the role of Notch1 in leukemia-initiating cell activity, we used the *Lck-Tal1/Lmo2* mouse model of T-ALL in which more than 75% of the mouse T-ALLs develop spontaneous mutations in *Notch1*. *In vivo* limiting dilution analyses have revealed that a rare L-IC population contributes to disease pathogenesis in this mouse T-ALL model. We found a committed thymic progenitor population enriched in disease potential and demonstrated that GSI treatment reduces and in some cases ablates L-IC activity. The present study reveals that L-ICs contribute to mouse T-ALL pathogenesis and provides evidence that Notch1 inhibition will target the L-ICs.

## Results

### **Preleukemic *Lck-Tal1/Lmo2* thymic progenitors exhibit aberrant Notch1 activity.**

The increase in the absolute number of Notch1-active DN3/4 progenitors revealed in the *TNR/Tal1/Lmo2* preleukemic mice (Kate Cullion<sup>251</sup>) suggested that sustained Notch1 activity might drive progenitor expansion during the preleukemic phase of the disease. To test this possibility, GFP-positive, Notch1 active, DN3 and DN4 cells from preleukemic *TNR/Tal1/Lmo2* mice were isolated and sequenced for the presence of *Notch1* mutations. We detected multiple *Notch1* mutations in the DN3 and DN4 progenitors isolated from preleukemic *TNR/Tal1/Lmo2* mice (Table 4). Similar to what we observed in *Tal1*-mediated mouse T-ALLs,<sup>248</sup> these mutations consisted of point mutations, insertions or deletions within exon 34 that introduce premature STOP codons or alter the reading frame, resulting in the truncation of PEST regulatory sequences. These mutations are predicted to increase Notch1 protein stability and explain the increased Notch1 reporter activity detected in the preleukemic *TNR/Tal1/Lmo2* thymic progenitor populations. Although PEST region mutations were observed (Table 1), 5' activating deletions were not detected in the preleukemic GFP-positive DN3/4 progenitors (Todd Ashworth, not shown), raising the possibility that PEST region mutations precede the 5' activating deletions in *Notch1* during leukemogenesis.

The presence of multiple *Notch1* mutations in the preleukemic thymic progenitors led us to hypothesize that mutant Notch1 contributes to the expansion of DN3/4 progenitor clones in these mice. This hypothesis predicts that the preleukemic thymus will be oligoclonal in nature and reflect the expansion of multiple progenitor clones. To analyze the clonality of the preleukemic progenitors, wild type and preleukemic GFP-positive DN3 and DN4 progenitors were purified and TCR-V $\beta$  family gene expression was determined by PCR amplification of the cDNA. In wild type thymocytes, we detect expression of 15 of the 22 TCR-V $\beta$  families examined, confirming the polyclonality of the wild type thymus (Figure 9). In each of the three *Lck-Tal1/Lmo2* preleukemic mice examined, the DN3 and DN4 subpopulations expressed 3-6 TCR-V $\beta$  families, consistent with an oligoclonal expansion (Figure 9). Although the TCR-V $\beta$  expression patterns differed among the three preleukemic mice examined, they were identical between the DN3 and DN4 progenitors within each mouse. The predominance of multiple identical TCR-V $\beta$  expressing clones in the preleukemic DN3 and DN4 populations suggests that the DN3 progenitors maintain their ability to differentiate to the DN4 stage. Thus, in this mouse T-ALL model, the preleukemic phase of the disease is associated with the expansion of multiple Notch1-active thymic progenitors.

### **Notch1 inhibition targets the L-ICs in a mouse T-ALL model**

The presence of *Notch1* mutations and the expansion of Notch1-active thymic progenitors in preleukemic *Lck-Tal1/Lmo2* mice raise the possibility that a

sustained Notch1 signal confers extensive proliferative capabilities on committed thymic progenitors. Once thymocytes are fully transformed, Notch1 protein expression is similar in DN3 and DP cells (Figure 10), suggesting that the expanded DN3 progenitors differentiate into the DP cells of the tumor. This is surprising because under normal developmental conditions, Notch1 expression is transcriptionally downregulated by the DP stage. It is possible that the 5' deletions and activation of the cryptic promoter in exon 25 of the *Notch1* locus removes the normal transcriptional regulatory elements responsible for Notch1 silencing at the DP stage. Although we demonstrated that GSI treatment extends the survival of end stage leukemic mice<sup>261</sup>, effects on L-IC frequency or activity were not addressed in the prior study. Since relapse is hypothesized to reflect an inability to eliminate the L-IC population, whether L-ICs are susceptible to Notch inhibitors remains a critical, unanswered question.

To examine the consequences of Notch1 inhibition on mouse L-IC activity, we initially treated mouse T-ALL cells *in vitro* with vehicle or GSI for 48 hours. This time period successfully decreases Notch1 protein levels *in vitro* (Figure 11). Serial dilutions of the vehicle- or GSI-treated leukemic cells were then transplanted into syngeneic recipients and treatment was maintained for 3 weeks. GSI was administered by oral gavage using an intermittent dosing regimen we have shown minimizes the gastrointestinal toxicity associated with Notch inhibition<sup>261</sup>. We have demonstrated that this GSI dosing regimen reduces Notch1 target gene expression in leukemic cells<sup>261</sup> (Figure 12). Five *Lck*-

*Tal1/Lmo2* tumors with mutations in *Notch1* were examined in this study and remarkably, complete or partial responses were observed in 4 of 5 mouse T-ALLs treated with GSI (Figure 13). For reasons not yet understood, GSI treatment of mouse T-ALL 1007 had minimal effects on leukemic cell viability (Table 7) and on disease latency and overall survival (Figure 13; log rank  $p < 0.28$ ).

Transplantation of  $10^5$  or  $10^4$  vehicle-treated leukemic cells from mouse T-ALLs 1426 or 2544 resulted in disease initiation in all transplanted recipients with an average latency of 31 and 55 days for 1426 and 28 and 39 days for 2544 (Figure 13). Mice transplanted with leukemic cells from mouse 1426 or 2544 treated with GSI failed to develop disease during the 180- or 90- day observation periods (Figure 13; log rank test  $p < 0.0004$  for 1426 and  $p < 0.001$  for 2544). These mice exhibited no evidence of disease at necropsy and histopathological examination of tissues failed to detect the presence of leukemic cells. GSI treatment of mice transplanted with leukemic cells from 1928 and 3304 reduced L-IC activity approximately 4- to 20-fold, respectively (Table 6) and significantly extended survival (Figure 13; log rank test  $p < 0.02$  for 1928 and  $p < 0.0003$  for 3304). Consistent with our published work<sup>261</sup>, transplanted mice treated with GSI continued to gain weight throughout the treatment period and exhibited no signs of gastrointestinal toxicity (Figure 14). This study demonstrates that in some cases Notch1 inhibition *in vivo* reduces L-IC activity below the limits of detection

of this limiting dilution assay. These findings have clear translational implications and support the continued development of Notch therapeutics for T-ALL patients.

It remains unclear why GSI treatment had no effect on mouse T-ALL 1007. All five mouse T-ALLs examined express high levels of intracellular Notch1 and harbor genomic insertions/deletions that result in PEST truncation (Figure 15A,B). All of these mouse T-ALLs also harbor 5' activating deletions in *Notch1* that result in ligand independent Notch1 activation (Todd Ashworth, Figure 15C). In 2 of 5 mouse T-ALLs analyzed (1007 and 3304) the deletions are likely Rag-mediated Type 1 deletions (not shown) and further support our finding that the Rag-active DN3 population is important in disease initiation. Mouse T-ALL 1007 fails to respond to GSI treatment potentially due to mutations in *Pten* or *Fbw7*<sup>260,420–422</sup>. Alternatively, L-IC activity in this mouse T-ALL may not depend on Notch1, but rather on the activation of other thymocyte self-renewal pathways potentially mediated by Lmo2<sup>137</sup>.

## Discussion

We hypothesized that deregulated Notch1 activity during the preleukemic phase may confer extensive proliferative properties on committed thymic progenitors. We demonstrate that the DN3 population is enriched in leukemia-initiating activity and provide evidence that Notch inhibition reduces and in some cases, eliminates L-IC activity. These findings have implications for translational research and suggest that Notch therapeutics may prove beneficial for T-ALL patients.

In spite of the L-IC frequency differences, both our study and the one conducted by Tremblay et al. find the DN3 subpopulation enriched in leukemia initiating potential<sup>113</sup>. Tremblay and colleagues also detect reduced L-IC activity in the DN4 population of *SCL/LMO1* mice and argue that transgenic expression of intracellular mutant *NOTCH1*, *SCL* and *LMO1* is sufficient to transform a thymic progenitor into a L-IC. Although we have not tested this, we predict that the DN4 population associated with *Lck-Tal1/Lmo2* tumors will also harbor L-ICs.

The time to disease progression and the estimates of L-IC frequency in our model suggest that additional genetic events define the L-ICs within the DN3 population. The detection of PEST region mutations in endogenous *Notch1* in an oligoclonal, thymic progenitor population roughly 60-90 days before disease is evident argues that a PEST mutation may not be sufficient for complete L-IC transformation in our model. Although 5' activating deletions in *Notch1* were readily observed in these mouse leukemic cells, we were unable to detect an



increase in 3' *Notch1* transcripts in preleukemic progenitors (Figure 15 and Todd Ashworth, data not shown). This result suggests that PEST region mutations precede 5' activating deletions in *Notch1*. This would leave us with the step-wise model of leukemogenesis being: Tal1/Lmo2 activation, Notch1 PEST mutations, Notch1 5' deletions, followed by additional pathway activation and/or the onset of leukemia.

Mouse L-ICs remain dependent on sustained Notch1 signals, as leukemia-initiating cell activity is significantly reduced in 4 of 5 mouse T-ALLs treated with GSIs. The L-IC dependence on Notch1 is consistent with the critical role of Notch1 in normal DN3 thymic expansion, survival and metabolism<sup>423,424</sup>. Additional support for NOTCH1 in the maintenance of L-IC activity comes from studies by Armstrong and colleagues who expand primary human T-ALL cells on a mouse stromal cell line that expresses the human NOTCH ligand DELTA-like 1. GSI treatment of these primary T-ALL cells arrests their growth *in vitro* and reduces the ability of these primary leukemic cells to initiate disease in NOD/SCID mice<sup>262</sup>. Collectively, both studies implicate NOTCH1 in the regulation of L-IC maintenance. To further solidify this finding, we GSI treatment reduced the absolute number of DN3 cells while the absolute numbers of DP, SP, and other DN populations remained unchanged (Figure 16). There is a possibility that because CD25 is a Notch1 target gene<sup>425</sup>, the apparent decrease in the DN3 population could reflect a population of DN3-like cells that has simply lost surface CD25 expression. However, because the absolute number of other T-ALL

populations analyzed did not appear to increase to indicate such a population, this is likely not the case. This provides additional evidence that the DN3 population is dependent on Notch1 for its survival.

Precisely how Notch1 contributes to L-IC activity is unknown. The Notch1 target genes c-Myc and Hes1, have been implicated in stem cell self-renewal and thymic progenitor expansion, respectively<sup>221,314,426,427</sup>. Leukemic or cancer stem cells have been shown to activate gene expression programs similar to those expressed in embryonic stem cells (ESC) and c-Myc expression is one of four transcription factors capable of reprogramming differentiated adult cells back to a pluripotent state<sup>428</sup>. Thus, constitutive Hes1 and/or c-Myc activation may confer “stem cell-like” properties on committed thymic progenitors and these signals may work in concert with survival pathways activated by Notch1.

Although this study reveals a clear L-IC dependence on Notch1, our data argue that additional genetic events contribute to complete L-IC transformation. The nature of these events will require further purification of the L-IC from the DN3 population to determine activation of specific pathways. Candidate genes for L-IC transformation are most likely involved in survival and the prevention of apoptosis. The activation of the Notch1 pathway drives the cells into rapid proliferation, a stress that in a normal cell would result in apoptosis. Thus, activation of genes such as Bcl-2 or Bcl-XL (possibly via c-Myb – see Appendix III) could contribute to L-IC transformation. While Notch1 and c-Myc (see Chapter IV) contribute to the self-renewal of L-ICs, it is also possible that additional self-

renewal genes may also need to be expressed in these cells to ensure that the L-IC does not become exhausted. Genes such as Lyl1, Hhex, Bmi1, and Gfi1 could be candidates for increased self-renewal in the L-IC population.

## Methods

### Mice

A cohort of *Lck-Tal1/Lmo2* transgenic mice was generated and monitored daily for the onset of leukemia<sup>112</sup>. To generate the *Tal/Lmo2/TNR* cohort, *Lck-Tal/Lmo2* mice were mated with *TNR/+* mice (STOCK Tg(Cp-EGFP)25Gaia/J # 005854, Jackson Laboratories, Bar Harbor, ME). *Tal1/Lmo2/TNR* mice are maintained on a mixed background ((C57BL/6J x SJL/J)F2 x FVB/N). To control for differences in genetic background, all preleukemic studies were performed using *TNR/+* control littermates. *Lck-Tal1/Lmo2* leukemic cells or purified subpopulations of leukemic cells were transplanted into syngeneic recipient FVB/N mice (6-8 weeks old, Jackson Lab, Bar Harbor, ME). All mice were maintained in pathogen-free conditions according to institutional animal care guidelines. L-IC frequency was determined using *Poisson* distribution statistics and the L-Calc Version 1.1 software program (StemCell Technologies, Inc., Vancouver, Canada). For the GSI studies, transplanted mice were treated with vehicle or GSI for 3 weeks as described previously<sup>261</sup>. Mice were monitored daily for disease development and weighed to monitor GSI-associated toxicity. Kaplan-Meier survival and statistical analyses were performed using GraphPad Prism 4.0 software (GraphPad Software, Inc.). The hazard ratio and its 95% confidence interval was also measured, comparing the vehicle- and GSI-treated groups and adjusting for the dilutions of leukemic cells, using the Cox

proportional hazards model analysis. A two-sided P value of <0.05 was considered statistically significant.

### **FACS analysis**

Single cell suspensions of *Lck-Tal1/Lmo2* leukemic cells were stained with CD4-PE-Cy5 and CD8-PE or with a lineage cocktail consisting of CD4-PE, CD8-PE, B220-PE, GR1-PE, MAC1-PE (BD Pharmingen, San Diego, CA Cat #553654, 553033, 553049, 553089, 553128, 557397). Lineage negative cells were then stained with CD44-APC (BD Pharmingen, San Diego, CA Cat #559250) and CD25-PE-Cy7 (eBioscience, San Diego, CA Cat #25-0251-82). Dead cells were excluded by propidium iodide staining. Flow cytometric analysis and sorting was performed on the FACS Caliber and FACS LSRII (Becton Dickinson, Franklin Lakes, NJ), respectively. Data was analyzed using Flow-Jo (Tree Star Inc., Ashland, OR).

### **RNA Analysis**

RNA was extracted from murine thymocytes or leukemic cells using Trizol. cDNA was synthesized using Superscript First Strand Synthesis Kit (Invitrogen). cDNA was quantified using the SYBR green kit (Qiagen) using specific primers to c-Myc F: 5'- CTGTTTGAAGGCTGGATTTCCT-3', R: 5'-CAGCACCGACAGACGCC-3'; and Deltex F: 5'- TGCCTGGTGGCCATGTACT-3', R: 5'- GACACTGCAGGCTGCCATC-3'. Copy number was normalized to  $\beta$ -Actin using the  $\Delta\Delta$ CT method.

### **Notch1 sequencing**

To determine the *Notch1* mutational status, DNA isolated from preleukemic sorted thymic populations or mouse T-ALL cells was amplified by PCR using *Pfu* DNA polymerase (Stratagene, Cedar Creek, TX) with primers specific for exon 34 of the *Notch1* gene<sup>248</sup>. PCR products were run on a 1.5% agarose gel, purified (QIAquick Gel Extraction Kit, Qiagen, Valencia, CA), and cloned into the TOPO TA cloning vector (Invitrogen, Carlsbad, CA) for sequencing using the universal M13 primers.

### **Clonality analysis**

To determine clonality, rearrangements of the TCR-V $\beta$  chain were assayed by standard qualitative PCR analysis, using *Pfu* DNA polymerase (Stratagene, Cedar Creek, TX) and primers specific for mouse TCR V $\beta$ 1-V $\beta$ 18 genes and constant region as described in<sup>429</sup>. V $\beta$ 1 –V $\beta$ 18 primers were each paired with the following V $\beta$  constant primer (V $\beta$  - 5'- GGCTCAAACAAGGAGACCTTGGGTGG - 3'). The amplification was performed using a Stratagene Robocycler Gradient 96 starting with a 2 minute 94°C denaturation, followed by 30 cycles consisting of 20 seconds at 94°C, 12 seconds at 55°C, and 30 seconds at 68°C and a final elongation step of 10 minutes at 68°C. PCR products were purified on a 2% agarose gel, subcloned and confirmed by sequencing.

**Table 4. Multiple *Notch1* mutations are detected in preleukemic *Lck-Tal1/Lmo2* thymic progenitors.**

Mouse #	Thymic Subset	Nucleotide Change	Amino Acid Change
9401	DN3	7161 C->G, ins G	2387 T->R
		7873 del TA	2626 Y->F
		7542 del C	2515 I->S
		7926 del A	2643 K->N
		7888 del T	2631 S->L
9401	DN4	7098 del T	2367 T->H
		7272 ins AAGGAAG	2425 G->R
		7313 del G	2438 G->E
		7264 ins C	2425 G->A
		7751 C->T	2584 A->V
		7722 del T	2576 W->G
		7788 ins G	2597 Y->I
9446	DN3	7883 ins T	2629 L->I
		7535 ins G	2512 P->R
		7792 del A	2599 R->E
		7844 del T	2616 L->Y
9446	DN4	7806 del A	2603 E->N
		7792 del A	2600 R->E
		7752 ins G	2586 G->W
9448	DN3	7831 T->C	2611 F->L
		7852 del TC	2618 S->H
		7775 del A	2594 M->C
		7869 del T	2626 Y->I
9448	DN4	7415 del TCCATGGTCCC	2472 L->H
		7673 T->C	2558 T->I
		7316 ins ACA	2439 A->D, ins T

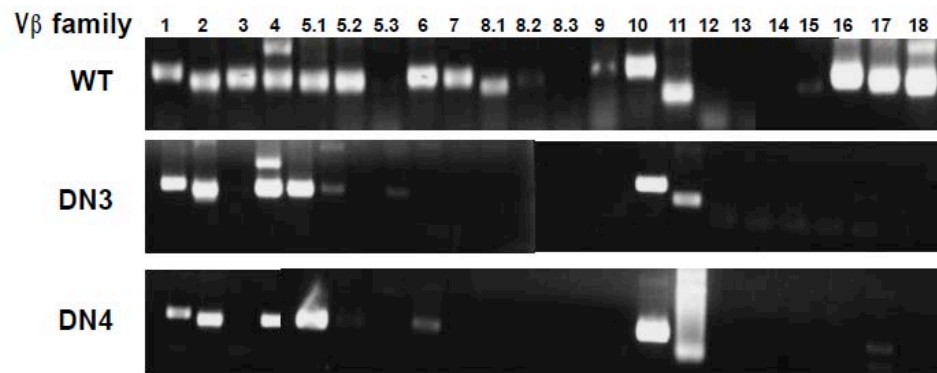


**Figure 9. Notch1-active thymic progenitors are oligoclonal.** Using specific primers for V $\beta$ 1-18, TCR V $\beta$  mRNA expression was examined in wild type and sorted GFP+ DN3 and 4 thymic progenitors isolated from preleukemic *Lck-Tal1/Lmo2* mice. Three mice were examined; one representative experiment is shown. Vertical lines have been inserted to indicate repositioned gel lanes. (Sorts performed by Kathleen Cullion, analysis performed by Jessica Tesell)



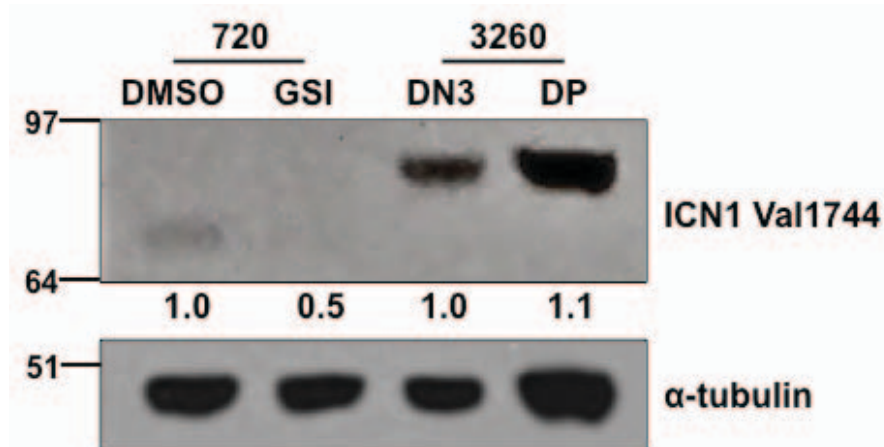


**Figure 10. Notch1 protein expression is similar in leukemic DN3 and DP cells.** One *Lck-Tal1/Lmo2* T-ALL was sorted into DN3 and DP populations. Cells were lysed and analyzed for Notch1 expression by immunoblotting. A murine T-ALL cell line (720) was treated with GSI for 48 hours as a control for the Notch1 Val1744 antibody. This data was presented for reviewers only.

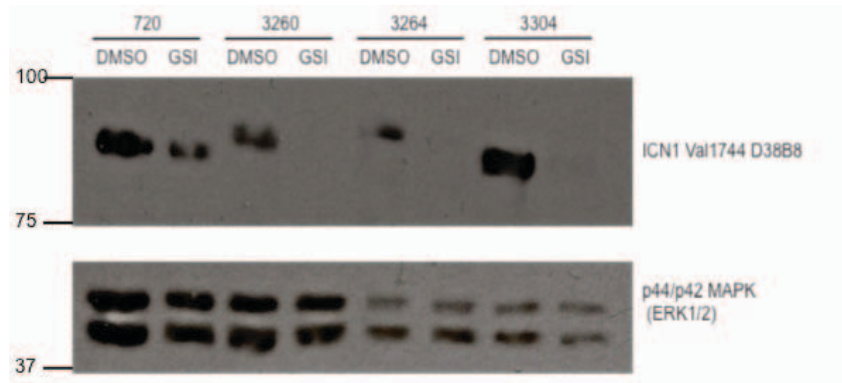


**Figure 11. GSI treatment reduces Notch1 protein expression in primary T-ALLs after 48 hours *in vitro*.** Three primary T-ALLs and the cell line 720 were treated *in vitro* with DMSO or Compound E for 48 hours. Cells were lysed and Notch1 protein levels were determined by immunoblotting. (This figure was presented for reviewers only)

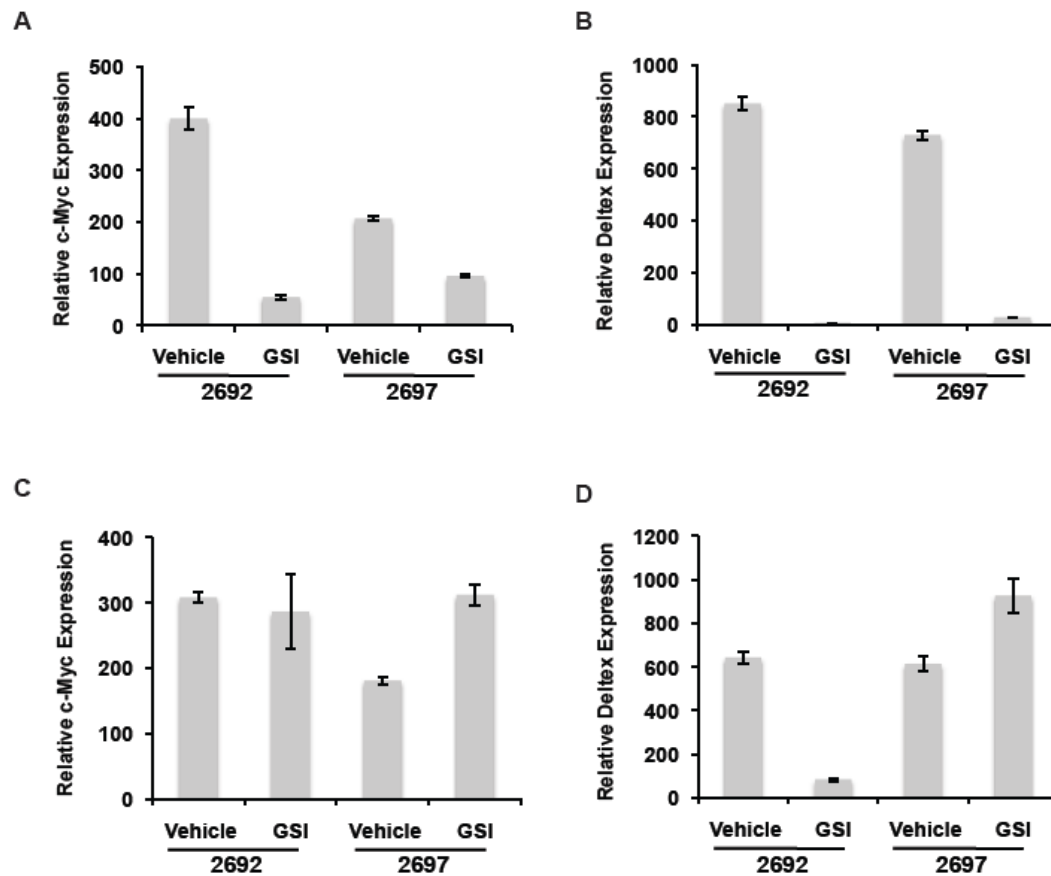


**Figure 12. GSI administration to leukemic mice results in decreased Notch1 target gene expression.** Mice transplanted with primary mouse leukemic cells were treated with vehicle or GSI, and c-Myc (A) or Deltex1 (B) expression analyzed by real time quantitative PCR. c-Myc (C) and Deltex1 (D) mRNA levels were also monitored at the time of disease recurrence. Copy number was normalized to  $\beta$ -actin using the  $\Delta\Delta CT$  method.

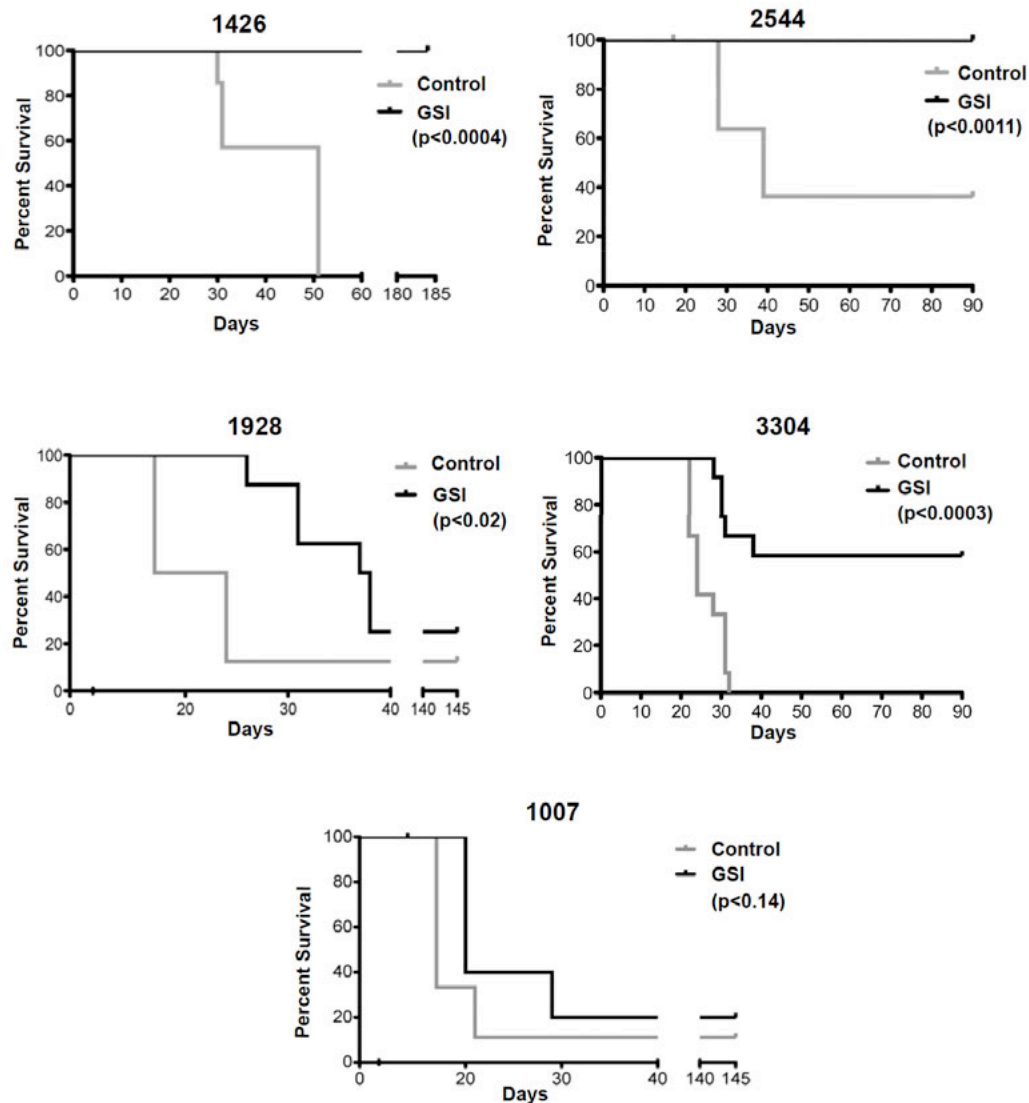


**Figure 13. Notch1 inhibition targets the L-IC in Lck-Tal1/Lmo2 mouse T-ALLs.** Mouse *Lck-Tal1/Lmo2* T-ALLs with *Notch1* mutations were treated with vehicle or GSI for 48 hours *in vitro*, stained and analyzed by flow cytometry. Leukemic cells were serially diluted and transplanted into syngeneic mice and treatment was continued for 3 weeks. GSI was administered using an intermittent dosing regimen and transplanted mice were monitored for disease development. Kaplan Meier survival curves were generated with GraphPad software.

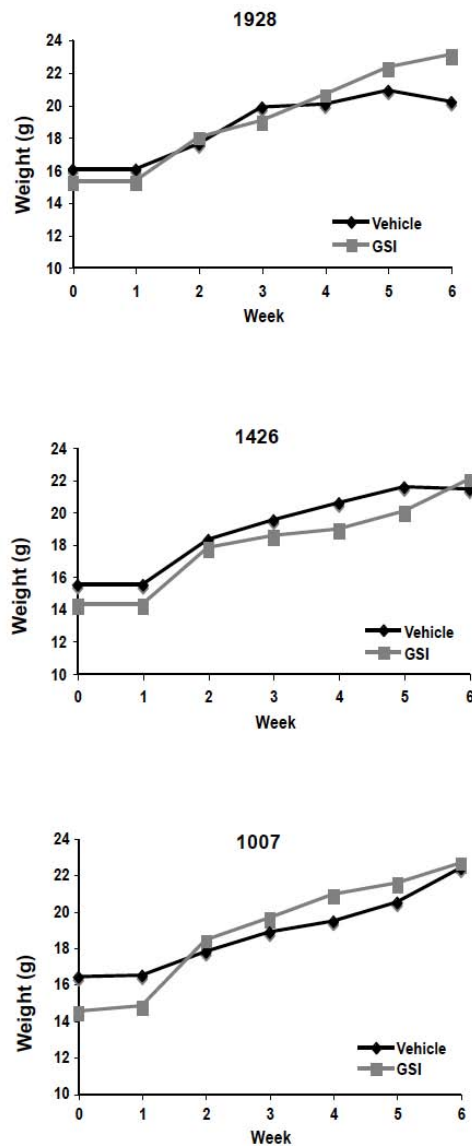


**Figure 14. Transplanted mice treated with GSI continued to gain weight throughout the treatment period.** Recipient mice transplanted with mouse T-ALLs 1928, 1426, and 1007 were treated with vehicle or 150mg/kg GSI (MRK-003) using an intermittent dosing regimen. Vehicle mice were given an equal volume of methylcellulose by oral gavage. The animals were weighed once per week, with GSI administered immediately following transplant and at 1 and 2 weeks post-transplant.

**Table 5. Notch1 inhibition reduces L-IC frequency and/or activity.**


Treatment	Number of Cells Injected			#diseased/ total	L-IC freq	CI
	100,000	10,000	1,000			
<b>Vehicle</b>	18/18	16/19	5/17	39/54	0.021%	0.036-0.013%
<b>GSI</b>	10/18	6/19	0/17	16/54	0.0011%	0.0019-0.0007%

**Table 6. Notch1 inhibition reduces L-IC frequency and/or activity.**

Cell Number	#Diseased mice/Total injected									
	1426		2544		3304		1928		1007	
	<u>Vehicle</u>	<u>GSI</u>	<u>Vehicle</u>	<u>GSI</u>	<u>Vehicle</u>	<u>GSI</u>	<u>Vehicle</u>	<u>GSI</u>	<u>Vehicle</u>	<u>GSI</u>
<b>100000</b>	3/3	0/3	4/4	0/4	4/4	4/4	4/4	3/4	3/3	3/3
<b>10000</b>	4/4	0/4	3/4	0/4	4/4	1/4	3/4	3/4	2/3	2/3
<b>1000</b>	0/3	0/3	1/4	0/4	4/4	0/4	0/3	0/3	1/3	0/3
<b>L-IC freq</b>	0.024%	N.D.	0.012%	N.D.	N.D.	0.003%	0.012%	0.003%	0.0149%	0.009%
<b>Fold change</b>	cure		cure		N.D.		4 fold		1.6 fold	

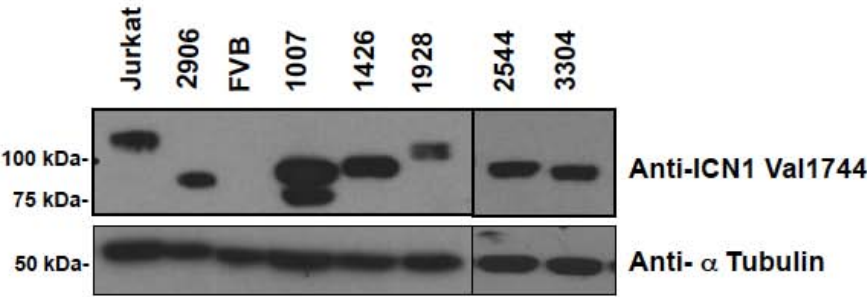
N.D. cannot calculate

**Table 7. Summary of GSI responses *in vivo*.**

	<div> <div>Complete Response</div>  <div>No Response</div> </div>				
	1426	2544	3304	1928	1007
<b>L-IC Frequency</b>	1:4,170	1:8,731	N.D.	1:8,731	1:6,695
<b>Mean Latency (days)</b>	51	39	24	21	17
<b>GSI Induced Cell Death</b>	24.1%	3.8%	16.4%	17.5%	1.1%



A



B

Tumor #	Genotype	Nucleic Acid Change	Amino Acid Change
1007	<i>Tal1/Lmo2</i>	7215 ins TTTT	2406 T->F
1426	<i>Tal1/Lmo2</i>	7161 C->G, ins G	2387 T-> R
1928	<i>Tal1/Lmo2</i>	7131 del G	2377 D->I
2544	<i>Tal1/Lmo2</i>	7162 del G, ins CCCTC	2388 A->P
3304	<i>Tal1/Lmo2</i>	7273 del G, ins AA	2425 G->K

C

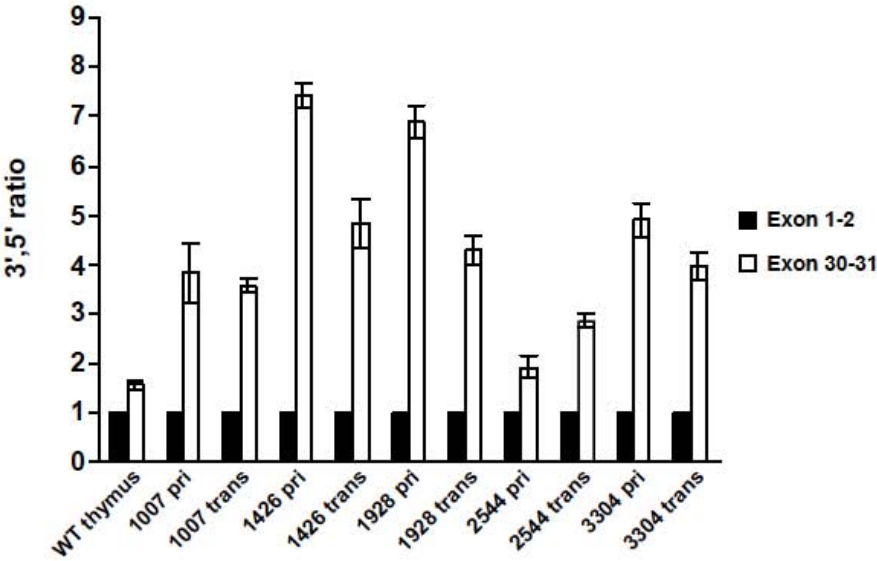


**Figure 15. Mouse T-ALLs examined in the GSI treatment study express high levels of intracellular Notch1, harbor insertions/deletions that result in PEST truncation and express aberrant 3' transcripts.** (A) Mouse T-ALL cell lysates were examined for intracellular Notch1 protein levels by immunoblotting with Notch1 Val1744 (Cell Signaling). Jurkat is a human T-ALL cell line that expresses full length ICN1; FVB is wild-type thymus; 2906 is a mouse tumor with truncated ICN1; 1007, 1426, 1928, 2544, and 3304 are the mouse *Lck-Tal1/Lmo2* T-ALLs examined in Figure 13. (B) DNA was isolated from the mouse TALLs and amplified with primers specific to exon 34 of the Notch1 gene. PCR product was cloned into the TOPO TA cloning vector for sequencing using the universal M13 primers. Mutations were then analyzed using MacVector software. (C) Ratiometric Notch1 quantitative RT-PCR analysis of mouse *Lck-Tal1/Lmo2* T-ALLs. The relative amounts of transcripts containing 5' (exons 1 and 2) and 3' (exons 30 and 31) Notch1 sequences were determined for primary tumors (pri) and transplanted tumors (trans) as previously described. Each determination was made in triplicate. (Data from section C performed by Todd Ashworth)

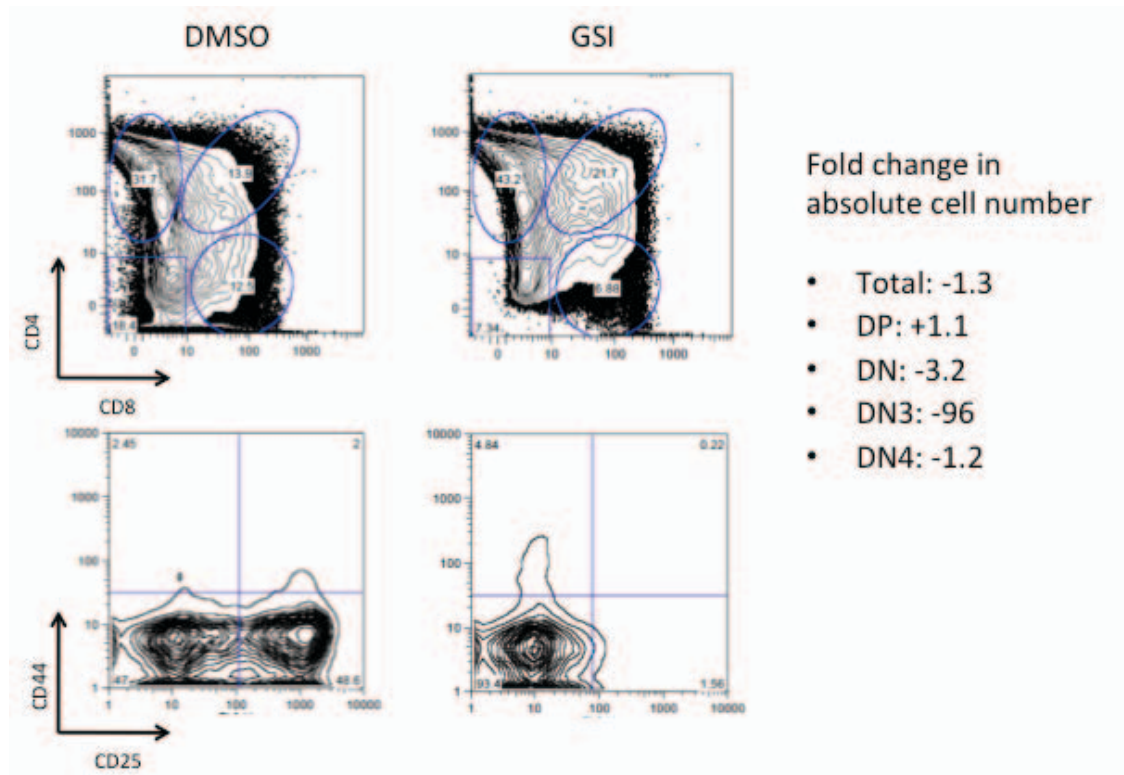


**Figure 16. GSI targets the L-IC population in *Lck-Tal1/Lmo2* T-ALLs.** Primary *Lck-Tal1/Lmo2* leukemic cells were treated with DMSO or GSI (Compound E) for 48 hours. Cells were counted using trypan blue exclusion, stained with CD4, CD8, CD25, and CD44 antibodies, and populations were analyzed by flow cytometry. Fold change in absolute number of each population are shown. Three T-ALLs were analyzed, one representative is shown. (This figure was presented for reviewers only)

## **CHAPTER IV**

**c-Myc silencing or inhibition prevents disease initiation in mice and impairs the growth of relapsed pediatric T-ALL cells**

Data from the following Chapter were a part of a manuscript not yet in print:

**Tesell, J.**, Roderick, J., Gutierrez, A., Qi, J., Brehm, M., Greiner, D., Look, A. T., Bradner, J.E., Kelliher, M. (2013) c-Myc inhibition prevents disease initiation in mice and impairs the growth of relapsed pediatric T-ALL cells. *J. Exp. Med.*, *in preparation*.

The manuscript has been edited for this thesis so that the results only include experiments performed by Jessica Tesell; data generated by others are noted.

## Introduction

We have demonstrated that Notch1 inhibition reduces the L-IC population and prevents disease initiation in our mouse T-ALL model (Chapter III). In this same model, we have shown that the L-IC is a subset of the DN3 population<sup>251</sup>. At this stage in development, Notch1 and its target gene c-Myc are critical for thymocyte differentiation. In the absence of either Notch1 or c-Myc, thymocyte development is blocked at the DN3 stage<sup>210,319,423,430,431</sup>. c-Myc in particular is critical for the expansion of DN3 cells to DN4 and DP cells<sup>319</sup>. These data led us to hypothesize that Notch1 may be acting through c-Myc in the leukemic DN3 cells to promote L-IC expansion and survival.

Notch1 regulates proliferation by directly stimulating c-Myc and Cyclin D3 expression<sup>110,170,172,259</sup> and by inhibiting the p53 pathway and cyclin dependent kinase inhibitors such as p21 and p27(reviewed in<sup>74</sup>). Retroviral expression of c-Myc had been shown to rescue mouse and human T-ALL cells from the effects of NOTCH1 inhibition<sup>110,172</sup>. As discussed in Chapter I, two recent reports have shown that c-Myc universally amplifies transcription. In contrast to conventional thinking, it is thought that c-Myc does not regulate the transcription of a set of target genes. Instead, c-Myc is able to amplify the transcription of active genes in a given cell type by binding E-box sites in “open” chromatin<sup>325,326</sup>.

These findings led us to hypothesize that c-Myc inhibition may interfere with multiple biological processes associated with L-ICs including extensive proliferation, survival and self-renewal, as well as metabolic and/or epigenetic

changes associated with drug resistance. In this Chapter, we used specific shRNAs to c-Myc as well as a pharmacological approach to examine the role of c-Myc in the murine T-ALL L-IC.

## Results

### ***c-Myc silencing prolongs survival and reduces the frequency of leukemia-initiating cells***

To test a requirement for c-Myc in L-IC expansion and self-renewal *in vivo*, we infected primary mouse T-ALLs with retroviruses encoding shRNAs to c-Myc or Renilla luciferase, with a separate promoter driving GFP expression. GFP-positive leukemic cells (Figure 17) were transplanted into syngeneic recipients and an *in vivo* limiting dilution assay performed to estimate L-IC frequency, as described previously<sup>251</sup>. In 3 of 4 primary mutant-*Notch1* mouse T-ALLs examined, silencing of c-Myc resulted in statistically significant increases in overall survival (Figure 18A-C) and an overall 17-fold decrease in L-IC frequency (Table 8).

None of nine mice transplanted with c-Myc silenced leukemic cells from mouse T-ALL 4673 developed disease, whereas 100% of the mice (n=9) transplanted with the Renilla transduced leukemic cells succumbed to disease with a mean latency of 28 days (Figure 18A;  $p < 0.0001$ ; Table 9). Since all of the mice transplanted with the control cells developed disease and c-Myc silencing completely interfered with leukemia initiation in transplanted mice, we were unable to estimate the fold reduction in L-IC frequency. We found no evidence of leukemia in the surviving mice, nor were GFP-positive cells detected in the bone marrow (Figure 21), suggesting that the L-ICs had been eliminated in these mice.



c-Myc suppression in mouse T-ALLs 5109 and 5059 also resulted in significant increases in overall survival (Figure 18B and C), with 4 and 6-fold reductions in L-IC frequency, respectively (Table 9). These studies reveal that c-Myc mediates L-IC survival and/or expansion *in vivo*.

In contrast, c-Myc inhibition in mouse T-ALL 6124 had no statistically significant effect on survival or L-IC frequency (Figure 18D  $p < 0.33$  and Table 9). At the time of transplant, all 4 mouse T-ALLs examined showed a similar reduction in c-Myc protein levels (Figure 19A, B average 47%, range 43-70%) and sort purity was consistently between 94-99% (Figure 17). Since a similar reduction in c-Myc protein levels was achieved (Figure 19 A/B), it is unclear why c-Myc suppression was less effective *in vivo* in this mouse T-ALL. One possibility is that leukemia 6124 is less dependent on c-Myc for its growth. To examine this possibility, remaining GFP-positive leukemic cells were cultured short-term *in vitro*. In the three mouse T-ALLs examined, c-Myc silencing interfered with growth *in vitro* and depleted the cultures of viable leukemic cells (Figure 19C). The increase in cell number observed in the shMyc-transduced 6124 cells reflected the emergence of GFP-negative or non-silenced leukemic cells (not shown). In spite of the variability observed *in vivo* (Figure 18), the growth of the 3 mouse T-ALLs examined including 6124 appeared similarly c-Myc dependent *in vitro* (Figure 19B). This likely reflects silencing of the LTR driving the expression of the shRNA *in vivo*.

***Tumors that develop from the transplantation of shMyc-transduced leukemic cells escape shRNA silencing.***

When animals became diseased after primary transplant, GFP and c-Myc expression levels were examined in tissues infiltrated with leukemic cells. In most transplanted mice, the leukemic cells remained GFP-positive and harbored the retroviral provirus (Table 10). One of fifteen mice transplanted with c-Myc-silenced 5059 leukemic cells developed GFP-negative disease and the proviral DNA was not detected; indicating that disease in this animal likely resulted from the expansion of contaminating GFP-negative leukemic cells that were not transduced with the retrovirus.

Eleven of 39 mice transplanted with shMyc-transduced cells developed disease but appeared to express c-Myc at levels similar to that observed in the Renilla-transduced leukemic cells (Figure 20A), suggesting that c-Myc suppression was not maintained in these diseased mice. The leukemic cells retained GFP expression (Figure 20B), but showed no detectable decrease in c-Myc RNA levels (Figure 20A and not shown). The LTR driving the expression of the c-Myc shRNA may have been silenced, leaving the PGK promoter driving expression of GFP intact (Figure 20C). Promoter methylation is common when using murine retroviruses that drive expression with an LTR. We saw an approximate 10-fold GFP fluorescence intensity in the recipient animals compared to pre-transplant (Figure 17 vs. Figure 20B), consistent with the loss of

transcription from the LTR. Thus, those mice transplanted with shMyc-transduced cells that developed disease escape from c-Myc-silencing, supporting our data that c-Myc is required for leukemia initiation.

### ***c-Myc mediates L-IC self-renewal***

In order to determine whether the Notch1-c-Myc pathway mediates L-IC self-renewal, we sacrificed the primary transplants that failed to develop disease after 120 days. Consistently, we were unable to detect GFP-positive leukemic cells in the spleen or bone marrow of these mice by flow cytometry (Figure 21 and data not shown). To further demonstrate that c-Myc silencing depletes the L-IC population and does not induce arrest or quiescence, bone marrow cells were pooled from primary transplants and  $5 \times 10^6$  cells were transplanted into secondary recipients. The secondary transplants were then monitored for evidence of disease for an additional period of 120 days. None of the 17 secondary recipients developed leukemia (data not shown), suggesting that c-Myc is required for the perpetuation or self-renewal of the L-IC.

### ***JQ1 treatment rapidly induces apoptosis of murine T-ALL cell lines in vitro.***

Although these c-Myc shRNAs have been reported to suppress c-Myc expression *in vivo*<sup>331</sup>, shRNAs can have off-targets effects<sup>432–434</sup>, which could have effects on L-IC activity. Therefore we also undertook a pharmacological approach to inhibit c-Myc using the bromodomain-4 (Brd4) inhibitor JQ1 developed by James Bradner and Jun Qi at DFCI. While not a specific c-Myc

inhibitor, JQ1 has been shown to reduce c-Myc mRNA and protein in hematologic malignancies<sup>435</sup>. Treatment with gamma secretase inhibitors (GSI) to prevent Notch1 activation reduces c-Myc expression. However, when human T-ALL cell lines are treated with GSI *in vitro*, it is growth arrest and not apoptosis that is primarily observed<sup>110,172,260,436</sup>. Agents that induce cell cycle arrest are not considered ideal cancer therapeutics, as they fail to induce apoptosis and may contribute to the development of drug resistance. Moreover, chronic GSI administration is associated with gastrointestinal toxicity due to on-target effects of Notch inhibition in the intestine<sup>207,437</sup>.

We hypothesized that JQ1 treatment may have greater anti-leukemic activity than to GSI on mouse T-ALL proliferation and survival *in vitro*. We treated mouse *Tal1/Lmo2* T-ALL cell lines with the GSI compound E (1uM) or with 250nM JQ1 for 24, 48 and 96 hours. We performed cell cycle analyses, monitored cell growth and viability and quantified the number of apoptotic leukemic cells. JQ1 treatment for 24 or 48 hours induced G0/G1 cell cycle arrest (Figure 22A and B) followed by an increase in subG1 cells evident at 96 hours (Figure 22B). In contrast and as expected, GSI-induced cell cycle arrest was detected at 96 hours (Figure 22B, third panel  $p < 0.0098$ ) with no significant increases in subG1 or Annexin V-positive leukemic cells (Figure 22B-D). Overall, JQ1 treatment reduced the proliferation of all 4 murine T-ALL cell lines examined (Figure 22C) and induced apoptosis by 96 hours (Figure 22D) GSI treatment arrested mouse leukemic growth but failed to induce apoptosis (Figure 22C,D).

This is in contrast to our published studies on *Lck-Tal1* mouse T-ALLs and cell lines, which undergo apoptosis following GSI treatment for 72 hours<sup>110</sup>.

To compare the effects of GSI or JQ1 treatment on c-Myc expression levels, mouse T-ALL cell lines were treated with DMSO, compound E (1 $\mu$ M) or increasing concentrations of JQ1 for 48 hours and c-Myc mRNA levels quantified by quantitative PCR. Optimal reductions in c-Myc mRNA levels were observed in leukemic cells treated with 250nM JQ1 (Figure 22E). Notably, similar reductions in c-Myc RNA levels were also observed in the GSI treated cultures (Figure 22E). We examined the expression of additional c-Myc target genes to determine if JQ1 treatment reduced c-Myc activity. Expression of four c-Myc target genes (*Cdk4*, *Apex1*, *Fbl*, and *Tk1*) were decreased upon JQ1 treatment (Figure 23), indicating that the c-Myc transcriptional program was impaired. These data suggest that JQ1 can be used as a tool to modulate c-Myc expression, although other genes are probably also targeted with JQ1 treatment.

Although GSI treatment resulted in an average 7-fold (range 3.8-11) reduction in intracellular Notch1 expression, more modest effects on c-Myc protein levels (average 1.5-fold, range 1.2 – 2.3) were observed in the GSI-treated cultures compared to controls (Figures 22F, 22G). In contrast, JQ1 treatment resulted in an average 4.3-fold decrease in c-Myc protein levels (Figures 22F, 22G, range 1.8 – 8.6). In sum, the mouse T-ALL cell lines appeared more sensitive to the effects of JQ1 treatment than to GSI *in vitro*.

### ***JQ1 treatment prolongs mouse T-ALL survival in vivo***

Treatment of mouse *Tal1/Lmo2* T-ALL cells with JQ1 *in vitro* induced apoptosis of the leukemic cells (Figure 22), suggesting that JQ1 treatment may extend the survival of leukemic mice. To examine the effects of JQ1 treatment on leukemic initiation, mice were transplanted with  $10^5$  leukemic cells and either vehicle or JQ1 was administered for three weeks. Mice were monitored for evidence of disease and effects of treatment on disease initiation and overall survival were determined. JQ1 treatment resulted in significant increases in overall survival in the 3 mouse T-ALLs examined (Figure 24; 8236 and 7624  $p < 0.0001$  and 7118  $p < 0.008$ ). JQ1 treatment prevented disease initiation in all 10 mice transplanted with cells from mouse T-ALL 8236 and in 8 of 10 JQ1 treated mice transplanted with leukemic cells from mouse T-ALL 7624. Although JQ1 treatment extended the survival of mice transplanted with leukemia 7118 ( $p < 0.008$ ), no significant effect on disease penetrance was observed. JQ1 treatment prolonged the survival of the transplanted mice, revealing that the inhibitor has clear anti-leukemia activity in mice and in some cases, the data suggested that JQ1 might interfere with disease initiation *in vivo*.

### ***JQ1 targets the mouse L-IC***

JQ1 treatment has been shown to interfere with c-Myc activity and reduce tumor cell line growth in conventional xenograft models of several hematological malignancies<sup>307,308,331,435,438</sup>, however its effect(s) on leukemia stem or -initiating

cells or on models of relapse has not yet been addressed. In order to quantify JQ1 effects on mouse L-IC frequency and/or activity, we transplanted three independent murine T-ALLs into recipient mice under *in vivo* limiting dilution conditions. Mice were then treated daily with vehicle or 50mg/kg of JQ1 for three consecutive weeks and transplanted mice were monitored for development of disease. JQ1 treatment reduced estimated L-IC frequencies (as measured by Poisson statistics) in all three mouse T-ALLs examined by an average of 9.3-fold (Table 11). JQ1 administration also significantly prolonged the survival of mice transplanted with mouse T-ALLs 7162 and 7116 (Figure 25  $p < 0.05$  and Table 12), where L-IC frequency decreased by 24-fold and 14-fold, respectively. However, in JQ1 treated mice transplanted with 7474 leukemic cells where L-IC activity was reduced only 3-fold, no significant effects on disease latency were observed (Figure 25  $p < 0.28$  and Table 12).

Overall, fifteen of thirty-two (47%) mice treated with vehicle developed disease whereas five of thirty-three mice (15%) treated with JQ1 succumbed to T-ALL (Table 11). To determine whether the JQ1 treated mice that developed disease remained responsive to the inhibitor, leukemic mice were given a single dose of vehicle or JQ1 prior to sacrifice and c-Myc mRNA levels quantified using real time quantitative PCR. We found c-Myc mRNA levels significantly reduced in the JQ1 treated mice compared to vehicle treated controls, indicating that the leukemic cells remained responsive to the inhibitor (in terms of c-Myc repression) and had not developed resistance *in vivo* (Figure 24D). Disease recurrence in the

JQ1-treated mice could reflect compound instability in mice<sup>435</sup> or indicate that treatment for 3 weeks is not sufficient and that continuous JQ1 administration may be required for complete remission.



## Discussion

c-Myc silencing by an shRNA approach or a non-specific pharmacologic approach to inhibit c-Myc reduces L-IC frequency and prevents disease initiation in most primary recipients (Figures 18, 24, and 25). Bone marrow cells isolated from primary recipients who failed to develop disease were pooled and transplanted into secondary recipients. None of these animals (n=17) developed disease, arguing that c-Myc suppression or inhibition eliminates the L-IC in these mice or interferes with the ability of these cells to self-renewal. In the c-Myc shRNA studies, transduced cells expressed GFP and GFP-positive cells could not be detected in primary or secondary recipients (Figure 21). These studies suggest that c-Myc suppression eliminates the L-IC population and reveal a critical role for c-Myc in mouse L-IC survival (or activity). These data also suggest that JQ1 may prove beneficial for T-ALL patients, either added to induction therapy or as a means to treat induction failure and relapse.

Consistent with its role as an amplifier of gene expression<sup>325,326</sup>, inhibiting c-Myc should also result in reduced expression of the genes already active in T-ALL. Classically, c-Myc was thought to control metabolism and cell growth, as well as proliferation, but it could also contribute to the activation of other self-renewal genes in the L-IC. While we do not yet have evidence that the T-ALL L-IC is quiescent, it is possible that c-Myc and its cell cycle target genes are able to push the L-ICs into S-phase in order to proliferate and initiate disease. Similarly,

c-Myc could control the metabolism of these cells resulting in a perfect balance of growth and quiescence.

Self-renewal of T-ALL L-ICs likely involves several pathways and thus c-Myc inhibition could be an efficient way to target many or possibly all of them. Administration of JQ1 to cell lines and to mice inhibits c-Myc expression and has effects on cell cycle, growth, ribogenesis, and nucleotide metabolism (reviewed in<sup>282</sup>), all of which could play a role in the generation or maintenance of T-ALL L-Cs. Of course, all these effects of JQ1 may not be directly due to c-Myc suppression, but also due to other genes affected by the compound.

JQ1 treatment significantly impaired the growth of murine T-ALL cell lines and was more effective at achieving cell cycle arrest and apoptosis than GSI (Figure 22). Although GSI treatment is expected to reduce intracellular Notch1 and c-Myc protein levels<sup>110,251,261</sup>, c-Myc protein levels were approximately 3-fold more reduced in the JQ1 treated mouse T-ALL cells than the GSI treated cells *in vitro*. Human T-ALL cell lines were also more sensitive to JQ1 than GSI treatment where 2-3 fold increases in apoptotic cells were observed in JQ1-treated cultures compared to GSI (Justine Roderick, data not shown). This may reflect more complete c-Myc inhibition in the JQ1 treated cells, where Notch1 independent pathways of c-Myc activation are also inhibited. Alternatively, other Brd4-dependent targets may be affected in the mouse leukemic cells.

Interestingly, we found that JQ1 was also able to reduce Notch1 target genes in addition to c-Myc target genes. Hes1, and PreT $\alpha$  expression were both significantly decreased upon JQ1 treatment (Figure 23). Notch1 mRNA was unaffected by JQ1 treatment, and protein levels were decreased in some lines, but not significantly reduced overall (Figure 22 F, H). It is possible that JQ1 is able to affect the processing of the Notch1 protein through downregulation of the proteases responsible for its maturation. This would result in decreases in Notch1 protein and its target genes, but not the mRNA. Alternatively, these Notch1-regulated genes may also be Brd4 dependent.

In the c-Myc shRNA experiments, the 4-6 fold differences in L-IC frequency observed in T-ALLs 5109 and 5059 had significant effects on disease latency (Figure 18 and Table 9). In contrast, transient JQ1 treatment resulted in 3-fold reductions in L-IC frequency in T-ALL 7474, but did not significantly extend survival (Figure 25 and Table 11). Presumably, the JQ1 treatment did not eliminate all of the L-ICs in this T-ALL, leaving these cells able to initiate disease once treatment had ceased.

T-ALL 6124 did not respond significantly to c-Myc silencing *in vivo*, but we do not believe that this is due to c-Myc independence. When transduced with c-Myc shRNA or treated with JQ1 *in vitro*, T-ALL 6124 exhibited reduced proliferation and increased apoptosis. It is likely that the c-Myc shRNA was silenced rapidly *in vivo*, resulting in re-expression of c-Myc and thus disease

initiation. Likewise, disease initiation was not impaired when T-ALL 7118 was treated with JQ1 *in vivo*, but JQ1 was able to reduce c-Myc mRNA and significantly extend disease latency. *In vitro*, T-ALL 7118 responded with similar kinetics as T-ALL cell lines 4673 and 5109 (Figure 26), again indicating that this T-ALL is JQ1-sensitive.

These findings reveal a central role for c-Myc in murine L-IC growth and survival. It remains to be determined whether JQ1 treatment targets the human L-IC *in vivo* but our data indicate that JQ1 is able to increase survival of mice engrafted with relapsed or IF T-ALL cells (Justine Roderick, data not shown). It is not clear from these studies whether c-Myc has a distinct role in the L-IC as compared to the leukemia as a whole. *In vitro* studies demonstrate a clear role for c-Myc in the growth and survival of T-ALL cells (Figures 19 and 22) while *in vivo* studies establish a necessity for c-Myc in the initiation of T-ALL in recipient mice (Figures 18 and 24). The precise c-Myc target genes involved in each of these biological processes are likely different, but are not currently understood.

## Methods

### Mice

*Tal1/Lmo2* transgenic mice were maintained and monitored daily for development of leukemia<sup>112,251</sup>. All animal procedures used in this study were approved by The University of Massachusetts Medical School Institutional Animal Care and Use Committee.

### *In vivo* studies

To estimate the effects of c-Myc silencing or JQ1 treatment on L-IC frequency, *Tal1/Lmo2* mouse T-ALLs were each serially diluted and transplanted into syngeneic recipient as described previously<sup>251</sup>. For shRNA studies, cells were sorted for GFP expression 48 hours post retroviral infection, serially diluted and transplanted into syngeneic recipient mice. For JQ1 studies, recipient mice were injected IP with vehicle (10:90 DMSO:10%hydroxypropyl-beta-cyclodextrin)(Sigma) or 50mg/kg JQ1 daily for 3 weeks. Mice were monitored for any signs of drug toxicity and sacrificed when disease was evident. L-IC frequency was calculated using Poisson distribution analysis and the ELDA software<sup>414</sup>.

### Cell culture

Primary mouse *Tal1/Lmo2* T-ALL cells were plated in RPMI with 20% FBS, 1% pen/strep and 1% L-glutamine (Gibco). IL7 (2ng/ml), Flt3L (5ng/ml) and SCF (10ng/ml) (R&D) were added to the culture media every 2-3 days until the

leukemic cells adapted to *in vitro* culture (approximately 2 weeks). At this time, cells were infected with retroviruses<sup>439</sup> encoding shRNA to c-Myc or Renilla luciferase. Leukemic cells were spininfected for 15 minutes with neat virus plus 20% serum and cytokines. Fresh media was added after 5 hours of incubation at 37°C.

### **FACS analysis**

Single-cell suspensions of *Tal1/Lmo2* leukemic cells were stained with cell surface antibodies and analyzed as previously described<sup>251</sup>. For *in vivo* shRNA studies, retrovirally transduced leukemic cells were sorted for GFP expression on the FACS Aria (BD Biosciences). For cell cycle analysis, leukemic cells were fixed in 70% ethanol overnight and then were stained with PI for DNA quantification.

### **Immunoblotting**

To monitor c-Myc expression levels, leukemic cells were lysed in RIPA buffer and total protein run on a 4-12% Bis-Tris gel (Invitrogen). Nitrocellulose membrane was probed with antibodies to c-Myc clone N262 (Santa Cruz), Notch1 Val1744 (Cell Signaling), and Erk1/2 loading control (Cell Signaling). Blots were imaged and quantified using ImageLab Software (BioRad).

### **Expression analyses**

RNA was extracted and cDNA synthesized as previously described; cDNA was quantified using specific c-Myc primers<sup>251</sup>. The copy number of c-Myc was normalized to the copy number for  $\beta$ -actin using the  $\Delta\Delta$ CT method. For *in vivo* target validation, mice were treated with a single dose of vehicle or JQ1

(50mg/kg) and leukemic tissues were harvested 2 hours later and analyzed as above.

DNA was isolated from recipient mice in shRNA study using Trizol (Invitrogen). Primers were designed against GFP (F: 5'-TATATCATGGCCGACAAGCA-3'; R: 5'-CCTACAGGTGGGGTCTTTCA-3') and standard qualitative PCR was performed with Taq polymerase. The amplification was performed using a Stratagene Robocycler Gradient starting with a 5-minute 95°C denaturation, followed by 30 cycles consisting of 1 minute at 95°C, 1 minute at 57°C, and 1 minute at 72°C with a final elongation at 72°C for 10 minutes. PCR products were run on a 1% agarose gel and imaged with UV light.

### **Cell viability and death assays**

*Tal1/Lmo2* leukemic cell lines were treated with 1uM Compound E (Alexis) or with increasing doses of JQ1 (Bradner, DFCI). The number of viable leukemic cells was calculated after 48 and 96 hours using a trypan blue exclusion assay. Cell cycle analysis was performed at 48 and 96 hours following treatment by staining cells with propidium iodide followed by flow cytometry. Metabolic activity was assayed after five days by the addition of CellTiter-Glo chemiluminescence reagent (Promega) and measured using a Beckman Coulter DTX 880 plate reader. Absorbance values were normalized to DMSO control for each patient sample and cell lines.

### **Statistical measures**

Kaplan-Meier survival curves and statistical analyses were performed

using GraphPad Prism software, Version 5.0. The hazard ratio and its 95% confidence interval was also measured, comparing the c-Myc and Renilla shRNA groups or vehicle and JQ1 treated groups and adjusting for the dilutions of leukemic cells, using the Cox proportional hazards model analysis. A 2-sided  $P < 0.05$  was considered statistically significant. Student's t-tests were performed on proliferation and Annexin V data using GraphPad Prism software, Version 5.0.



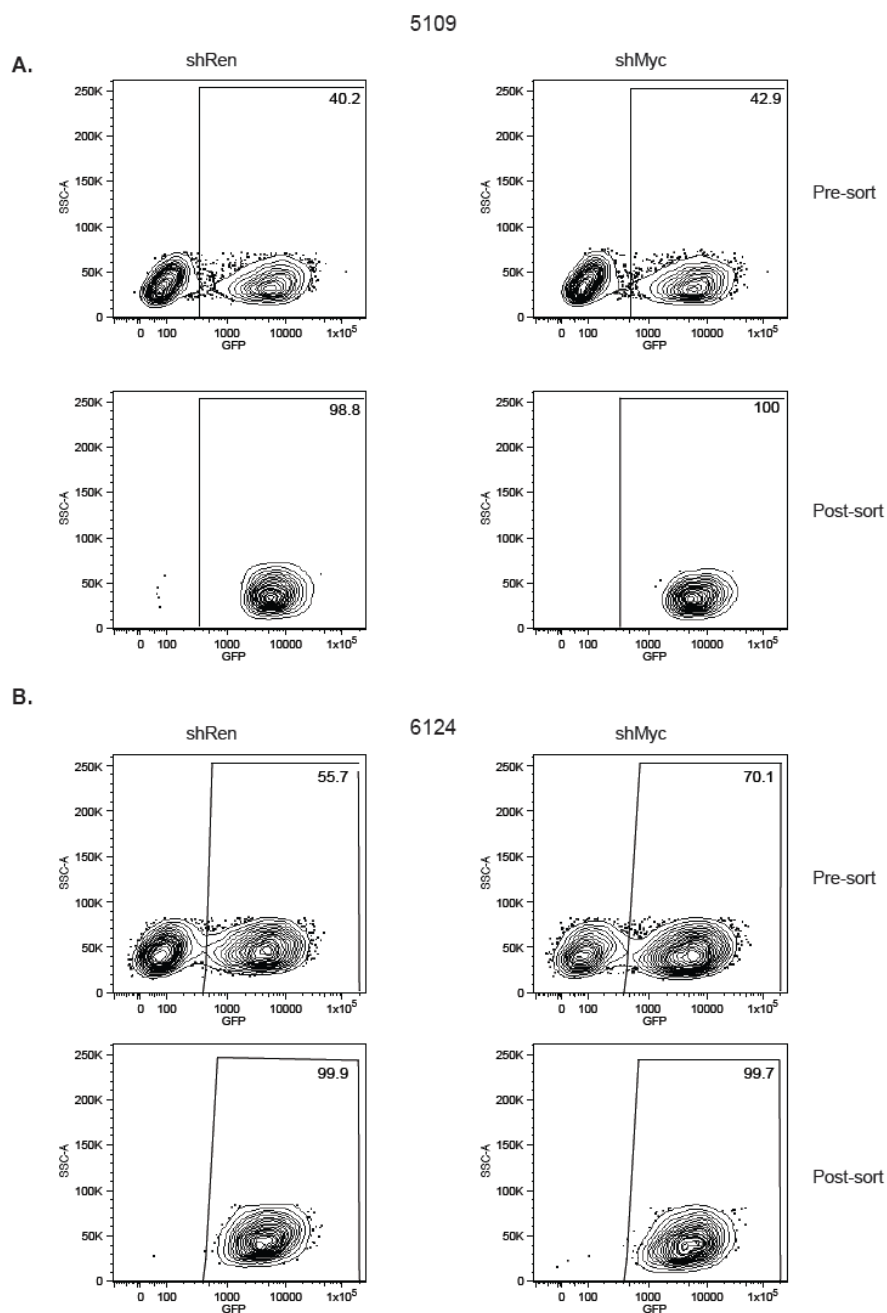


**Figure 17. Sort purity of shRNA-infected leukemic cells prior to transplant.** Post-infection with retrovirus, cells were sorted on a FACS Aria (BD Biosciences) for GFP expression. Percent of GFP-positive cells before and after sorts are shown for tumors **A** 5109 and **B** 6124.

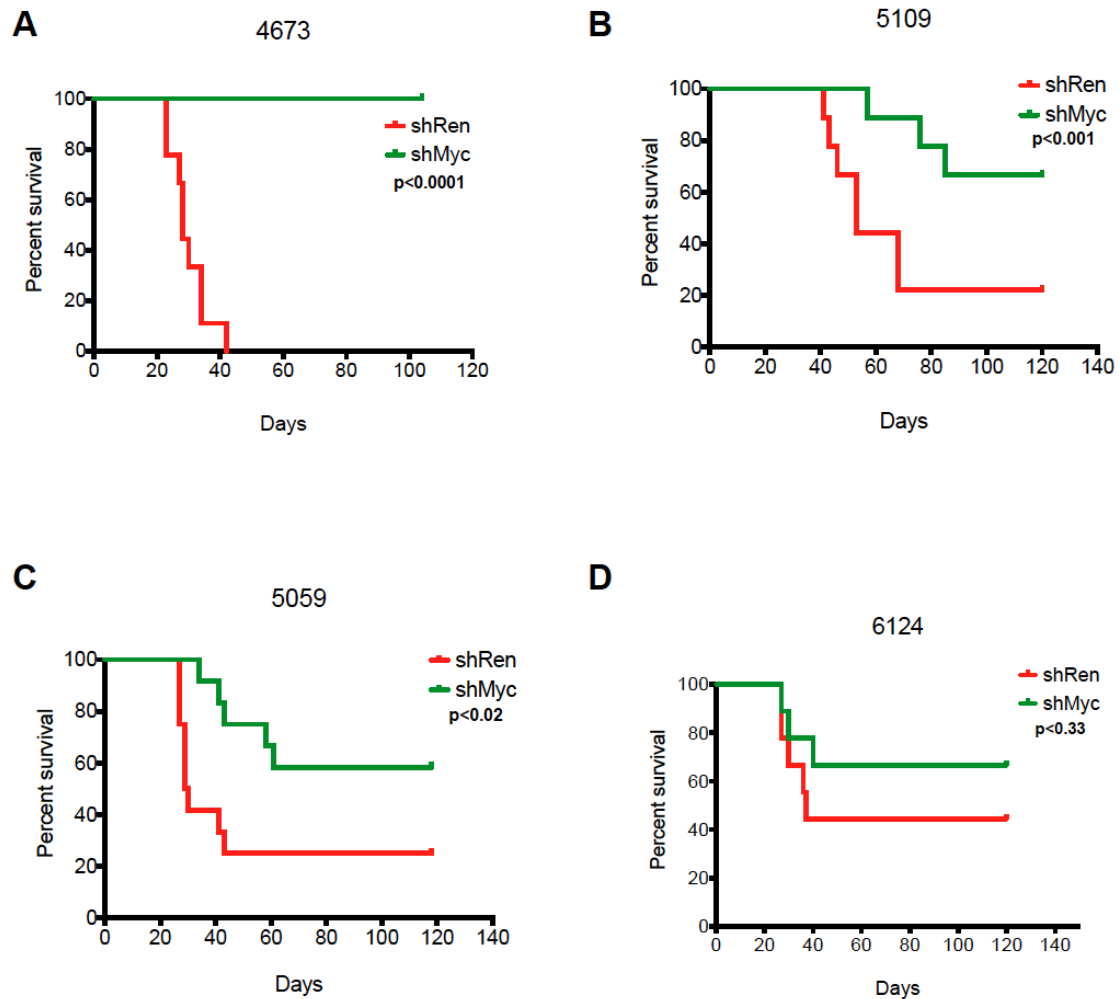


**Figure 18. Silencing of c-Myc prolongs survival in mice transplanted with murine T-ALL cells.** Four independent murine *Tal1/Lmo2* T-ALL cells were infected with retroviruses encoding an shRNA to c-Myc or Renilla luciferase. Cells were sorted for GFP expression, serially diluted and transplanted into syngeneic recipients via intraperitoneal (IP) injection. Transplanted mice were monitored for evidence of disease. The survival curve for each group of mice was estimated using the Kaplan-Meier method and the difference in overall survival between the two groups assessed by the log-rank test. **A** 4673  $p < 0.0001$ , **B** 5109  $p < 0.02$ , **C** 5059  $p < 0.024$ , **D** 6124  $p = 0.33$ .

**Table 8. Silencing of c-Myc reduces L-IC frequency.**

shRNA	Number of Cells Injected				#diseased/ total	L-IC freq	CI
	100,000	10,000	1,000	100			
<b>shRen</b>	6/7	10/13	8/13	4/6	28/39	0.034%	0.064-0.018%
<b>shMyc</b>	5/7	4/13	2/13	0/6	11/39	0.002%	0.004-0.001%

CI: Confidence Interval

Table 9. Silencing of c-Myc reduces L-IC frequency.

Cell #	#Diseased mice/Total injected							
	4673		5109		5059		6124	
	shRen	shMyc	shRen	shMyc	shRen	shMyc	shRen	shMyc
100000	--	--	2/3	1/3	4/4	4/4	--	--
10000	3/3	0/3	2/3	1/3	3/4	0/4	2/3	3/3
1000	3/3	0/3	1/3	1/3	2/4	1/4	2/3	0/3
100	3/3	0/3	--	--	--	--	1/3	0/3
L-IC freq	N.D.	N.D.	N.D.	0.0007%	0.02%	0.0034%	N.D.	0.023%
Fold Change	cure		N.D.		5.8-fold		N.D.	

N.D. Cannot calculate

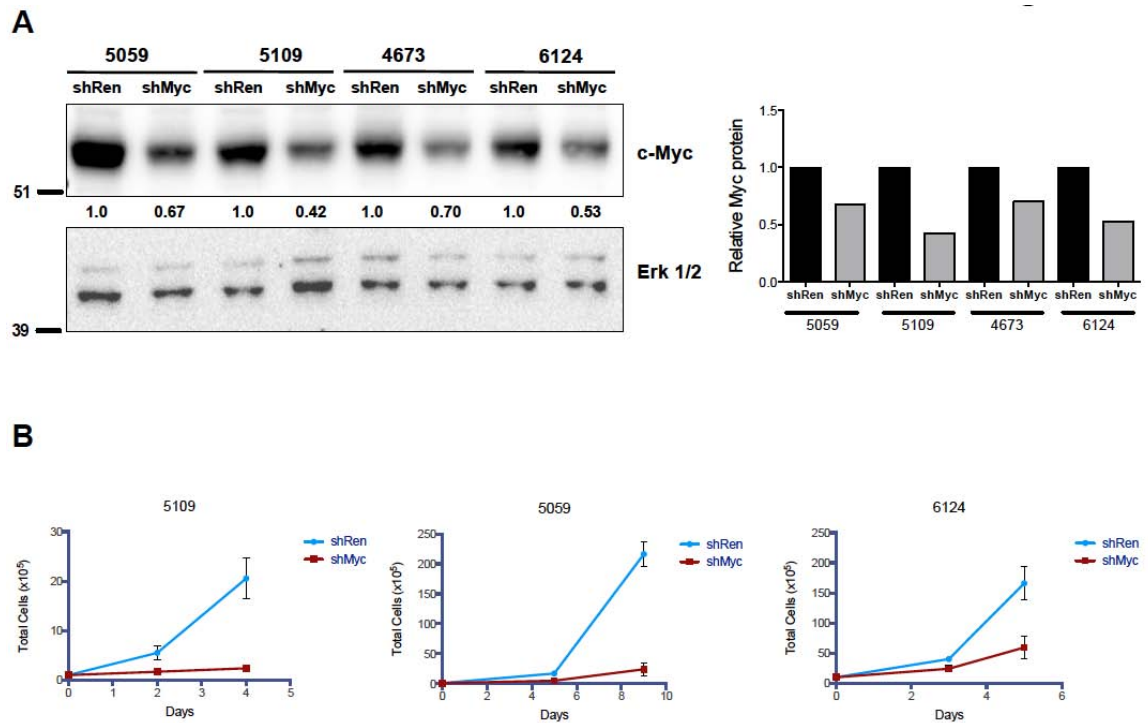


**Figure 19. Reduced c-Myc protein levels and impaired growth in vitro in c-Myc-silenced leukemic cells.** **A.** Reduced c-Myc protein levels in c-Myc-silenced leukemic cells. Protein was isolated from murine *Tal1/Lmo2* T-ALLs infected with retroviruses encoding shRNAs to c-Myc or Renilla luciferase and c-Myc and Erk1/2 protein levels were determined by immunoblotting. **B. c-Myc suppression impairs bulk leukemic growth in vitro.** Cell viability was calculated via a trypan blue exclusion assay. Four independent mouse T-ALLs were analyzed; three are shown.

Table 10. Most leukemic mice contained GFP+ and proviral+ cells.

Mouse T-ALL	# GFP+ mice/ total	# Proviral+ mice/ total
5059	3/5	4/5
5109	2/3	3/3
4673	0/0	N.D
6124	3/3	N.D

N.D. not done

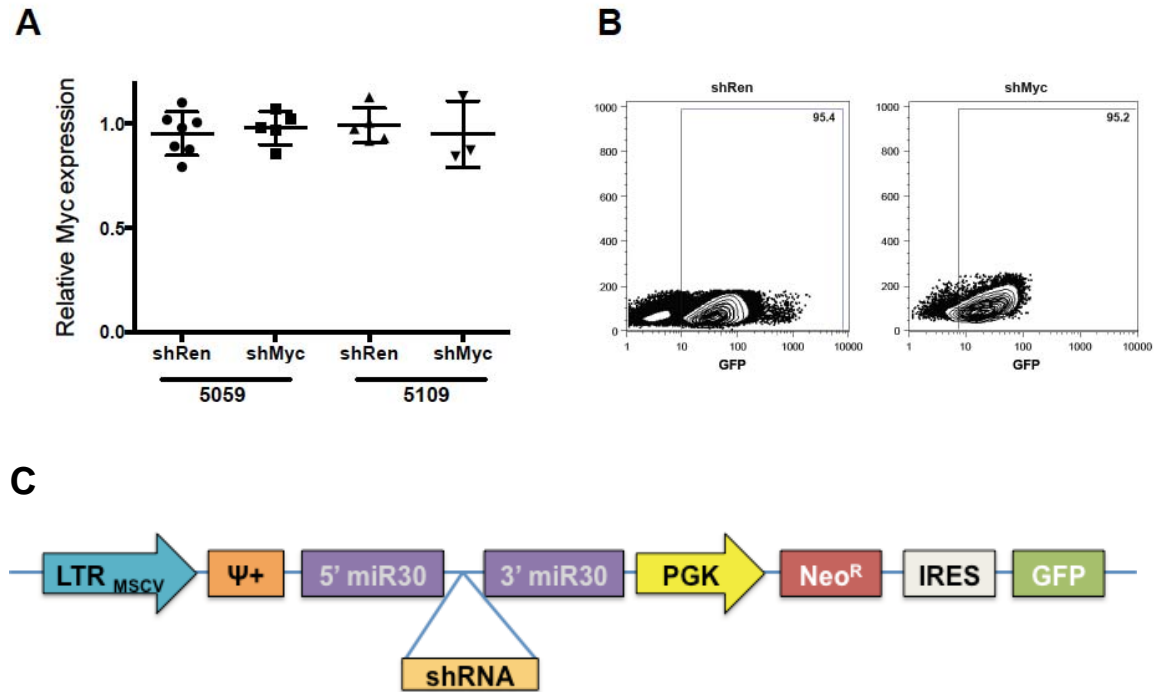


**Figure 20. Myc-silenced mice that develop disease contain GFP+ cells but do not exhibit Myc knockdown.** **A.** Mouse leukemic cells were isolated from mice transplanted with shRen or shMyc infected mice. RNA was isolated and *c-Myc* mRNA levels determined by quantitative real time PCR. Copy number was normalized to  $\beta$ -actin using the  $\Delta\Delta$ CT method. Each point represents a single mouse examined. **B.** Leukemic tissues were dissociated into a single cell suspension and GFP expression determined by flow cytometry. One representative from each group of tumor 5059 is shown. **C.** Map of pLMN vector used in these studies.

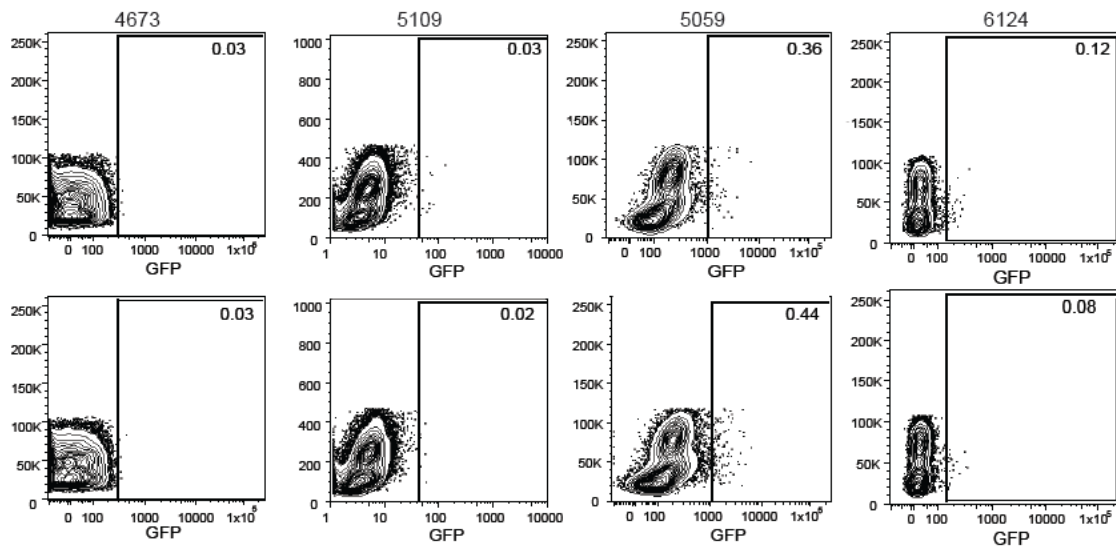


**Figure 21. No GFP-positive cells remained in transplanted animals 120 days post-transplant.** Mice that failed to develop disease 120 days post-transplant were sacrificed. Bone marrow cells were isolated and analyzed by flow cytometry. No GFP-positive cells were present in any animals examined. Two representative mice from each group are shown.



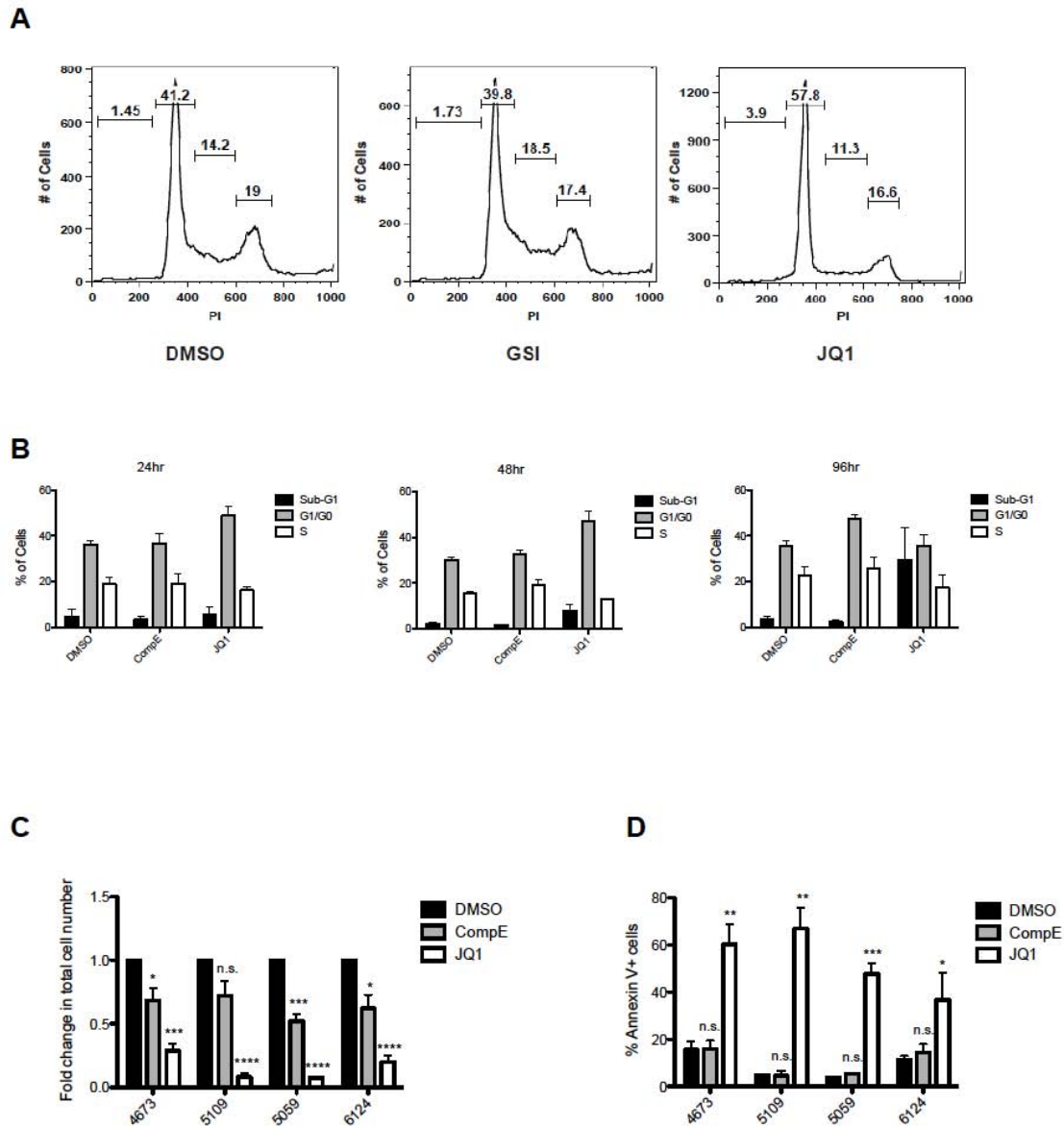


**Figure 22. JQ1 treatment induces rapid cell cycle arrest and apoptosis of murine T-ALL cells.** Murine T-ALL cell lines were treated with JQ1 (250nM) or with Compound E (1uM), unless otherwise noted. **A.** Murine T-ALL cell lines were left untreated or treated with JQ1 or compound E for 24 hours and then stained with propidium iodide followed by flow cytometry. One representative plot from mouse T-ALL 5109 is shown. **B. JQ1-induced cell cycle arrest is evident at 24 hours.** Murine T-ALL cell line 5109 was treated with JQ1 or compound E for 24, 48 and 96 hours and the percentage of cells in subG1, G0/G1 and S phases determined. **C. Mouse T-ALL cell lines are more sensitive to treatment with JQ1 than GSI.** Four mouse T-ALL cell lines (4673, 5109, 5059 and 6124) were treated with DMSO, JQ1 or compound E for 96 hours and the total number of viable cells was calculated via trypan blue exclusion assay.

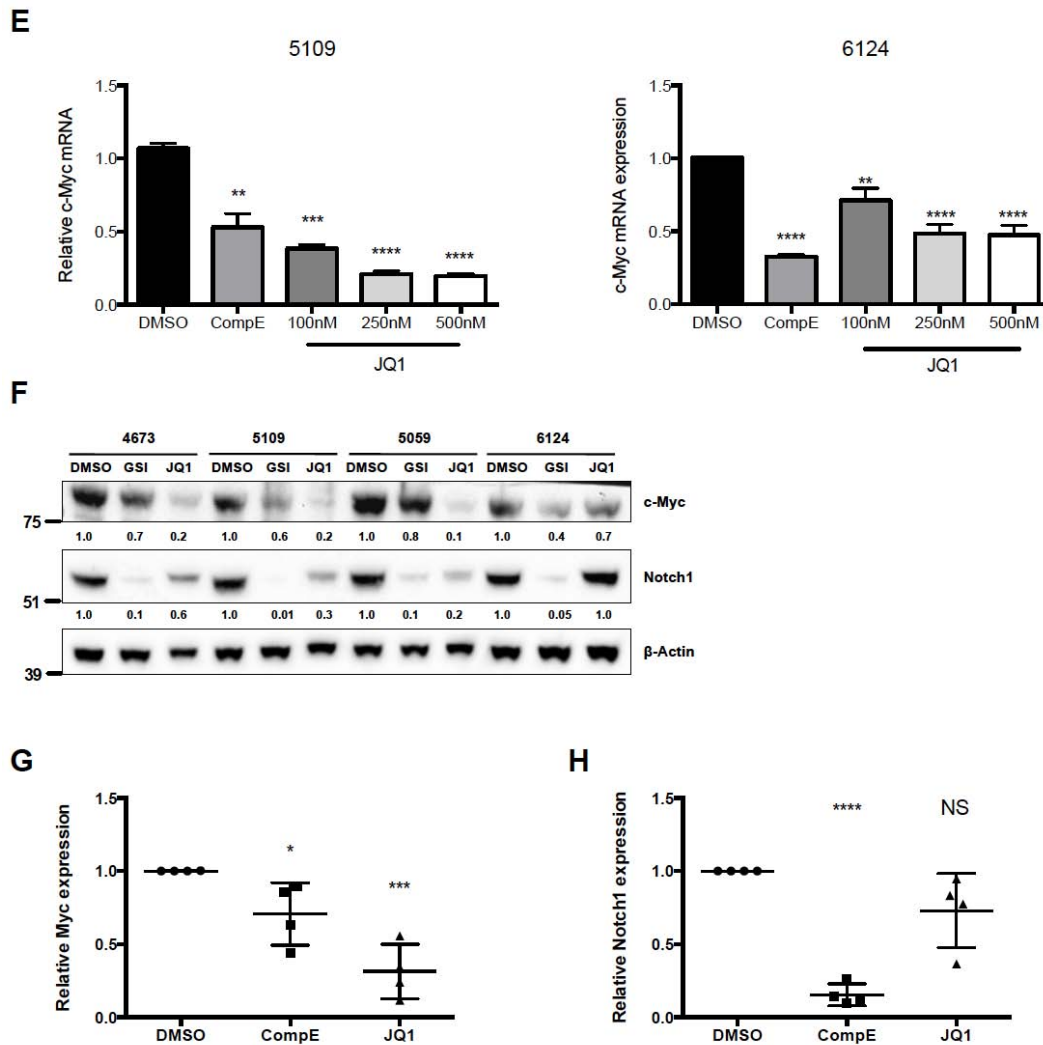


**Figure 22, continued. D. JQ1 induces apoptosis of mouse T-ALL cells.** Four mouse T-ALL cell lines were treated with vehicle, JQ1 or compound E and the percentage of apoptotic cells determined by Annexin V and 7AAD staining followed by flow cytometry. Combined analysis of Annexin V+ and Annexin V/7AAD+ cells are shown. **E. Reduced c-Myc mRNA levels in JQ1 and compound E treated cells.** RNA was isolated from leukemic cultures treated with vehicle, JQ1 or compound E for 48 hours and *c-Myc* expression was analyzed by quantitative real-time PCR. Copy number was normalized to  $\beta$ -actin using the  $\Delta\Delta C_T$  method. **F. c-Myc protein levels were significantly reduced upon treatment with JQ1.** Protein was isolated cells treat with from DMSO, JQ1 and Compound E for 48 hours. Intracellular Notch1, c-Myc, and Actin levels were determined by immunoblotting. **G., H. c-Myc protein is more significantly decreased with JQ1 compared to GSI, but Notch1 is not affected by JQ1.** Four biological replicates were performed as in F. Average fold change in c-Myc protein (G) or Notch1 protein (H) was calculated for each treatment and is represented by each point on the graph. Data are means  $\pm$  SD. \* $p < 0.05$ , \*\* $p < 0.01$ , \*\*\* $p < 0.001$ , \*\*\*\* $p < 0.0001$ ; NS, not significant.

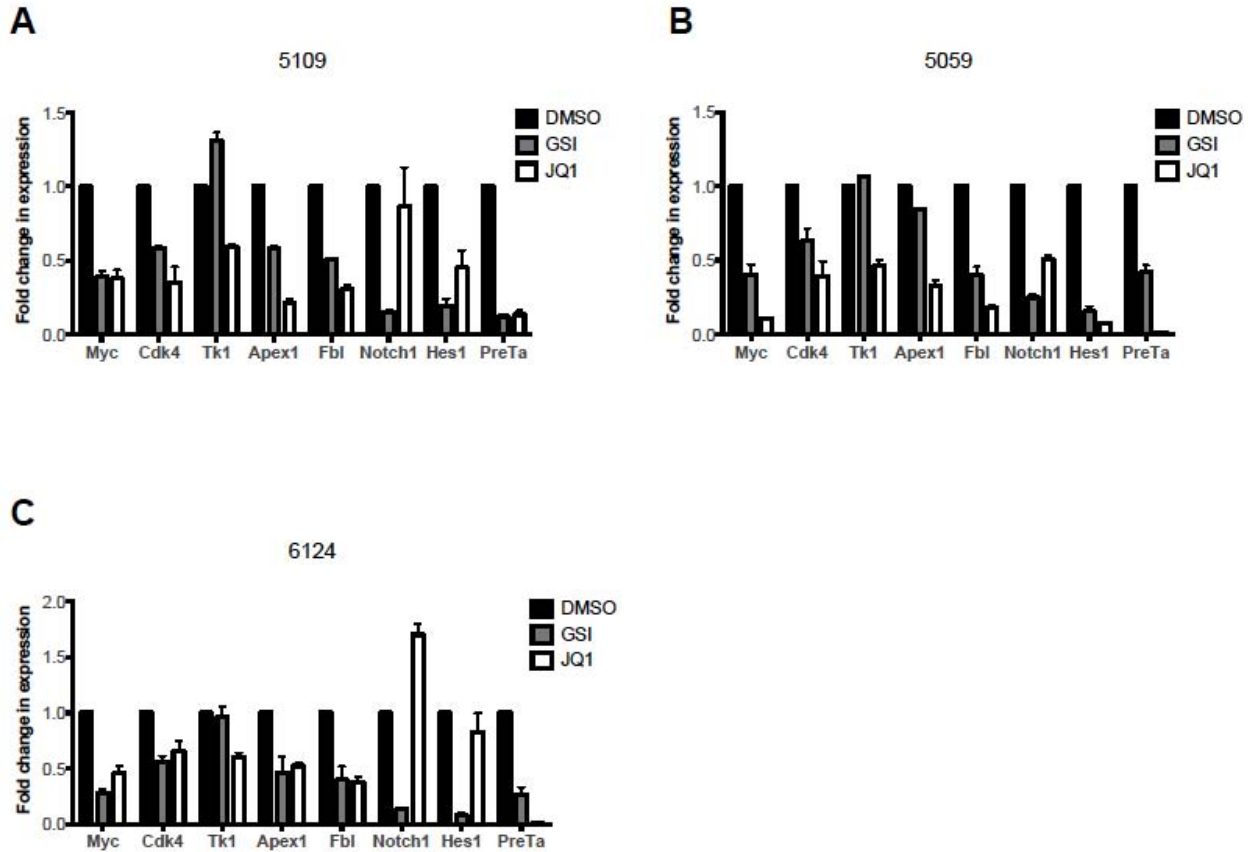


**Figure 23. JQ1 treatment reduces c-Myc mRNA, expression of c-Myc target genes, and expression of Notch1 target genes.** Murine T-ALL cell lines were treated with JQ1 (250nM) or Compound E (1uM) for 48 hours. RNA was isolated and *c-Myc*, *Cdk4*, *Apex1*, *Fbl*, *Tk1*, *Notch1*, *Hes1*, and *PreTa* expression were analyzed by qPCR. Copy number was normalized to  $\beta$ -actin using the  $\Delta\Delta$ CT method. **A.** 5109, **B.** 5059, **C.** 6124.

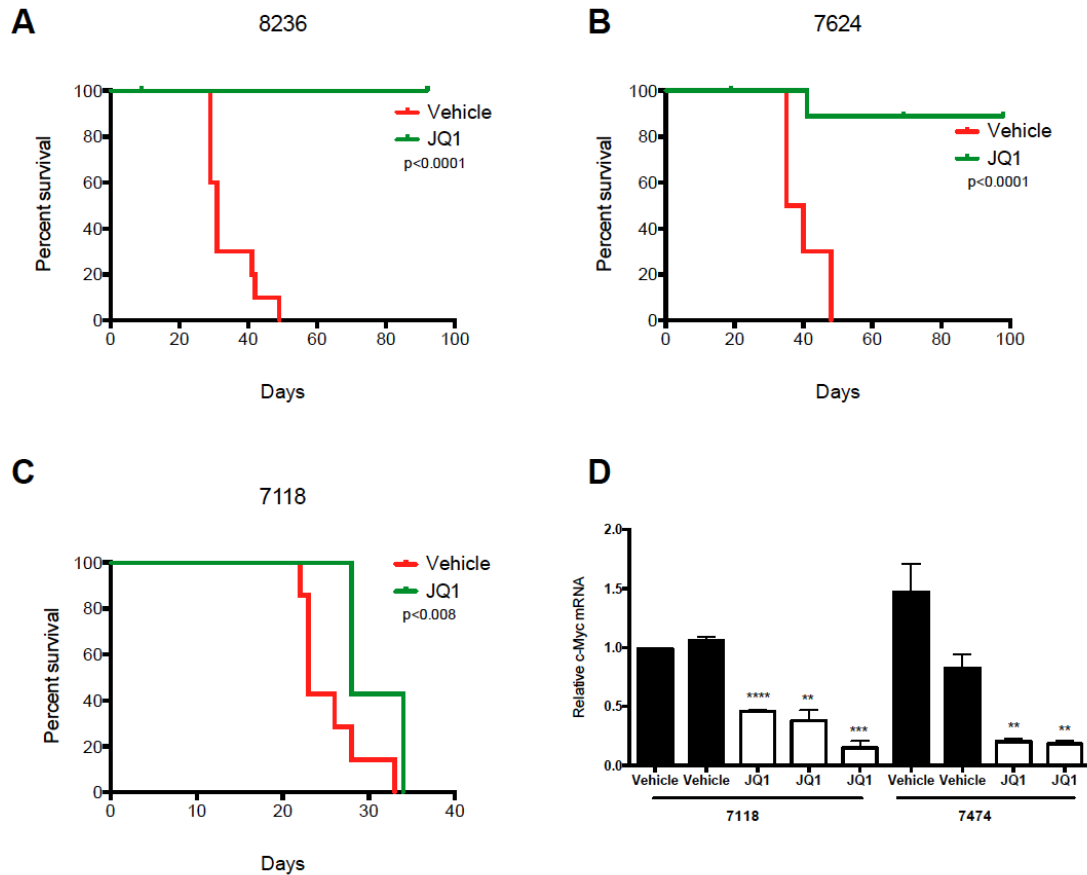


**Figure 24. JQ1 treatment of leukemic mice significantly prolongs survival and reduces c-Myc expression. A-C.** *Tal1/Lmo2* mouse T-ALLs were transplanted into syngeneic recipients. JQ1 was administered at 50mg/kg daily starting the time of transplant and continuing for 3 consecutive weeks. Mice were monitored for disease and sacrificed when they became moribund. Survival was estimated using the Kaplan-Meier method and the difference in overall survival between the two groups assessed by the log-rank test. **D. Diseased mice remain responsive to JQ1 treatment.** At disease presentation, mice were re-treated with a single dose of JQ1 at 50mg/kg. Leukemic tissues were harvested after two hours and RNA isolated. *c-Myc* expression was analyzed by quantitative real-time PCR. Copy number was normalized to  $\beta$ -actin using the  $\Delta\Delta CT$  method. Data are means  $\pm$  SD. \*\* $p < 0.01$ , \*\*\* $p < 0.001$ , \*\*\*\* $p < 0.0001$

Table 11. JQ1 treatment reduces L-IC frequency.

Treatment	Number of Cells Injected			#diseased/ total	L-IC freq	CI
	100,000	10,000	1,000			
<b>Vehicle</b>	10/10	5/11	0/11	15/32	0.0056%	0.012-0.003%
<b>JQ1</b>	4/11	1/11	0/11	5/33	0.0006%	0.0014-0.0003%

CI: Confidence interval

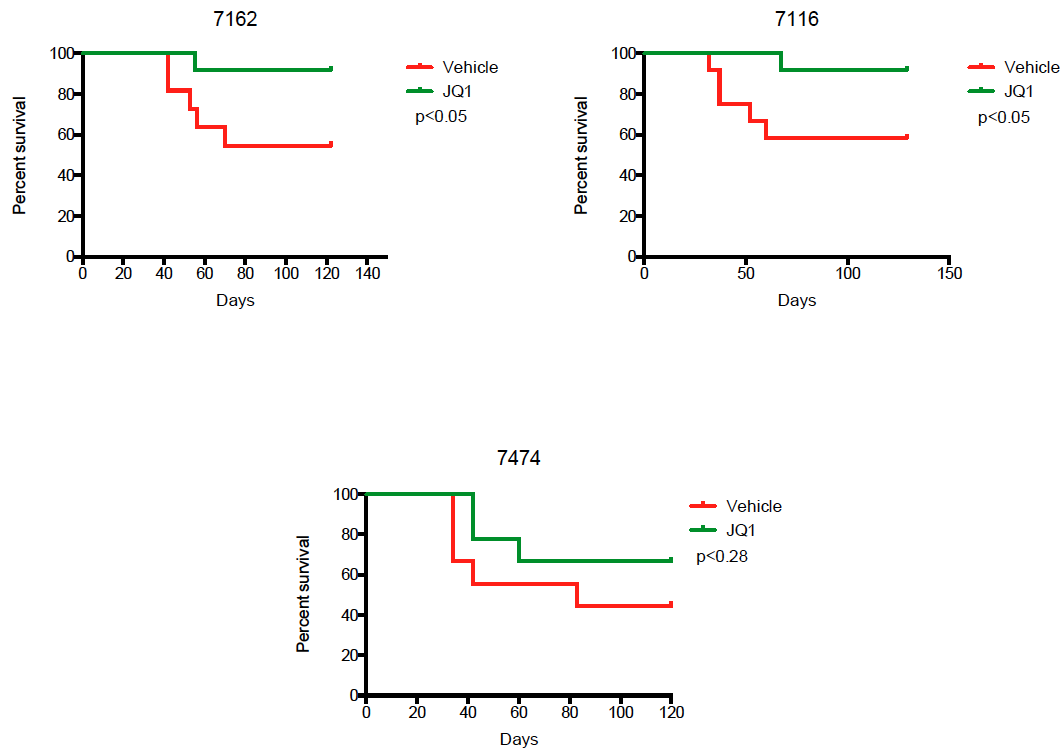


**Figure 25. JQ1 treatment extends survival of recipient mice when cells are transplanted in limiting dilution.** *Ta11/Lmo2* mouse T-ALLs were transplanted into syngeneic recipients via limiting dilution. JQ1 was administered at 50mg/kg daily starting the time of transplant and continuing for 3 consecutive weeks. Mice were monitored for disease and sacrificed when they became moribund. Survival was estimated using the Kaplan-Meier method and the difference in overall survival between the two groups assessed by the log-rank test.

Table 12. JQ1 treatment reduces L-IC frequency.

Cell Number	<u>#Diseased mice/Total injected</u>					
	7474		7116		7162	
	<u>Vehicle</u>	<u>JQ1</u>	<u>Vehicle</u>	<u>JQ1</u>	<u>Vehicle</u>	<u>JQ1</u>
100000	3/3	2/3	4/4	1/4	3/3	1/4
10000	2/3	1/3	1/4	0/4	2/4	0/4
1000	0/3	0/3	0/4	0/4	0/4	0/4
L-IC freq	0.0043%	0.0014%	0.0036%	0.0003%	0.0062%	0.0003%
Fold change	3 fold		14 fold		24 fold	

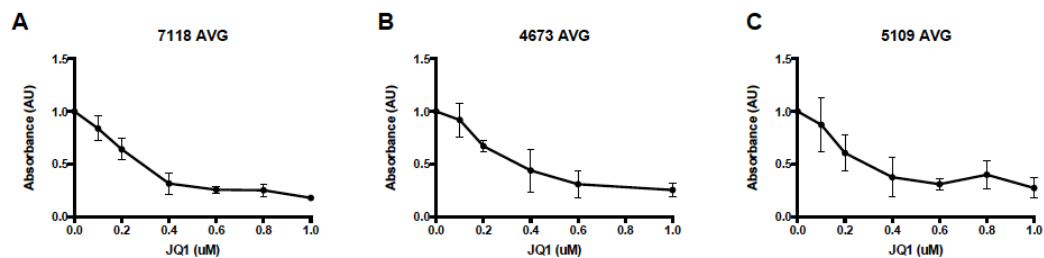


**Figure 26. Similar growth inhibition is observed among T-ALLs following JQ1 treatment.** Primary T-ALL 7118 (A) and T-ALL cell lines 4673 (B) and 5109 (C) were cultured in the presence of DMSO or increasing concentrations of JQ1 (100-1000nM) for 48 hours. Metabolic activity was assessed by MTS. Results are presented as an average of 3 biological replicates.



## **CHAPTER V**

### **Discussion**

This thesis research has focused on defining and understanding the T-ALL L-IC. An extraordinary amount of emphasis must be placed on accurately estimating L-IC frequency so that this assay can be used as a tool for testing targeted therapeutics. I have validated the assay for measuring L-IC frequency using two different transplantation methods and have shown that L-IC frequency is not influenced by transplantation method or microenvironment. I have also tested therapeutics in the *Lck-Tal1/Lmo2* mouse model using this assay and have shown that both Notch1 and c-Myc inhibition target the L-IC.

### **Inhibiting the Notch1-c-Myc pathway in L-ICs**

It is clear from our studies (and others) that oncogenic pathways can drive L-ICs. The Notch1-c-Myc pathway is critical for T-ALL maintenance, and I have shown that the pathway drives T-ALL L-ICs as well. I showed that inhibiting either Notch1 (Chapter III) or c-Myc (Chapter IV) reduces the L-IC frequency and/or activity in murine T-ALL, confirming that this pathway is important in L-IC biology. Because of the inappropriate activation of this pathway in patient samples and mouse models of T-ALL, there is likely a therapeutic window for drug development. Directly targeting an active pathway involved in self-renewal of the L-IC will eliminate these cells while hopefully leaving normal tissues unharmed. Targeting the L-IC could also reduce or eliminate cardiac toxicities and morbidities caused by harsh chemotherapy, steroids, and radiation regimens<sup>23,440,441</sup>.

In my hands, both GSI and JQ1 resulted in decreases in murine T-ALL L-IC frequency (Tables 5 and 12, respectively). While GSI was approximately 2-fold better than JQ1 (19-fold vs. 9.3 fold) at reducing the frequency of L-ICs, it is likely that this reflects JQ1 instability *in vivo*. The specific shRNAs to c-Myc resulted in a 17-fold decrease in L-IC frequency, very similar to that of GSI. This could suggest that c-Myc is the critical gene regulated by Notch1 in the L-IC population, as both GSI and c-Myc silencing resulted in an almost identical phenotype. However, other Notch1 target genes such as Cyclin D3 and Hes1 would have to be inhibited to definitively come to this conclusion. The half-life of JQ1 *in vivo* is only approximately 1.5 hours, while the half-life of the MRK-003 compound (GSI) is close to 18 hours and is not cleared from the system for up to 3 days after administration. JQ1 is able to reduce c-Myc expression to a greater degree than GSI or c-Myc shRNA (Figure 22 and Figure 19, respectively), but probably has other targets than c-Myc in T-ALL. Together, these data suggest that perhaps if JQ1 were more stable, it would be as effective, if not better than GSI treatment in terms of L-IC inhibition.

Historically, a definitive c-Myc signature has not been defined in cancer cells, despite c-Myc expression being detected in almost 70% of human cancers (reviewed in<sup>282</sup>). During the course of our experiments, we became aware of several papers revealing insight into the c-Myc transcriptional program. First, c-Myc was found to be a universal amplifier of gene expression using ChIP-seq studies and total mRNA quantifications in multiple cell types, including T-

cells<sup>325,326</sup>. Second, “super-enhancers” were found at the c-Myc locus, and other critical genes, in multiple myeloma. Using ChIP-seq to the chromatin activator Brd4, these super-enhancers were found to be up to 15 times larger than normal enhancers, have increased occupancy of chromatin modulators and activated histone marks. This results in increased gene transcription at a particular locus. Moreover, it was shown that super-enhancers were found genes important for the survival and proliferation of multiple myeloma cells, such as IRF4 and PRDM1. Importantly, these super-enhancers can be disrupted with agents that inhibit transcription initiation and elongation complexes, such as JQ1 and a homologue, iBET<sup>442</sup>.

JQ1 is able to disrupt chromatin and global transcriptional programs by inhibiting the binding of Brd4 to acetylated histones, specifically at super-enhancers, like the one controlling c-Myc<sup>442</sup>. While Notch1-inhibition results in the downregulation of a discrete set of genes, JQ1 has the ability to disrupt critical growth genes within a cell in a fairly nonspecific manner. It is thought that the super-enhancers are located at gene necessary for the growth and survival of a given tissue or malignancy, so disrupting these has great potential for efficacy and the possibility of a therapeutic window. In multiple myeloma, JQ1 treatment was able to disrupt the super-enhancers and affect the expression of multiple genes critical to the survival of the multiple myeloma cells<sup>442</sup>. While our attempt at a JQ1 microarray was not successful (Appendix IV, Table 18 and data not shown), there is other evidence that JQ1 does inhibit a broad spectrum of genes

that have roles in cell growth and survival<sup>307,308,331,438</sup>. This indicates that the effects of JQ1 on leukemic cells are likely not due solely to c-Myc repression, but also due to broader effects on chromatin and other critical cellular processes.

Notch1 inhibitors reduced L-IC frequency and/or activity in the *Lck-Tal1/Lmo2* mouse model of T-ALL in 4 out of 5 T-ALLs tested (Figure 13). Two of the five T-ALLs were completely cured with GSI treatment while an additional two T-ALLs showed significant increases in survival and decreases in L-IC frequency upon GSI treatment. T-ALL 1007 did not respond at all to GSI treatment. It is unclear as to what caused these differences in response, but if these drugs were to be used in the clinic, it would be helpful to understand which patients would respond to GSI treatment and which would not. In our hands, the GSI response did not correlate to Notch1 expression or mutational status. All T-ALLs tested expressed high amounts of intracellular Notch1 and sequencing revealed mutations in the PEST domain. All of these T-ALLs also were found to have 5' deletions in the *Notch1* locus (Figure 15), indicating that these T-ALLs theoretically should have responded to Notch1 inhibition. Our T-ALL model has activation of the PI3K/mTOR pathway<sup>261</sup>, as well as inactivation of the *Ink4a/Arf* locus<sup>111</sup>. Both of these events could contribute to GSI resistance. Under conditions of Notch1 inhibition, even though there is evidence of Notch1 mutations, the T-ALLs can upregulate an alternative pathway to facilitate their survival. Specifically, T-ALL 1007 did present with decreased Pten protein and

activated Akt (Appendix I), which could have allowed for its survival during GSI treatment.

We currently do not have a way to identify which patients will benefit from GSI therapy. Because of this and the GSI-associated toxicities, c-Myc may be a better target in this disease. In T-ALL, c-Myc is the most critical gene regulated by Notch1, being the only gene tested so far to be able to fully rescue the cell cycle arrest and apoptosis caused by GSI administration<sup>110,172</sup>. It is becoming increasingly evident that c-Myc is the driver of proliferation and differentiation in T-ALL cells and that cells can find many ways to upregulate its expression. As discussed in Appendix III, TAL1 has been shown to upregulate c-MYC in human T-ALL cell lines and patient samples<sup>119</sup>. c-Myc is also a target of c-Myb<sup>443</sup>, so this could be an additional pathway that activates the c-Myc oncogene. Under conditions of Notch1 inhibition, this Tal1-Myb-Myc pathway should still be active and so c-Myc may be able to mediate GSI resistance. The Akt pathway and loss of Pten expression can also increase c-Myc transcriptional activity by inactivating the kinase activity of GSK-3 $\beta$ , which phosphorylates c-Myc and targets it for degradation<sup>444</sup>.

In *Lck-Tal1/Lmo2* T-ALLs, JQ1 inhibited proliferation and induced apoptosis in leukemic cell lines *in vitro* (Figure 22) and prolonged survival *in vivo* (Figure 24). Importantly, JQ1 treatment decreased L-IC frequency *in vivo* (Table 11), demonstrating that the drug could prevent or treat relapse in patients. When

compared to GSI *in vitro*, JQ1 treatment resulted in increased apoptosis, decreased proliferation, and greater inhibition of c-Myc activity (Figures 22, 23). The increase in apoptosis compared to GSI is most likely due to JQ1 inhibiting additional Brd4-dependent targets that affect leukemic growth and survival. Possible candidates for these additional target genes could be c-Myb, Bcl-XL, or other critical T-cell differentiation genes.

Some mouse T-ALLs did not fully respond to c-Myc suppression or inhibition *in vivo* (T-ALLs 6124 and 7118 in Chapter IV). We do not believe that these data point to the presence of a “Myc-independent” subset of T-ALLs. In contrast, our evidence suggests that there are a number of complex events that take place when these leukemias are transplanted *in vivo*. T-ALL 6124 did not respond significantly to c-Myc shRNA *in vivo*, but did show decreases in proliferation *in vitro*. These cells also underwent cell cycle arrest and apoptosis following JQ1 treatment *in vitro*. Notably, greater effects on proliferation in T-ALL line 6124 were seen with JQ1 when compared side by side to a re-infection with c-Myc shRNA (not shown). As mentioned in Chapter IV, it is likely that the c-Myc shRNA was rapidly silenced in T-ALL 6124 *in vivo*. The pressures of initiating disease *in vivo* are likely very strong and therefore cells that have an advantage, such as a clone that has silenced the retroviral LTR, are selected to initiate disease. Likewise, a clone that has other specific molecular characteristics such as additional pathway activation (i.e. PI3K/Akt or Ras) could be selected for *in vivo* and thus result in a different phenotype than what was seen *in vitro*. This

may have been the case in T-ALL 7118 (Chapter IV) or 1007 (Chapter III, Appendix I).

While JQ1 treatment significantly extended survival *in vivo*, it failed to inhibit disease initiation in any of the recipient mice from T-ALL 7118. We do not think that the decreased response in T-ALL 7118 is due to issues with drug administration or the emergence of a Myc-independent clone. Re-administration of JQ1 decreased c-Myc expression *in vivo*. This revealed that c-Myc is inhibited with the 50mg/kg dose of JQ1 in leukemic tissues *in vivo*, but may not inhibit other important target genes at this dose in T-ALL 7118. It is also possible that this repression is short lived, as JQ1 has been shown to have a half-life on the order of 1.5 hours *in vivo*. Coupled with the short, approximately 30-minute half-life of the c-Myc protein itself, this could have resulted in rapid re-expression of c-Myc *in vivo*. Primary cells from the 7118 T-ALL were treated with JQ1 *in vitro* and showed sensitivity similar to murine leukemic cell lines (Figure 26;  $IC_{50}=273nM$ , cell line range 163-343nM, not shown), indicating that this T-ALL is not inherently resistant to JQ1 treatment.

### **Possible causes of GSI resistance**

We have seen variable responses to GSI *in vivo* and so it is probable that additional genetic events contribute to T-ALL development and may influence responses to GSI treatment. We did find evidence of Pten loss and Akt pathway activation in T-ALLs with moderate to no GSI response *in vivo* (Appendix I). Pten



loss and subsequent Akt pathway activation correlated with decreased disease latency (Table 13), suggesting that Pten loss results in development of more aggressive T-ALLs. It is still unclear if the activation of the Akt pathway enriches for L-ICs or if it results in accelerated growth of existing L-ICs. It is also possible that the loss of Pten made the leukemic cells GSI resistant, a mechanism of GSI resistance in human T-ALL cell lines<sup>420</sup>. Mutations in additional oncogenes or tumor suppressors may also emerge upon transplant and is an area of active interest in our lab.

Over the course of these experiments, we have noticed that treating the *Lck-Tal1/Lmo2* T-ALLs *in vitro* resulted in a decreased GSI response compared to what was seen with *Lck-Tal1* T-ALLs. Previously, our lab showed robust cell cycle arrest followed by apoptosis in GSI-treated murine cell lines within 48 hours<sup>248</sup>. The *Lck-Tal1/Lmo2* T-ALL cell lines tested in Chapter IV did not undergo cell cycle arrest until 96 hours of treatment and did not undergo apoptosis at all in that time. It is possible that Lmo2 expression somehow is able to confer Notch1-independent survival signals.

Studies in *CD2-Lmo2* transgenic mice have revealed a unique gene signature associated with overexpression of Lmo2 in the developing thymus<sup>137,405</sup>. The Lmo2 gene signature is closely associated with the Lyl1 T-ALL signature, a more immature subclass of T-ALL, and with ETP-ALL samples. These signatures are associated with the induction of stem cell genes such as

*Hhex*, *c-Kit*, and *Nfe2*. *Hhex* in particular has been shown to induce self-renewal in thymocytes, like *Lmo2*<sup>18</sup>. *Hhex* is a transcriptional repressor that activates Wnt signaling by repressing the transcriptional repressor *Tle4*<sup>445</sup>. In *Lmo2*-expressing cells, Wnt activation may be one mechanism whereby cells resist the effects of Notch1 inhibition through upregulation of genes such as Cyclin D1 or c-Myc. Wnt activation may not override the requirement for Notch1 signaling, but under conditions of Notch1 inhibition, this parallel pathway could contribute to leukemic cell survival and a GSI-resistant phenotype.

Recently, in the same mouse model, *Lmo2*-expressing thymocytes were shown to induce a hematopoietic stem cell-like signature in part by upregulating *Nfe2*, *Hhex*, *Lyl1*, *Gata2*, and *N-Myc* while downregulating death receptor genes such as *Fas1*<sup>405</sup>. This Notch1-independent, and possible *Tal1*-independent, signature may be able to keep cells alive longer under conditions of Notch1 inhibition and prevent apoptosis by continuing the production of key cell growth genes.

### **Defining and characterizing the L-IC**

We are confident in the validity of the assay used to calculate the L-IC frequency in murine T-ALL (Chapter II), so we can use it to further define characteristics of the L-IC. The critical need for additional cell surface markers to define the L-IC is discussed in Appendix II. At this point, we are confident that the L-IC is a subset of the DN3 population, but the precise cell has not yet been

defined. Once we further enrich the population by using additional cell surface markers, we may be able to define additional pathways that mediate L-IC activity and design targeted therapies.

c-Kit positivity ranges from 1-60% of DN3 cells (average 16%, Table 14) and could potentially enrich for the L-IC by 2-100 fold. While c-Kit could potentially define functional subsets of the L-ICs (Appendix II), it is likely that additional markers will be needed because of the low frequency (0.003-0.05%) estimated in *Lck-Tal1/Lmo2* T-ALLs. For the purpose of sorting cells and enriching the L-IC population, it would be most beneficial to start with members expressed on the extracellular surface and those shown to export chemotherapeutics. Other intracellular transporters may also be analyzed to determine other biological characteristics of the L-IC.

In breast cancer, chemotherapy enriches for T-ICs<sup>374</sup>. Drugs like topoisomerase inhibitors, alkylating agents, and anti-metabolites kill the rapidly dividing cells in the tumor, leaving a slow cycling T-IC population behind, primed to mediate relapse. It may be possible to enrich for an L-IC population in T-ALL by using conventional T-ALL induction therapies such as vincristine or methotrexate. A recent study reported that glucocorticoid (dexamethasone) treatment selects for a resistant population in T-ALL that expresses L-IC markers<sup>447</sup>, but further analysis was not performed on this population beyond clonality assessment. A short burst of treatment that does not eradicate disease

should leave a population of cells that could be then be analyzed for cell cycle status, altered gene expression, cell surface markers, and L-IC activity. Murine T-ALLs and T-ALL patients usually show a very good initial response rate to induction regimens, however, so determining an appropriate therapeutic window would be critical.

Other possibilities for L-IC enrichment could be targeted toward the altered metabolic state found in cancer cells. Because of rapid cell growth and availability of key nutrients, cancer cells will often switch from normal glycolysis to glutaminolysis<sup>448</sup>. This process will produce energy from glutamine instead of glucose and is controlled in part by c-Myc<sup>449</sup>. Therefore in T-ALL, looking at glutamine transporters such as ASCT2, may be a beneficial way to enrich for L-ICs. ASCT2 has been shown to mediate malignant growth in a variety of malignancies such as brain, breast, prostate, and lung cancers<sup>450,451</sup>. It is also possible that glucose transporters are still important to the L-ICs, as GLUT3 has been shown to be implicated in maintenance of germinal, neural, and skeletal muscle stem cells<sup>452–454</sup> and has roles in angiogenesis in cancer cells (reviewed in<sup>455</sup>).

### **L-IC assay validation**

While we have validated the L-IC assay and are confident with the L-IC frequency calculated in our model, some questions still remain. Other groups have measured L-IC frequency in animals that are either sub-lethally irradiated or

immunodeficient<sup>113</sup>. Tremblay and colleagues used a similar mouse model *pSIL-Tal1/Lck-Lmo1*, and reported L-IC frequencies of 1%, approximately 10-fold higher than what we have found. Importantly, my colleague Kathleen Cullion and the Tremblay group found the DN3/DN4 thymocyte population enriched in L-IC activity, indicating that the L-IC population is the same in two models with similar driving oncogenes. This points to additional differences in assay design and mouse models to yield such different L-IC frequencies. These differences could range from sublethal irradiation to genetic background to the oncogenic promoter.

Sublethally irradiating mice serves to make space in the thymus and bone marrow by killing some, but not all, of the hematopoietic cells and lymphocytes<sup>456</sup>. This reduction in thymic and bone marrow cellularity reduces competition in these niches<sup>398</sup>. Changes in microenvironment can also occur with irradiation including stromal remodeling, increased cytokine production, and DNA damage(reviewed in<sup>457</sup>). Theoretically, sublethal irradiation might result in the engraftment of more L-ICs due to the increased space and decreased competition. However, my preliminary data do not suggest that irradiation affects the frequency of the T-ALL L-IC (not shown). This is consistent with the data presented in Chapter II, in that the T-ALL L-IC is not influenced by changes in microenvironment. Additional T-ALLs will need to be analyzed to solidify these results.

The effect of the recipient immune system on L-IC frequency is a more difficult issue to address. Severely immunocompromised mice such as NOD/SCID (NS) or NSG mice have little to no functional lymphocytes, decreased dendritic cell function and defective macrophages. NS mice have no B- or T-cells and thus no adaptive immunity<sup>458</sup> while NSG mice also have limited innate immune capabilities, with likely only limited natural killer (NK) cells contributing to an immune response. Not only do these deficiencies reduce cellularity in the bone marrow and thymus, but they also prevent any sort of competition or host immune response<sup>459</sup>. As a result, these mice are used to engraft normal and malignant human cells. Because these mice can be used to engraft normal cells (without self-renewal capabilities), it may be too permissive to accurately calculate L-IC frequency. Tremblay and colleagues used a Rag<sup>-/-</sup> host<sup>113</sup>, which results in a lack of mature T-cells, so this could be another source of variation between our data.

Recently, increasing evidence has surfaced that the host (or patient) immune system plays a valuable role in eliminating cancer cells from the body. NK cells are able to recognize tumor cells based on their cell surface expression of various proteins and target these cells with cytotoxic perforin and granzyme molecules (reviewed in<sup>460</sup>). Specifically, NK cells can recognize if a cancer cell is expressing too little or too much major histocompatibility complex (MHC) I on the cell surface and remove these cells from the body<sup>461</sup>. In our murine transplantation model, the NK cells in the syngeneic transplants could be

eliminating some of the T-ALL cells from circulation before they are able to initiate disease, thus resulting in an apparently low L-IC frequency. Other immune cells such as cytotoxic T-lymphocytes (CTLs) or innate immune cells other than NK cells could contribute to this response as well. In preliminary experiments comparing wild type recipients and NSG mice, murine T-ALL cells showed a 10-fold increased penetrance (L-IC frequency) and slightly decreased latency in the NSG mice in two out of three experiments (not shown).

These data could indicate that the L-IC assay in syngeneic recipients may not be the best readout for L-IC frequency, as it may be underestimating the number of cells contributing to disease. Alternatively, one could argue that a patient would likely have at least some level of NK and other immune cell activity in the body and therefore an assay should be conducted where these cells are present. We have not conducted experiments to examine the cell surface molecules present on our murine T-ALLs to see if different populations may be more immunogenic than others, but it is also possible that the only reason we do not see L-IC activity in more mature DP populations is that they are able to trigger an immune response in the host animal. Sort experiments will need to be done to determine whether DP cells have any L-IC activity in immunocompromised mice.

Lastly, a source of L-IC frequency variation could be traced to genetic differences in the oncogenes used to drive T-ALL. Tremblay and colleagues used

the *SIL-Tal1* model, where Tal1 expression is driven by a ubiquitous promoter in the genome<sup>107,108</sup>, while the *Lck* promoter is only expressed in immature T-cells. Expression levels of Tal1 have not been compared between these two models; however, variation could be present that cause differences in L-IC frequency. The differences between Lmo1 and Lmo2 used as cooperating oncogenes in the two T-ALL models are probably negligible, as the two genes share homology and functional overlap.

### **T-ALL Heterogeneity**

In Chapter II and Appendix I, I showed that clonal selection events take place when primary murine T-ALLs are transplanted into recipient mice. Not all leukemic clones have the same ability to transfer disease, providing additional evidence for functional heterogeneity in these T-ALLs. I also noticed that leukemic clones that exhibit Pten loss emerge in transplanted mice, where the primary leukemia expressed wild-type levels of the protein. This clone presumably possesses all the same qualities of an L-IC, but the proliferative and survival advantages gained from the Pten mutation allowed this clone to become dominant. These data indicate that while we know that T-ALL is organized in a functional hierarchy, there is emerging evidence of clonal dominance in T-ALL as well.

The data presented in this thesis, along with recently published work, help to reveal a more detailed picture of T-ALL pathogenesis (Figure 27). We have



known that the *Lck-Tal1/Lmo2* model of T-ALL results in a DN3 block in thymocyte differentiation before leukemogenesis. We now know that Lmo2 is able to induce self-renewal in these cells and that Notch1 mutations occur preleukemically (Table 2). This aberrant pool of DN3 thymocytes expands but retains the ability to differentiate, most likely once the Notch1-c-Myc pathway becomes prominently activated. There must also be additional genetic events that occur before the onset of disease because Notch1 mutations occur in the preleukemic state, before the onset of T-ALL. One possible event is 5' deletions in the *Notch1* locus that remove the extracellular domain and render the protein ligand-independent. These mutations were not detected at the preleukemic stage (4-6 weeks old), but are prominent in murine T-ALLs (6/7 examined)<sup>249,251</sup>. The leukemic DN3 cells remain dependent on the Notch1-c-Myc pathway as they initiate disease in the mouse in a cell autonomous manner. This thesis provides evidence that T-ALL is driven by both the cancer stem cell (hierarchical) model of leukemogenesis and the clonal evolution model. These data advocate for the development of anti-L-IC therapies in T-ALL. Specifically, I have shown evidence for the further development of inhibitors that target the Notch1-c-Myc pathway while maintaining a low toxicity profile in patients.

### **Future directions:**

Our main goal for this project is to define and target the L-ICs in our murine T-ALL mouse model, and ultimately in patients. To do this, we must purify the L-IC based on surface markers and/or biological properties (discussed in

Appendix II). Options on how to do this have also been discussed already in this thesis. It would also be interesting to determine whether the L-IC population is different in *Lck-Tal1*, *Lck-Lmo2* and/or *Lck-Tal1/Ink4aArf<sup>+/−</sup>* mice (models we already have available in the lab). The immunophenotypes of these T-ALLs are slightly more differentiated than the *Lck-Tal1/Lmo2* mice described here and so it is possible that the L-IC population or resulting L-IC frequency may be different. This type of analysis could reveal differing roles for the *Tal1* and *Lmo2* oncogenes in the disease in terms of self-renewal and/or L-IC frequency. Performing L-IC assays in these additional mouse models will also solidify the universality of the L-IC/stem cell hypothesis in the pathogenesis of T-ALL.

Future experiments will revolve around determining the functional characteristics of the human T-ALL L-IC. An L-IC frequency has not yet been definitively determined in T-ALL patients using immunodeficient mice, but functional populations have been defined. In human T-ALL, the initiating cell is thought to be an early T-cell progenitor that is CD34<sup>+</sup> and CD7<sup>+</sup>. In human T-cell development, this would compare to a DN2/DN3 cell that is beginning to commit fully to the T-lineage. These data correlate roughly to the population defined in mouse models of the disease. These data also indicate that the NSG model for engrafting T-cells is not entirely permissive, as CD34<sup>−</sup> and CD7<sup>−</sup> cells had limited engraftment abilities in these mice.

Along with defining an L-IC population in human T-ALL patient samples, we will attempt to target this L-IC with therapies, and potentially shRNAs to specific oncogenic pathways. This latter experiment has been daunting in the past due to viability issues with primary patient samples, but progress is being made in the lab and we are optimistic that we will soon be able to infect these cells. If infection of the patient samples is successful, we should be able to perform unbiased *in vivo* shRNA screens with the samples to determine critical pathways involved in the self-renewal of T-ALL patient samples.

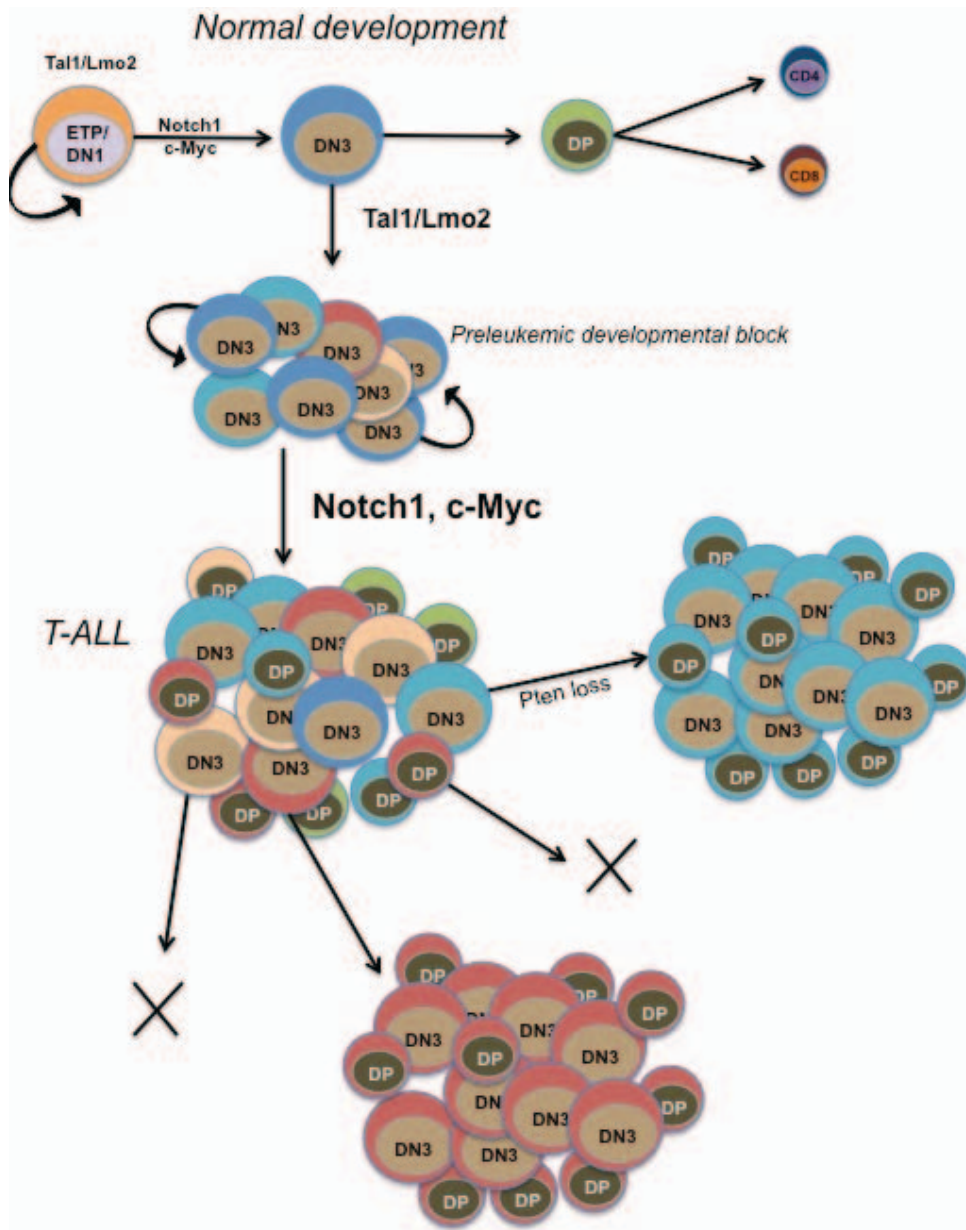


**Figure 27. A model for T-ALL development.** The forced expression of Tal1 and Lmo2 in the developing thymus causes a block in development and the accumulation of DN3 cells that gain the ability to self-renew. Activation of the Notch1-c-Myc pathway occurs in these cells via PEST region mutations and 5' deletions at the Notch1 locus. The self-renewing DN3 thymocytes gain the ability to expand into an oligoclonal T-ALL. Only the DN3 cells in the tumor have the ability to transfer disease to recipient mice, but there can be clones within the T-ALL with differing transplant capabilities. One event documented in this thesis was the loss of Pten upon T-ALL transplant, thus giving a leukemic clone a selective advantage. In theory, if one DN3 cell could be transplanted or if a clonal DN3 population could be sorted out, resulting disease should be clonal.

## **Appendix I: Clonal selection for Pten loss occurs upon T-ALL transplant**

## Introduction

*Pten* was discovered as a tumor suppressor in the 1980's when a part of chromosome 10 was found to be deleted in a set of malignant gliomas<sup>462</sup>. Later it was identified as the cause of a number of familial benign hamartoma syndromes, including Cowden syndrome<sup>463</sup> and mapped to the 10q23 deletion<sup>464</sup>. *Pten* is considered a haploinsufficient tumor suppressor because even partial losses in protein expression can result in large phenotypic changes<sup>465</sup>. The *Pten* model of tumorigenesis is considered a continuum model because slight changes in *Pten* dosage can dictate not only tumor susceptibility but also the progression of disease(reviewed in<sup>466</sup>).

*Pten* is a lipid phosphatase involved in negatively regulating the PI3K-Akt signaling pathway<sup>467,468</sup>. *Pten* dephosphorylates and thus deactivates PIP<sub>3</sub>, which activates PDK1. Once activated, PDK1 phosphorylates Akt at Thr308, thus activating the Akt and mTOR signaling cascades. The Akt pathway promotes cell survival, proliferation, cell growth, angiogenesis, and metabolism by phosphorylating downstream proteins such as GSK3 $\beta$ , FOXO, Bcl-2, BAD, MDM2, and p27(reviewed in<sup>469</sup>). Akt is also able to activate the mTORC1 complex, which phosphorylates the p70S6K and promotes cell growth and survival(reviewed in<sup>470</sup>). Thus, many tumors find ways to decrease *Pten* expression, therefore activating these critical oncogenic pathways.

Both the PI3K and Akt pathways are able to help promote the metabolic reprogramming of cancer cells, known as the Warburg effect<sup>471</sup>. Cancer cells, due to their excessive growth, increase glycolysis and lactate production in cells (reviewed in<sup>472</sup>). The PI3K and Akt pathways help to increase glucose uptake<sup>473</sup> and allow cells to increase lipid and macromolecule synthesis pathways<sup>474</sup>. *Pten* deletion has also been linked to promoting tumor-permissive stroma in mouse models of breast cancer and human breast cancer cell lines<sup>475,476</sup> and is indeed deleted in many breast cancer patient samples<sup>386,477</sup>.

In adult tissue stem cells, such as HSCs, *Pten* deletion caused a decrease in the HSC pool and a coordinate increase in T-ALL and AML L-IC populations<sup>339,478,479</sup>. Treatment of mice with rapamycin, an inhibitor of mTOR signaling, decreased the L-IC pool and restored the self-renewal capacity to HSCs<sup>340,480</sup>. This is consistent with additional reports, which found that increased mTOR signaling depletes stem cells by activating critical cell cycle and senescence checkpoints (reviewed in<sup>480</sup>). *Pten*-null mice are viable, but develop a variety of malignancies, including T-ALL and AML<sup>481</sup>. *Pten* deletions have also been found in T-ALL patient samples at diagnosis, and after relapse of the disease<sup>336,482,483</sup>. These findings indicate a critical role for *Pten* loss in the transformation of normal stem and progenitor cells.

*Pten* is regulated by a variety of genetic and epigenetic processes. Notch1 signaling, for example, is able to promote *Pten* transcription through CSL or

repress its transcription through activation of c-Myc<sup>484,485</sup>. *Pten* transcription is also repressed by the proto-oncogenes Bmi-1 and c-Jun<sup>486,487</sup>. miRNAs<sup>488</sup> and competitive endogenous RNAs (ceRNAs)<sup>489</sup> regulate *Pten* at the translational level by inhibiting translation or acting as decoys to miRNA repression, respectively. At the post-translational level, Pten can be modified by phosphorylation, acetylation, or ubiquitination events and the number and location of these modifications will dictate whether the activity of Pten is increased or decreased. These modifications can also affect the localization of the protein, which can in turn affect the ability of Pten to act on its targets. Finally, Pten can be regulated by protein-protein interactions, which can increase or decrease the phosphatase activity of the catalytic domain by stabilizing or destabilizing particular residues (reviewed in <sup>490</sup>).

In some human T-ALL cell lines, *Pten* loss has correlated with GSI resistance<sup>420</sup>. The Notch1 target gene Hes1 is a repressor of Pten, such that when Notch1 is active in cells, Pten expression decreases and Akt signaling increases, furthering T-ALL cell growth and proliferation<sup>491</sup>. When GSIs are administered to cell lines with intact Pten, Hes1 repression of Pten decreases and therefore so does Akt signaling; the cells respond by undergoing G1 arrest. In cell lines where Pten expression is lost, GSIs seem ineffective because the activation of the Akt pathway continues in the absence of Notch1 signaling. This observation was not corroborated when using murine T-ALL cell lines or T-ALL patient samples, so the notion that Pten loss confers GSI resistance is still under



debate. Recent reports, however, have shown that *Pten* loss is able to deregulate c-Myc expression, thus increasing its oncogenic potential<sup>444,492</sup>. Because c-Myc has been shown to rescue the effects of Notch1-inhibition<sup>110,172,259</sup>, c-Myc deregulation via *Pten* loss could be another way T-ALLs appear resistant to GSI treatments.

In this Appendix, I will discuss experiments undertaken to determine the cause of the variability seen in GSI responses in our mouse model of T-ALL (III). We examined the *Pten* locus in the T-ALLs used for the study described in Chapter III and found that some tumors underwent *Pten* loss upon transplant in recipient mice. However, attempts to determine the mechanism by which this loss occurred in these T-ALLs were not entirely successful.

## Results

As I completed the *in vivo* GSI studies described in Chapter III of this thesis, we tried to explain the differences in the responses to GSI across the various tumors. We found a correlation between disease latency and response to GSI; specifically, aggressive leukemic growth was associated with GSI resistance *in vivo* (Table 4). Some tumors (1007, 1928, 3304) were more aggressive than the others (1426, 2544) but this aggressiveness did not correlate with an increase in L-IC frequency. Thus we hypothesized that additional growth and survival pathways may be activated in these leukemias.

We started our investigation with looking at Pten expression in these T-ALLs, based on evidence that *Pten* loss confers GSI resistance in human T-ALL cell lines. We found that in the three T-ALLs that were most aggressive (1007, 1928, 3304), decreased disease latency was associated with decreased Pten expression (Figure 28). Because Pten is a prominent negative regulator of Akt signaling, we examined levels of phosphorylated Akt (p-Akt). Indeed, the T-ALLs that expressed Pten upon transplant (1426, 2544) expressed little to no p-Akt while the T-ALLs that lost some degree of Pten expression showed increased levels of p-Akt (Figure 28B and Table 13).

In order to determine the mechanism of Pten loss/decrease in these murine T-ALLs, we analyzed mRNA and protein of the tumor tissues before and after transplant (Table 13). The T-ALLs examined expressed low levels of miR-

19b (Figure 29A), a miRNA that negatively regulates Pten translation<sup>493,494</sup>. This was surprising, as miR-19b is expressed as a part of the miR-17-92 cluster, which is activated by c-Myc. It is still possible that Pten levels in these murine T-ALLs are being modulated by other miRNAs.

T-ALL 3304 expressed a decreased amount of Pten mRNA as compared to T-ALLs 1426 and 2544 (Figure 29B), which maintained Pten protein expression upon transplant. It is possible that the Pten mRNA is being targeted for degradation by a miRNA other than miR-19b. More likely, the L-ICs developed a mutation or deletion in the Pten genomic sequence in the recipient mice, either resulting in decreased mRNA expression or decreased mRNA stability. Alternatively, this particular clone existed in the primary T-ALL and that the mutation gave the clone a selective advantage in the recipient mice, as seen in patient samples when engrafted into immunodeficient mice<sup>336</sup>. Lastly, epigenetic silencing could have taken place in T-ALL 3304. SALL4 has been shown to remodel the Pten locus by recruiting HDACs<sup>495</sup>; or it is possible that the locus underwent DNA methylation to prevent transcription(reviewed in<sup>466</sup>).

In T-ALL 1928, Pten mRNA was decreased in the recipient mice, however very low levels of Pten mRNA were detected in the primary T-ALL (Figure 29B). It is unclear why Pten protein was detected with little to no mRNA expression being detected. The primary tumor material from these studies were used to publish the manuscript described in Chapter III, and so unfortunately not enough

material remained to repeat these experiments. In T-ALL 1007, no changes in Pten mRNA were detected in recipient mice, while protein levels were quite low in the recipient animals (Figure 28B, 30B). In this T-ALL, it is likely that miRNAs are important, although it is unclear which one(s). Possible candidates include miR-17, another member of the oncogenic miR-17-92 cluster<sup>494,496–498</sup>, and miR-21, a miRNA implicated in solid tumors for inhibiting Pten translation<sup>499,500</sup>.

Technical hurdles throughout these experiments prevented optimal data analysis. Primary T-ALL material was limiting and was not prepared in buffers to preserve phosphorylated epitopes and so p-Akt could not be compared before and after transplant. There were also difficulties in preparing lysates from frozen leukemic tissues from recipient mice. We think that this may explain why increased p-Akt was not observed in 1007 and 3304 (Figure 28). In retrospect, lysates should have been prepared from fresh leukemic tissues so that phosphorylated proteins could be examined.

We obtained *Pten*<sup>fl/fl</sup> mice<sup>501</sup> to determine if loss of Pten alters murine T-ALL L-IC frequency or if loss simply activates the Akt pathway and results in increased T-ALL growth and survival. It was difficult to determine this by using data from the tumors in our GSI study because at the time of analysis, some tumors had lost Pten and some had retained it. The L-IC frequency in the *Lck-Tal1/Lmo2* model of T-ALL is highly variable, so it would be best to compare the effects of Pten expression within a single tumor, not across a small sampling of

tumors. Since data was inconclusive, we turned our focus to the Notch1 target gene c-Myc to examine self-renewal and proliferation of T-ALL L-ICs (Chapter IV).

## Discussion

In this small study, we have shown that genetic selection occurs in murine T-ALLs upon transplant into recipient mice. Pten loss, either *de novo* or through selection for a specific clone, takes place in a subset of T-ALLs and this loss correlates to more aggressive disease *in vivo*. Although in this cohort of mice the loss of Pten expression did not correlate with GSI resistance, other groups have shown that *PTEN* loss does mediate resistance in human T-ALL cell lines<sup>420</sup>. A larger number of leukemias and more rigorous genetic experimentation are required to resolve these issues and to find a definitive answer as to what mediates GSI resistance.

It is possible that when Pten loss is selected for in T-ALL, this event also increases the L-IC frequency. Increased Akt pathway signaling has not yet been linked to increased cancer initiating cell activity, but it has been shown to increase oncogenic potential of T-ALL<sup>482,502</sup>. We hypothesized that the apparent increase in T-ALL aggressiveness could be a reflection of increased L-IC frequency. Because murine T-ALLs are oligoclonal, and not all clones remain in transplanted mice (Chapter II), transplantation of single clones may resolve some of the inconsistencies in Pten expression that we see upon transplant. Transplanting clones in this way from a single T-ALL would also determine whether Pten loss confers changes in L-IC frequency, within a single leukemia.

Coupled with the TCR-V $\beta$  clonality selection discussed in Chapter II, these experiments show that serial transplantation selects for leukemic clones in recipient mice. Thus, serial transplantation could be used as a model for relapsed T-ALL because transplantation selects for the most aggressive leukemic sub-clones. We know that the disease is oligoclonal based on TCR-V $\beta$  expression. It is possible that with serial transplantation, we could bring this down to a clonal T-ALL. If we are able to transplant a single L-IC, we would be able to come to a conclusion about the role of Pten in T-ALL initiation.

## Methods

### Mice

All mouse experiments were performed according to IACUC standards as described in Chapters II, III, and IV of this thesis.

### Immunoblotting

Protein was isolated from primary T-ALLs and leukemic tissues from recipient mice. Samples were run on a 4-12% Bis-Tris gel (Invitrogen) and blotted with antibodies to Pten (Cell Signaling catalog #9552), phospho-Akt (Cell Signaling catalog # 4060S), total Akt (Santa Cruz catalog # sc-8312), and total Erk1/2 (Cell Signaling catalog # 9102S).

### Expression analyses

mRNA was isolated from primary T-ALLs and leukemic tissues from recipient mice using Trizol reagent (Invitrogen). cDNA was synthesized and expression of Pten mRNA quantified by qPCR using specific primers: F5-TGGATTGACTTAGACTTGACCT'-3', R5'- GCGGTGTCATAATGTCTCTCAG-3'. Expression was normalized to  $\beta$ -Actin expression using the  $\Delta\Delta$ CT method.

miRNA was isolated from primary T-ALLs and leukemic tissues from recipient mice using the miRVana kit (Ambion). Specific miRNA cDNA was generated using the TaqMan kit for miR-19b and expression was quantified by qPCR.



Expression of miR-19b was normalized to expression of the housekeeping miRNA sno202.

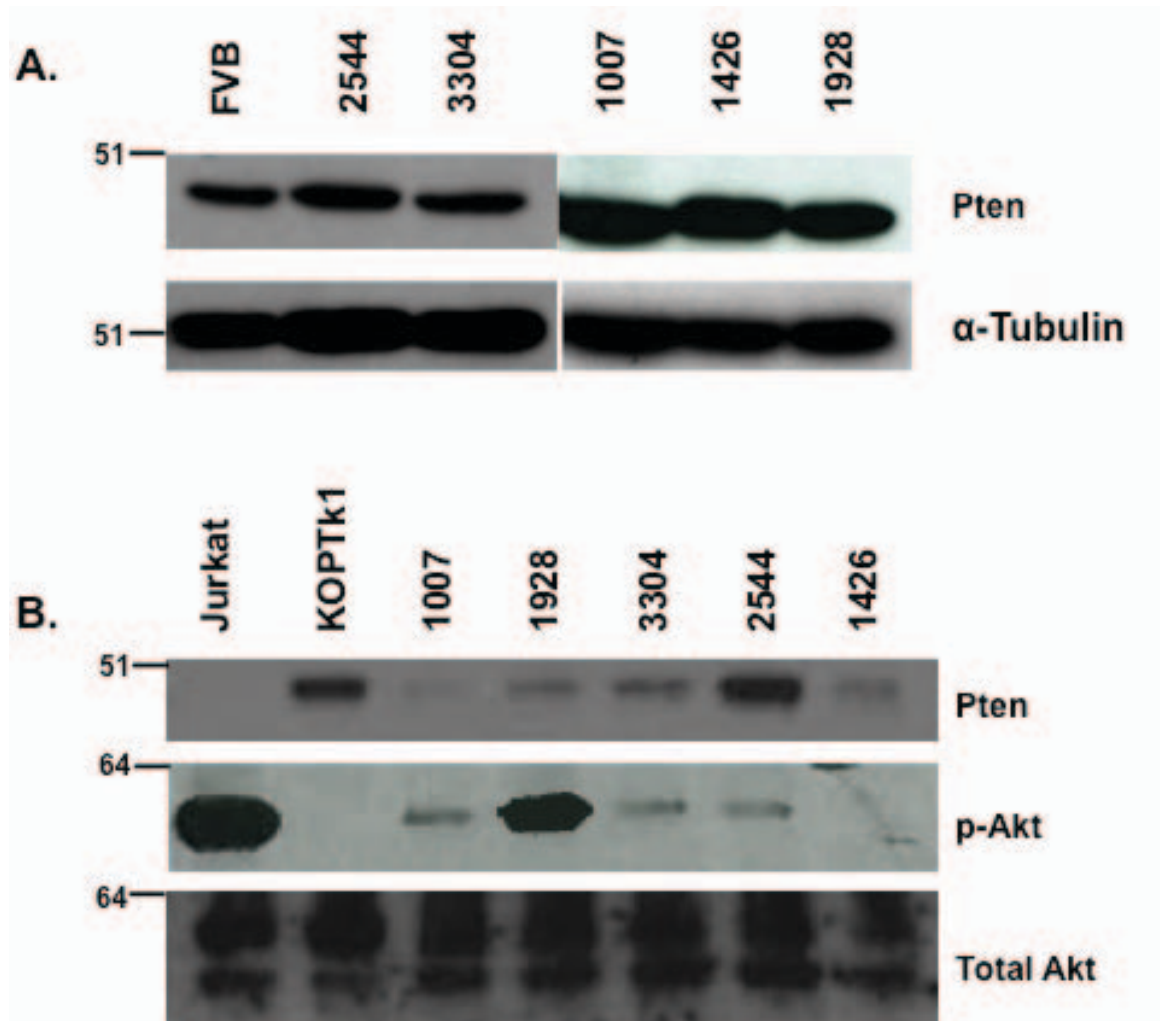


**Figure 28. Pten protein decreases upon transplant and results in increased Akt signaling.** **A.** Protein was isolated from primary T-ALLs before transplant and Pten expression was analyzed by immunoblotting. **B.** Protein was isolated from snap-frozen tissue from recipient mice. Pten, p-Akt, and total Akt levels were analyzed by immunoblotting.

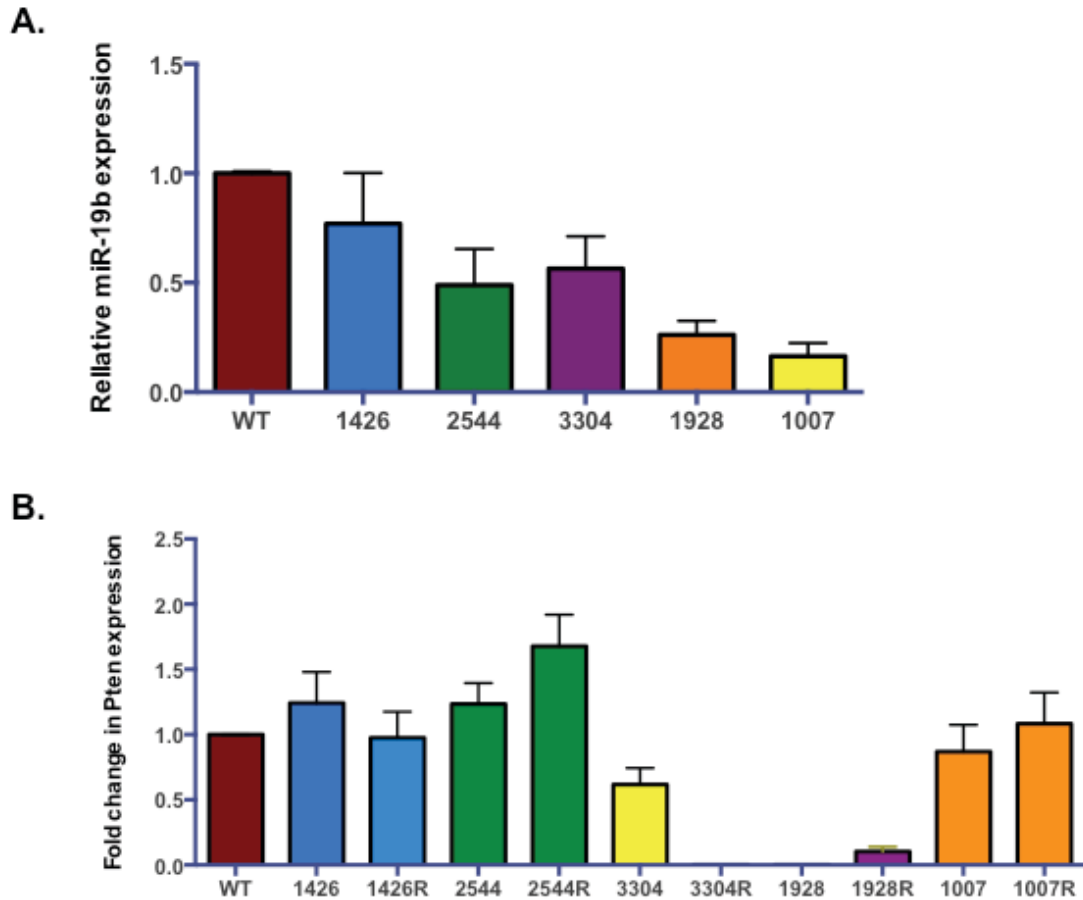


**Figure 29. There is no correlation between miR-19b expression and reduced Pten expression in transplanted T-ALLs** **A.** miRNA was isolated from leukemic tissues of recipient mice. miR-19b expression was analyzed using the TaqMan qPCR assay and was normalized to snoRNA202. Data shown are the average of three experiments. **B.** Total mRNA was isolated from leukemic tissues from primary leukemias and recipient mice (denoted R) and cDNA synthesized. Pten expression was analyzed by qPCR and normalized to  $\beta$ -Actin via the  $\Delta\Delta CT$  method. Data shown are the average of three experiments.

**Table 13. Loss of Pten expression correlates with decreased GSI sensitivity and increased p-Akt.**

	<b>GSI Response</b>	<b>Disease Latency (days)</b>	<b>Pten mRNA</b>	<b>Pten protein</b>	<b>p-Akt</b>	<b>miR-19b</b>
1426	complete	51	+	+	low/+	~WT
2544	complete	39	+	+	low/+	50% of WT
1928	partial	21	-	-	+++	50% of WT
3304	partial	24	low	low	low/+	30% of WT
1007	resistant	17	+	low	++	10% of WT

## **Appendix II: Attempts to further characterize the L-IC population**

## Introduction

The focus of my dissertation research has been to identify and characterize the murine T-ALL L-IC and then target pathways to inhibit its growth and survival. Our current data on the *Lck-Ta11/Lmo2* L-IC suggest that the L-IC is a subset of the DN3 population (<sup>251</sup> and Table 1). The percent of DN3 cells does not correlate with L-IC frequency (Table 1) and therefore further purification is necessary in order for a definitive L-IC population can be determined. Because of the low frequency of L-ICs in the *Lck-Ta11/Lmo2* model of T-ALL, it is likely that more than one marker will be necessary to purify the population.

c-Kit, also known as CD117, is a cell surface cytokine receptor that binds stem-cell factor (SCF) and initiates PI3K, Stat(1,3,5), and MAPK signaling cascades<sup>503,504</sup>, all of which promote cell survival, proliferation, and differentiation of hematopoietic cells<sup>505</sup>. c-Kit<sup>-/-</sup> mice present with hematopoietic, germ cell, and melanoblast defects<sup>506</sup>. Expression of c-Kit is critical to early thymocyte development, specifically thymocytes in the DN1 and DN2 stages<sup>507</sup>. Its expression is decreased in T-cells between the DN2b and DN3a stages of thymocyte development, but low expression is retained until the cells reach DN4/DP. Single-positive T-cells do not express c-Kit, except briefly during CD8 stimulation(reviewed in<sup>40</sup>).

The interleukin-7 receptor (IL7R) consists of a heterodimer of 2 subunits: IL7R $\alpha$  (CD127) and the common- $\gamma$  receptor (CD132). Once engaged with its

ligand, IL7, the IL7R initiates a signaling cascade mediated by the JAK/STAT5 and PI3K/mTOR pathways(reviewed in<sup>399</sup>). One of the main functions of the IL7R is to promote survival and inhibit apoptosis in developing thymocytes. The expression of IL7R is critical for early T-cell specification and differentiation, but expression decreases starting at the DN3 stage until it is undetectable in single positive thymocytes<sup>508,509</sup>.

As mentioned in the Chapter I, the DN3 population can be divided into two subpopulations (DN3a and DN3b) based on the expression of CD27<sup>53</sup>. CD27 is a member of the TNF family of cell surface receptors and initiates MAPK and NFκB signaling after binding its ligand CD70, thereby promoting proliferation of T-cells<sup>510–512</sup>. Expression is absent in T-cells until the DN3b stage of development as the receptor has critical roles in developing long-term immunity in mature T-cells. The expression of CD27 also correlates with the downregulation of Notch1 signaling in normal developing thymocytes<sup>419</sup>. The transition of T-cells from the DN3a to DN3b stage marks the transition from quiescence to rapid proliferation(reviewed in<sup>40</sup>). This marker also has leukemic implications: in CML, the expression of CD27 is associated with increased L-IC activity<sup>513</sup>.

This Appendix will discuss attempts to define the L-IC based on cell surface markers normally expressed on T-cells (CD27) and those expressed on more immature progenitor cells (c-kit and IL7R). I also conducted some preliminary experiments with BrdU incorporation to determine if the L-IC

population consists of quiescent or rapidly dividing cells within our murine T-ALLs.



## Results

I stained seventeen primary T-ALLs and four preleukemic thymi (mice age 4-6 weeks) for the expression of c-Kit because of its role in early thymocyte survival and differentiation. Normal thymocytes express c-Kit at the DN1 and DN2 stages, but expression begins to decrease during the transition from DN2 to DN3. On 3/4 preleukemic DN3 and 4/4 preleukemic DN4 cells, there appears to be some aberrant expression of c-Kit (Table 14). This expression is decreased or undetected in transformed T-ALLs, except for two leukemias (3264 and 4018) that expressed high levels of c-Kit in the DN3 compartment. These data suggest that c-Kit may have a role in the preleukemic differentiation block caused by overexpression of Tal1 and/or Lmo2 and potentially could contribute to self-renewal of this population. In fact, the Tal1 complex is thought to control the expression of c-Kit at the DN1/DN2 stage in normal hematopoiesis<sup>94</sup>, so it likely drives expression of c-Kit in these preleukemic progenitors.

c-Kit expression appears to decrease upon leukemic transformation, but can still be detected on 9/17 of the T-ALL DN3 populations examined. This is somewhat surprising, as Notch1, whose expression is high in murine T-ALLs, can also influence c-Kit expression<sup>514</sup>. c-Kit could be used as a marker to sort T-ALLs and enrich for the L-IC population but it does not seem to be a universal or consistent marker on the leukemic DN3 cells. Based on its expression in leukemic DN3 cells, c-Kit could potentially result in a 3-10 fold enrichment of the

L-IC population. Unfortunately, we did not perform L-IC assays with the 17 T-ALLs examined, so a correlation between c-Kit expressing DN3 cells and L-IC frequency was not made.

Because the IL7R promotes survival in thymocytes, we hypothesized that it may also promote survival in the T-ALL L-IC and possibly serve as a marker to enrich the LIC population. Eleven primary murine T-ALLs and four preleukemic thymi were analyzed for expression of IL7R $\alpha$  on the surface of DN3 cells (not shown), but results were inconclusive. Staining needs to be optimized and analysis repeated. IL7R expression is still an interest in our lab, especially in light of recent reports citing activating IL7R mutations in T-ALL<sup>515</sup>.

In order to determine the DN3a/DN3b profile in the *Lck-Ta11/Lmo2* mouse model of T-ALL, staining was performed on three primary T-ALLs and four preleukemic thymi. This analysis revealed that nearly all the preleukemic and leukemic DN3 cells expressed CD27 and potentially were derived from the DN3b subset (Table 15). Based on the characteristics of normal DN3a/b cells<sup>40</sup>, we could hypothesize that T-ALL L-ICs are highly proliferative. This would be consistent with the activation of the Notch1-c-Myc pathway at this stage in T-ALL. Alternatively, it is possible that there is a small quiescent population in the DN3a subset and that this subset contains the L-IC.

A population of quiescent L-ICs has been described in AML that is consistent with normal HSC biology<sup>342,361</sup>. We attempted to examine the

proliferative properties of the *Lck-Tal1/Lmo2* L-ICs by performing *in vivo* BrdU uptake assays. Leukemic mice were injected with BrdU and leukemic cells were stained for flow cytometry one hour later. BrdU staining of three primary T-ALLs along with thymi of two age-matched wild-type mice revealed that only a small portion of the leukemic DN3 cells are dividing at any given time, similar to the phenotype in normal thymocytes (Figure 30). These experiments may have been limited by the timing of the BrdU injections or by age of the wild type mice. Because the wild-type mice were age-matched to the diseased mice, perhaps the thymus had involuted to a point where cells were no longer cycling. As they stand, these data do not provide enough evidence to claim that there is a quiescent DN3 population in murine T-ALLs.

## Discussion

The expression of c-Kit on the surface of DN3 cells could serve as a marker to sort DN3 cells and determine the L-IC frequency of the positive and negative populations (Table 14). It is possible that c-Kit helps contribute to the accumulation of pre-L-ICs in the thymus as judged by the increased expression of c-Kit on 3/4 preleukemic DN3 populations examined. Upon transformation, c-Kit expression may only remain on the small population L-ICs. Consistently, c-Kit is present on preleukemic DN4 cells, but absent on the leukemic DN4 population. This could reflect the developmental block at the DN stage in preleukemic mice where expression decreases once the cells transform and differentiate towards DP blasts. It has been shown that c-Kit activation confers radioprotection to cells<sup>516,517</sup>. The activation of c-Kit on a subset of the DN3 population could mediate the radioprotection observed in *CD2-Lmo2* thymocytes.

Because most of the cells in the preleukemic and leukemic the *Lck-Tal1/Lmo2* thymi do express CD27, this population is unlikely to be helpful in enriching for the L-IC population, but could elucidate more about L-IC biology. In one of the preleukemic thymi examined, there appeared to be a small population of cells that did not stain positively for CD27 expression (Table 15). This CD27-negative population did not persist in any of the three T-ALLs examined. If further analysis confirms these preleukemic data, perhaps a lack of CD27 expression could indicate a population enriched in L-IC activity. The DN3a population is

blocked in the G1 phase of the cell cycle while the TCR-V $\beta$  chain is rearranged and expressed; cells then progress through the cell cycle once positive selection of the thymocytes begins<sup>40</sup>. This G1 population could represent a quiescent L-IC population in T-ALL. At this point, however, this CD27-negative population does not persist in our murine T-ALLs, and we do not have evidence of a quiescent L-IC.

Until the L-IC is further purified, an alternative to BrdU staining might need to be used to define cycling status of the L-IC population. The low percentage of BrdU incorporation in the murine T-ALLs could be an indication that the leukemic cells are not proliferating in the thymus. When disease is evident, the thymus is enlarged and it is probable that cells are unable to obtain the proper amount of nutrients; cells egress from the thymus and infiltrate the spleen, liver, bone marrow, kidneys, and lymph nodes. Analysis of these other sites of leukemic burden could distinguish whether leukemic DN3 are cycling more in other areas of the body.

Alternatively, Hoechst 33342 staining could be performed. This stain is incorporated into the minor groove of DNA and can be used for cell cycle analysis<sup>518</sup>. However, when excited using both the red and blue lasers, the fluorescence can be plotted and a side population identified<sup>519</sup>. In murine bone marrow, the side population enriches for the HSC population<sup>520</sup>. This staining technique could be used with the *Lck-Tal1/Lmo2* T-ALLs to determine if there is a

population that effluxes the Hoechst stain. Most importantly, cells stained with Hoechst stain can be sorted and live cells potentially transplanted into the L-IC assay to determine if there is a functional consequence of dye efflux.

## **Methods**

### **Flow cytometry**

All flow cytometry experiments were performed as previously described using either the FACSCalibur or LSRII machines (BD). Antibodies to c-Kit (eBioscience catalog #35-1171-82), CD27 (eBioscience catalog#11-0271-85) and IL7R (BD catalog#555288) were titrated and used at optimal concentrations for this cell type. The IL7R antibody was biotinylated and used with a streptavidin secondary antibody (eBioscience catalog#17-4317-82). BrdU uptake assays and staining were performed according to instructions provided in the APC BrdU Flow Kit (BD catalog #552598).

**Table 14. c-Kit expression on *Lck-Tal1/Lmo2* preleukemic and leukemic thymic subsets**

PRE-LEUKEMIA				
Thymic subsets				
Mouse	DN1	DN2	DN3	DN4
WT	++	+++	++	-
3255	low	+	low	++
3258	low	++	+	++
3237	+	++	+++	++
3294	++	+	++	+
T-ALL				
Leukemic subsets				
Mouse	DN1	DN2	DN3	DN4
WT	++	+++	++	-
3706	+	N.A.	N.A.	-
3708	N.A.	N.A.	+	-
3700	N.A.	N.A.	+	-
3664	++	N.A.	N.A.	-
3265	+	+	N.A.	N.A.
3209	N.A.	N.A.	+	low
3234	N.A.	low	low	-
3239	N.A.	N.A.	+	low
3264	-	-	+++ (59%)	N.A.
3233	+	+++ (80%)	++	N.A.
3260	N.A.	N.A.	+	+
4004	N.A.	N.A.	+	-
4018	N.A.	N.A.	+++ (30%)	-
4170	N.A.	N.A.	low	-
3299	N.A.	N.A.	low	-
4122	N.A.	N.A.	low	-
4001	N.A.	N.A.	low	low

low, slight MFI shift only; +, 1-10%; ++, 10-29%; +++, >30%; N.A., not applicable



**Table 15. Increased CD27 expression is found on preleukemic and leukemic DN3 cells**

PRE-LEUKEMIA		
Thymic subset		
Mouse	DN3a	DN3b
WT	+++	+
3553	-	+++
3237	-	+++
3294	-	+++
2596	low	+++
T-ALL		
Leukemic subset		
Mouse	DN3a	DN3b
WT	+++	+
3700	-	+++
3702	-	+++
3708	-	+++

+, 1-10%; ++, 10-50%; +++, >50%;

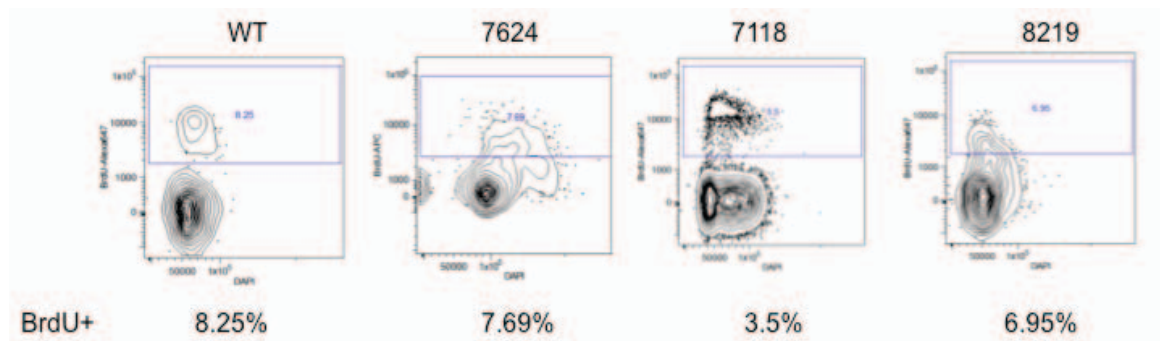


**Figure 30. BrdU uptake assays reveal that leukemic DN3 cells have similar cycling status to wild-type thymocytes.** Three mice with T-ALL and age-matched wild-type mice were injected with BrdU and rested for one hour before thymomas (T-ALL) or thymi (wild-type) were harvested and stained for surface antibodies and internal BrdU. DAPI is used as a DNA dye. Plots shown were gated on live DN3 cells.

## **Appendix III: c-Myb plays a role in T-ALL L-IC survival and/or activity**

## Introduction

The c-Myb transcription factor is encoded by the cellular homologue of the *v-myb* oncogene discovered in the avian leukemia viruses AMV and E26. It is a helix-loop-helix transcription factor expressed in hematopoietic cells<sup>521,522</sup>, intestinal epithelial cells<sup>523</sup>, and the adult brain<sup>524</sup> and recognizes the DNA sequence C/T-A-A-C-G/T-G<sup>525</sup>. c-Myb has been shown to regulate self-renewal in these normal tissues and has been implicated in the pathogenesis of breast cancer<sup>526,527</sup>, colon cancer<sup>528,529</sup>, and a variety of leukemias (AML, CML, T-ALL)<sup>79,530–535</sup>.

The target genes of c-MYB range from housekeeping genes to T-cell genes to proto-oncogenes (reviewed in<sup>443</sup>). Many of the genes activated by c-MYB are involved in cell cycle progression, such as cyclins and cyclin-dependent kinases<sup>536–538</sup>. Other target genes of c-MYB inhibit apoptosis, such as *BCL-2* and *BCL-XL*<sup>539–541</sup>. In murine knockout models, it was found that c-Myb is required for erythropoiesis in the fetal liver; null mice were severely anemic and did not survive to birth<sup>521</sup>. Using a conditional knockout model in the hematopoietic system, Lieu and colleagues showed that c-Myb is required for self-renewal of hematopoietic stem cells<sup>542</sup> and the development of T-cells<sup>543</sup>. c-Myb is required for progression through the DN3 stage, survival of DP thymocytes, and maturation of CD4-single positive cells<sup>544,545</sup>. Any of these checkpoints could be critical to the survival of T-ALL cells.

In human T-ALL, both somatic duplications and translocation events have been shown to activate the *c-MYB* locus and contribute to disease pathogenicity<sup>532,533</sup>. In the case of translocation t(6;7)(q23;q34), the *c-MYB* locus is introduced into the TCR $\beta$  locus, which drives its expression in differentiated T-cell blasts<sup>532</sup>. *c-Myb* expression is normally decreased after T-cells reach the DN3 stage of thymocyte development, but not entirely eliminated<sup>545,546</sup>. A proliferation/mitosis signature, consistent with the activation of *c-Myc*, *Cdk1*, and Cyclins A, B, and E, characterizes this unique subset of T-ALL<sup>532</sup>.

In MLL-AF9 driven AML, *c-Myb* was found to promote self-renewal of the L-ICs and inhibition of *c-Myb* ablated leukemia in diseased mice<sup>439</sup>. In human T-ALL, *c-MYB* was found to be a direct target of TAL1 and is highly expressed in TAL1-positive T-ALL cell lines. Together, these data led us to hypothesize that *c-Myb* may control self-renewal in our *Lck-Tal1/Lmo2* mouse model of T-ALL. The experiments described in this appendix show that silencing of *c-Myb* in murine T-ALLs led to increased survival and decreased L-IC frequency in recipient mice. *c-Myb* inhibition was also shown to reduce self-renewal of L-ICs and reduce proliferation of bulk leukemic cells.

## Results

In order to determine if c-Myb plays a role in the T-ALL L-IC, we silenced expression of the protein using retroviruses expressing shRNA to *c-Myb*, as described in Chapter IV of this thesis. The same primary murine leukemias were used and manipulated simultaneously with the shMyc cells, therefore the same shRen cells from that experiment were used as the control for these experiments. When we transplanted the shMyb cells into recipient mice, we saw very similar results to the shMyc study. Three out of four T-ALLs showed significant increases in overall survival (Figure 31 A-C) and an overall 34-fold reduction in L-IC frequency (Table 16), range 7-fold to cure (Table 17). This indicates a critical role for c-Myb in leukemic initiation and maintenance.

As in the shMyc study, mice transplanted with T-ALL 4673 shMyb cells did not develop disease (n=9). There was no evidence of disease in the surviving mice and no GFP-positive cells found in the bone marrow, suggesting that the L-IC had been completely eliminated. T-ALLs 5109 and 5059 showed significant increases in survival upon c-Myb silencing and 7- to 18-fold decreases in L-IC frequency, respectively (Figure 31B-C;  $p < 0.007$ ,  $p < 0.008$ ; Table 17). These data confirm that c-Myb expression is required for L-IC expansion *in vivo*. Surprisingly, these results are actually more dramatic than what we saw with the shMyc cells (Figure 18, Tables 8 and 9) suggesting that c-Myb plays a larger role in the T-ALL L-IC compared to c-Myc. In contrast to the c-Myc study, T-ALL 6124 showed

a 3-fold decrease in L-IC frequency upon c-Myb silencing (Table 17). However, this decrease in L-IC frequency did not result in a significant increase in overall survival of the recipient mice (Figure 31D,  $p < 0.18$ ).

It is unclear why all T-ALLs did not respond to the c-Myb shRNA in a similar manner *in vivo*. We examined the effects of c-Myb inhibition on leukemic growth by plating the GFP-positive sorted cells in an *in vitro* growth assay and monitoring their proliferation over time. In all three T-ALLs tested, c-Myb silencing resulted in decreased proliferation and increased dead cells in the culture (Figure 32A). Consistent with the shMyc studies, T-ALL 6124 showed the least response to the Myb shRNA and a coordinate increase in GFP-negative cells in the culture. All murine T-ALLs appeared dependent on c-Myb for their growth. Knockdown of c-Myb protein in the retrovirally infected cultures was quite strong (Figure 32B), with an average knockdown of 5-fold (range 2- to 8- fold). This could explain the increased response to the shRNA *in vivo* compared to the shMyc experiments where knockdown averaged only 2-fold (range 1.4- to 2.3- fold).

When animals became diseased after transplantation with leukemic cells, GFP expression and c-Myb levels were examined in tissues exhibiting leukemic burden. Most of the mice that we were able to analyze had GFP-positive leukemia (not shown), but several animals were found deceased so we were unable to determine GFP expression. Unlike the shMyc studies, decreased c-Myb expression was apparent in all recipient mice examined (Figure 33). This

suggests that the shRNA was not silenced in the recipient mice and therefore disease initiation occurred even with decreased c-Myb levels.

To investigate the effects of c-Myb silencing on self-renewal of the murine T-ALLs, we performed secondary transplant experiments. 120 days after initial transplant, all surviving mice were sacrificed and tissues analyzed for GFP expression. We were unable to detect GFP-positive cells in the bone marrow or other lymphoid tissues, indicating a lack of transplanted leukemic cells (Figure 34). Bone marrow cells were pooled and  $5 \times 10^6$  cells were transplanted into secondary recipients. None of the 17 secondary transplants became diseased after an additional 120 days (not shown), suggesting that c-Myb is required for L-IC self-renewal, despite the fact that knockdown was maintained in primary recipients that became diseased. This assay ensures that shRNA to c-Myb did not simply induce quiescence of the leukemic cells in the primary recipients.



## Discussion

Here, I have shown a clear role for c-Myb in the maintenance and self-renewal of T-ALL L-ICs. Silencing of c-Myb with specific shRNAs resulted in decreased proliferation of T-ALL cells in culture. Importantly, decreased expression of c-Myb resulted in an average of 34-fold fewer L-ICs and significant effects on overall survival.

Probably the most interesting result in this study was that leukemic mice maintained knockdown of c-Myb at disease presentation. This finding suggests that that c-Myb may not be required for L-IC activity because c-Myb depleted L-ICs were capable of disease initiation. This contrasts with our study of c-Myc in Chapter IV where all diseased animals had silenced or escaped the shRNA and restored c-Myc expression in order to initiate disease. However, compared to the c-Myc study with the same exact tumors transplanted at the same time, c-Myb silencing resulted in a 34-fold decrease in L-IC frequency whereas c-Myc silencing resulted in a 17-fold reduction of L-ICs. This could indicate a more prominent role for c-Myb in L-ICs or could simply reflect a discrepancy in the levels of knockdown between the two experiments. Additionally, these results indicate that T-ALL dependence on a particular gene for growth *in vitro* does not correlate to the dependence *in vivo*.

Upstream of c-Myb, Tal1 could be mediating a stem cell phenotype in these T-ALL cells. TAL1 directly activates *c-MYB* in T-ALL<sup>119</sup> and c-Myb is

involved in the maintenance of normal HSCs<sup>521,522</sup>. The transcriptional program initiated by c-Myb expression points to increased cell survival and decreased apoptosis<sup>529,536,537,539–541,547,548</sup>. Enforced Tal1 expression causes a block in T-cell differentiation<sup>112,114</sup>, and it is possible that c-Myb expression is what allows these cells to remain alive long enough to incur additional mutations such as activating mutations and 5' deletions in the *Notch1* locus<sup>138,248</sup>. This protection from death could then be extended to the L-IC, as c-Myb activates *Bcl-XL* and *Bcl-2*<sup>539,540,547</sup>, two genes shown to be elevated in certain chemotherapy-resistant L-ICs.

Future experiments could include *in vitro* studies such as ChIP-seq, array CGH, and other types of profiling to reveal additional mechanisms of c-Myb activation, but these questions are not as interesting as the potential functional experiments. Completely ablating c-Myb at various points of leukemic transformation would allow us to further define its role in the L-IC. By using *c-Myb<sup>fl/fl</sup>* mice mated into our *Lck-Tal1/Lmo2* transgenic mouse lines, we could use various transgenic or knock-in Cre lines to confirm our shRNA results. Depending on which specific Cre is used, deletion should be more efficient than shRNA and this method would allow for deletion at different time points in development prior to leukemia. This strategy would also allow us to differentiate effects of leukemic cell engraftment and leukemia-initiating capabilities. Our lab has obtained these mice and begun the mating process.

The role of c-Myb in T-ALL is not entirely clear, but these preliminary studies support an important role in the self-renewal of the murine L-IC.

## **Methods**

### **Mice, Cell Culture, Flow cytometry**

All experiments described in this Appendix were performed at the same time and with the same reagents as experiments described in Chapter IV of this thesis.

### **Expression Analyses**

mRNA was isolated from retrovirally infected T-ALLs and T-ALL cell lines treated with JQ1 as described in Chapter IV. qPCR was performed on cDNA using the following primers for c-Myb expression: F:5' GAGCACCCAACTGTTCTC-3', R:5'- CACCAGGGGCCTGTTCTTAG-3' Protein expression was evaluated by immunoblotting using a monoclonal anti-c-Myb antibody (Millipore Cat# 05-175).

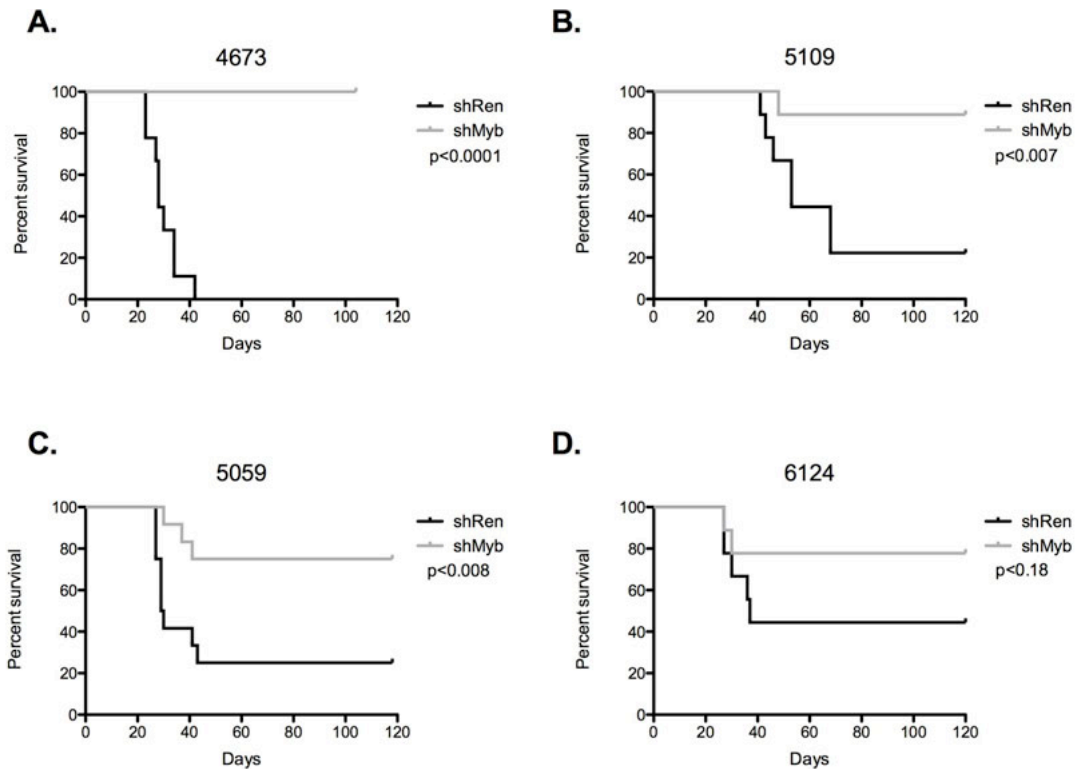


**Figure 31. Silencing of c-Myb prolongs survival in mice transplanted with murine T-ALL cells.** Four independent murine *Tal1/Lmo2* T-ALL cells were infected with retroviruses encoding an shRNA to c-Myb or Renilla luciferase. Cells were sorted for GFP expression, serially diluted and transplanted into syngeneic recipients via intraperitoneal (IP) injection. Transplanted mice were monitored for evidence of disease. The survival curve for each group of mice was estimated using the Kaplan-Meier method and the difference in overall survival between the two groups assessed by the log-rank test. **A** 4673  $p < 0.0001$ , **B** 5109  $p < 0.007$ , **C** 5059  $p < 0.008$ , **D** 6124  $p < 0.18$ .

**Table 16. Silencing of c-Myb reduces L-IC frequency.**

shRNA	Number of Cells Injected				#diseased/ total	L-IC freq	CI
	100,000	10,000	1,000	100			
shRen	6/7	10/13	8/13	4/6	28/39	0.034%	0.064-0.018%
shMyb	4/7	2/13	0/13	0/6	6/39	0.001%	0.002-0.0004%

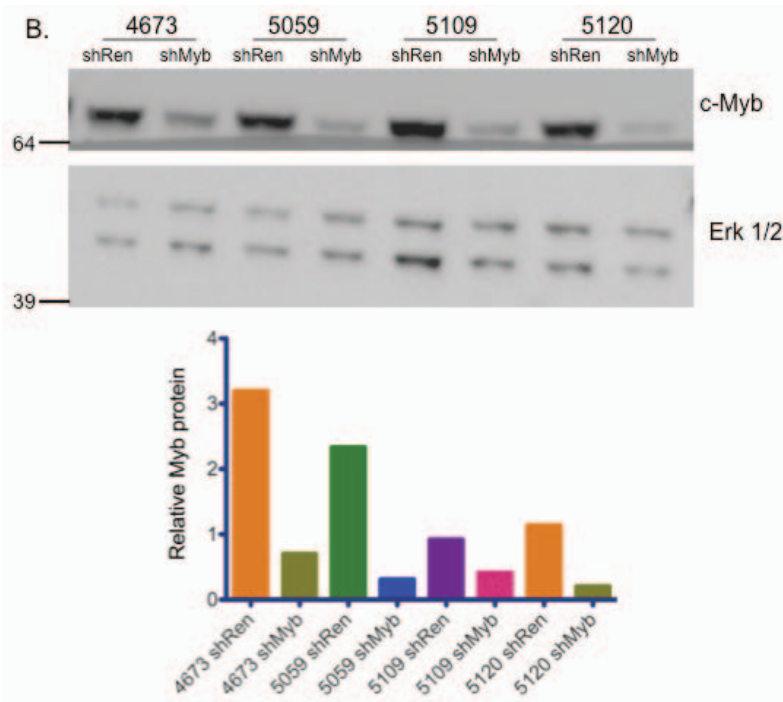
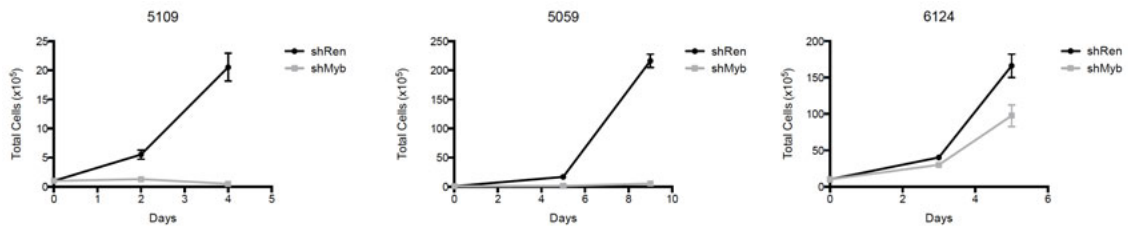
CI: Confidence Interval

Table 17. Silencing of c-Myb reduces L-IC frequency.

Cell Number	<u>#Diseased mice/Total injected</u>							
	4673		5109		5059		6124	
	<u>shRen</u>	<u>shMyb</u>	<u>shRen</u>	<u>shMyb</u>	<u>shRen</u>	<u>shMyb</u>	<u>shRen</u>	<u>shMyb</u>
<b>100000</b>	--	--	2/3	1/3	4/4	3/4	--	--
<b>10000</b>	3/3	0/3	2/3	0/3	3/4	0/4	2/3	2/3
<b>1000</b>	3/3	0/3	1/3	0/3	2/4	0/4	2/3	0/3
<b>100</b>	3/3	0/3	--	--	--	--	1/3	0/3
<b>L-IC freq</b>	N.D.	N.D.	N.D.	0.0004%	0.02%	0.0011%	N.D.	0.009%
<b>Fold Change</b>	cure		~7-fold		18-fold		~3-fold	

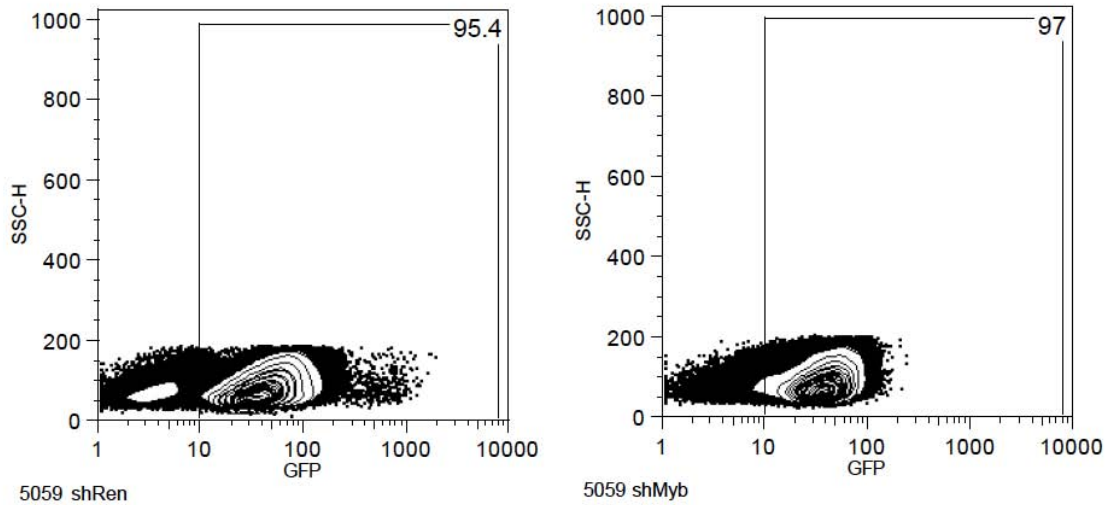
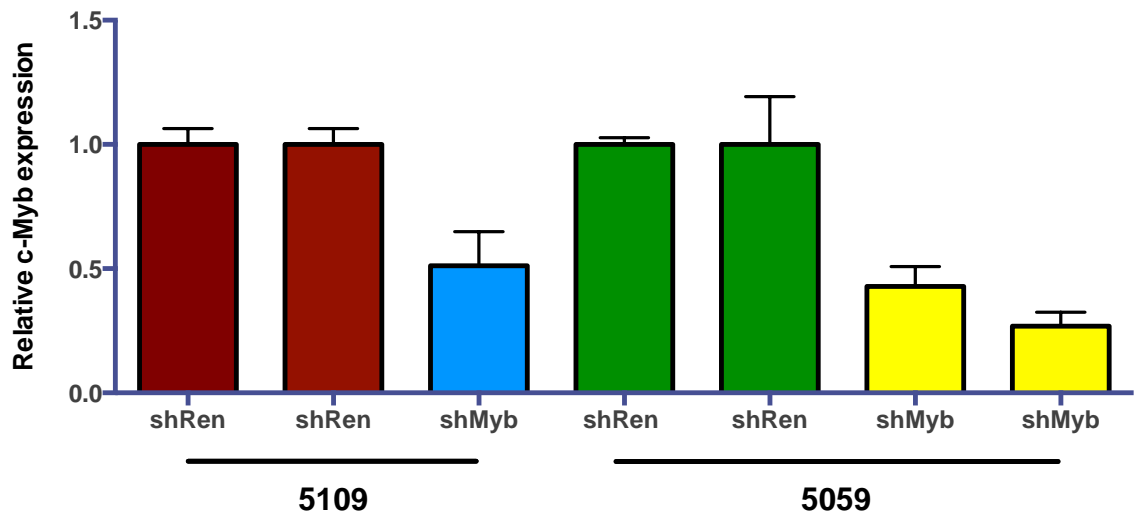
N.D. Cannot calculate

A.



**Figure 32. Impaired cell growth and reduced c-Myb expression in c-Myb-silenced leukemic cells. A. c-Myb suppression impairs bulk leukemic growth in vitro.** Cell viability was calculated via a trypan blue exclusion assay. Four independent mouse T-ALLs were analyzed; three are shown. **B. Reduced c-Myb protein levels in c-Myb-silenced leukemic cells.** Protein was isolated from murine *Tal1/Lmo2* T-ALLs infected with retroviruses encoding shRNAs to c-Myb or Renilla luciferase and c-Myb and Erk1/2 protein levels were determined by immunoblotting. Quantification of the blot is shown below



**A.****B.**

**Figure 33. Myb-silenced mice that develop disease contain GFP+ cells and exhibit Myb knockdown.** **A.** Mouse leukemic cells were isolated from mice transplanted with shRen or shMyb infected mice. Thymi were dissociated into a single cell suspension and GFP expression determined by flow cytometry. One representative from each group of tumor 5059 is shown. **B.** RNA was isolated from thymi and *c-Myb* mRNA levels determined by quantitative real time PCR. Copy number was normalized to  $\beta$ -actin using the  $\Delta\Delta$ CT method.

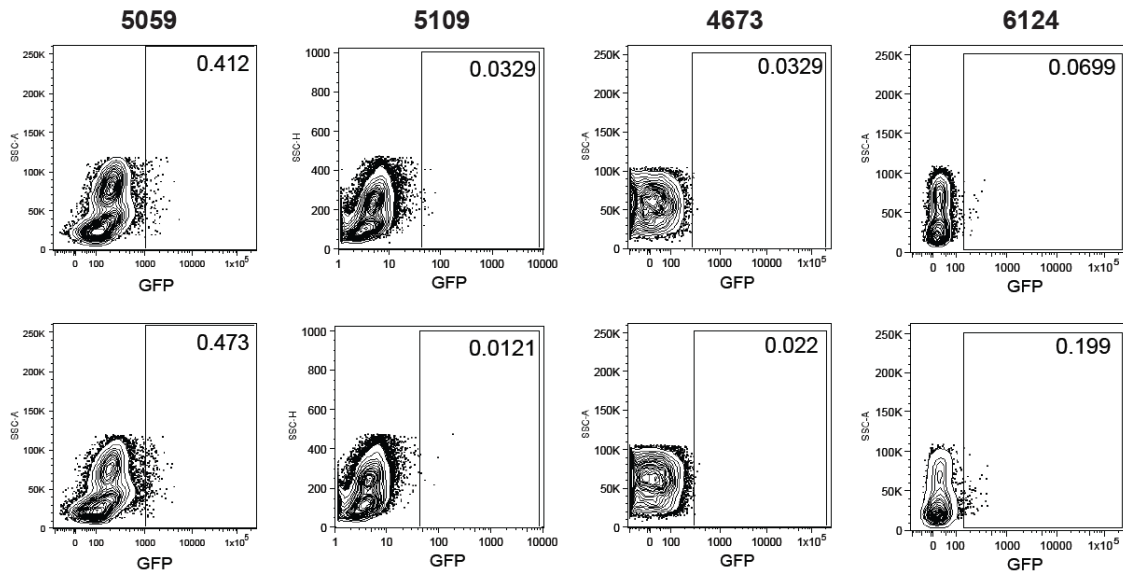


**Figure 34. No GFP-positive cells remained in transplanted animals 120 days post-transplant.** Mice that failed to develop disease 120 days post-transplant were sacrificed. Bone marrow cells were isolated and analyzed by flow cytometry. No GFP-positive cells were present in any animals examined. Two representative mice from each group are shown.

## **Appendix IV: Microarray following JQ1 treatment *in vivo***

The data presented in this Appendix go with Chapter IV. A gene expression array was attempted using murine T-ALLs treated with JQ1 *in vivo*. Results were inconclusive and so were not included in the main body of this thesis.

## Results

### ***JQ1 inhibits c-Myc in vivo***

To determine the mechanism of action of JQ1 in T-ALL, we designed an *in vivo* microarray. Three independent murine T-ALLs were each transplanted into four recipient mice. Upon disease presentation, two mice were treated with vehicle or 50mg/kg of JQ1. Two hours post-injection, tumor tissue was harvested and total RNA isolated and sent for oligonucleotide profiling (see Methods for greater detail). JQ1 treatment significantly ( $p < 0.05$ ) changed the expression of 524 genes with a fold change cutoff of 1.5; 376 were downregulated upon treatment while 148 were induced (not shown). Upon ranking this list (Table 18), we found that the E47/HEB-regulated gene *Rag1* was the most highly modulated (fold change, -5.7,  $p < 0.03$ ) and *c-Myc* was ranked 13th (fold change of -3.2,  $p < 0.04$ ). We found a relatively small number of genes to be modulated in our microarray, especially considering the vast number of genes known to be regulated by *c-Myc*. Known target genes such as *Cdk4*, *Fbl*, *Apex1*, and *Tk1* were not found on the array, despite being reduced by JQ1 in all three cell lines tested (Figure 23).

Technical error introduced by attempting to perform a microarray with leukemic tissues might have caused variation in gene expression among the T-ALLs examined. Normal cells in the tissue could have also affected the results or compound availability *in vivo* may have not been uniform across the animals

examined. Indeed, gene expression values differed from one vehicle-treated mouse to the next, within a single T-ALL analyzed. Because JQ1 reduces cell cycle and inhibits apoptosis (Figure 22C,D), it is likely that genes controlling these pathways should be found on an array for JQ1 treatment. If the tissues processed from the animals were at different proliferation states at the time of harvest, this could increase variability even further.

Gene expression profiling should be repeated with murine T-ALL cell lines where technical variation would be limited. An ideal experiment would take place at an early time point during JQ1 treatment when gene expression is changing, but when the arrest and apoptosis are not yet apparent. Established cell lines would be treated for a time course to determine the optimum balance of these factors and then both technical (2-3 repeats of same cell line) and biological (2-3 cell lines) replicates would be submitted for microarray analysis. Hopefully, this would reduce the noise and variability both within and across T-ALL samples examined. Further analysis of the effects of significantly changed genes on T-ALL biology could determine a genetic mechanism of action for JQ1. This experiment could also elucidate additional genes critical for T-ALL maintenance that have not yet be studied.

**Table 18. Top 50 repressed and induced genes following JQ1 treatment**

<b>Gene Symbol</b>	<b>Gene Description</b>	<b>P</b>	<b>FC</b>
Rag1	recombination activating gene 1	0.0341	-5.7260
Ccr4	chemokine (C-C motif) receptor 4	0.0159	-5.7188
Slc16a5	solute carrier family 16, member 5	0.0049	-4.3560
Tmem229b	transmembrane protein 229B	0.0091	-4.0645
Naip3	NLR family, apoptosis inhibitory protein 3	0.0205	-3.5799
Arpp21	cyclic AMP-regulated phosphoprotein, 21	0.0423	-3.4594
Sla	src-like adaptor	0.0146	-3.4116
Il1rl2	interleukin 1 receptor-like 2	0.0066	-3.3810
Arsi	arylsulfatase i	0.0027	-3.3637
Tcrg-V3 Tcrg-V2	T-cell receptor gamma, V3   T-cell receptor gamma, V2	0.0155	-3.3450
Lpar4	lysophosphatidic acid receptor 4	0.0263	-3.1848
Myc	myelocytomatosis oncogene	0.0437	-3.1729
Il12rb2	interleukin 12 receptor, beta 2	0.0033	-3.1584
Trat1	T cell receptor associated transmembrane adaptor 1	0.0051	-3.1435
Il5ra	interleukin 5 receptor, alpha	0.0004	-3.0937
Tnfrsf8	tumor necrosis factor receptor superfamily, member 8	0.0052	-3.0010
Tnfsf10	tumor necrosis factor (ligand) superfamily, member 10	0.0007	-2.9721
Cd226	CD226 antigen	0.0174	-2.9180
Gpr174	G protein-coupled receptor 174	0.0229	-2.9110
Cd27	CD27 antigen	0.0091	-2.8525
Gm239	predicted gene 239	0.0017	-2.7914
Gm885	predicted gene 885	0.0006	-2.7681
Narg2	NMDA receptor-regulated gene 2	0.0473	-2.7680
Rpp38	ribonuclease P/MRP 38 subunit (human)	0.0087	-2.7397
Ubash3a	ubiquitin associated and SH3 domain containing, A	0.0455	-2.7359
Mir363	microRNA 363	0.0377	-2.7308
Tmem173	transmembrane protein 173	0.0053	-2.7060
Ikzf2	IKAROS family zinc finger 2	0.0121	-2.6943
Zfp72	zinc finger protein 72	0.0075	-2.6593
Ifi202b	interferon activated gene 202B	0.0068	-2.6467
Prssl1 Fstl3	protease, serine-like 1   follistatin-like 3	0.0014	-2.6351
Prkcq	protein kinase C, theta	0.0241	-2.5738
Ifi203	interferon activated gene 203	0.0441	-2.5049
Art2b	ADP-ribosyltransferase 2b	0.0086	-2.4902
Cd28	CD28 antigen	0.0002	-2.4796
Rasgrp1	RAS guanyl releasing protein 1	0.0387	-2.4744
Mcoln3	mucolipin 3	0.0437	-2.4548
Ms4a6b	membrane-spanning 4-domains, subfamily A, member 6B	0.0127	-2.4358
Prr11	proline rich 11	0.0486	-2.4039
Gm10673	predicted gene 10673	0.0194	-2.4036
Cd2	CD2 antigen	0.0342	-2.4021
Ccdc125	coiled-coil domain containing 125	0.0142	-2.3834
Slfn8	schlafen 8	0.0466	-2.3777
Rtp4	receptor transporter protein 4	0.0118	-2.3632
Slc40a1	solute carrier family 40, member 1	0.0484	1.9810

Chchd7	coiled-coil-helix-coiled-coil-helix domain containing 7	0.0066	1.9876
Lyn	Yamaguchi sarcoma viral (v-yes-1) oncogene homolog	0.0152	1.9888
Dag1	dystroglycan 1	0.0249	1.9935
Ifrd1	interferon-related developmental regulator 1	0.0025	2.0117
Larp1b	La ribonucleoprotein domain family, member 1B	0.0065	2.0211
Chka	choline kinase alpha	0.0105	2.0244
Zfand2a	zinc finger, AN1-type domain 2A	0.0045	2.0245
Csf1r	colony stimulating factor 1 receptor	0.0076	2.0752
Ppp1r13b	protein phosphatase 1, regulatory (inhibitor) subunit 13B	0.0288	2.0811
Cited2	Cbp/p300-interacting transactivator 2	0.0039	2.0962
Arid5a	AT rich interactive domain 5A (MRF1-like)	0.0367	2.1071
Jund	Jun proto-oncogene related gene d	0.0389	2.1471
Hist1h2bg	histone cluster 1, H2bg	0.0367	2.1539
Sgk1	serum/glucocorticoid regulated kinase 1	0.0240	2.1610
Mfge8	milk fat globule-EGF factor 8 protein	0.0495	2.1719
6430548M08Rik	RIKEN cDNA 6430548M08 gene	0.0024	2.1733
Serpina1e	serine (or cysteine) peptidase inhibitor, clade A, member 1E	0.0470	2.1760
B230325K18Rik	RIKEN cDNA B230325K18 gene	0.0193	2.1850
Dnajb9	DnaJ (Hsp40) homolog, subfamily B, member 9	0.0484	2.2274
Gcg	glucagon	0.0123	2.2588
Ero1lb	ERO1-like beta (S. cerevisiae)	0.0123	2.2663
Arrdc3	arrestin domain containing 3	0.0424	2.2860
Mylip	myosin regulatory light chain interacting protein	0.0221	2.2905
Rnf146	ring finger protein 146	0.0304	2.3479
Sesn2	sestrin 2	0.0269	2.3558
Serpina1b	serine (or cysteine) preptidase inhibitor, clade A, member 1B	0.0158	2.3571
Baiap2	brain-specific angiogenesis inhibitor 1-associated protein 2	0.0190	2.4263
Hist1h3d	histone cluster 1, H3d	0.0381	2.4478
Cnnm4	cyclin M4	0.0278	2.5110
Tiparp	TCDD-inducible poly(ADP-ribose) polymerase	0.0218	2.5171
Cirbp	cold inducible RNA binding protein	0.0488	2.5373
Rgs2	regulator of G-protein signaling 2	0.0136	2.5410
Habp4	hyaluronic acid binding protein 4	0.0033	2.5806
Ins2	insulin II	0.0217	2.6836
Txnip	thioredoxin interacting protein	0.0081	2.7543
Hexim1	hexamethylene bis-acetamide inducible 1	0.0042	2.7566
Iapp	islet amyloid polypeptide	0.0114	2.9620
Lyve1	lymphatic vessel endothelial hyaluronan receptor 1	0.0411	3.0694
Gadd45b	growth arrest and DNA-damage-inducible 45 beta	0.0253	3.0923
Ins1	insulin I	0.0330	3.2085
Larp1b	La ribonucleoprotein domain family, member 1B	0.0075	3.3594
Chac1	ChaC, cation transport regulator-like 1 (E. coli)	0.0237	3.6694
Hist2h3c2	histone cluster 2, H3c2	0.0258	4.3948
Cd74	CD74 antigen	0.0344	4.6995
Hist1h2bc	histone cluster 1, H2bc	0.0198	5.2753
Hist1h1c	histone cluster 1, H1c	0.0037	6.8435

P, p-value; FC, fold change



## Methods

### Gene expression array

Three independent murine T-ALLs were each transplanted into four recipient mice. Upon disease presentation, two mice were treated with vehicle or 50mg/kg of JQ1. Two hours post-injection, tumor tissue was harvested and total RNA isolated, followed by cleanup using the RNeasy kit (Qiagen). Quality of mRNA was assessed using a nanochip on the Agilent Bioanalyzer 2100 (Agilent Technologies) and samples were processed for oligonucleotide microarray profiling. Affymetrix Mouse Exon 1.0 ST arrays were processed and analyzed using GeneSpring GX12.1 software (Agilent Technologies). Data was normalized using the Robust Multi-Array Analysis (RMA) summarization algorithm with data transformation set to the median of each sample. Probe sets were filtered on expression and *P* values for differential expression were determined, with  $p < 0.05$  being considered statistically significant, and a cutoff of 1.5-fold being used for further analysis.

### List of primers

Gene	Forward 5'-3'	Reverse 5'-3'
$\beta$ -Actin	CGGTTGGCCTTAGGGTTCAG	CGAGGCCCCAGAGCAAGAGAG
Apex1	ACGGGGAAGAACCCAAGTC	GGTGAGGTTTTCTGATCTGGAG
c-Myb	GAGCACCCAACCTGTTCTC	CACCAGGGGCCTGTTCTTAG
c-Myc	CTGTTTGAAGGCTGGATTTCCCT	CAGCACCGACAGACGCC
Cdk4	ATGGCTGCCACTCGATATGAA	TCCTCCATTAGGAACTCTCACAC
Deltex-1	TGCCTGGTGGCCATGTACT	GACACTGCAGGCTGCCATC
Fbl	CAAAATTGAGTACAGAGCCTGGA	CGGGCCGACAATATCAGAGA
GFP*	TATATCATGGCCGACAAGCA	CCTACAGGTGGGGTCTTTCA
Hes1	AAGACGGCCTCTGAGCACA	CCTTCGCCTCTTCTCCATGAT
Mcl1	TGTAAGGACGAAACGGGACT	AAAGCCAGCAGCACATTTCT
Notch1	CCCTTGCTCTGCCTAACGC	GGAGTCCTGGCATCGTTGG
Pre-T $\alpha$	CTGCTTCTGGGCGTCAGGT	TGCCTTCCATCTACCAGCAGT
Pten	TGGATTCGACTTAGACTTGACCT	GCGGTGTCATAATGTCTCTCAG
Rag1	CATTCTAGCACTCTGGCCGG	TCATCGGGTGCAGAACTGAA
Rag2	TTAATTCCTGGCTTGGCCG	TTCCTGCTTGTGGATGTGAAAT
Tk1	AAGTGCCTGGTCATCAAGTATG	GCTGCCACAATTACTGTCTTGC

\*genomic DNA PCR

### List of antibodies

<b>FACS</b>	<b>Antibody</b>	<b>Company</b>	<b>Catalog#</b>
	Annexin V-FITC	BD Pharmingen	556419
	B220-PE	BD Pharmingen	553089
	BrdU-APC (kit)	BD Pharmingen	552598
	CD117-PECY5	eBioscience	35-1171-82
	CD127-biotin	BD Pharmingen	555288
	CD25-PECY7	eBioscience	25-0251-82
	CD27-FITC	eBioscience	11-0271-85
	CD4-PE	BD Pharmingen	553033
	CD4-PECy5	BD Pharmingen	553654
	CD44-APC	BD Pharmingen	559250
	CD8-FITC	BD Pharmingen	553031
	CD8-PE	BD Pharmingen	553049
	Gr-1-PE	BD Pharmingen	553128
	Mac1-PE	BD Pharmingen	557397
	Streptavidin-APC	eBioscience	17-4317-82
	Streptavidin-PE	BD Pharmingen	554061
<b>IB</b>	<b>Antibody</b>	<b>Company</b>	<b>Catalog#</b>
	$\beta$ -Actin clone AC-15	Sigma	A5441
	Notch1 Val1744 clone D3B8	Cell Signaling	4147S
	c-Myb clone 1-1	Millipore	05-175
	c-Myc clone 9E10	Santa Cruz	sc-764
	c-Myc clone N262	Santa Cruz	sc-40
	p-Akt (S473) clone D9E	Cell Signaling	4060S
	Pten	Cell Signaling	9552
	Total Akt	Santa Cruz	sc-8312
	Total Erk1/2	Cell Signaling	9102S
	anti-mouse secondary	GE Healthcare	NA934V
	anti-rabbit secondary	GE Healthcare	NA931V

## REFERENCES

1. Jemal A, Siegel R, Ward E, et al. Cancer statistics, 2008. *CA Cancer J Clin.* 2008;58(2):71–96.
2. Gurney J, Severson R, Davis S, Robison L. Incidence of cancer in children in the united states: sex-, race-, and 1-year age-specific rates by histologic type. *Cancer.* 1995;75(8):2186–2195.
3. Pizzo PA, M.D., Poplack DG. Principles and practice of pediatric oncology. Wolters Kluwer Health/Lippincott Williams & Wilkins; 2010.
4. Sinigaglia R, Gigante C, Bisinella G, et al. Musculoskeletal manifestations in pediatric acute leukemia. *Journal of Pediatric Orthopedics.* 2008;28(1):20–8.
5. Simone J V, Verzosa MS, Rudy J a. Initial features and prognosis in 363 children with acute lymphocytic leukemia. *Cancer.* 1975;36(6):2099–108.
6. Lilleyman JS, Hann IM, Stevens RF. The clinical significance of blast cell morphology in childhood lymphoblastic leukaemia. *Medical and Pediatric Oncology.* 1986;14(3):144–7.
7. Buonamici S, Trimarchi T, Ruocco MG, et al. Ccr7 signalling as an essential regulator of cns infiltration in t-cell leukaemia. *Nature.* 2009;459(7249):1000–4.
8. Pui C-H, Mullighan CG, Evans WE, Relling M V. Pediatric acute lymphoblastic leukemia: where are we going and how do we get there? *Blood.* 2012;120(6):1165–74.
9. Pui C-H, Evans WE. Treatment of acute lymphoblastic leukemia. *The New England Journal of Medicine.* 2006;354(2):166–78.
10. Pui C, Sandlund J, Pei D, et al. Improved outcome for children with acute lymphoblastic leukemia: results of total therapy study xiiib at st jude children's research hospital. *Blood.* 2004;104(9):2690–2696.
11. Thomas DA, Kantarjian H, Smith TL, et al. Primary refractory and relapsed adult acute lymphoblastic leukemia: characteristics, treatment results, and prognosis with salvage therapy. *Cancer.* 1999;86(7):1216–30.
12. Zhang J, Ding L, Holmfeldt L, et al. The genetic basis of early t-cell precursor acute lymphoblastic leukaemia. *Nature.* 2012;481(7380):157–63.

13. Coustan-Smith E, Mullighan CG, Onciu M, et al. Early t-cell precursor leukaemia: a subtype of very high-risk acute lymphoblastic leukaemia. *The Lancet Oncology*. 2009;10(2):147–56.
14. Inukai T, Kiyokawa N, Campana D, et al. Clinical significance of early t-cell precursor acute lymphoblastic leukaemia: results of the tokyo children's cancer study group study l99-15. *British Journal of Haematology*. 2012;156(3):358–65.
15. Goldberg JM, Silverman LB, Levy DE, et al. Childhood t-cell acute lymphoblastic leukemia: the dana-farber cancer institute acute lymphoblastic leukemia consortium experience. *Journal of Clinical Oncology*. 2003;21(19):3616–22.
16. Silverman LB, Declerck L, Gelber RD, et al. Results of dana-farber cancer institute consortium protocols for children with newly diagnosed acute lymphoblastic leukemia (1981-1995). *Leukemia*. 2000;14(12):2247–56.
17. Harris MB, Shuster JJ, Pullen DJ, et al. Consolidation therapy with antimetabolite-based therapy in standard-risk acute lymphocytic leukemia of childhood: a pediatric oncology group study. *Journal of Clinical Oncology*. 1998;16(8):2840–7.
18. Möricke A, Reiter A, Zimmermann M, et al. Risk-adjusted therapy of acute lymphoblastic leukemia can decrease treatment burden and improve survival: treatment results of 2169 unselected pediatric and adolescent patients enrolled in the trial all-bfm 95. *Blood*. 2008;111(9):4477–89.
19. Vora A, Mitchell CD, Lennard L, et al. Toxicity and efficacy of 6-thioguanine versus 6-mercaptopurine in childhood lymphoblastic leukaemia: a randomised trial. *Lancet*. 2006;368(9544):1339–48.
20. Conter V, Valsecchi MG, Silvestri D, et al. Pulses of vincristine and dexamethasone in addition to intensive chemotherapy for children with intermediate-risk acute lymphoblastic leukaemia: a multicentre randomised trial. *Lancet*. 2007;369(9556):123–31.
21. De Moerloose B, Suciu S, Bertrand Y, et al. Improved outcome with pulses of vincristine and corticosteroids in continuation therapy of children with average risk acute lymphoblastic leukemia (all) and lymphoblastic non-hodgkin lymphoma (nhl): report of the eortc randomized phase 3 trial 58951. *Blood*. 2010;116(1):36–44.
22. Chessells JM, Veys P, Kempinski H, et al. Long-term follow-up of relapsed childhood acute lymphoblastic leukaemia. *British Journal of Haematology*. 2003;123(3):396–405.

23. Rubnitz JE, Lensing S, Zhou Y, et al. Death during induction therapy and first remission of acute leukemia in childhood: the st. jude experience. *Cancer*. 2004;101(7):1677–84.
24. Maule M, Scélo G, Pastore G, et al. Risk of second malignant neoplasms after childhood leukemia and lymphoma: an international study. *Journal of the National Cancer Institute*. 2007;99(10):790–800.
25. Kimball Dalton VM, Gelber RD, Li F, et al. Second malignancies in patients treated for childhood acute lymphoblastic leukemia. *Journal of Clinical Oncology*. 1998;16(8):2848–53.
26. Zúñiga-Pflücker J, Lenardo M. Regulation of thymocyte development from immature progenitors. *Current Opinion in Immunology*. 1996;44:
27. Zúñiga-Pflücker JC. T-cell development made simple. *Nature reviews: Immunology*. 2004;4(1):67–72.
28. Osawa M, Hanada K, Hamada H, Nakauchi H. Long-term lymphohematopoietic reconstitution by a single cd34-low/negative hematopoietic stem cell. *Science*. 1996;273(1995):3–6.
29. Cheshier SH, Morrison SJ, Liao X, Weissman IL. In vivo proliferation and cell cycle kinetics of long-term self-renewing hematopoietic stem cells. *Proceedings of the National Academy of Sciences*. 1999;96(6):3120–5.
30. Morrison SJ, Weissman IL. The long-term repopulating subset of hematopoietic stem cells is deterministic and isolatable by phenotype. *Immunity*. 1994;1(8):661–73.
31. Ikuta K, Weissman I. Evidence that hematopoietic stem cells express mouse c-kit but do not depend on steel factor for their generation. ... of the *National Academy of Sciences*. 1992;89:1502–1506.
32. Spangrude G, Heimfeld S, Weissman I. Purification and characterization of mouse hematopoietic stem cells. *Science*. 1988;241:58–62.
33. Smith LG, Weissman IL, Heimfeld S. Clonal analysis of hematopoietic stem-cell differentiation in vivo. *Proceedings of the National Academy of Sciences*. 1991;88(7):2788–92.
34. Uchida N, Aguila HL, Fleming WH, Jerabek L, Weissman IL. Rapid and sustained hematopoietic recovery in lethally irradiated mice transplanted with purified thy-1.1lo lin-sca-1+ hematopoietic stem cells. *Blood*. 1994;83(12):3758–79.

35. Kiel MJ, Yilmaz OH, Iwashita T, et al. Slam family receptors distinguish hematopoietic stem and progenitor cells and reveal endothelial niches for stem cells. *Cell*. 2005;121(7):1109–21.
36. Yilmaz OH, Kiel MJ, Morrison SJ. Slam family markers are conserved among hematopoietic stem cells from old and reconstituted mice and markedly increase their purity. *Blood*. 2006;107(3):924–30.
37. Schroeder T. Hematopoietic stem cell heterogeneity: subtypes, not unpredictable behavior. *Cell Stem Cell*. 2010;6(3):203–7.
38. Morrison SJ, Wandycz a M, Hemmati HD, Wright DE, Weissman IL. Identification of a lineage of multipotent hematopoietic progenitors. *Development*. 1997;124(10):1929–39.
39. Kondo M, Weissman IL, Akashi K. Identification of clonogenic common lymphoid progenitors in mouse bone marrow. *Cell*. 1997;91(5):661–72.
40. Rothenberg E V, Moore JE, Yui M a. Launching the t-cell-lineage developmental programme. *Nature Reviews: Immunology*. 2008;8(1):9–21.
41. Benz C, Martins VC, Radtke F, Bleul CC. The stream of precursors that colonizes the thymus proceeds selectively through the early t lineage precursor stage of t cell development. *The Journal of Experimental Medicine*. 2008;205(5):1187–99.
42. Heinzl K, Benz C, Martins V, Haidl I, Bleul CC. Bone marrow-derived hemopoietic precursors commit to the t cell lineage only after arrival in the thymic microenvironment. *The Journal of Immunology*. 2007;178:858–868.
43. Bhandoola A, Von Boehmer H, Petrie HT, Zúñiga-Pflücker JC. Commitment and developmental potential of extrathymic and intrathymic t cell precursors: plenty to choose from. *Immunity*. 2007;26(6):678–89.
44. Porritt HE, Rumfelt LL, Tabrizifard S, et al. Heterogeneity among dn1 prothymocytes reveals multiple progenitors with different capacities to generate t cell and non-t cell lineages. *Immunity*. 2004;20(6):735–45.
45. Massa S, Balciunaite G, Ceredig R, Rolink AG. Critical role for c-kit (cd117) in t cell lineage commitment and early thymocyte development in vitro. *European Journal of Immunology*. 2006;36(3):526–32.
46. Balciunaite G, Ceredig R, Fehling H-J, Zúñiga-Pflücker J-C, Rolink AG. The role of notch and il-7 signaling in early thymocyte proliferation and differentiation. *European Journal of Immunology*. 2005;35(4):1292–300.

47. Allman D, Sambandam A, Kim S, et al. Thymopoiesis independent of common lymphoid progenitors. *Nature Immunology*. 2003;4(2):168–74.
48. Harman BC, Jenkinson EJ, Anderson G. Entry into the thymic microenvironment triggers notch activation in the earliest migrant t cell progenitors. *Journal of Immunology*. 2003;170(3):1299–303.
49. Pui JC, Allman D, Xu L, et al. Notch1 expression in early lymphopoiesis influences b versus t lineage determination. *Immunity*. 1999;11(3):299–308.
50. Tan JB, Visan I, Yuan JS, Guidos CJ. Requirement for notch1 signals at sequential early stages of intrathymic t cell development. *Nature Immunology*. 2005;6(7):671–9.
51. Ceredig R, Rolink T. A positive look at double-negative thymocytes. *Nature Reviews: Immunology*. 2002;2(11):888–97.
52. Shinkal Y, Ma A, Cheng H-L, Alt FW. Cd3e and cd34z cytoplasmic domains can independently generate signals for t cell development and function. *Immunity*. 1995;2:401–411.
53. Taghon T, Yui M a, Pant R, Diamond R a, Rothenberg E V. Developmental and molecular characterization of emerging beta- and gammadelta-selected pre-t cells in the adult mouse thymus. *Immunity*. 2006;24(1):53–64.
54. Dudley EC, Petrie HT, Shah LM, Owen MJ, Hayday a C. T cell receptor beta chain gene rearrangement and selection during thymocyte development in adult mice. *Immunity*. 1994;1(2):83–93.
55. Saint-Ruf C, Ungewiss K, Groettrup M, et al. Analysis and expression of a cloned pre-t cell receptor gene. *Science*. 1994;266(5188):1208–12.
56. Fehllng H, Krotkova A, Saint-Ruf C, Von Boehmer H. Crucial role of the pre-t-cell receptor a gene in development of ab but not gd t cells. *Nature*. 1995;375:795–798.
57. Aifantis I, Gounari F, Scorrano L, Borowski C, Von Boehmer H. Constitutive pre-tcr signaling promotes differentiation through ca<sup>2+</sup> mobilization and activation of nf-kappab and nfat. *Nature Immunology*. 2001;2(5):403–9.
58. Eyquem S, Chemin K, Fasseu M, Bories J-C. The ets-1 transcription factor is required for complete pre-t cell receptor function and allelic exclusion at the t cell receptor beta locus. *Proceedings of the National Academy of Sciences*. 2004;101(44):15712–7.



59. Michie A, Zúñiga-Pflücker J. Regulation of thymocyte differentiation: pre-tcr signals and  $\beta$ -selection. *Seminars in Immunology*. 2002;14(02):311–323.
60. Neilson JR, Winslow MM, Hur EM, Crabtree GR. Calcineurin b1 is essential for positive but not negative selection during thymocyte development. *Immunity*. 2004;20(3):255–66.
61. Voll RE, Jimi E, Phillips RJ, et al. Nf-kappa b activation by the pre-t cell receptor serves as a selective survival signal in t lymphocyte development. *Immunity*. 2000;13(5):677–89.
62. Mallick C a, Dudley EC, Viney JL, Owen MJ, Hayday a C. Rearrangement and diversity of t cell receptor beta chain genes in thymocytes: a critical role for the beta chain in development. *Cell*. 1993;73(3):513–9.
63. Kisielow P, Von Boehmer H. Development and selection of t cells: facts and puzzles. *Advances in Immunology*. 1995;58:87–209.
64. Kisielow P, Miazek A. Positive selection of t cells: rescue from programmed cell death and differentiation require continual engagement of the t cell receptor. *The Journal of Experimental Medicine*. 1995;181(June):1975–1984.
65. Surh CD, Sprent J. T-cell apoptosis detected in situ during positive and negative selection in the thymus. *Nature*. 1994;372:100–103.
66. Boehm T. Self-renewal of thymocytes in the absence of competitive precursor replenishment. *The Journal of Experimental Medicine*. 2012;209(8):1397–400.
67. Martins VC, Ruggiero E, Schlenner SM, et al. Thymus-autonomous t cell development in the absence of progenitor import. *The Journal of Experimental Medicine*. 2012;209(8):1409–1417.
68. Peaudecerf L, Lemos S, Galgano A, et al. Thymocytes may persist and differentiate without any input from bone marrow progenitors. *The Journal of Experimental Medicine*. 2012;209(8):1401–8.
69. Lin Y, Aplan PD. Leukemic transformation. *Cancer Biology and Therapy*. 2004;3(1):13–20.
70. Van Vlierberghe P, Van Grotel M, Beverloo HB, et al. The cryptic chromosomal deletion del(11)(p12p13) as a new activation mechanism of lmo2 in pediatric t-cell acute lymphoblastic leukemia. *Blood*. 2006;108(10):3520–9.
71. Aifantis I, Raetz E, Buonamici S. Molecular pathogenesis of t-cell leukaemia and lymphoma. *Nature reviews: Immunology*. 2008;8(5):380–90.

72. Hatano M, Roberts CWM, Minden M, Crist WM, Korsmeyer SJ. Deregulation of a homeobox gene , hox11 , by the t(i0;14) in t cell leukemia. *Science*. 1991;253:79–82.
73. Riz I, Hawley TS, Luu T V, Lee NH, Hawley RG. Tlx1 and notch coregulate transcription in t cell acute lymphoblastic leukemia cells. *Molecular Cancer*. 2010;9:181.
74. Demarest RM, Ratti F, Capobianco a J. It's t-all about notch. *Oncogene*. 2008;27(38):5082–91.
75. McCormack M, Forster A, Drynan L, Pannell R, Rabbitts TH. Lmo2 t-cell oncogene is activated via chromosomal translocations or retroviral insertion during gene therapy but has no mandatory role in normal t-cell development. *Molecular and Cellular Biology*. 2003;23(24):9003.
76. Ferrando A a, Neuberg DS, Staunton J, et al. Gene expression signatures define novel oncogenic pathways in t cell acute lymphoblastic leukemia. *Cancer Cell*. 2002;1(1):75–87.
77. Mellentin JD, Smith SD, Cleary ML. Lyl-1, a novel gene altered by chromosomal translocation in t cell leukemia, codes for a protein with a helix-loop-helix dna binding motif. *Cell*. 1989;58(1):77–83.
78. Larson Gedman a, Chen Q, Kugel Desmoulin S, et al. The impact of notch1, fbw7 and pten mutations on prognosis and downstream signaling in pediatric t-cell acute lymphoblastic leukemia: a report from the children's oncology group. *Leukemia*. 2009;23(8):1417–25.
79. Lahortiga I, De Keersmaecker K, Van Vlierberghe P, et al. Duplication of the myb oncogene in t cell acute lymphoblastic leukemia. *Nature Genetics*. 2007;39(5):593–5.
80. Chervinsky DS, Zhao XF, Lam DH, et al. Disordered t-cell development and t-cell malignancies in scl lmo1 double-transgenic mice: parallels with e2a-deficient mice. *Molecular and Cellular Biology*. 1999;19(7):5025–35.
81. Kallianpur A, Jordan J, Brandt S. The scl/tal-1 gene is expressed in progenitors of both the hematopoietic and vascular systems during embryogenesis. *Blood*. 1994;83(5):1200–1208.
82. Drake CJ, Brandt SJ, Trusk TC, Little CD. Tal1/scl is expressed in endothelial progenitor cells/angioblasts and defines a dorsal-to-ventral gradient of vasculogenesis. *Developmental Biology*. 1997;192(1):17–30.

83. Green AR, Lints T, Visvader J, Harvey R, Begley CG. Scl is coexpressed with gata-1 in hemopoietic cells but is also expressed in developing brain. *Oncogene*. 1992;7(4):653–60.
84. Robb L, Lyons I, Li R, et al. Absence of yolk sac hematopoiesis from mice with a targeted disruption of the scl gene. *Proceedings of the National Academy of Sciences*. 1995;92(15):7075–9.
85. Shivdasani R, Mayer E, Orkin S. Absence of blood formation in mice lacking t-cell leukaemia oncoprotein tal-1/scl. *Nature*. 1995;373:432–434.
86. Porcher C, Swat W, Rockwell K, et al. The t cell leukemia oncoprotein scl/tal-1 is essential for development of all hematopoietic lineages. *Cell*. 1996;86(1):47–57.
87. Robb L, Elwood NJ, Elefanty a G, et al. The scl gene product is required for the generation of all hematopoietic lineages in the adult mouse. *The EMBO Journal*. 1996;15(16):4123–9.
88. Visvader JE, Fujiwara Y, Orkin SH. Unsuspected role for the t-cell leukemia protein scl/tal-1 in vascular development. *Genes & Development*. 1998;12(4):473–9.
89. Mouthon M a, Bernard O, Mitjavila MT, et al. Expression of tal-1 and gata-binding proteins during human hematopoiesis. *Blood*. 1993;81(3):647–55.
90. Tremblay M, Herblot S, Lecuyer E, Hoang T. Regulation of pt alpha gene expression by a dosage of e2a, heb, and scl. *The Journal of biological chemistry*. 2003;278(15):12680–7.
91. Hsu H, Wadman I, Baer R. Formation of in vivo complexes between the tal1 and e2a polypeptides of leukemic t cells. *Proceedings of the National Academy of Sciences*. 1994;91(April):3181–3185.
92. Voronova AF, Lee F. The e2a and tal-1 helix-loop-helix proteins associate in vivo and are modulated by id proteins during interleukin 6-induced myeloid differentiation. *Proceedings of the National Academy of Sciences*. 1994;91(13):5952–6.
93. Hsu HL, Cheng JT, Chen Q, Baer R. Enhancer-binding activity of the tal-1 oncoprotein in association with the e47/e12 helix-loop-helix proteins. *Molecular and Cellular Biology*. 1991;11(6):3037–42.
94. Lécuyer E, Herblot S, Saint-Denis M, et al. The scl complex regulates c-kit expression in hematopoietic cells through functional interaction with sp1. *Blood*. 2002;100(7):2430–40.

95. Valge-Archer V, Osada H, Warren A, et al. The lim protein rbtn2 and the basic helix-loop-helix protein tal1 are present in a complex in erythroid cells. *Proceedings of the National Academy of Sciences*. 1994;91:8617–8621.
96. Wadman I a, Osada H, Grütz GG, et al. The lim-only protein lmo2 is a bridging molecule assembling an erythroid, dna-binding complex which includes the tal1, e47, gata-1 and ldb1/nli proteins. *The EMBO Journal*. 1997;16(11):3145–57.
97. Huang S, Qiu Y, Stein RW, Brandt SJ. P300 functions as a transcriptional coactivator for the tal1/scl oncoprotein. *Oncogene*. 1999;18(35):4958–67.
98. Huang S, Qiu Y, Shi Y, Xu Z, Brandt SJ. P/caf-mediated acetylation regulates the function of the basic helix-loop-helix transcription factor tal1/scl. *The EMBO Journal*. 2000;19(24):6792–803.
99. Huang S, Brandt SJ. Msin3a regulates murine erythroleukemia cell differentiation through association with the tal1 (or scl) transcription factor. *Molecular and Cellular Biology*. 2000;20(6):2248–59.
100. Begley CG, Aplan PD, Denning SM, et al. The gene scl is expressed during early hematopoiesis and encodes a differentiation-related dna-binding motif. *Proceedings of the National Academy of Sciences*. 1989;86(24):10128–32.
101. Fitzgerald TJ, Neale G a, Raimondi SC, Goorha RM. C-tal, a helix-loop-helix protein, is juxtaposed to the t-cell receptor-beta chain gene by a reciprocal chromosomal translocation: t(1;7)(p32;q35). *Blood*. 1991;78(10):2686–95.
102. Aplan PD, Lombardi DP, Kirsch IR. Structural characterization of sil, a gene frequently disrupted in t-cell acute lymphoblastic leukemia. *Molecular and Cellular Biology*. 1991;11(11):5462–9.
103. Aplan PD, Lombardi DP, Reaman GH, et al. Involvement of the putative hematopoietic transcription factor scl in t-cell acute lymphoblastic leukemia. *Blood*. 1992;79(5):1327–33.
104. Bash R, Hall S, Timmons C, et al. Does activation of the tal1 gene occur in a majority of patients with t-cell acute lymphoblastic leukemia? a pediatric oncology group study. *Blood*. 1995;86(2):666–676.
105. Breit TM, Mol EJ, Wolvers-Tettero IL, et al. Site-specific deletions involving the tal-1 and sil genes are restricted to cells of the t cell receptor alpha/beta lineage: t cell receptor delta gene deletion mechanism affects multiple genes. *The Journal of Experimental Medicine*. 1993;177(4):965–77.

106. Robb L, Rasko JE, Bath ML, Strasser A, Begley CG. Scl, a gene frequently activated in human t cell leukaemia, does not induce lymphomas in transgenic mice. *Oncogene*. 1995;10(1):205–9.
107. Aplan PD, Jones C a, Chervinsky DS, et al. An scl gene product lacking the transactivation domain induces bony abnormalities and cooperates with lmo1 to generate t-cell malignancies in transgenic mice. *The EMBO Journal*. 1997;16(9):2408–19.
108. Cheng Y, Zhang Z, Slape C, Aplan PD. cre-loxp–mediated recombination between the sil and scl genes leads to a block in t-cell development at the cd4–cd8– to cd4+cd8+ transition. *Neoplasia*. 2007;9(4):315–321.
109. Kelliher MA, Seldin DC, Leder P. Tal-1 induces t cell acute lymphoblastic leukemia accelerated by casein kinase iialpha. *The EMBO Journal*. 1996;15(19):5160–6.
110. Sharma VM, Calvo J a, Draheim KM, et al. Notch1 contributes to mouse t-cell leukemia by directly inducing the expression of c-myc. *Molecular and Cellular Biology*. 2006;26(21):8022–31.
111. Shank-Calvo J, Draheim K, Bhasin M, Kelliher M. P16ink4a or p19arf loss contributes to tal1-induced leukemogenesis in mice. *Oncogene*. 2006;25(21):3023–31.
112. Draheim KM, Hermance N, Yang Y, et al. A dna-binding mutant of tal1 cooperates with lmo2 to cause t cell leukemia in mice. *Oncogene*. 2010;30(10):1252–60.
113. Tremblay M, Tremblay CS, Herblot S, et al. Modeling t-cell acute lymphoblastic leukemia induced by the scl and lmo1 oncogenes. *Genes & Development*. 2010;24(11):1093–105.
114. O’Neil J, Shank J, Cusson N, Murre C, Kelliher M. Tal1/scl induces leukemia by inhibiting the transcriptional activity of e47/heb. *Cancer Cell*. 2004;5(6):587–96.
115. Schlissel M, Voronova a, Baltimore D. Helix-loop-helix transcription factor e47 activates germ-line immunoglobulin heavy-chain gene transcription and rearrangement in a pre-t-cell line. *Genes & Development*. 1991;5(8):1367–1376.
116. Takeuchi A, Yamasaki S, Takase K, et al. E2a and heb activate the pre-tcr alpha promoter during immature t cell development. *Journal of Immunology*. 2001;167(4):2157–63.

117. Jones-Mason ME, Zhao X, Kappes D, et al. E protein transcription factors are required for the development of cd4(+) lineage t cells. *Immunity*. 2012;36(3):348–61.
118. O’Neil J, Billa M, Oikemus S, Kelliher M. The dna binding activity of tal-1 is not required to induce leukemia/lymphoma in mice. *Oncogene*. 2001;20(29):3897–905.
119. Sanda T, Lawton LN, Barrasa MI, et al. Core transcriptional regulatory circuit controlled by the tal1 complex in human t cell acute lymphoblastic leukemia. *Cancer Cell*. 2012;22(2):209–21.
120. Palii CG, Perez-Iratxeta C, Yao Z, et al. Differential genomic targeting of the transcription factor tal1 in alternate haematopoietic lineages. *The EMBO Journal*. 2011;30(3):494–509.
121. Wilson NK, Miranda-Saavedra D, Kinston S, et al. The transcriptional program controlled by the stem cell leukemia gene scl/tal1 during early embryonic hematopoietic development. *Blood*. 2009;113(22):5456–65.
122. Gowney JD, Shigematsu H, Li Z, et al. Loss of runx1 perturbs adult hematopoiesis and is associated with a myeloproliferative phenotype. *Blood*. 2005;106(2):494–504.
123. O’Neil J, Look AT. Mechanisms of transcription factor deregulation in lymphoid cell transformation. *Oncogene*. 2007;26(47):6838–49.
124. Larson RC, Osada H, Larson TA, Lavenir I, Rabbitts TH. The oncogenic lim protein rbtn2 causes thymic developmental aberrations that precede malignancy in transgenic mice. *Oncogene*. 1995;11(5):853–62.
125. Boehm T, Foroni L, Kaneko Y, Perutz MF, Rabbitts TH. The rhombotin family of cysteine-rich lim-domain oncogenes: distinct members are involved in t-cell translocations to human chromosomes 11p15 and 11p13. *Proceedings of the National Academy of Sciences*. 1991;88(10):4367–71.
126. Royer-Pokora B, Loos U, Ludwig WD. Ttg-2, a new gene encoding a cysteine-rich protein with the lim motif, is overexpressed in acute t-cell leukaemia with the t(11;14)(p13;q11). *Oncogene*. 1991;6(10):1887–93.
127. McCormack M, Rabbitts T. Activation of the t-cell oncogene lmo2 after gene therapy for x-linked severe combined immunodeficiency. *New England Journal of Medicine*. 2004;350(9):913–922.
128. Howe S, Mansour M, Schwarwaelder K, et al. Insertional mutagenesis combined with acquired somatic mutations causes leukemogenesis following gene therapy of scid-x1 patients. *The Journal of clinical ....* 2008;118(9):

129. Hacein-Bey-Abina S, Garrigue A, Wang GP, et al. Insertional oncogenesis in 4 patients after retrovirus-mediated gene therapy of scid-x1. *The Journal of Clinical Investigation*. 2008;118(9):3132–3142.
130. Hacein-Bey-Abina S, Von Kalle C, Schmidt M, et al. Lmo2-associated clonal t cell proliferation in two patients after gene therapy for scid-x1. *Science*. 2003;302(5644):415–9.
131. Larson R, Lavenir I, Larson T, et al. Protein dimerization between lmo2 (rbtn2) and tal1 alters thymocyte development and potentiates t cell tumorigenesis in transgenic mice. *The EMBO Journal*. 1996;15(5):1021–1027.
132. Wadman I, Li J, Bash RO, et al. Specific in vivo association between the bhlh and lim proteins implicated in human t cell leukemia. *The EMBO Journal*. 1994;13(20):4831–9.
133. Warren a J, Colledge WH, Carlton MB, et al. The oncogenic cysteine-rich lim domain protein rbtn2 is essential for erythroid development. *Cell*. 1994;78(1):45–57.
134. Rabbitts TH. Lmo t-cell translocation oncogenes typify genes activated by chromosomal translocations that alter transcription and developmental processes. *Genes & Development*. 1998;12(17):2651–2657.
135. Nam C-H, Rabbitts T. The role of lmo2 in development and in t cell leukemia after chromosomal translocation or retroviral insertion. *Molecular Therapy*. 2006;13(1):15–25.
136. Larson RC, Fisch P, Larson TA, et al. T cell tumours of disparate phenotype in mice transgenic for rbtn-2. *Oncogene*. 1994;9(12):3675–81.
137. McCormack MP, Young LF, Vasudevan S, et al. The lmo2 oncogene initiates leukemia in mice by inducing thymocyte self-renewal. *Science*. 2010;327(5967):879–83.
138. Weng AP, Ferrando A a, Lee W, et al. Activating mutations of notch1 in human t cell acute lymphoblastic leukemia. *Science*. 2004;306(5694):269–71.
139. Artavanis-Tsakonas S, Rand MD, Lake RJ. Notch signaling: cell fate control and signal integration in development. *Science*. 1999;284(5415):770–776.
140. Felli MP, Maroder M, Mitsiadis T a, et al. Expression pattern of notch1, 2 and 3 and jagged1 and 2 in lymphoid and stromal thymus components: distinct ligand-receptor interactions in intrathymic t cell development. *International Immunology*. 1999;11(7):1017–25.

141. Shimizu K, Chiba S, Saito T, et al. Functional diversity among notch1, notch2, and notch3 receptors. *Biochemical and Biophysical Research Communications*. 2002;291(4):775–9.
142. Jönsson JI, Xiang Z, Pettersson M, Lardelli M, Nilsson G. Distinct and regulated expression of notch receptors in hematopoietic lineages and during myeloid differentiation. *European Journal of Immunology*. 2001;31(11):3240–7.
143. Lee AH, Jeong EG, Yoo NJ, Lee SH. Mutational analysis of notch1, 2, 3, and 4 genes in common solid cancers and acute leukemias. *APMIS*. 2007;115:1357–1363.
144. De La Coste A, Freitas A a. Notch signaling: distinct ligands induce specific signals during lymphocyte development and maturation. *Immunology Letters*. 2006;102(1):1–9.
145. Lissemore JL, Starmer WT. Phylogenetic analysis of vertebrate and invertebrate delta/serrate/lag-2 (dsl) proteins. *Molecular phylogenetics and evolution*. 1999;11(2):308–19.
146. Irvin D, Nakano I, Paucar A, Kornblum H. Patterns of jagged1, jagged2, delta-like 1 and delta-like 3 expression during late embryonic and postnatal brain development suggest multiple functional roles in progenitors and differentiated cells. *Journal of Neuroscience Research*. 2004;75:330–343.
147. Chillakuri CR, Sheppard D, Lea SM, Handford P a. Notch receptor-ligand binding and activation: insights from molecular studies. *Seminars in cell & developmental biology*. 2012;23(4):421–8.
148. Logeat F, Bessia C, Brou C, et al. The notch1 receptor is cleaved constitutively by a furin-like convertase. *Proceedings of the National Academy of Sciences*. 1998;95(14):8108–12.
149. Rebay I, Fleming RJ, Fehon RG, et al. Specific egf repeats of notch mediate interactions with delta and serrate: implications for notch as a multifunctional receptor. *Cell*. 1991;67(4):687–99.
150. Kurooka H, Kuroda K, Honjo T. Roles of the ankyrin repeats and c-terminal region of the mouse notch1 intracellular region. *Nucleic Acids Research*. 1998;26(23):5448–55.
151. Lubman OY, Ilagan MXG, Kopan R, Barrick D. Quantitative dissection of the notch:cs1 interaction: insights into the notch-mediated transcriptional switch. *Journal of Molecular Biology*. 2007;365(3):577–89.



152. Kovall RA, Blacklow SC. Mechanistic insights into notch receptor signaling from structural and biochemical studies. *Current Topics in Developmental Biology*. 2010;92:31–71.
153. Rechsteiner M. Regulation of enzyme levels by proteolysis: the role of pest regions. *Advances in Enzyme Regulation*. 1988;27:135–51.
154. Bettenhausen B, Hrabě de Angelis M, Simon D, Guénet JL, Gossler A. Transient and restricted expression during mouse embryogenesis of *dll1*, a murine gene closely related to *drosophila delta*. *Development*. 1995;121(8):2407–18.
155. Lindsell CE, Shawber CJ, Boulter J, Weinmaster G. Jagged: a mammalian ligand that activates notch1. *Cell*. 1995;80(6):909–17.
156. Vooijs M, Schroeter EH, Pan Y, Blandford M, Kopan R. Ectodomain shedding and intramembrane cleavage of mammalian notch proteins is not regulated through oligomerization. *The Journal of Biological Chemistry*. 2004;279(49):50864–73.
157. Brou C, Logeat F, Gupta N, et al. A novel proteolytic cleavage involved in notch signaling: the role of the disintegrin-metalloprotease tace. *Molecular Cell*. 2000;5(2):207–16.
158. De Strooper B, Annaert W, Cupers P, et al. A presenilin-1-dependent gamma-secretase-like protease mediates release of notch intracellular domain. *Nature*. 1999;398(6727):518–22.
159. Oswald F, Täuber B, Dobner T, et al. P300 acts as a transcriptional coactivator for mammalian notch-1. *Molecular and Cellular Biology*. 2001;21(22):7761–7774.
160. Tamura K, Taniguchi Y, Minoguchi S, et al. Physical interaction between a novel domain of the receptor notch and the transcription factor rbp-j kappa/su(h). *Current Biology*. 1995;5(12):1416–23.
161. Wu L, Sun T, Kobayashi K, Gao P, Griffin JD. Identification of a family of mastermind-like transcriptional coactivators for mammalian notch receptors. *Molecular and Cellular Biology*. 2002;22(21):7688–7700.
162. Fuentes-Pananá E, Ling P. Characterization of the cbf2 binding site within the epstein-barr virus latency c promoter and its role in modulating ebna2-mediated transactivation. *Journal of Virology*. 1998;72(1):693–700.
163. Jeffries S, Capobianco A. Neoplastic transformation by notch requires nuclear localization. *Molecular and Cellular Biology*. 2000;20(11):3928–3941.

164. Hsieh JJ, Zhou S, Chen L, Young DB, Hayward SD. Cir, a corepressor linking the dna binding factor cbf1 to the histone deacetylase complex. *Proceedings of the National Academy of Sciences of the United States of America*. 1999;96(1):23–8.
165. Zhou S, Fujimuro M, Hsieh JJ, et al. Skip , a cbf1-associated protein , interacts with the ankyrin repeat domain of notchic to facilitate notchic function. *Molecular and Cellular Biology*. 2000;20(7):2400–2410.
166. Taniguchi Y, Furukawa T, Tun T, Han H, Honjo T. Lim protein kyot2 negatively regulates transcription by association with the rbp-j dna-binding protein. *Molecular and Cellular Biology*. 1998;18(1):644–654.
167. Kao H-Y, Ordentlich P, Koyano-Nakagawa N, et al. A histone deacetylase corepressor complex regulates the notch signal transduction pathway. *Genes & Development*. 1998;12(15):2269–2277.
168. Laherty CD, Billin a N, Lavinsky RM, et al. Sap30, a component of the msin3 corepressor complex involved in n-cor-mediated repression by specific transcription factors. *Molecular Cell*. 1998;2(1):33–42.
169. Waltzer L, Bourillot PY, Sergeant A, Manet E. Rbp-j kappa repression activity is mediated by a co-repressor and antagonized by the epstein-barr virus transcription factor ebna2. *Nucleic Acids Research*. 1995;23(24):4939–45.
170. Joshi I, Minter LM, Telfer J, et al. Notch signaling mediates g1/s cell-cycle progression in t cells via cyclin d3 and its dependent kinases. *Blood*. 2009;113(8):1689–98.
171. Maillard I, Fang T, Pear WS. Regulation of lymphoid development, differentiation, and function by the notch pathway. *Annual Review of Immunology*. 2005;23(Figure 1):945–74.
172. Weng AP, Millholland JM, Yashiro-Ohtani Y, et al. C-myc is an important direct target of notch1 in t-cell acute lymphoblastic leukemia/lymphoma. *Genes & Development*. 2006;20(15):2096–109.
173. Liu H, Chi AWS, Arnett KL, et al. Notch dimerization is required for leukemogenesis and t-cell development. *Genes & Development*. 2010;24(21):2395–407.
174. Yang L-T, Nichols JT, Yao C, et al. Fringe glycosyltransferases differentially modulate notch1 proteolysis induced by delta1 and jagged1. *Molecular Biology of the Cell*. 2005;16(2):927–42.
175. Moloney DJ, Panin VM, Johnston SH, et al. Fringe is a glycosyltransferase that modifies notch. *Nature*. 2000;406(6794):369–75.

176. Hicks C, Johnston SH, DiSibio G, et al. Fringe differentially modulates jagged1 and delta1 signalling through notch1 and notch2. *Nature Cell Biology*. 2000;2(8):515–20.
177. Chastagner P, Israël A, Brou C. Aip4/itch regulates notch receptor degradation in the absence of ligand. *PLoS One*. 2008;3(7):e2735.
178. Qiu L, Joazeiro C, Fang N, et al. Recognition and ubiquitination of notch by itch, a hect-type e3 ubiquitin ligase. *The Journal of Biological Chemistry*. 2000;275(46):35734–7.
179. Matesic LE, Haines DC, Copeland NG, Jenkins N a. Itch genetically interacts with notch1 in a mouse autoimmune disease model. *Human Molecular Genetics*. 2006;15(24):3485–97.
180. McGill M a, McGlade CJ. Mammalian numb proteins promote notch1 receptor ubiquitination and degradation of the notch1 intracellular domain. *The Journal of Biological Chemistry*. 2003;278(25):23196–203.
181. Gupta-Rossi N, Le Bail O, Gonen H, et al. Functional interaction between sel-10, an f-box protein, and the nuclear form of activated notch1 receptor. *The Journal of Biological Chemistry*. 2001;276(37):34371–8.
182. Oberg C, Li J, Pauley A, et al. The notch intracellular domain is ubiquitinated and negatively regulated by the mammalian sel-10 homolog. *The Journal of Biological Chemistry*. 2001;276(38):35847–53.
183. Tsunematsu R, Nakayama K, Oike Y, et al. Mouse fbw7/sel-10/cdc4 is required for notch degradation during vascular development. *The Journal of Biological Chemistry*. 2004;279(10):9417–23.
184. Wu G, Lyapina S, Das I, Li J. Sel-10 is an inhibitor of notch signaling that targets notch for ubiquitin-mediated protein degradation. *Molecular and Cellular Biology*. 2001;21(21):7403–7415.
185. Nakayama KI, Nakayama K. Regulation of the cell cycle by scf-type ubiquitin ligases. *Seminars in Cell & Developmental Biology*. 2005;16(3):323–33.
186. Fryer CJ, White JB, Jones K a. Mastermind recruits cycc:cdk8 to phosphorylate the notch icd and coordinate activation with turnover. *Molecular Cell*. 2004;16(4):509–20.
187. Nateri AS, Riera-Sans L, Da Costa C, Behrens A. The ubiquitin ligase scffbw7 antagonizes apoptotic jnk signaling. *Science*. 2004;303(5662):1374–8.

188. Koepp DM, Schaefer LK, Ye X, et al. Phosphorylation-dependent ubiquitination of cyclin e by the scffbw7 ubiquitin ligase. *Science*. 2001;294(5540):173–7.
189. Yada M, Hatakeyama S, Kamura T, et al. Phosphorylation-dependent degradation of c-myc is mediated by the f-box protein fbw7. *The EMBO Journal*. 2004;23(10):2116–25.
190. Mao J-H, Kim I-J, Wu D, et al. Fbxw7 targets mtor for degradation and cooperates with pten in tumor suppression. *Science*. 2008;321(5895):1499–502.
191. Swiatek PJ, Lindsell CE, Del Amo FF, Weinmaster G, Gridley T. Notch1 is essential for postimplantation development in mice. *Genes & Development*. 1994;8(6):707–719.
192. Hamada Y, Kadokawa Y, Okabe M, et al. Mutation in ankyrin repeats of the mouse notch2 gene induces early embryonic lethality. *Development*. 1999;126(15):3415–24.
193. Hrabe de Angelis M, McIntyre J, Gossler A. Maintenance of somite borders in mice requires the delta homologue dll1. *Nature*. 1997;386:717–721.
194. Xue Y, Gao X, Lindsell CE, et al. Embryonic lethality and vascular defects in mice lacking the notch ligand jagged1. *Human Molecular Genetics*. 1999;8(5):723–30.
195. Domenga V, Fardoux P, Lacombe P, et al. Notch3 is required for arterial identity and maturation of vascular smooth muscle cells. *Genes & Development*. 2004;18(22):2730–5.
196. Li L, Krantz I, Deng Y, Genin A. Alagille syndrome is caused by mutations in human jagged1, which encodes a ligand for notch1. *Nature Genetics*. 1997;16:243–251.
197. Oda T, Elkahouloun A, Pike B, Okajima K. Mutations in the human jagged1 gene are responsible for alagille syndrome. *Nature Genetics*. 1997;16:235–242.
198. Joutel A, Corpechot C, Ducros A, Vahedi K. Notch3 mutations in cadasil, a hereditary adult-onset condition causing stroke and dementia. *Nature*. 1996;383:707–710.
199. Bogenrieder T, Herlyn M. The molecular pathology of cutaneous melanoma. *Cancer Biomarkers*. 2010;9(1-6):267–86.
200. Dotto GP. Notch tumor suppressor function. *Oncogene*. 2008;27(38):5115–23.

201. Estrach S, Ambler C a, Lo Celso C, Hozumi K, Watt FM. Jagged 1 is a beta-catenin target gene required for ectopic hair follicle formation in adult epidermis. *Development*. 2006;133(22):4427–38.
202. Vauclair S, Nicolas M, Barrandon Y, Radtke F. Notch1 is essential for postnatal hair follicle development and homeostasis. *Developmental Biology*. 2005;284(1):184–93.
203. Yamamoto N, Tanigaki K, Han H, Hiai H, Honjo T. Notch/rbp-j signaling regulates epidermis/hair fate determination of hair follicular stem cells. *Current Biology*. 2003;13(4):333–8.
204. Villa N, Walker L, Lindsell CE, et al. Vascular expression of notch pathway receptors and ligands is restricted to arterial vessels. *Mechanisms of Development*. 2001;108(1-2):161–4.
205. Lawson ND, Scheer N, Pham VN, et al. Notch signaling is required for arterial-venous differentiation during embryonic vascular development. *Development*. 2001;128(19):3675–83.
206. Fre S, Huyghe M, Mourikis P, et al. Notch signals control the fate of immature progenitor cells in the intestine. *Nature*. 2005;435(7044):964–8.
207. Van Es JH, Van Gijn ME, Riccio O, et al. Notch/gamma-secretase inhibition turns proliferative cells in intestinal crypts and adenomas into goblet cells. *Nature*. 2005;435(7044):959–63.
208. Real PJ, Tosello V, Palomero T, et al. Gamma-secretase inhibitors reverse glucocorticoid resistance in t cell acute lymphoblastic leukemia. *Nature Medicine*. 2009;15(1):50–8.
209. Wilson A, MacDonald HR, Radtke F. Notch 1-deficient common lymphoid precursors adopt a b cell fate in the thymus. *The Journal of Experimental Medicine*. 2001;194(7):1003–12.
210. Radtke F, Wilson a, Stark G, et al. Deficient t cell fate specification in mice with an induced inactivation of notch1. *Immunity*. 1999;10(5):547–58.
211. Nwabo Kamdje AH, Krampera M. Notch signaling in acute lymphoblastic leukemia: any role for stromal microenvironment? *Blood*. 2011;118(25):6506–14.
212. Hasserjian RP, Aster JC, Davi F, Weinberg DS, Sklar J. Modulated expression of notch1 during thymocyte development. *Blood*. 1996;88(3):970–6.
213. Jaleco a C, Neves H, Hooijberg E, et al. Differential effects of notch ligands delta-1 and jagged-1 in human lymphoid differentiation. *The Journal of Experimental Medicine*. 2001;194(7):991–1002.

214. Rothenberg E V, Dionne CJ. Lineage plasticity and commitment in t-cell development. *Immunological Reviews*. 2002;187:96–115.
215. Han H, Tanigaki K, Yamamoto N, et al. Inducible gene knockout of transcription factor recombination signal binding protein-j reveals its essential role in t versus b lineage decision. *International Immunology*. 2002;14(6):637–45.
216. Passegué E, Jamieson CHM, Ailles LE, Weissman IL. Normal and leukemic hematopoiesis: are leukemias a stem cell disorder or a reacquisition of stem cell characteristics? *Proceedings of the National Academy of Sciences*. 2003;100 Suppl:11842–9.
217. Dick JE. Stem cell concepts renew cancer research. *Blood*. 2008;112(13):4793–807.
218. Dontu G, Jackson KW, McNicholas E, et al. Role of notch signaling in cell-fate determination of human mammary stem/progenitor cells. *Breast Cancer Research*. 2004;6(6):R605–15.
219. Bouras T, Pal B, Vaillant F, et al. Notch signaling regulates mammary stem cell function and luminal cell-fate commitment. *Cell Stem Cell*. 2008;3(4):429–41.
220. Shen Q, Goderie SK, Jin L, et al. Endothelial cells stimulate self-renewal and expand neurogenesis of neural stem cells. *Science*. 2004;304(5675):1338–40.
221. Hitoshi S, Alexson T, Tropepe V, et al. Notch pathway molecules are essential for the maintenance , but not the generation , of mammalian neural stem cells. *Genes & Development*. 2002;16:846–858.
222. Hitoshi S, Seaberg RM, Kosciuk C, et al. Primitive neural stem cells from the mammalian epiblast differentiate to definitive neural stem cells under the control of notch signaling. *Genes & Development*. 2004;18:1806–1811.
223. Kumano K, Chiba S, Kunisato A, et al. Notch1 but not notch2 is essential for generating hematopoietic stem cells from endothelial cells. *Immunity*. 2003;18(5):699–711.
224. Varnum-Finney B, Purton LE, Yu M, et al. The notch ligand, jagged-1, influences the development of primitive hematopoietic precursor cells. *Blood*. 1998;91(11):4084–91.
225. Varnum-Finney B, Xu L, Brashem-Stein C, et al. Pluripotent, cytokine-dependent, hematopoietic stem cells are immortalized by constitutive notch1 signaling. *Nature Medicine*. 2000;6(11):1278–81.

226. Reya T, Duncan AW, Ailles L, et al. A role for wnt signalling in self-renewal of haematopoietic stem cells. *Nature*. 2003;423(6938):409–14.
227. Maillard I, Koch U, Dumortier A, et al. Canonical notch signaling is dispensable for the maintenance of adult hematopoietic stem cells. *Cell Stem Cell*. 2008;2(4):356–66.
228. Mancini SJC, Mantei N, Dumortier A, et al. Jagged1-dependent notch signaling is dispensable for hematopoietic stem cell self-renewal and differentiation. *Blood*. 2005;105(6):2340–2.
229. Rathinam C, Matesic LE, Flavell R a. The e3 ligase itch is a negative regulator of the homeostasis and function of hematopoietic stem cells. *Nature Immunology*. 2011;12(5):399–407.
230. Varnum-Finney B, Halasz L, Sun M, Gridley T, Radtke F. Notch2 governs the rate of generation of mouse long- and short-term repopulating stem cells. *The Journal of Clinical Investigation*. 2011;121(3):1207–1216.
231. Asnafi V, Buzyn A, Le Noir S, et al. Notch1/fbxw7 mutation identifies a large subgroup with favorable outcome in adult t-cell acute lymphoblastic leukemia (t-all): a group for research on adult acute lymphoblastic leukemia (graall) study. *Blood*. 2009;113(17):3918–24.
232. Liu H, Chiang M, Pear W. Critical roles of notch1 in acute t-cell lymphoblastic leukemia. *International Journal of Hematology*. 2011;94:118–125.
233. Koch U, Radtke F. Notch in t-all: new players in a complex disease. *Trends in Immunology*. 2011;32(9):434–42.
234. Ellisen LW, Bird J, West DC, et al. Tan-1, the human homolog of the drosophila notch gene, is broken by chromosomal translocations in t lymphoblastic neoplasms. *Cell*. 1991;66(4):649–61.
235. Capobianco A, Zagouras P, Blaumueller C, Artavanis-Tsakonas S, Bishop J. Neoplastic transformation by truncated alleles of human notch1/tan1 and notch2. *Molecular and Cellular Biology*. 1997;17(11):6265–6273.
236. Pear WS, Aster JC, Scott ML, et al. Exclusive development of t cell neoplasms in mice transplanted with bone marrow expressing activated notch alleles. *The Journal of Experimental Medicine*. 1996;183(5):2283–91.
237. Beverly LJ, Capobianco AJ. Perturbation of ikaros isoform selection by mlv integration is a cooperative event in notch(ic)-induced t cell leukemogenesis. *Cancer Cell*. 2003;3(6):551–64.

238. Aster J, Xu L, Karnell F, et al. Essential roles for ankyrin repeat and transactivation domains in induction of t-cell leukemia by notch1. *Molecular and Cellular Biology*. 2000;20(20):7505–7515.
239. Malecki MJ, Sanchez-Irizarry C, Mitchell JL, et al. Leukemia-associated mutations within the notch1 heterodimerization domain fall into at least two distinct mechanistic classes. *Molecular and Cellular Biology*. 2006;26(12):4642–51.
240. Haydu JE, De Keersmaecker K, Duff MK, et al. An activating intragenic deletion in notch1 in human t-all. *Blood*. 2012;119(22):5211–4.
241. Sulis ML, Williams O, Palomero T, et al. Notch1 extracellular juxtamembrane expansion mutations in t-all. *Blood*. 2008;112(3):733–40.
242. Chiang M, Xu L, Shestova O, et al. Leukemia-associated notch1 alleles are weak tumor initiators but accelerate k-ras–initiated leukemia. *The Journal of Clinical Investigation*. 2008;118(9):3181–3194.
243. Bellavia D, Campese AF, Checquolo S, et al. Combined expression of ptalpha and notch3 in t cell leukemia identifies the requirement of pretcr for leukemogenesis. *Proceedings of the National Academy of Sciences*. 2002;99(6):3788–93.
244. Bellavia D, Campese AF, Alesse E, et al. Constitutive activation of nf-kb and t-cell leukemia/lymphoma in notch3 transgenic mice. *The EMBO Journal*. 2000;19(13):3337–3348.
245. Lin YW, Nichols RA, Letterio JJ, Aplan PD. Notch1 mutations are important for leukemic transformation in murine models of precursor-t leukemia/lymphoma. *Blood*. 2006;107(6):2540–2543.
246. Kindler T, Cornejo MG, Scholl C, et al. K-rasg12d-induced t-cell lymphoblastic lymphoma/leukemias harbor notch1 mutations and are sensitive to gamma-secretase inhibitors. *Blood*. 2008;112(8):3373–82.
247. Göthert JR, Brake RL, Smeets M, et al. Notch1 pathway activation is an early hallmark of scl t leukemogenesis. *Blood*. 2007;110(10):3753–62.
248. O’Neil J, Calvo J, McKenna K, et al. Activating notch1 mutations in mouse models of t-all. *Blood*. 2006;107(2):781–5.
249. Ashworth TD, Pear WS, Chiang MY, et al. Deletion-based mechanisms of notch1 activation in t-all: key roles for rag recombinase and a conserved internal translational start site in notch1. *Blood*. 2010;116(25):5455–64.



250. Jeannet R, Mastio J, Macias-Garcia A, et al. Oncogenic activation of the notch1 gene by deletion of its promoter in ikaros-deficient t-all. *Blood*. 2010;116(25):5443–54.
251. Tatarek J, Cullion K, Ashworth T, et al. Notch1 inhibition targets the leukemia-initiating cells in a tal1/lmo2 mouse model of t-all. *Blood*. 2011;118(6):1579–90.
252. Fortini ME. Gamma-secretase-mediated proteolysis in cell-surface-receptor signalling. *Nature Reviews: Molecular Cell Biology*. 2002;3(9):673–84.
253. Francis R, McGrath G, Zhang J, et al. Aph-1 and pen-2 are required for notch pathway signaling, gamma-secretase cleavage of betaapp, and presenilin protein accumulation. *Developmental Cell*. 2002;3(1):85–97.
254. De Strooper B. Aph-1, pen-2, and nicastrin with presenilin generate an active g-secretase complex. *Neuron*. 2003;38:9–12.
255. Cowan JW, Wang X, Guan R, et al. Growth hormone receptor is a target for presenilin-dependent gamma-secretase cleavage. *The Journal of Biological Chemistry*. 2005;280(19):19331–42.
256. Hass MR, Yankner B a. A {gamma}-secretase-independent mechanism of signal transduction by the amyloid precursor protein. *The Journal of Biological Chemistry*. 2005;280(44):36895–904.
257. Lammich S, Okochi M, Takeda M, et al. Presenilin-dependent intramembrane proteolysis of cd44 leads to the liberation of its intracellular domain and the secretion of an abeta-like peptide. *The Journal of Biological Chemistry*. 2002;277(47):44754–9.
258. Ni CY, Murphy MP, Golde TE, Carpenter G. Gamma -secretase cleavage and nuclear localization of erbb-4 receptor tyrosine kinase. *Science*. 2001;294(5549):2179–81.
259. Palomero T, Lim WK, Odom DT, et al. Notch1 directly regulates c-myc and activates a feed-forward-loop transcriptional network promoting leukemic cell growth. *Proceedings of the National Academy of Sciences*. 2006;103(48):18261–6.
260. O’Neil J, Grim J, Strack P, et al. Fbw7 mutations in leukemic cells mediate notch pathway activation and resistance to gamma-secretase inhibitors. *The Journal of Experimental Medicine*. 2007;204(8):1813–24.
261. Cullion K, Draheim KM, Hermance N, et al. Targeting the notch1 and mtor pathways in a mouse t-all model. *Blood*. 2009;113(24):6172–81.

262. Armstrong F, Brunet de la Grange P, Gerby B, et al. Notch is a key regulator of human t-cell acute leukemia initiating cell activity. *Blood*. 2009;113(8):1730–40.
263. Weng A, Nam Y, Wolfe M, et al. Growth suppression of pre-t acute lymphoblastic leukemia cells by inhibition of notch signaling. *Molecular and Cellular Biology*. 2003;23(2):655–664.
264. Rizzo P, Osipo C, Foreman K, et al. Rational targeting of notch signaling in cancer. *Oncogene*. 2008;27(38):5124–31.
265. Nam Y, Sliz P, Song L, Aster JC, Blacklow SC. Structural basis for cooperativity in recruitment of maml coactivators to notch transcription complexes. *Cell*. 2006;124(5):973–83.
266. Nam Y, Sliz P, Pear WS, Aster JC, Blacklow SC. Cooperative assembly of higher-order notch complexes functions as a switch to induce transcription. *Proceedings of the National Academy of Sciences*. 2007;104(7):2103–8.
267. Moss ML, Stoeck A, Yan W, Dempsey PJ. Adam10 as a target for anti-cancer therapy. *Current Pharmaceutical Biotechnology*. 2008;9(1):2–8.
268. Wong GT, Manfra D, Poulet FM, et al. Chronic treatment with the gamma-secretase inhibitor ly-411,575 inhibits beta-amyloid peptide production and alters lymphopoiesis and intestinal cell differentiation. *The Journal of Biological Chemistry*. 2004;279(13):12876–82.
269. NCI. Ro4929097 in treating patients with stage iv melanoma. NCT01120275. 2013;
270. Merck. Study of mk-0752 in combination with tamoxifen or letrozole to treat early stage breast cancer. NCT00756717. 2011;
271. Bristol-Meyers-Squibb. Study to evaluate the safety and tolerability of weekly intravenous (iv) doses of bms-906024 in subjects with acute t-cell lymphoblastic leukemia or t-cell lymphoblastic lymphoma. NCT01363817. 2012;
272. Beverly LJ, Felsher DW, Capobianco AJ. Suppression of p53 by notch in lymphomagenesis: implications for initiation and regression. *Cancer Research*. 2005;65(16):7159–68.
273. Armelin HA, Armelin MC, Kelly K, et al. Functional role for c-myc in mitogenic response to platelet-derived growth factor. *Nature*. 1984;310(5979):655–60.

274. Kelly K, Cochran BH, Stiles CD, Leder P. Cell-specific regulation of the c-myc gene by lymphocyte mitogens and platelet-derived growth factor. *Cell*. 1983;35(3 Pt 2):603–10.
275. Seoane J, Poupponnot C, Staller P, et al. Tgf $\beta$  influences myc, miz-1 and smad to control the cdk inhibitor p15<sup>ink4b</sup>. *Nature Cell Biology*. 2001;3:400–409.
276. He T-C, Sparks A, Rago C, et al. Identification of c-myc as a target of the apc pathway. *Science*. 1998;281(5382):1509–1512.
277. Soudon J, Bernard O, Mathieu-Mahul D, Larsen CJ. C-myc gene expression in a leukemic t-cell line bearing a t(8;14) (q24;q11) translocation. *Leukemia*. 1991;5(1):60–5.
278. Taub R, Kirsch I, Morton C, et al. Translocation of the c-myc gene into the immunoglobulin heavy chain locus in human burkitt lymphoma and murine plasmacytoma cells. *Proceedings of the National Academy of Sciences*. 1982;79:7837–7841.
279. Dalla-Favera R, Bregni M, Erikson J, et al. Human c-myc onc gene is located on the region of chromosome 8 that is translocated in burkitt lymphoma cells. *Proceedings of the National Academy of Sciences*. 1982;79:7824–7827.
280. Duesberg PH, Vogt PK. Avian acute leukemia viruses mc29 and mh2 share specific rna sequences: evidence for a second class of transforming genes. *Proceedings of the National Academy of Sciences*. 1979;76(4):1633–7.
281. Hu SS, Lai MM, Vogt PK. Genome of avian myelocytomatosis virus mc29: analysis by heteroduplex mapping. *Proceedings of the National Academy of Sciences*. 1979;76(3):1265–8.
282. Dang C V. Myc on the path to cancer. *Cell*. 2012;149(1):22–35.
283. Shou Y, Martelli ML, Gabrea A, et al. Diverse karyotypic abnormalities of the c-myc locus associated with c-myc dysregulation and tumor progression in multiple myeloma. *Proceedings of the National Academy of Sciences*. 2000;97(1):228–33.
284. Land H, Parada LF, Weinberg RA. Tumorigenic conversion of primary embryo fibroblasts requires at least two cooperating oncogenes. *Nature*. 1983;304(5927):596–602.
285. Adams JM, Harris AW, Pinkert CA, et al. The c-myc oncogene driven by immunoglobulin enhancers induces lymphoid malignancy in transgenic mice. *Nature*. 1985;318(6046):533–8.

286. Chesi M, Robbiani DF, Sebag M, et al. Aid-dependent activation of a myc transgene induces multiple myeloma in a conditional mouse model of post-germinal center malignancies. *Cancer Cell*. 2008;13(2):167–80.
287. Leder A, Pattengale P, Kuo A, Stewart T, Leder P. Consequences of widespread deregulation of the c-myc gene in transgenic mice: multiple neoplasms and normal development. *Cell*. 1986;45:485–495.
288. Beer S, Zetterberg A, Ihrle R a, et al. Developmental context determines latency of myc-induced tumorigenesis. *PLoS Biology*. 2004;2(11):e332.
289. Ellwood-Yen K, Graeber TG, Wongvipat J, et al. Myc-driven murine prostate cancer shares molecular features with human prostate tumors. *Cancer Cell*. 2003;4(3):223–38.
290. Felsher DW, Bishop JM. Reversible tumorigenesis by myc in hematopoietic lineages. *Molecular Cell*. 1999;4(2):199–207.
291. Amati B, Brooks M, Levy N, et al. Oncogenic activity of the c-myc protein requires dimerization with max. *Cell*. 1993;72:233–245.
292. Blackwood E, Eisenman R. Max: a helix-loop-helix zipper protein that forms a sequence-specific dna-binding complex with myc. *Science*. 1991;251:1211–1217.
293. Grinberg A, Hu C, Kerppola T. Visualization of myc/max/mad family dimers and the competition for dimerization in living cells. *Molecular and Cellular Biology*. 2004;24(10):4294–4308.
294. Kato GJ, Lee WM, Chen LL, Dang C V. Max: functional domains and interaction with c-myc. *Genes & Development*. 1992;6(1):81–92.
295. Kretzner L, Blackwood E, Eisenman R. Myc and max proteins possess distinct transcriptional activities. *Nature*. 1992;359:426–429.
296. Chang T-C, Zeitels LR, Hwang H-W, et al. Lin-28b transactivation is necessary for myc-mediated let-7 repression and proliferation. *Proceedings of the National Academy of Sciences*. 2009;106(9):3384–9.
297. O'Donnell K a, Wentzel E a, Zeller KI, Dang C V, Mendell JT. C-myc-regulated micrnas modulate e2f1 expression. *Nature*. 2005;435(7043):839–43.
298. Chang T-C, Yu D, Lee Y-S, et al. Widespread micrna repression by myc contributes to tumorigenesis. *Nature Genetics*. 2008;40(1):43–50.

299. Cowling VH, Cole MD. The myc transactivation domain promotes global phosphorylation of the rna polymerase ii carboxy-terminal domain independently of direct dna binding. *Molecular and Cellular Biology*. 2007;27(6):2059–73.
300. Cole MD, Cowling VH. Transcription-independent functions of myc: regulation of translation and dna replication. *Nature Reviews: Molecular Cell Biology*. 2008;9(10):810–5.
301. Schneider A, Peukert K, Eilers M, Hänel F. Association of myc with the zinc-finger protein miz-1 defines a novel pathway for gene regulation by myc. *Current topics in microbiology and immunology*. 1997;224:137–46.
302. Zindy F, Eischen CM, Randle DH, et al. Myc signaling via the arf tumor suppressor regulates p53-dependent apoptosis and immortalization. *Genes & Development*. 1998;12(15):2424–33.
303. Eischen CM, Weber JD, Roussel MF, Sherr CJ, Cleveland JL. Disruption of the arf-mdm2-p53 tumor suppressor pathway in myc-induced lymphomagenesis. *Genes & Development*. 1999;13(20):2658–69.
304. Trudel M, Lanoix J, Barisoni L, et al. C-myc-induced apoptosis in polycystic kidney disease is bcl-2 and p53 independent. *The Journal of Experimental Medicine*. 1997;186(11):1873–84.
305. Sakamuro D, Eviner V, Elliott KJ, et al. C-myc induces apoptosis in epithelial cells by both p53-dependent and p53-independent mechanisms. *Oncogene*. 1995;11(11):2411–8.
306. Levens D. You don't muck with myc. *Genes & Cancer*. 2010;1(6):547–554.
307. Delmore JE, Issa GC, Lemieux ME, et al. Bet bromodomain inhibition as a therapeutic strategy to target c-myc. *Cell*. 2011;146(6):904–17.
308. Mertz J a, Conery AR, Bryant BM, et al. Targeting myc dependence in cancer by inhibiting bet bromodomains. *Proceedings of the National Academy of Sciences*. 2011;108(40):16669–74.
309. Gregory M a, Qi Y, Hann SR. Phosphorylation by glycogen synthase kinase-3 controls c-myc proteolysis and subnuclear localization. *The Journal of Biological Chemistry*. 2003;278(51):51606–12.
310. Gregory M, Hann S. C-myc proteolysis by the ubiquitin-proteasome pathway: stabilization of c-myc in burkitt's lymphoma cells. *Molecular and Cellular Biology*. 2000;2423–2435.

311. Salghetti SE, Kim SY, Tansey WP. Destruction of myc by ubiquitin-mediated proteolysis: cancer-associated and transforming mutations stabilize myc. *The EMBO Journal*. 1999;18(3):717–26.
312. Herbst A, Salghetti SE, Kim SY, Tansey WP. Multiple cell-type-specific elements regulate myc protein stability. *Oncogene*. 2004;23(21):3863–71.
313. Laurenti E, Varnum-Finney B, Wilson A, et al. Hematopoietic stem cell function and survival depend on c-myc and n-myc activity. *Cell Stem Cell*. 2008;3(6):611–24.
314. Wilson A, Murphy MJ, Oskarsson T, et al. C-myc controls the balance between hematopoietic stem cell self-renewal and differentiation. *Genes & Development*. 2004;18(22):2747–63.
315. Reavie L, Della Gatta G, Crusio K, et al. Regulation of hematopoietic stem cell differentiation by a single ubiquitin ligase-substrate complex. *Nature Immunology*. 2010;11(3):207–15.
316. Thompson BJ, Jankovic V, Gao J, et al. Control of hematopoietic stem cell quiescence by the e3 ubiquitin ligase fbw7. *The Journal of Experimental Medicine*. 2008;205(6):1395–408.
317. Takeishi S, Matsumoto A, Onoyama I, et al. Ablation of fbwx7 eliminates leukemia-initiating cells by preventing quiescence. *Cancer Cell*. 2013;23(3):347–361.
318. Reavie L, Buckley SM, Loizou E, et al. Regulation of c-myc ubiquitination controls chronic myelogenous leukemia initiation and progression. *Cancer Cell*. 2013;23(3):362–375.
319. Dose M, Khan I, Guo Z, et al. C-myc mediates pre-tcr-induced proliferation but not developmental progression. *Blood*. 2006;108(8):2669–77.
320. Perna D, Fagà G, Verrecchia a, et al. Genome-wide mapping of myc binding and gene regulation in serum-stimulated fibroblasts. *Oncogene*. 2012;31(13):1695–709.
321. Ji H, Wu G, Zhan X, et al. Cell-type independent myc target genes reveal a primordial signature involved in biomass accumulation. *PloS One*. 2011;6(10):e26057.
322. Xie X, Lu J, Kulbokas EJ, et al. Systematic discovery of regulatory motifs in human promoters and 3' utrs by comparison of several mammals. *Nature*. 2005;434(7031):338–45.

323. Li Z, Van Calcar S, Qu C, et al. A global transcriptional regulatory role for c-myc in burkitt's lymphoma cells. *Proceedings of the National Academy of Sciences*. 2003;100(14):8164–9.
324. Rahl PB, Lin CY, Seila AC, et al. C-myc regulates transcriptional pause release. *Cell*. 2010;141(3):432–45.
325. Lin CY, Lovén J, Rahl PB, et al. Transcriptional amplification in tumor cells with elevated c-myc. *Cell*. 2012;151(1):56–67.
326. Nie Z, Hu G, Wei G, et al. C-myc is a universal amplifier of expressed genes in lymphocytes and embryonic stem cells. *Cell*. 2012;151(1):68–79.
327. Amati B, Alevizopoulos K, Vlach J. Myc and the cell cycle. *Frontiers in Bioscience*. 1998;3:250–268.
328. Shim H, Chun YS, Lewis BC, Dang C V. A unique glucose-dependent apoptotic pathway induced by c-myc. *Proceedings of the National Academy of Sciences*. 1998;95(4):1511–6.
329. Yuneva M, Zamboni N, Oefner P, Sachidanandam R, Lazebnik Y. Deficiency in glutamine but not glucose induces myc-dependent apoptosis in human cells. *The Journal of Cell Biology*. 2007;178(1):93–105.
330. Sodik NM, Swigart LB, Karnezis AN, et al. Endogenous myc maintains the tumor microenvironment. *Genes & Development*. 2011;25(9):907–16.
331. Zuber J, Shi J, Wang E, et al. Rnai screen identifies brd4 as a therapeutic target in acute myeloid leukaemia. *Nature*. 2011;478(7370):524–8.
332. Clausen D, Guo J, Parise R, et al. In vitro cytotoxicity and in vivo efficacy, pharmacokinetics, and metabolism of 10074-g5 , a novel small-molecule inhibitor of c-myc/max dimerization. *Pharmacology and Experimental Therapeutics*. 2010;335(3):715–727.
333. Follis AV, Hammoudeh DI, Daab AT, Metallo SJ. Small-molecule perturbation of competing interactions between c-myc and max. *Bioorganic & medicinal chemistry letters*. 2009;19(3):807–10.
334. Yang D, Liu H, Goga A, et al. Therapeutic potential of a synthetic lethal interaction between the myc proto-oncogene and inhibition of aurora-b kinase. *Proceedings of the National Academy of Sciences*. 2010;107(31):13836–41.
335. Den Hollander J den, Rimpi S, Doherty JR, Rudelius M, Buck A. Aurora kinases a and b are up-regulated by myc and are essential for maintenance of the malignant state. *Blood*. 2010;116(9):1498–1505.

336. Clappier E, Gerby B, Sigaux F, et al. Clonal selection in xenografted human t cell acute lymphoblastic leukemia recapitulates gain of malignancy at relapse. *The Journal of Experimental Medicine*. 2011;208(4):653–61.
337. Cox C V, Martin HM, Kearns PR, et al. Characterization of a progenitor cell population in childhood t-cell acute lymphoblastic leukemia. *Blood*. 2007;109(2):674–82.
338. Magee J a, Piskounova E, Morrison SJ. Cancer stem cells: impact, heterogeneity, and uncertainty. *Cancer Cell*. 2012;21(3):283–96.
339. Yilmaz OH, Valdez R, Theisen BK, et al. Pten dependence distinguishes haematopoietic stem cells from leukaemia-initiating cells. *Nature*. 2006;441(7092):475–82.
340. Lee JY, Nakada D, Yilmaz OH, et al. Mtor activation induces tumor suppressors that inhibit leukemogenesis and deplete hematopoietic stem cells after pten deletion. *Cell Stem Cell*. 2010;7(5):593–605.
341. Abrahamsson AE, Geron I, Gotlib J, et al. Glycogen synthase kinase 3beta missplicing contributes to leukemia stem cell generation. *Proceedings of the National Academy of Sciences*. 2009;106(10):3925–9.
342. Hope KJ, Jin L, Dick JE. Acute myeloid leukemia originates from a hierarchy of leukemic stem cell classes that differ in self-renewal capacity. *Nature Immunology*. 2004;5(7):738–43.
343. Bonnet D, Dick J. Human acute myeloid leukemia is organized as a hierarchy that originates from a primitive hematopoietic stem cell. *Nature Medicine*. 1997;
344. Dick JE, Lapidot T. Biology of normal and acute myeloid leukemia stem cells. *International Journal of Hematology*. 2005;82(5):389–96.
345. Reya T, Morrison SJ, Clarke MF, Weissman IL. Stem cells, cancer, and cancer stem cells. *Nature*. 2001;414(6859):105–11.
346. Cozzio A, Passegué E, Ayton PM, et al. Similar mll-associated leukemias arising from self-renewing stem cells and short-lived myeloid progenitors. *Genes & Development*. 2003;17(24):3029–35.
347. So CW, Karsunky H, Passegué E, et al. Mll-gas7 transforms multipotent hematopoietic progenitors and induces mixed lineage leukemias in mice. *Cancer Cell*. 2003;3(2):161–71.



348. Krivtsov A V, Twomey D, Feng Z, et al. Transformation from committed progenitor to leukaemia stem cell initiated by mll-af9. *Nature*. 2006;442(7104):818–22.
349. Somervaille TCP, Cleary ML. Identification and characterization of leukemia stem cells in murine mll-af9 acute myeloid leukemia. *Cancer Cell*. 2006;10(4):257–68.
350. Huntly BJP, Shigematsu H, Deguchi K, et al. Moz-tif2, but not bcr-abl, confers properties of leukemic stem cells to committed murine hematopoietic progenitors. *Cancer Cell*. 2004;6(6):587–96.
351. Kuo Y-H, Landrette SF, Heilman S a, et al. Cbf beta-smmhc induces distinct abnormal myeloid progenitors able to develop acute myeloid leukemia. *Cancer Cell*. 2006;9(1):57–68.
352. Jamieson CHM, Ailles LE, Dylla SJ, et al. Granulocyte-macrophage progenitors as candidate leukemic stem cells in blast-crisis cml. *The New England Journal of Medicine*. 2004;351(7):657–67.
353. Minami Y, Stuart S a, Ikawa T, et al. Bcr-abl-transformed gmp as myeloid leukemic stem cells. *Proceedings of the National Academy of Sciences*. 2008;105(46):17967–72.
354. Gerby B, Clappier E, Armstrong F, et al. Expression of cd34 and cd7 on human t-cell acute lymphoblastic leukemia discriminates functionally heterogeneous cell populations. *Leukemia*. 2011;25(8):1249–58.
355. Ma W, Gutierrez A, Goff DJ, et al. Notch1 signaling promotes human t-cell acute lymphoblastic leukemia initiating cell regeneration in supportive niches. *PLoS One*. 2012;7(6):e39725.
356. Chiang MY, Xu ML, Histen G, et al. Identification of a conserved negative regulatory sequence that influences the leukemogenic activity of notch1. *Molecular and Cellular Biology*. 2006;26(16):6261–71.
357. Wilson A, Laurenti E, Oser G, et al. Hematopoietic stem cells reversibly switch from dormancy to self-renewal during homeostasis and repair. *Cell*. 2008;135(6):1118–29.
358. Fuchs E. The tortoise and the hair: slow-cycling cells in the stem cell race. *Cell*. 2009;137(5):811–9.
359. Essers MAG, Offner S, Blanco-Bose WE, et al. Ifnalpha activates dormant haematopoietic stem cells in vivo. *Nature*. 2009;458(7240):904–8.

360. Ishikawa F, Yoshida S, Saito Y, et al. Chemotherapy-resistant human aml stem cells home to and engraft within the bone-marrow endosteal region. *Nature Biotechnology*. 2007;25(11):1315–21.
361. Saito Y, Uchida N, Tanaka S, et al. Induction of cell cycle entry eliminates human leukemia stem cells in a mouse model of aml. *Nature Biotechnology*. 2010;28(3):275–80.
362. Dieter SM, Ball CR, Hoffmann CM, et al. Distinct types of tumor-initiating cells form human colon cancer tumors and metastases. *Cell Stem Cell*. 2011;9(4):357–65.
363. Pece S, Tosoni D, Confalonieri S, et al. Biological and molecular heterogeneity of breast cancers correlates with their cancer stem cell content. *Cell*. 2010;140(1):62–73.
364. Essers MAG, Trumpp A. Targeting leukemic stem cells by breaking their dormancy. *Molecular Oncology*. 2010;4(5):443–50.
365. Seita J, Weissman I. Hematopoietic stem cell: self-renewal versus differentiation. *Wiley Interdisciplinary Reviews: ....* 2010;2(6):640–653.
366. Aguirre-Ghiso J a. Models, mechanisms and clinical evidence for cancer dormancy. *Nature Reviews: Cancer*. 2007;7(11):834–46.
367. Pantel K, Alix-Panabières C, Riethdorf S. Cancer micrometastases. *Nature Reviews: Clinical Oncology*. 2009;6:339–351.
368. Goldman JM. Chronic myeloid leukemia: a historical perspective. *Seminars in Hematology*. 2010;47(4):302–11.
369. Druker BJ, Guilhot F, O'Brien SG, et al. Five-year follow-up of patients receiving imatinib for chronic myeloid leukemia. *The New England Journal of Medicine*. 2006;355(23):2408–17.
370. Oravec-Wilson KI, Philips ST, Yilmaz OH, et al. Persistence of leukemia-initiating cells in a conditional knockin model of an imatinib-responsive myeloproliferative disorder. *Cancer Cell*. 2009;16(2):137–48.
371. Perrotti D, Jamieson C, Goldman JM, Skorski T. Chronic myeloid leukemia: mechanisms of blastic transformation. *The Journal of Clinical Investigation*. 2010;120(7):2254–64.
372. Barnes DJ, Melo J V. Primitive, quiescent and difficult to kill. *Cell Cycle*. 2006;5(24):2862–2866.

373. Ross DM, Hughes TP, Melo J V. Do we have to kill the last cml cell? *Leukemia*. 2011;25(2):193–200.
374. Li X, Lewis MT, Huang J, et al. Intrinsic resistance of tumorigenic breast cancer cells to chemotherapy. *Journal of the National Cancer Institute*. 2008;100(9):672–9.
375. Dean M, Fojo T, Bates S. Tumour stem cells and drug resistance. *Nature Reviews: Cancer*. 2005;5(4):275–84.
376. Konopleva M, Konoplev S, Hu W, et al. Stromal cells prevent apoptosis of aml cells by up-regulation of anti-apoptotic proteins. *Leukemia*. 2002;16(9):1713–24.
377. Konopleva M, Zhao S, Hu W, et al. The anti-apoptotic genes *bcl-x(l)* and *bcl-2* are over-expressed and contribute to chemoresistance of non-proliferating leukaemic cd34+ cells. *British journal of Haematology*. 2002;118(2):521–34.
378. Bao S, Wu Q, McLendon RE, et al. Glioma stem cells promote radioresistance by preferential activation of the dna damage response. *Nature*. 2006;444(7120):756–60.
379. Diehn M, Cho RW, Lobo N a, et al. Association of reactive oxygen species levels and radioresistance in cancer stem cells. *Nature*. 2009;458(7239):780–3.
380. Notta F, Mullighan CG, Wang JCY, et al. Evolution of human bcr-abl1 lymphoblastic leukaemia-initiating cells. *Nature*. 2011;469(7330):362–7.
381. Mullighan C, Phillips L, Su X, Ma J. Genomic analysis of the clonal origins of relapsed acute lymphoblastic leukemia. *Science*. 2008;5(November):1377–1380.
382. Anderson K, Lutz C, Van Delft FW, et al. Genetic variegation of clonal architecture and propagating cells in leukaemia. *Nature*. 2011;469(7330):356–61.
383. Baylin S, Jones P. A decade of exploring the cancer epigenome — biological and translational implications. *Nature Reviews Cancer*. 2011;11:726–734.
384. Aparicio S, Caldas C. The implications of clonal genome evolution for cancer medicine. *New England Journal of Medicine*. 2013;368(9):842–851.
385. Polyak K, Haviv I, Campbell IG. Co-evolution of tumor cells and their microenvironment. *Trends in Genetics*. 2009;25(1):30–8.
386. Hu M, Yao J, Cai L, et al. Distinct epigenetic changes in the stromal cells of breast cancers. *Nature Genetics*. 2005;37(8):899–905.

387. Campbell PJ, Yachida S, Mudie LJ, et al. The patterns and dynamics of genomic instability in metastatic pancreatic cancer. *Nature*. 2010;467(7319):1109–13.
388. Chen J, Li Y, Yu T-S, et al. A restricted cell population propagates glioblastoma growth after chemotherapy. *Nature*. 2012;488(7412):522–6.
389. Schepers AG, Snippert HJ, Stange DE, et al. Lineage tracing reveals lgr5+ stem cell activity in mouse intestinal adenomas. *Science*. 2012;337(6095):730–5.
390. Driessens G, Beck B, Caauwe A, Simons BD, Blanpain C. Defining the mode of tumour growth by clonal analysis. *Nature*. 2012;488(7412):527–30.
391. Charrad RS, Li Y, Delpech B, et al. Ligation of the cd44 adhesion molecule reverses blockage of differentiation in human acute myeloid leukemia. *Nature medicine*. 1999;5(6):669–76.
392. Jin L, Hope KJ, Zhai Q, Smadja-Joffe F, Dick JE. Targeting of cd44 eradicates human acute myeloid leukemic stem cells. *Nature Medicine*. 2006;12(10):1167–74.
393. Tallman MS. Differentiating therapy in acute myeloid leukemia. *Leukemia*. 1996;10(8):1262–8.
394. Wulf G, Wang R-Y, Kuehnle I, et al. A leukemic stem cell with intrinsic drug efflux capacity in acute myeloid leukemia. *Blood*. 2001;98(4):1166–1173.
395. Singh S, Hawkins C, Clarke I, Squire J. Identification of human brain tumour initiating cells. *Nature*. 2004;432:396–401.
396. Secomb TW, Konerding M a, West C a, et al. Microangiectasias: structural regulators of lymphocyte transmigration. *Proceedings of the National Academy of Sciences*. 2003;100(12):7231–4.
397. Hsiai TK, Cho SK, Wong PK, et al. Micro sensors: linking real-time oscillatory shear stress with vascular inflammatory responses. *Annals of Biomedical Engineering*. 2004;32(2):189–201.
398. Harrison D, Astle C. Loss of stem cell repopulating ability upon transplantation: effects of donor age, cell number, and transplantation procedure. *The Journal of Experimental Medicine*. 1982;156:1767–1779.
399. Anderson MK. At the crossroads: diverse roles of early thymocyte transcriptional regulators. *Immunological Reviews*. 2006;209:191–211.

400. Hager-Theodorides AL, Outram S V, Shah DK, et al. Bone morphogenetic protein 2/4 signaling regulates early thymocyte differentiation. *Journal of immunology* (Baltimore, Md. : 1950). 2002;169(10):5496–504.
401. Johnson SE, Shah N, Bajer A a, LeBien TW. Il-7 activates the phosphatidylinositol 3-kinase/akt pathway in normal human thymocytes but not normal human b cell precursors. *Journal of immunology* (Baltimore, Md. : 1950). 2008;180(12):8109–17.
402. Scollay RG, Butcher EC, Weissman IL. Thymus cell migration. quantitative aspects of cellular traffic from the thymus to the periphery in mice. *European Journal of Immunology*. 1980;10(3):210–8.
403. Rooke R, Waltzinger C, Benoist C, Mathis D. Targeted complementation of mhc class ii deficiency by intrathymic delivery of recombinant adenoviruses. *Immunity*. 1997;7(1):123–34.
404. Siegelman MH, DeGrendele HC, Estess P. Activation and interaction of cd44 and hyaluronan in immunological systems. *Journal of Leukocyte Biology*. 1999;66(2):315–21.
405. Cleveland SM, Smith S, Tripathi R, et al. Lmo2 induces hematopoietic stem cell like features in t-cell progenitor cells prior to leukemia. *Stem Cells*. 2013;(615):
406. Yamamoto S, Sato Y, Maruyama S, et al. Analysis of the influence of portal venous pressure (shear stress) to the movement of mononuclear cells in the liver. *Transplantation Proceedings*. 2000;32(7):2289.
407. Koch U, Radtke F. Mechanisms of t cell development and transformation. *Annual Review of Cell and Developmental Biology*. 2011;27:539–62.
408. Zlotoff D a, Schwarz B a, Bhandoola A. The long road to the thymus: the generation, mobilization, and circulation of t-cell progenitors in mouse and man. *Seminars in Immunopathology*. 2008;30(4):371–82.
409. Guttinger M, Sutti F, Panigada M, et al. Epithelial v-like antigen (eva), a novel member of the immunoglobulin superfamily, expressed in embryonic epithelia with a potential role as homotypic adhesion molecule in thymus histogenesis. *The Journal of Cell Biology*. 1998;141(4):1061–71.
410. Iacovelli S, Iosue I, Di Cesare S, Guttinger M. Lymphoid eva1 expression is required for dn1-dn3 thymocytes transition. *PloS One*. 2009;4(10):e7586.
411. Haanstra KG, Hofman SO, Lopes Estêvão DM, et al. Antagonizing the  $\alpha 4 \beta 1$  integrin, but not  $\alpha 4 \beta 7$ , inhibits leukocytic infiltration of the central nervous

system in rhesus monkey experimental autoimmune encephalomyelitis. *Journal of Immunology*. 2013;190(5):1961–73.

412. Ahrendt M, Hammerschmidt S, Pabst O, Pabst R, Bode U. Stromal cells confer lymph node-specific properties by shaping a unique microenvironment influencing local immune responses. *The Journal of Immunology*. 2008;181:1898–1907.

413. Mebius RE, Streeter PR, Michie S, Butcher EC, Weissman IL. A developmental switch in lymphocyte homing receptor and endothelial vascular addressin expression regulates lymphocyte homing and permits cd4+ cd3- cells to colonize lymph nodes. *Proceedings of the National Academy of Sciences*. 1996;93(20):11019–24.

414. Hu Y, Smyth GK. Elda: extreme limiting dilution analysis for comparing depleted and enriched populations in stem cell and other assays. *Journal of Immunological Methods*. 2009;347(1-2):70–8.

415. Dumortier A, Jeannet R, Kirstetter P, Kleinmann E, Sellars M. Notch activation is an early and critical event during t-cell leukemogenesis in ikaros-deficient mice. *Molecular and Cellular Biology*. 2006;26(1):209–220.

416. Duncan AW, Rattis FM, DiMascio LN, et al. Integration of notch and wnt signaling in hematopoietic stem cell maintenance. *Nature Immunology*. 2005;6(3):314–22.

417. Mizutani K, Yoon K, Dang L, Tokunaga A, Gaiano N. Differential notch signalling distinguishes neural stem cells from intermediate progenitors. *Nature*. 2007;449(7160):351–5.

418. Hellström M, Phng L-K, Hofmann JJ, et al. Dll4 signalling through notch1 regulates formation of tip cells during angiogenesis. *Nature*. 2007;445(7129):776–80.

419. Yashiro-Ohtani Y, He Y, Ohtani T, et al. Pre-tcr signaling inactivates notch1 transcription by antagonizing e2a. *Genes & Development*. 2009;23(14):1665–76.

420. Palomero T, Sulis ML, Cortina M, et al. Mutational loss of pten induces resistance to notch1 inhibition in t-cell leukemia. *Nature Medicine*. 2007;13(10):1203–10.

421. Thompson BJ, Buonamici S, Sulis ML, et al. The scffbw7 ubiquitin ligase complex as a tumor suppressor in t cell leukemia. *The Journal of Experimental Medicine*. 2007;204(8):1825–35.

422. Maser RS, Choudhury B, Campbell PJ, et al. Chromosomally unstable mouse tumours have genomic alterations similar to diverse human cancers. *Nature*. 2007;447(7147):966–71.
423. Ciofani M, Zúñiga-Pflücker JC. Notch promotes survival of pre-t cells at the beta-selection checkpoint by regulating cellular metabolism. *Nature Immunology*. 2005;6(9):881–8.
424. Maillard I, Schwarz B a, Sambandam A, et al. Notch-dependent t-lineage commitment occurs at extrathymic sites following bone marrow transplantation. *Blood*. 2006;107(9):3511–9.
425. Adler SH, Chiffoleau E, Xu L, et al. Notch signaling augments t cell responsiveness by enhancing cd25 expression. *Journal of Immunology*. 2003;171(6):2896–903.
426. Kunisato A, Chiba S, Nakagami-Yamaguchi E, et al. Hes-1 preserves purified hematopoietic stem cells ex vivo and accumulates side population cells in vivo. *Blood*. 2003;101(5):1777–83.
427. Tomita K, Hattori M, Nakamura E, et al. The bhlh gene hes1 is essential for expansion of early t cell precursors. *Genes & Development*. 1999;13(9):1203–10.
428. Takahashi K, Yamanaka S. Induction of pluripotent stem cells from mouse embryonic and adult fibroblast cultures by defined factors. *Cell*. 2006;126(4):663–76.
429. Cornberg M, Chen A, Wilkinson L, et al. Narrowed tcr repertoire and viral escape as a consequence of heterologous immunity. *Journal of Clinical Investigation*. 2006;116(5):1443–1456.
430. Wolfer A, Wilson A, Nemir M, MacDonald HR, Radtke F. Inactivation of notch1 impairs vjbeta rearrangement and allows pre-tcr-independent survival of early alpha beta lineage thymocytes. *Immunity*. 2002;16(6):869–79.
431. Maillard I, Tu L, Sambandam A, et al. The requirement for notch signaling at the beta-selection checkpoint in vivo is absolute and independent of the pre-t cell receptor. *The Journal of Experimental Medicine*. 2006;203(10):2239–45.
432. Jackson A, Bartz S, Schelter J, et al. Expression profiling reveals off-target gene regulation by rna. *Nature biotechnology*. 2003;21(6):635–638.
433. Pei Y, Tuschl T. On the art of identifying effective and specific sirnas. *Nature Methods*. 2006;3(9):670–676.

434. Svoboda P. Off-targeting and other non-specific effects of rna experiments in mammalian cells. *Current Opinion in Molecular Therapeutics*. 2007;9(3):248–57.
435. Filippakopoulos P, Qi J, Picaud S, et al. Selective inhibition of bet bromodomains. *Nature*. 2010;468(7327):1067–73.
436. Lewis HD, Leveridge M, Strack PR, et al. Apoptosis in t cell acute lymphoblastic leukemia cells after cell cycle arrest induced by pharmacological inhibition of notch signaling. *Chemistry & Biology*. 2007;14(2):209–19.
437. Milano J, McKay J, Dagenais C, et al. Modulation of notch processing by gamma-secretase inhibitors causes intestinal goblet cell metaplasia and induction of genes known to specify gut secretory lineage differentiation. *Toxicological Sciences*. 2004;82(1):341–58.
438. Ott CJ, Kopp N, Bird L, et al. Bet bromodomain inhibition targets both c-myc and il7r in high-risk acute lymphoblastic leukemia. *Blood*. 2012;
439. Zuber J, Rappaport AR, Luo W, et al. An integrated approach to dissecting oncogene addiction implicates a myb-coordinated self-renewal program as essential for leukemia maintenance. *Genes & Development*. 2011;25(15):1628–40.
440. Möricke a, Zimmermann M, Reiter A, et al. Long-term results of five consecutive trials in childhood acute lymphoblastic leukemia performed by the all-bfm study group from 1981 to 2000. *Leukemia*. 2010;24(2):265–84.
441. Moghrabi A, Levy DE, Asselin B, et al. Results of the dana-farber cancer institute all consortium protocol 95-01 for children with acute lymphoblastic leukemia. *Blood*. 2007;109(3):896–904.
442. Lovén J, Hoke H a, Lin CY, et al. Selective inhibition of tumor oncogenes by disruption of super-enhancers. *Cell*. 2013;153(2):320–34.
443. Ramsay RG, Gonda TJ. Myb function in normal and cancer cells. *Nature Reviews: Cancer*. 2008;8(7):523–34.
444. Bonnet M, Loosveld M, Montpellier B, et al. Posttranscriptional deregulation of myc via pten constitutes a major alternative pathway of myc activation in t-cell acute lymphoblastic leukemia. *Blood*. 2011;117(24):6650–9.
445. Marfil V, Moya M, Pierreux CE, et al. Interaction between hhex and sox13 modulates wnt/tcf activity. *The Journal of Biological Chemistry*. 2010;285(8):5726–37.



446. Lou H, Dean M. Targeted therapy for cancer stem cells: the patched pathway and abc transporters. *Oncogene*. 2007;26(9):1357–60.
447. Chiu PPL, Jiang H, Dick JE. Leukemia-initiating cells in human t-lymphoblastic leukemia exhibit glucocorticoid resistance. *Blood*. 2010;116(24):5268–79.
448. Daye D, Wellen KE. Metabolic reprogramming in cancer: unraveling the role of glutamine in tumorigenesis. *Seminars in Cell & Developmental Biology*. 2012;23(4):362–9.
449. Wang R, Dillon CP, Shi LZ, et al. The transcription factor myc controls metabolic reprogramming upon t lymphocyte activation. *Immunity*. 2011;35(6):871–82.
450. Fuchs BC, Bode BP. Amino acid transporters asct2 and lat1 in cancer: partners in crime? *Seminars in Cancer Biology*. 2005;15(4):254–66.
451. Hassanein M, Hoeksema MD, Shiota M, et al. Slc1a5 mediates glutamine transport required for lung cancer cell growth and survival. *Clinical Cancer Research*. 2013;19(3):560–70.
452. Korkola JE, Houldsworth J, Chadalavada RS V, et al. Down-regulation of stem cell genes, including those in a 200-kb gene cluster at 12p13.31, is associated with in vivo differentiation of human male germ cell tumors. *Cancer Research*. 2006;66(2):820–7.
453. Maurer MH, Geomor HK, Bürgers HF, Schelshorn DW, Kuschinsky W. Adult neural stem cells express glucose transporters glut1 and glut3 and regulate glut3 expression. *FEBS Letters*. 2006;580(18):4430–4.
454. Natalicchio A, De Stefano F, Perrini S, et al. Involvement of the p66shc protein in glucose transport regulation in skeletal muscle myoblasts. *American Journal of Physiology, Endocrinology, and Metabolism*. 2009;296(2):E228–37.
455. Macheda ML, Rogers S, Best JD. Molecular and cellular regulation of glucose transporter (glut) proteins in cancer. *Journal of Cellular Physiology*. 2005;202(3):654–62.
456. Hayes LL, Claman HN. Recovery of immunocompetence of bone marrow and spleen following sublethal irradiation. *Proceedings of the Society for Experimental Biology and Medicine*. 1970;133(1):57–61.
457. Barcellos-Hoff MH, Park C, Wright EG. Radiation and the microenvironment - tumorigenesis and therapy. *Nature Reviews: Cancer*. 2005;5(11):867–75.

458. Lapidot T, Fajerman Y, Kollet O. Immune-deficient scid and nod/scid mice models as functional assays for studying normal and malignant human hematopoiesis. *Journal of Molecular Medicine*. 1997;75(9):664–73.
459. Agliano A, Martin-Padura I, Mancuso P, et al. Human acute leukemia cells injected in nod/ltsz-scid/il-2rgamma null mice generate a faster and more efficient disease compared to other nod/scid-related strains. *International Journal of Cancer*. 2008;123(9):2222–7.
460. Rutkowski MR, Stephen TL, Conejo-Garcia JR. Anti-tumor immunity: myeloid leukocytes control the immune landscape. *Cellular immunology*. 2012;278(1-2):21–6.
461. Parham P, Moffett A. Variable nk cell receptors and their mhc class i ligands in immunity, reproduction and human evolution. *Nature Reviews: Immunology*. 2013;13(2):133–44.
462. Bigner SH, Mark J, Mahaley MS, Bigner DD. Patterns of the early, gross chromosomal changes in malignant human gliomas. *Hereditas*. 1984;101(1):103–13.
463. Liaw D, Marsh D, Li J, Dahia P, Wang S. Germline mutations of the pten gene in cowden disease, an inherited breast and thyroid cancer syndrome. *Nature*. 1997;16:64–67.
464. Steck P, Pershouse M, Jasser S, et al. Identification of a candidate tumour suppressor gene, mmac1, at chromosome 10q23.3 that is mutated in multiple advanced cancers. *Nature Genetics*. 1997;15:356–362.
465. Alimonti A, Carracedo A, Clohessy JG, et al. Subtle variations in pten dose determine cancer susceptibility. *Nature Genetics*. 2010;42(5):454–8.
466. Hollander MC, Blumenthal GM, Dennis P a. Pten loss in the continuum of common cancers, rare syndromes and mouse models. *Nature Reviews: Cancer*. 2011;11(4):289–301.
467. Sun H, Lesche R, Li DM, et al. Pten modulates cell cycle progression and cell survival by regulating phosphatidylinositol 3,4,5,-trisphosphate and akt/protein kinase b signaling pathway. *Proceedings of the National Academy of Sciences*. 1999;96(11):6199–204.
468. Stambolic V, Suzuki a, De la Pompa JL, et al. Negative regulation of pkb/akt-dependent cell survival by the tumor suppressor pten. *Cell*. 1998;95(1):29–39.
469. Manning BD, Cantley LC. Akt/pkb signaling: navigating downstream. *Cell*. 2007;129(7):1261–74.

470. Ma XM, Blenis J. Molecular mechanisms of mtor-mediated translational control. *Nature Reviews: Molecular Cell Biology*. 2009;10(5):307–18.
471. Warburg O. On respiratory impairment in cancer cells. *Science*. 1956;124(3215):269–70.
472. Vander Heiden MG, Cantley LC, Thompson CB. Understanding the warburg effect: the metabolic requirements of cell proliferation. *Science*. 2009;324(5930):1029–33.
473. Eguez L, Lee A, Chavez J a, et al. Full intracellular retention of glut4 requires as160 rab gtpase activating protein. *Cell metabolism*. 2005;2(4):263–72.
474. Fang M, Shen Z, Huang S, et al. The er udpase entpd5 promotes protein n-glycosylation, the warburg effect, and proliferation in the pten pathway. *Cell*. 2010;143(5):711–24.
475. Bronisz a, Godlewski J, Wallace J a, et al. Reprogramming of the tumour microenvironment by stromal pten-regulated mir-320. *Nature Cell Biology*. 2012;14(2):159–67.
476. Trimboli AJ, Cantemir-Stone CZ, Li F, et al. Pten in stromal fibroblasts suppresses mammary epithelial tumours. *Nature*. 2009;461(7267):1084–91.
477. Kurose K, Gilley K, Matsumoto S, et al. Frequent somatic mutations in pten and tp53 are mutually exclusive in the stroma of breast carcinomas. *Nature Genetics*. 2002;32(3):355–7.
478. Zhang J, Grindley JC, Yin T, et al. Pten maintains haematopoietic stem cells and acts in lineage choice and leukaemia prevention. *Nature*. 2006;441(7092):518–22.
479. Magee J a, Ikenoue T, Nakada D, et al. Temporal changes in pten and mtorc2 regulation of hematopoietic stem cell self-renewal and leukemia suppression. *Cell Stem Cell*. 2012;11(3):415–28.
480. Ito K, Bernardi R, Pandolfi PP. A novel signaling network as a critical rheostat for the biology and maintenance of the normal stem cell and the cancer-initiating cell. *Current Opinion in Genetics & Development*. 2009;19(1):51–9.
481. Guo W, Lasky JL, Chang C-J, et al. Multi-genetic events collaboratively contribute to pten-null leukaemia stem-cell formation. *Nature*. 2008;453(7194):529–33.
482. Gutierrez A, Sanda T, Grebliunaite R, et al. High frequency of pten, pi3k, and akt abnormalities in t-cell acute lymphoblastic leukemia. *Blood*. 2009;114(3):647–50.

483. Jotta PY, Ganazza M a, Silva A, et al. Negative prognostic impact of pten mutation in pediatric t-cell acute lymphoblastic leukemia. *Leukemia*. 2010;24(1):239–42.
484. Whelan J, Forbes S, Bertrand F. Cbf-1 (rbp-jk) binds to the pten promoter and regulates pten gene expression. *Cell Cycle*. 2007;6(1):80–84.
485. Palmero I, Pantoja C, Serrano M. P19arf links the tumour suppressor p53 to ras. *Nature*. 1998;395(6698):125–6.
486. Xia D, Srinivas H, Ahn Y-H, et al. Mitogen-activated protein kinase kinase-4 promotes cell survival by decreasing pten expression through an nf kappa b-dependent pathway. *The Journal of Biological Chemistry*. 2007;282(6):3507–19.
487. Song L, Li J, Liao W, Feng Y. The polycomb group protein bmi-1 represses the tumor suppressor pten and induces epithelial-mesenchymal transition in human nasopharyngeal epithelial. *The Journal of Clinical Investigation*. 2009;119(12):3626–3636.
488. Bartel DP. Micrnas: target recognition and regulatory functions. *Cell*. 2009;136(2):215–33.
489. Salmena L, Poliseno L, Tay Y, Kats L, Pandolfi PP. A cerna hypothesis: the rosetta stone of a hidden rna language? *Cell*. 2011;146(3):353–8.
490. Song MS, Salmena L, Pandolfi PP. The functions and regulation of the pten tumour suppressor. *Nature Reviews: Molecular Cell Biology*. 2012;13(5):283–96.
491. Palomero T, Dominguez M, Ferrando A. The role of the pten/akt pathway in notch1-induced leukemia. *Cell Cycle*. 2008;7(8):965–970.
492. Gutierrez A, Grebliunaite R, Feng H, et al. Pten mediates myc oncogene dependence in a conditional zebrafish model of t cell acute lymphoblastic leukemia. *The Journal of Experimental Medicine*. 2011;208(8):1595–603.
493. Olive V, Bennett MJ, Walker JC, et al. Mir-19 is a key oncogenic component of mir-17-92. *Genes & Development*. 2009;23(24):2839–49.
494. Mu P, Han Y-C, Betel D, et al. Genetic dissection of the mir-17~92 cluster of micrnas in myc-induced b-cell lymphomas. *Genes & Development*. 2009;23(24):2806–11.
495. Lu J, Jeong H-W, Jeong H, et al. Stem cell factor sall4 represses the transcriptions of pten and sall1 through an epigenetic repressor complex. *PLoS One*. 2009;4(5):e5577.

496. Li H, Yang B. Stress response of glioblastoma cells mediated by mir-17-5p targeting pten and the passenger strand mir-17-3p targeting mdm2. *Oncotarget*. 2012;1–16.
497. Rao E, Jiang C, Ji M, et al. The mirna-17~92 cluster mediates chemoresistance and enhances tumor growth in mantle cell lymphoma via pi3k/akt pathway activation. *Leukemia*. 2012;26(5):1064–72.
498. Shan S, Fang L, Shatseva T, et al. Mature mir-17-5p and passenger mir-17-3p induce hepatocellular carcinoma by targeting pten, galnt7, and vimentin in different signal pathways. *Journal of Cell Science*. 2013;(February 2013):
499. Meng F, Henson R, Wehbe-Janek H, et al. Microrna-21 regulates expression of the pten tumor suppressor gene in human hepatocellular cancer. *Gastroenterology*. 2007;133(2):647–58.
500. Ma X, Kumar M, Choudhury S, Buscaglia L, Barker J. Loss of the mir-21 allele elevates the expression of its target genes and reduces tumorigenesis. *Proceedings of the National Academy of Sciences*. 2011;108(25):10144–10149.
501. Lesche R, Groszer M, Gao J, Wang Y. Cre/loxp-mediated inactivation of the murine pten tumor suppressor gene. *Genesis*. 2002;149:148–149.
502. Silva A, Yunes J, Cardoso B, LR M, Jotta P. Pten posttranslational inactivation and hyperactivation of the pi3k/akt pathway sustain primary t cell leukemia viability. *The Journal of Clinical Investigation*. 2008;118(11):3762–3774.
503. Scheijen B, Griffin J. Tyrosine kinase oncogenes in normal hematopoiesis and hematological disease. *Oncogene*. 2002;3314–3333.
504. Masson K, Rönnstrand L. Oncogenic signaling from the hematopoietic growth factor receptors c-kit and flt3. *Cellular Signalling*. 2009;21(12):1717–26.
505. Kent D, Copley M, Benz C, et al. Regulation of hematopoietic stem cells by the steel factor/kit signaling pathway. *Clinical Cancer Research*. 2008;14(7):1926–30.
506. Nocka K, Tan JC, Chiu E, et al. Molecular bases of dominant negative and loss of function mutations at the murine c-kit/white spotting locus: w37, wv, w41 and w. *The EMBO journal*. 1990;9(6):1805–13.
507. Godfrey DI, Zlotnik a, Suda T. Phenotypic and functional characterization of c-kit expression during intrathymic t cell development. *Journal of immunology (Baltimore, Md. : 1950)*. 1992;149(7):2281–5.
508. González-García S, García-Peydró M, Martín-Gayo E, et al. Csl-maml-dependent notch1 signaling controls t lineage-specific il-7{alpha} gene

expression in early human thymopoiesis and leukemia. *The Journal of Experimental Medicine*. 2009;206(4):779–91.

509. Park J, Yu Q, Erman B, et al. Suppression of il7ralpha transcription by il-7 and other prosurvival cytokines: a novel mechanism for maximizing il-7-dependent t cell survival. *Immunity*. 2004;21(2):289–302.

510. Gravestien L a, Amsen D, Boes M, et al. The tnfr receptor family member cd27 signals to jun n-terminal kinase via traf-2. *European Journal of Immunology*. 1998;28(7):2208–16.

511. Lens SM, Tesselaar K, Van Oers MH, Van Lier R a. Control of lymphocyte function through cd27-cd70 interactions. *Seminars in Immunology*. 1998;10(6):491–9.

512. Claus C, Riether C, Schürch C, et al. Cd27 signaling increases the frequency of regulatory t cells and promotes tumor growth. *Cancer Research*. 2012;72(14):3664–76.

513. Schürch C, Riether C, Matter MS, Tzankov A, Ochsenbein AF. Cd27 signaling on chronic myelogenous leukemia stem cells activates wnt target genes and promotes disease progression. *The Journal of Clinical Investigation*. 2012;122(2):624–638.

514. Höflinger S, Kesavan K, Fuxa M, et al. Analysis of notch1 function by in vitro t cell differentiation of pax5 mutant lymphoid progenitors. *Journal of immunology (Baltimore, Md. : 1950)*. 2004;173(6):3935–44.

515. Zenatti PP, Ribeiro D, Li W, et al. Oncogenic il7r gain-of-function mutations in childhood t-cell acute lymphoblastic leukemia. *Nature Genetics*. 2011;43(10):932–9.

516. Maddens S, Charruyer A, Plo I, et al. Kit signaling inhibits the sphingomyelin-ceramide pathway through plcγ1: implication in stem cell factor radioprotective effect. *Blood*. 2013;100(4):1294–1301.

517. Pérez-Losada J, Sánchez-Martín M, Pérez-Caro M, Pérez-Mancera P a, Sánchez-García I. The radioresistance biological function of the scf/kit signaling pathway is mediated by the zinc-finger transcription factor slug. *Oncogene*. 2003;22(27):4205–11.

518. Darzynkiewicz Z, Huang X. Analysis of cellular dna content by flow cytometry. *Current protocols in immunology / edited by John E. Coligan ... [et al.]*. 2004;Chapter 5:Unit 5.7.

519. Goodell M, Brose K. Isolation and functional properties of murine hematopoietic stem cells that are replicating in vivo. *The Journal of Experimental Medicine*. 1996;183(A):1797–1806.
520. Ergen A V, Jeong M, Lin KK, Challen GA, Goodell MA. Isolation and characterization of mouse side population cells. *Methods in molecular biology* (Clifton, N.J.). 2013;946:151–62.
521. Mucenski ML, McLain K, Kier a B, et al. A functional c-myb gene is required for normal murine fetal hepatic hematopoiesis. *Cell*. 1991;65(4):677–89.
522. Emambokus N, Vegiopoulos A, Harman B, et al. Progression through key stages of haemopoiesis is dependent on distinct threshold levels of c-myb. *The EMBO Journal*. 2003;22(17):4478–88.
523. Malaterre J, Carpinelli M, Ernst M, et al. C-myb is required for progenitor cell homeostasis in colonic crypts. *Proceedings of the National Academy of Sciences*. 2007;104(10):3829–34.
524. Malaterre J, Mantamadiotis T, Dworkin S, et al. C-myb is required for neural progenitor cell proliferation and maintenance of the neural stem cell niche in adult brain. *Stem Cells*. 2008;26(1):173–81.
525. Biedenkapp H, Borgmeyer U, Sippel AE, Klempnauer KH. Viral myb oncogene encodes a sequence-specific dna-binding activity. *Nature*. 1988;335(6193):835–7.
526. Kauraniemi P, Hedenfalk I, Persson K, et al. Myb oncogene amplification in hereditary brca1 breast cancer. *Cancer Research*. 2000;60(19):5323–8.
527. Guérin M, Sheng ZM, Andrieu N, Riou G. Strong association between c-myb and oestrogen-receptor expression in human breast cancer. *Oncogene*. 1990;5(1):131–5.
528. Trainer D, Kline T, McCabe F, et al. Biological characterization and oncogene expression in human colorectal carcinoma cell lines. *International Journal of Cancer*. 2006;296:287–296.
529. Torelli G, Venturelli D, Coló A, Zanni C. Expression of c-myb protooncogene and other cell cycle-related genes in normal and neoplastic human colonic mucosa. *Cancer Research*. 1987;47:5266–5269.
530. Anfossi G, Gewirtz a M, Calabretta B. An oligomer complementary to c-myb-encoded mrna inhibits proliferation of human myeloid leukemia cell lines. *Proceedings of the National Academy of Sciences*. 1989;86(9):3379–83.

531. Calabretta B, Sims RB, Valtieri M, et al. Normal and leukemic hematopoietic cells manifest differential sensitivity to inhibitory effects of c-myc antisense oligodeoxynucleotides: an in vitro study relevant to bone marrow purging. *Proceedings of the National Academy of Sciences*. 1991;88(6):2351–5.
532. Clappier E, Cuccuini W, Kalota A, et al. The c-myc locus is involved in chromosomal translocation and genomic duplications in human t-cell acute leukemia (t-all), the translocation defining a new t-all subtype in very young children. *Blood*. 2007;110(4):1251–61.
533. O’Neil J, Tchinda J, Gutierrez A, et al. Alu elements mediate myb gene tandem duplication in human t-all. *The Journal of Experimental Medicine*. 2007;204(13):3059–66.
534. Hess JL, Bittner CB, Zeisig DT, et al. C-myc is an essential downstream target for homeobox-mediated transformation of hematopoietic cells. *Blood*. 2006;108(1):297–304.
535. Lidonnici MR, Corradini F, Waldron T, Bender TP, Calabretta B. Requirement of c-myc for p210(bcr/abl)-dependent transformation of hematopoietic progenitors and leukemogenesis. *Blood*. 2008;111(9):4771–9.
536. Thompson CB, Challoner PB, Neiman PE, Groudine M. Expression of the c-myc proto-oncogene during cellular proliferation. *Nature*. 1986;319(6052):374–80.
537. Weston K. Myb proteins in life, death and differentiation. *Current Opinion in Genetics & Development*. 1998;8(1):76–81.
538. Cures a, House C, Kanei-Ishii C, Kemp B, Ramsay RG. Constitutive c-myc amino-terminal phosphorylation and dna binding activity uncoupled during entry and passage through the cell cycle. *Oncogene*. 2001;20(14):1784–92.
539. Yuan J, Crittenden RB, Bender TP. C-myc promotes the survival of cd4+cd8+ double-positive thymocytes through upregulation of bcl-xl. *Journal of Immunology*. 2010;184(6):2793–804.
540. Zhou F, Zhang L, Van Laar T, Van Dam H, Ten Dijke P. Gsk3 $\beta$  inactivation induces apoptosis of leukemia cells by repressing the function of c-myc. *Molecular Biology of the Cell*. 2011;22(18):3533–40.
541. Corradini F, Bussolari R, Cerioli D, Lidonnici MR, Calabretta B. A degradation-resistant c-myc mutant cooperates with bcl-2 in enhancing proliferative potential and survival of hematopoietic cells. *Blood Cells, Molecules & Diseases*. 2007;39(3):292–6.



542. Lieu YK, Reddy EP. Conditional c-myb knockout in adult hematopoietic stem cells leads to loss of self-renewal due to impaired proliferation and accelerated differentiation. *Proceedings of the National Academy of Sciences*. 2009;106(51):21689–94.
543. Lieu YK, Kumar A, Pajeroski AG, Rogers TJ, Reddy EP. Requirement of c-myb in t cell development and in mature t cell function. *Proceedings of the National Academy of Sciences*. 2004;101(41):14853–8.
544. Bender TP, Kremer CS, Kraus M, Buch T, Rajewsky K. Critical functions for c-myb at three checkpoints during thymocyte development. *Nature Immunology*. 2004;5(7):721–9.
545. Allen RD, Bender TP, Siu G. C-myb is essential for early t cell development. *Genes & Development*. 1999;13:1073–1078.
546. Bender T, Thompson C, Kuehl W. Differential expression of c-myb mrna in murine b lymphomas by a block to transcription elongation. *Science*. 1987;235(5213):1473–1476.
547. Taylor D, Badiani P, Weston K. A dominant interfering myb mutant causes apoptosis in t cells. *Genes & Development*. 1996;10(21):2732–2744.
548. Graf T. Myb: a transcriptional activator linking proliferation and differentiation in hematopoietic cells. *Current Opinion in Genetics & Development*. 1992;2(2):249–55.